ISSN 0021-9673

VOL. 538 NO. 2 FEBRUARY 1, 1991

THIS ISSUE COMPLETES VOL. 538

JOURNAL OF CHROMATOGRAPHY

INCLUDING ELECTROPHORESIS AND OTHER SEPARATION METHODS

ELSEVIER

JOURNAL OF CHROMATOGRAPHY

Scope. The *Journal of Chromatography* publishes papers on all aspects of chromatography, electrophoresis and related methods. Contributions consist mainly of research papers dealing with chromatographic theory, instrumental development and their applications. The section *Biomedical Applications*, which is under separate editorship, deals with the following aspects: developments in and applications of chromatographic and electrophoretic techniques related to clinical diagnosis or alterations during medical treatment; screening and profiling of body fluids or tissues with special reference to metabolic disorders; results from basic medical research with direct consequences in clinical practice; drug level monitoring and pharmacokinetic studies; clinical toxicology; analytical studies in occupational medicine.

Submission of Papers. Manuscripts (in English; *four* copies are required) should be submitted to: Editorial Office of *Journal of Chromatography*, P.O. Box 681, 1000 AR Amsterdam, The Netherlands, Telefax (+31-20) 5862 304, or to: The Editor of *Journal of Chromatography, Biomedical Applications*, P.O. Box 681, 1000 AR Amsterdam, The Netherlands. Review articles are invited or proposed by letter to the Editors. An outline of the proposed review should first be forwarded to the Editors for preliminary discussion prior to preparation. Submission of an article is understood to imply that the article is original and unpublished and is not being considered for publication elsewhere. For copyright regulations, see below.

Subscription Orders. Subscription orders should be sent to: Elsevier Science Publishers B.V., P.O. Box 211, 1000 AE Amsterdam, The Netherlands, Tel. (+31-20) 5803 911, Telex 18582 ESPA NL, Telefax (+31-20) 5803 598. The *Journal of Chromatography* and the *Biomedical Applications* section can be subscribed to separately.

Publication. The *Journal of Chromatography* (incl. *Biomedical Applications*) has 38 volumes in 1991. The subscription prices for 1991 are:

J. Chromatogr. (incl. *Cum. Indexes, Vols. 501–550*) + *Biomed. Appl.* (Vols. 535–572):
Dfl. 7220.00 plus Dfl. 1140.00 (p.p.h.) (total *ca.* US$ 4696.50)

J. Chromatogr. (incl. *Cum. Indexes, Vols. 501–550*) only (Vols. 535–561):
Dfl. 5859.00 plus Dfl. 810.00 (p.p.h.) (total *ca.* US$ 3746.50)

Biomed. Appl. only (Vols. 562–572):
Dfl. 2387.00 plus Dfl. 330.00 (p.p.h.) (total *ca.* US$ 1526.50).

Our p.p.h. (postage, package and handling) charge includes surface delivery of all issues, except to subscribers in Argentina, Australia, Brasil, Canada, China, Hong Kong, India, Israel, Malaysia, Mexico, New Zealand, Pakistan, Singapore, South Africa, South Korea, Taiwan, Thailand and the U.S.A. who receive all issues by air delivery (S.A.L. — Surface Air Lifted) at no extra cost. For Japan, air delivery requires 50% additional charge; for all other countries airmail and S.A.L. charges are available upon request. Back volumes of the *Journal of Chromatography* (Vols. 1–534) are available at Dfl. 195.00 (plus postage). Claims for missing issues will be honoured, free of charge, within three months after publication of the issue. Customers in the U.S.A. and Canada wishing information on this and other Elsevier journals, please contact Journal Information Center, Elsevier Science Publishing Co. Inc., 655 Avenue of the Americas, New York, NY 10010, U.S.A., Tel. (+1-212) 633 3750, Telefax (+1-212) 633 3990.

Abstracts/Contents Lists published in Analytical Abstracts, Biochemical Abstracts, Biological Abstracts, Chemical Abstracts, Chemical Titles, Chromatography Abstracts, Clinical Chemistry Lookout, Current Contents/Life Sciences, Current Contents/Physical, Chemical & Earth Sciences, Deep-Sea Research/Part B: Oceanographic Literature Review, Excerpta Medica, Index Medicus, Mass Spectrometry Bulletin, PASCAL-CNRS, Pharmaceutical Abstracts, Referativnyi Zhurnal, Research Alert, Science Citation Index and Trends in Biotechnology.

See inside back cover for Publication Schedule, Information for Authors and information on Advertisements.

0021-9673/91/$03.50

Printed in The Netherlands

VOL. 538, NO. 2 JOURNAL OF CHROMATOGRAPHY FEBRUARY 1, 1991

CONTENTS

(Abstracts/Contents Lists published in Analytical Abstracts, Biochemical Abstracts, Biological Abstracts, Chemical Abstracts, Chemical Titles, Chromatography Abstracts, Current Contents/Life Sciences, Current Contents/Physical, Chemical & Earth Sciences, Deep-Sea Research/Part B: Oceanographic Literature Review, Excerpta Medica, Index Medicus, Mass Spectrometry Bulletin, PASCAL-CNRS, Referativnyi Zhurnal, Research Alert and Science Citation Index)

REGULAR PAPERS

Gas Chromatography

Column Liquid Chromatography

(Continued overleaf)

Column Liquid Chromatography

BOOK REVIEW

In articles with more than one author, the name of the author to whom correspondence should be addressed is indicated in the article heading by a 6-pointed asterisk (*)

Chemometrics Tutorials

Collected from Chemometrics and Intelligent Laboratory Systems - An International Journal, Volumes 1-5

edited by **D.L. Massart,** *Brussels,* **R.G. Brereton,** *University of Bristol, Bristol, UK,* **R.E.Dessy,** *Blacksburg, VA,* **P.K. Hopke,** *Potsdam, NY,* **C.H. Spiegelman,** *College Station, TX,* **W. Wegscheider,** *Graz, Austria*

The journal *Chemometrics and Intelligent Laboratory Systems* has a specific policy of publishing tutorial papers, (i.e. articles aiming to discuss and illustrate the application of chemometric and other techniques) solicited from leading experts in the varied disciplines relating to this subject. This book comprises reprints of tutorials from the first 5 volumes of this journal, covering the period from late 1986 to mid 1989. The authors of the papers include analytical, organic and environmental chemists, statisticians, pharmacologists, geologists, geochemists, computer scientists and biologists, which reflects the strong interdisciplinary communication. The papers have been reorganized into major themes, covering most of the main areas of chemometrics. This book is intended both as a personal reference text and as a useful background for courses in chemometrics and laboratory computing.

1990 viii + 428 pages (Paperback)
Price: US$ 66.75 / Dfl. 130.00
ISBN 0-444-88837-3

Elsevier Science Publishers
P.O. Box 211, 1000 AE Amsterdam, The Netherlands
P.O. Box 882, Madison Square Station, New York, NY 10159, USA

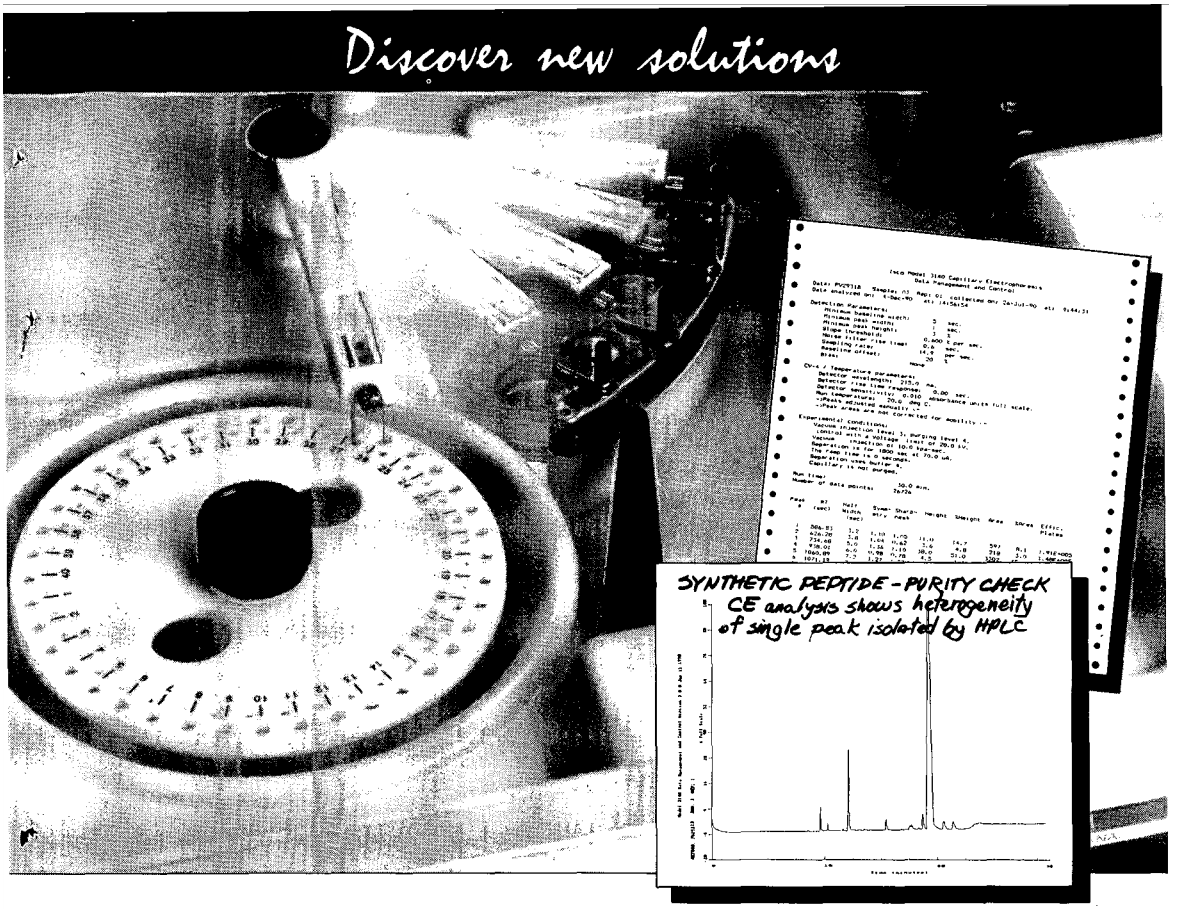

Find out if CE is right for your peptides, oligonucleotides, or pharmaceuticals

If you're considering capillary electrophoresis for fast, efficient separation of your samples, let us run a test analysis for you on our new Model 3140 Electropherograph™. We'll give you real-world results to help you make the right choice in automated CE.

- Model 3140's powerful PC-based method/data software generates comprehensive reports showing separation conditions and data analysis results.
- Its autosampler holds up to 40 covered microvials and allows multiple injections per vial from just microliters of sample.
- Programmable buffer selection facilitates method optimization.

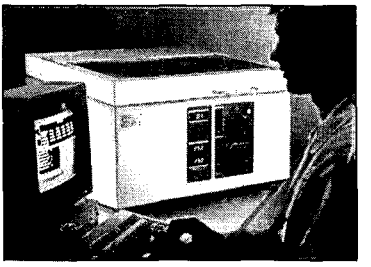

- Slip-through capillary holder provides convenience with flexibility and economy. Install any coated or uncoated capillary in less than two minutes.
- Exclusive sample-metering injection and ±0.5 °C temperature control assure reproducible analyses.

Our free analysis offer entails no obligation. We're glad to do it for any researcher who is seriously considering the purchase of a CE system. Contact your Isco distributor for details.

Isco Europe AG, Brüschstr. 17
CH8708 Männedorf, Switzerland
Fax: **(41-1)920 62 08**

Isco, Inc., P.O. Box 5347
Lincoln NE 68505, U.S.A.
Tel: **(800)228-4250**

ISCO

Distributors • **Australia:** Australian Chromatography Co. • **Austria:** INULA • **Belgium:** SA HVL NV • **Canada:** Canberra Packard Canada, Ltd. • **Denmark:** Mikrolab Aarhus • **Finland:** ETEK OY • **France:** Ets. Roucaire, S.A. • **Germany:** Colora Messtechnik GmbH • **Hungary:** Lasis Handelsges. mbH • **Italy:** Analytical Control Italia S.p.A. • **Japan:** JSI Co. Ltd. • **Korea:** Sang Chung, Ltd. • **The Netherlands:** Beun-de Ronde B.V. • **Norway:** Dipl. Ing. Houm A.S. • **Spain:** CHEMICONTROL, S.L. • **Sweden:** Spectrochrome AB • **Switzerland:** IG Instrumenten-Gesellschaft AG • **U.K.:** Jones Chromatography Ltd. •

Ion Chromatography

Principles and Applications

by **P.R. Haddad,** *University of New South Wales, Kensington, N.S.W., Australia and* **P.E. Jackson,** *Waters Chromatography Division, Milford, MA, USA*

(Journal of Chromatography Library, 46)

Ion chromatography (IC) was first introduced in 1975 for the determination of inorganic anions and cations and water soluble organic acids and bases. Since then, the technique has grown in usage at a phenomenal rate. The growth of IC has been accompanied by a blurring of the original definition of the technique, so that it now embraces a very wide range of separation and detection methods, many of which bear little resemblance to the initial concept of ion-exchange separation coupled with conductivity detection.

Ion Chromatography is the first book to provide a comprehensive treatise on all aspects of ion chromatography. Ion-exchange, ion-interaction, ion-exclusion and other pertinent separation modes are included, whilst the detection methods discussed include conductivity, amperometry, potentiometry, spectroscopic methods (both molecular and atomic) and post-column reactions. The theoretical background and operating principles of each separation and detection mode are discussed in detail. A unique extensive compilation of practical applications of IC (1250 literature citations) is presented in tabular form. All relevant details of each application are given to accommodate reproduction of the method in the laboratory without access to the original publication.

This truly comprehensive text on ion chromatography should prove to be the standard reference work for researchers and those involved in the use of the subject in practical situations.

1990 798 pages
Price: US$ 191.50 / Dfl. 335.00
ISBN 0-444-88232-4

Elsevier Science Publishers
P.O. Box 211, 1000 AE Amsterdam, The Netherlands
P.O. Box 882, Madison Square Station, New York, NY 10159, USA

Journal of Chromatography, 538 (1991) 233–240
Elsevier Science Publishers B.V., Amsterdam

CHROM. 22 841

Performance of an extraction disk in synthetic organic chemical analysis using gas chromatography–mass spectrometry

ANNA KRAUT-VASS* and JERRY THOMA
Environmental Health Laboratories, 110 S. Hill Street, South Bend, IN 46617 (U.S.A.)
(Received June 13th, 1990)

ABSTRACT

Forty-three semi-volatile organic compounds listed in Method 525 of the U.S. Environmental Protection Agency were investigated by gas chromatography–mass spectroscopy in order to test the applicability of the Empore™ extraction disk in water analysis. Accuracy and precision data was determined at two concentrations and compounds were identified by retention time and by comparison with the National Institute of Standards and Testing (National Bureau of Standards) computerized mass spectral library. The results indicate, that the speed of routine analysis can be increased considerably by using the extraction disk instead of extraction cartridges, with practically the same reliability. Data acquired after the completion of the initial work demonstrates that the performance for pentachlorophenol can be markedly enhanced by the use of an unpacked insert in the gas chromatography injector.

INTRODUCTION

As the concern over the quality of our water resources continues to intensify, the demand is increasing for faster and more reliable methods of detecting potentially harmful organic compounds in surface and ground waters. Using automated gas chromatography–mass spectroscopy (GC–MS) techniques a large number of samples can be analyzed per day with a high degree of reliability [1]. However, in semi-volatile analysis, the preparation and pre-concentration of the sample extracts is the time-consuming step. To avoid manipulations with large volumes of solvents, solid-phase extraction was introduced [2,3], and later proposed by the U.S. Environmental Protection Agency (EPA) in a draft method [4]. The cartridge procedure, as presented in EPA Method 525 requires multiple transfers of 10 to 75 ml sample aliquots to the cartridge or cartridge reservoir. At the recommended flow rate, the total extraction time is 2–3 h. The speed of liquid–solid extraction of the semi-volatile organic compounds from the water samples can be dramatically increased by substituting extraction disks in place of extraction cartridges [5].

In the present study we report the performance of the Empore™ extraction disk for 43 semi-volatile organic chemicals and compare the results with those published in the EPA Method 525 [4], where an extraction cartridge was applied.

0021-9673/91/$03.50

EXPERIMENTAL

Chemicals

Standards for individual compounds were prepared using analytical-grade materials (Supelco, Bellefonte, PA, U.S.A.). Standard mixtures were provided by Finnigan MAT (San Jose, CA, U.S.A.). [$^2H_{10}$]Acenaphthene, [$^2H_{10}$]phenanthrene and [$^2H_{12}$]chrysene were applied as internal standards (IS) and [$^2H_{12}$]perylene as surrogate standard (SS). The solvents (dichloromethane, ethylacetate and methanol) were high purity pesticide quality (Burdick & Jackson Labs., Muskegon, MI, U.S.A.).

Instrumentation and capillary column

A Varian (Sunnyvale, CA, U.S.A.) 3500 capillary gas chromatograph was fitted with a J&W Scientific (Folsom, CA, U.S.A.) 30 m × 0.25 mm I.D. fused-silica capillary column (DB-5.625, 0.25 μm film thickness) directly coupled to the ion trap detector. A Varian Model 8035 autosampler and a 1093 SPI injector was used during the study.

Analytical operating parameters. The final selected GC system conditions were as follows. Carrier gas: ultrapure helium (Air Products). Carrier gas flow-rate: 2.8 ml min^{-1}. Initial oven temperature: 45°C, initial hold time: 2 min; ramp rate 1: 50°C/min, oven temperature 2: 160°C; ramp rate 2: 6°C/min, oven temperature 3: 210°C; ramp rate 3: 20°C/in, oven temperature 4: 250°C; ramp rate 4: 5°C/min, oven temperature 5: 300°C, final hold time 4 min.

Mass spectrometer. A Finnigan MAT ITD 700 ion trap detector was used. Transfer line and exit nozzle were maintained at 250°C and the manifold at 220°C.

Other special equipments and materials

For the extraction Empore™ extraction disk (C_8 bonded, 47 mm diameter) was used (Analytichem International, Harbor City, CA, U.S.A.), in a 47 mm microanalysis holder (Fisher Scientific, Pittsburg, PA, U.S.A.), in a fashion similar to membrane filters.

For the concentration of the extracts a Turbo-vap evaporation apparatus (Zymark, Hopkinton, MA, U.S.A.) was used.

The chromatograms were interpreted by reference to retention indices and retention times derived from comparison with pure standard mixtures. Mass spectra were interpreted by comparison with pure standard mixtures. Mass spectra were interpreted by comparison with a NIST (NBS) computerized mass spectral library (provided by Finnigan MAT). Concentration range of calibration: 0.1–10.0 μg/l in the original 1 l water sample.

Standard procedure

Summary of the method. Organic compound analytes, internal and surrogate standards were extracted from a water sample by pulling one liter of sample through the Empore disk placed in a 300 ml glass funnel with a fritted glass base. The organic compounds were eluted with 10 ml ethylacetate followed by 10 ml methylene chloride and concentrated to 1 ml final volume. The sample components were separated, identified and measured by injecting 1–3 μl of extract into a high resolution fused silica capillary column of the GC–MS system.

Extraction. 1000 ml water sample was acidified with 2 ml 6 *M* HCl to pH < 2. A 10-μl volume of a 500 μg/ml IS–SS solution was added to the water sample. A 47 mm Empore extraction disk was placed into a fritted glass funnel and washed with 10 ml ethylacetate:dichloromethane 1:1 mixture with vacuum on. The disk was then dried with air suction for 1 min.

The vacuum system used had sufficient capacity to maintain a slight vacuum of about 13 cm (5 in.) of mercury in the vacuum flask.

First 10 ml methanol, then 10 ml organic-free water were pulled through the disk. The vacuum was released immediately after all the water has passed through the disk to prevent the disk from drying.

Immediately after this step a 1000-ml water sample was extracted, with the vacuum adjusted to yield a 20 min extraction time. Finally the disk was dried by air suction for 1 min[a].

Elution. A 50-ml test tube was placed into the suction flask. The sample bottle was rinsed with 10 ml ethyl acetate, then the solvent transferred into the funnel. Gentle vacuum was applied until the first drops of solvent passed the disk. The vacuum was then stopped to allow the elution solvent to penetrate into the disk and elute the chemicals of interest. Approximately 1 min later the vacuum was switched on again and the ethyl acetate was collected in the test tube. This step was repeated with 10 ml dichloromethane. The combined extract was dried over anhydrous sodium sulfate for a few minutes.

Evaporation. The dry extract was transferred into an evaporation flask and the volume was reduced to 0.5 ml using nitrogen flow. Then the extract was transferred into the GC autosampler vial, the evaporation flask was rinsed with a small amount of dichloromethane and this solution was added into the autosampler vial. The final volume in the vial was adjusted to 1 ml.

A 1–3-μl sample was injected into the capillary column.

RESULTS AND DISCUSSION

In Table I the 43 synthetic compounds included in this study are compiled. These compounds represent a variety in chemical structure and applications in agriculture and industry. Included are pesticides, plasticizers, additives etc. A typical standard chromatogram is shown on Fig. 1. Mean accuracy data and relative standard deviations for all 43 compounds are shown in Table II for 2.0 and 0.2 μg/l target concentrations. The results represent an average of seven replicate determinations, where the experimental conditions were kept as close to those of the Method 525 [4] as possible, except for the extraction method.

The analysis time is drastically reduced using the extraction disk as the extraction is complete within 20 min compared with the 2–3 h required for the cartridge. Despite the short contact time, the general performance of the disk competes well with that of the extraction cartridge. The mean average method accuracy[b]

---

[a] Prolonged air suction may result in losses.

[b] For the sake of comparison with the results published in Method 525, compounds 39 and 43 have been excluded from the means.

TABLE I

COMPILATION OF THE SYNTHETIC ORGANIC COMPOUNDS INVESTIGATED

Compound	Mol.wt.[a]	Chem. Abstracts Service registry number
1 Acenaphthylene	152	208-96-8
2 Alachlor	269	15972-60-8
3 Aldrin	362	309-00-2
4 Anthracene	178	120-12-7
5 Atrazine	215	1912-24-9
6 Benz[*a*]anthracene	228	56-55-3
7 Benzo[*b*]fluoranthene	252	205-82-3
8 Benzo[*k*]fluoranthene	252	207-08-9
9 Benzo[*a*]pyrene	252	50-32-8
10 Benzo[*g,h,i*]perylene	276	191-24-2
11 Butylbenzyl phthalate	312	85-68-7
12 α-Chlordane	406	5103-71-9
13 γ-Chlordane	406	5103-72-2
14 *trans*-Nonachlor	440	39765-80-5
15 Chrysene	228	218-01-9
16 Dibenz[*a,h*]anthracene	278	53-70-3
17 Di-*n*-butyl phthalate	278	84-72-2
18 Diethyl phthalate	222	84-66-2
19 Di(2-ethylhexyl) phthalate	390	177-81-7
20 Di(2-ethylhexyl) adipate	370	103-23-1
21 Dimethyl phthalate	194	131-11-3
22 Endrin	378	72-20-8
23 Fluorene	166	86-73-7
24 Heptachlor	370	76-44-8
25 Heptachlor epoxide	386	1024-57-3
26 Hexachlorobenzene	282	118-74-1
27 Hexachlorocyclopentadiene	270	77-47-7
28 Indeno[1,2,3,*c,d*]pyrene	276	193-39-5
29 Lindane	288	58-89-9
30 Methoxychlor	344	72-43-5
31 2-Chlorobiphenyl	188	2051-607
32 2,3-Dichlorobiphenyl	222	16605-91-7
33 2,4,5-Trichlorobiphenyl	256	15862-07-4
34 2,2′,4,4′-Tetrachlorobiphenyl	290	2437-79-8
35 2,2′,3′,4,6-Pentachlorobiphenyl	324	60233-25-2
36 2,2′,4,4′,5,6′-Hexachlorobiphenyl	358	60145-22-4
37 2,2′,3,3′,4,4′,6-Heptachlorobiphenyl	392	52663-71-8
38 2,2′,3,3′,4,5′,6,6′-Octachloribiphenyl	426	40186-71-8
39 Pentachlorophenol	264	87-865
40 Phenanthrene	178	85-01-8
41 Pyrene	202	129-00-0
42 Simazine	201	122-34-9
43 Toxaphene mixture		8001-35-2

[a] Monoisotopic molecular weight (mol.wt.) calculated from the atomic masses of the isotopes with the smallest masses.

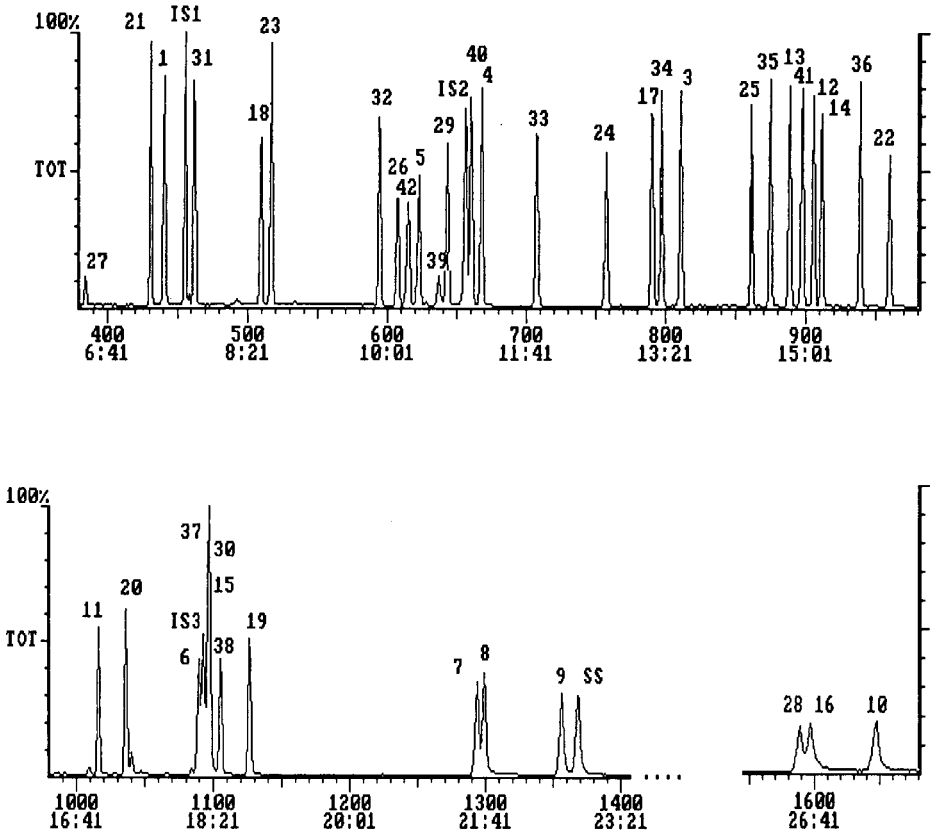

Fig. 1. A typical total ion chromatogram of the compounds investigated (except compound 2). Direct injection of 3 μl of a 5 ng/μl solution (20 ng/μl for pentachlorophenol). For other experimental conditions see text. Horizontal scales: scan No. (top) and time in min:s (bottom).

(concentration determined as a % of the true concentration) for the 43 compounds at 2.0 and 0.2 μg/l target concentration is 108 and 103% respectively, compared with the 91 and 95% of the cartridge method [4]. The average relative standard deviation in our measurements is 15 and 33% for the high and low concentration range respectively. The experiments with cartridge extraction [4] gave 15 and 25%. These figures indicate that the disk is more sensitive for the concentration of the compounds investigated. As we go from 2 μg/l target concentration to 0.2 μg/l, the number of compounds with relative standard deviations higher than 10% increaseses from 14 to 37. In the case of the extraction cartridge these figures are 25 and 33, respectively. The number of cases, where the systematic error is higher than 50% increases from 3 to 16; for the cartridge these values are 4 and 9. Our results with packed extraction columns [6] support the observation, that the cartridge generally performs better in the low concentration range than the disk.

The results presented here apply for the C_8 bonded disk. Results for a C_{18} disk under the same experimental conditions were very close to those with the C_8 bonded

TABLE II

ACCURACY AND PRECISION DATA (%) FROM SEVEN DETERMINATIONS FOR THE 43 COMPOUNDS INVESTIGATED

R.S.D. = Relative standard deviation.

Compound number	True concentration (μg/l)			
	2.0[a]		0.2[b]	
	R.S.D.	Mean accuracy	R.S.D.	Mean accuracy
1	4.8	116	19.5	58
2	6.8	103	9.0	103
3	5.7	114	13.5	99
4	3.4	118	13.1	46
5	11.9	139	8.2	129
6	2.6	103	30.0	39
7	8.5	93	18.6	81
8	10.4	97	39.8	61
9	4.4	111	18.8	51
10	2.9	111	20.3	68
11	6.1	109	52.4	242
12	49.5	82	55.8	68
13	31.4	82	27.3	85
14	23.8	18	139.8	37
15	6.2	96	27.5	40
16	3.5	114	24.8	62
17	7.3	149	37.2	519
18	5.8	134	46.7	167
19	14.1	133	22.8	372
20	4.7	108	17.0	161
21	7.1	117	11.9	123
22	10.0	126	34.5	128
23	8.1	114	15.8	51
24	3.2	116	8.4	131
25	11.4	122	11.4	141
26	52.5	60	120.1	27
27	18.9	131	23.0	98
28	6.8	93	67.6	19
29	12.4	113	11.7	122
30	6.1	95	24.6	48
31	8.3	112	10.9	78
32	10.5	125	8.2	101
33	7.0	108	12.7	90
34	8.1	144	11.6	97
35	9.6	118	16.3	106
36	9.5	131	27.9	95
37	134.5	15	134.7	30
38	52.5	102	90.9	45
39	15.1	132	68.0	773
40	6.2	113	14.3	51
41	4.9	119	31.6	41
42	6.5	112	9.8	110
43	6.6	304	–	–

[a] For compounds 39 and 43 the real concentrations were 12 and 37.5 μg/l, respectively.
[b] For compound 39 the real concentration was 0.8 μg/l.

disk. The average mean acuracy with C_{18} disk is slightly worse but the mean standard deviation is smaller in the low concentration range than the values presented above for the C_8 bonded disk. It should be noted, however, that in the case of the C_{18} bonded disk the extraction time was only 10 min, and 2 × 5 ml eluent was used.

Besides the differences mentioned above, the "problem compounds" are slightly different for the two kinds of liquid–solid extraction. In the case of the extraction

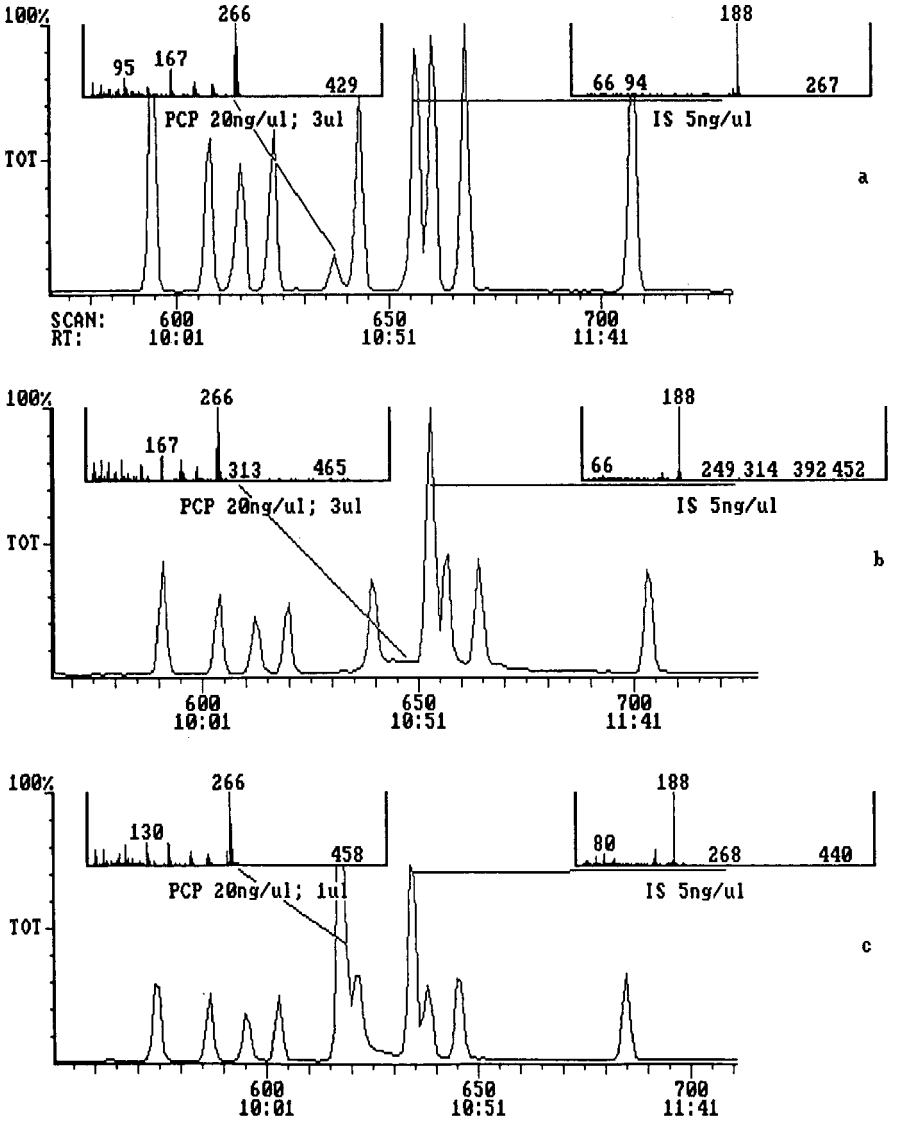

Fig. 2. Effect of the insert packing on the separation and detection limit for pentachlorophenol (PCP), direct injection. (a) Lightly packed insert, new DB-5.625 column, 60 ng PCP. (b) Tightly packed insert, six months old column, 60 ng PCP. (c) Unpacked high-performance insert, six months old column, 20 ng PCP.

cartridge some polycyclic aromatic compound have relatively low recovery, while the disk gave better results both in accuracy and precision (*e.g.* compounds 6, 10, 16, 28). The systematic error for phthalate esters and similar plasticizers is high due to the high and mostly uncontrollable background concentration.

Pentachlorophenol is problematic in both cases, the disk performance is especially poor in the low concentration range.

Despite the general recommendations, our results indicate, that for this compound an unpacked insert in the GC injector is more satisfactory, as shown in Fig. 2. Compared with an average glass wool packing (Fig. 2a), a tightly packed insert results in a broad, nearly undetectable pentachlorophenol peak (Fig. 2b). In the latter case the quantitation ion can be found everywhere in the 630–675 scan number range (10:30–11:20 retention time). This makes the quantitative analysis unreliable. The adsorption on the glass wool packing can be avoided by using a high performance unpacked insert (Varian), Fig. 2c, in this case 1 μl injection is enough. (Due to the ageing of the column and the corresponding changes in the column length, the retention times are slightly different on the chromatograms. There are differences in the concentration of the other compounds as well, but these parameters hardly affect the separation). It is also worth noting, that in some cases solid particles in the water sample can plug the pores of the disk. To avoid this a pre-filtration step may be necessary. However, potential losses of extraction efficiency must be investigated.

CONCLUSION

The results presented here demonstrate that the speed of routine analysis and consequently the productivity of a testing laboratory can be increased considerably by using extraction disks in place of packed columns with practically the same reliability under normal conditions. The applicability of the extraction disk for extremely low target concentrations is subject to further investigation.

ACKNOWLEDGEMENTS

The research described here was supported in part by Finnigan MAT. We also thank the 3M Co. for providing the Empore disks used during this investigation.

REFERENCES

1 P. MacCarthy, R. W. Klusman and J. A. Rice, *Anal. Chem.*, 61 (1989) 269R; and references cited therein.
2 L. Renberg and K. Lindstrom, *J. Chromatogr.*, 214 (1981) 327.
3 C. E. Rostad, W. E. Pereira and S. M. Ratcliff, *Anal. Chem.*, 56 (1984) 2856.
4 *Method 525: Revision 2.1*, U.S. Environmental Protection Agency, Environmental Monitoring System Laboratory, Cincinnati, OH, 1988.
5 D. F. Hagen, C. G. Markell and G. A. Schmitt, personal communication.
6 A. Kraut-Vass and J. Thoma, unpublished results.

Journal of Chromatography, 538 (1991) 241–248
Elsevier Science Publishers B.V., Amsterdam

CHROM. 22 785

Solubility of gasoline components in different lubricants for combustion engines determined by gas–liquid partition chromatography

JESPER SCHRAMM and SPENCER C. SORENSON*
Laboratory for Energetics, Technical University of Denmark, Lyngby (Denmark)
(First received April 3rd, 1990; revised manuscript received August 31st, 1990)

ABSTRACT

The solubility of typical gasoline fuel components in different lubricants for gasoline engines was determined at temperatures between 90 and 150°C. Solubility is an important parameter in combustion engine research, as the fuel during intake and compression dissolves in the lubricant film on the cylinder wall, thus escaping from the combustion processes. During the expansion and exhaust stroke the fuel is desorbed again and in this way contributes to the formation of unburned hydrocarbons in the exhaust gas. The solubility is characterized by Henry's constant. A gas–liquid partition chromatographic technique was used for the determination of Henry's constants, and gave values in good agreement with the known values for selected reference components.

INTRODUCTION

Hydrocarbon emissions from passenger cars constitute a serious environmental problem. The presence of unburned hydrocarbons in the exhaust gas from gasoline vehicles is partly due to the fact that the fuel dissolves in the lubricant film on the cylinder wall during intake and compression. Later, during the expansion and exhaust strokes, the fuel is desorbed at a time where the cylinder temperature is too low for total oxidation of the desorbed fuel, and part of the fuel is thus exhausted unburned to the environment.

There is therefore a need for more insight into the absorption/desorption phenomena, including information about the solubility of fuel components in the lubricant. Henry's constant describes the relationship between the fuel concentration in the gas phase and the concentration in the lubricant film and is therefore a measure of the solubility. From an automotive engineer's point of view, it would be advantageous to be able to select lubricans and fuels with favourable solubility characteristics in order to reduce emissions. For this study a broad range of fuel components and lubricants were selected in order to measure Henry's constant. Gas–liquid partition chromatography (GLC) was chosen as the experimental method, as this is a rapid and well documented method for this purpose [1,2].

0021-9673/91/$03.50

EXPERIMENTAL

The lubricant in question was coated on Celite 545 (80–100 mesh). The coating was carried out by dissolving the support material and the lubricant in an ether. The ether was then removed by heating until only the coated material was left. The material was packed in a 1 m × 1/8 in I.D. glass column and conditioned for 24 h at 150°C. A level of 10% (w/w) of coating material was used, as 10–15% was recommended by Sugiyama *et al.* [1].

The gas chromatograph used was a Shimadzu GC 9A equipped with a thermal conductivity detector. Helium was used as the carrier gas at a flow-rate of *ca.* 25 ml/min. According to Sugiyama *et al.* [1], the influence of carrier gas flow-rate on the specific retention volume is very small. The column temperature was held constant in each experiment. The amount of fuel injected was a small as possible to ensure that Henry's law holds.

THEORY

Henry's law can be written in the following way:

$$p_2 = HX_2 \tag{1}$$

where p_2 is the partial pressure of the fuel in the gas phase, H is Henry's constant and X_2 is the molar concentration of the fuel in the liquid phase.

Henry's constant for the fuel dissolved in the lubricant can be derived from the specific retention volume according to the following equation (see, *e.g.*, Sugiyama *et al.* [1], Schramm [3] and Schramm and Sorenson [4]):

$$H = \frac{RT}{V_R' M_1} \tag{2}$$

where R is the gas constant, T the column temperature, V_R' the specific retention volume and M_1 the molar weight of the lubricant. As the molar weight of the lubricant can only be approximated and in some practical situations is unknown, it is more convenient to express the solubility as another constant, H^*, which is proportional to H according to

$$H^* = \frac{M_1}{M_2} \cdot H \tag{3}$$

where M_2 is the molar weight of the fuel component. The meaning of H^* can be seen by rewriting eqn. 1 in the following way:

$$p_2 = HX_2 = H \cdot \frac{n_2}{n_1 + n_2} \approx H \cdot \frac{n_2}{n_1}$$

$$= H \cdot \frac{m_2/M_2}{m_1/M_1}$$

$$= H^* \cdot \frac{m_2}{m_1}$$

$$= H^* Y_2 \tag{4}$$

where n_1 is the number of moles of lubricant in the liquid phase, n_2 the number of moles of fuel component in the liquid phase, m_1 the mass of lubricant in the liquid phase, m_2 the mass of fuel component in the liquid phase and Y_2 the mass concentration of fuel component in the liquid phase.

By introducing H^* instead of H, eqn. 2 can be rewritten as

$$H^* = \frac{RT}{V_R M_2} \tag{5}$$

where M_2 is known exactly for pure hydrocarbons.

RESULTS

Henry's constants were measured at 90, 110, 130 and 150°C, as this covers the normal range for the oil-film temperature in gasoline engines. The lubricants chosen for investigation were two crude oil-based lubricants, two partly synthetic lubricants and two fully synthetic lubricants. Data for the lubricants are given in Table I. The following fuel components were tested:

paraffins: *n*-hexane, *n*-heptane, isooctane (2,2,4-trimethylpentane), cyclohexane;

olefins: 2-methyl-2-butene, trimethylpentene;

aromatics: benzene, toluene, *o*-, *m*- and *p*-xylene, ethylbenzene, *n*-propylbenzene, isopropylbenzene, trimethylbenzene;

ethers: methyl *tert.*-butyl ether (MTB).

TABLE I

PROPERTIES OF LUBRICANTS

Property	Lubricant					
	A	B	C	D	E	F
Molecular weight	425	550	550	500	–	–
Density (kg/m^3) at 15°C	870	864	961	881	874	884
Viscosity (cSt) at 40°C	82.8	107	81.5	95.5	91.4	121.7
Viscosity (cSt) at 100°C	12.0	18.1	13.7	14.3	13.9	17.0
SAE classification	10W–30	5W–50	10W–40	10W–40	10W–40	15W–50
Base oil composition						
Synthetic-based (%)	40[a]	100[a]	100[b]	0	30[a]	0
Crude oil-based (%)	60	0	0	100	70	100

[a] Based on poly(α-olefin).

[b] Based on polyol ester.

TABLE II

Lubricant	Temperature (°C)	Fuel component					
		Methyl-*tert.*-butyl-ether	2-Methyl-2-butene	Trimethyl-pentene	Cyclo-hexane	*n*-Hexane	*n*-Heptane
A	90	796	1401	188	343	597	248
	110	1114	1642	304	551	772	385
	130	1302	–	478	745	–	554
	150	1521	2655	604	926	1366	724
B	90	730	1119	177	334	514	233
	110	1060	1333	299	484	723	355
	130	1138	–	388	645	900	468
	150	1527	2065	529	823	1206	745
C	90	1011	1817	257	487	893	365
	110	1112	2006	434	715	1065	554
	130	–	3340	658	1146	–	1009
	150	1987	5433	1053	1484	1512	1506
D	90	1161	1506	191	355	610	244
	110	1237	1968	325	578	–	414
	130	1400	2135	447	737	1060	575
	150	2584	2982	635	1083	1496	781
E	90	767	–	–	–	–	–
	110	982	–	–	–	–	–
	130	1498	–	–	–	–	–
	150	1502	–	–	–	–	–
F	90	672	–	–	–	–	–
	110	1121	–	–	–	–	–
	130	1465	–	–	–	–	–
	150	2188	–	–	–	–	–

MTB was chosen because it is commonly added to unleaded gasoline to increase the octane number.

Henry's constants, H^*, calculated from eqn. 5 are given in Table II. H^* is shown as a curve for isooctane and *m*-xylene in Figs. 1 and 2 to give a clearer impression of the temperature dependence.

It can be seen that H^* generally increases with increasing temperature. The increase in most instances is almost proportional to the temperature although some curves have a tendency to approach a potential function:

$$H^* = aT^b + c \tag{6}$$

where b is slightly larger than 1. This tendency is most pronounced for lubricant C.

Some general features of the lubricants' influence on solubility can be seen. The differences in H^* values are generally small from one lubricant to another, except for lubricant C. The differences seem to increase with increasing temperature. Lubricant

Iso-octane	Benzene	Toluene	*o*-Xylene	*m*-Xylene	*p*-Xylene	Ethyl-benzene	*n*-Propyl benzene	Isopropyl-benzene	Trimethyl-benzene
222	411	160	52	61	62	68	31	39	24
343	596	264	95	108	111	124	58	72	47
498	957	381	156	179	187	197	102	125	82
700	1124	537	235	271	270	287	160	186	135
211	388	148	50	59	61	67	30	38	24
315	549	239	88	105	105	118	56	70	45
446	–	341	141	163	157	193	94	108	76
551	971	482	205	238	241	252	143	162	119
335	385	153	51	61	62	68	30	40	–
476	567	250	92	110	111	123	60	74	49
769	1124	452	181	212	229	238	127	148	103
1034	1524	638	300	321	320	342	207	234	161
299	429	160	51	60	61	69	31	39	24
363	677	270	92	108	111	121	57	72	46
507	807	388	150	175	179	192	101	117	80
853	1227	572	250	274	277	294	166	193	135
220	400	154	–	–	–	–	–	–	–
323	599	250	–	–	–	–	–	–	–
464	815	386	–	–	–	–	–	–	–
609	1070	525	–	–	–	–	–	–	–
211	371	145	–	–	–	–	–	–	–
321	587	258	–	–	–	–	–	–	–
477	920	384	–	–	–	–	–	–	–
659	1082	563	–	–	–	–	–	–	–

C shows the highest H^* value in almost every instance, the only exceptions being with MTB, benzene and toluene. For all the paraffins and olefins tested the performance of lubricant C is considerably different. This is obviously due to the special structure of lubricant C, which is a fully synthetic lubricant with a polyol ester structure. As an ester is a much more polar compound than paraffins and olefins it will not dissolve these components as easily as the other lubricants that mainly consist of paraffins and olefins.

From Figs. 1 and 2 it can also be seen that lubricant B in every instance gives the lowest H^* value although the deviations from the other lubricants are smaller than with lubricant C.

The measurements have thus show that the fully synthetic lubricants B and C lie in the outer sections of the observed H^* range. This indicates that the use of more specialized (synthetic) lubricants results in solubility behaviour that is substantially different from that of typical crude oil-based lubricants. This could be important in efforts to reduce hydrocarbon emissions from gasoline engines, as the use of synthetic

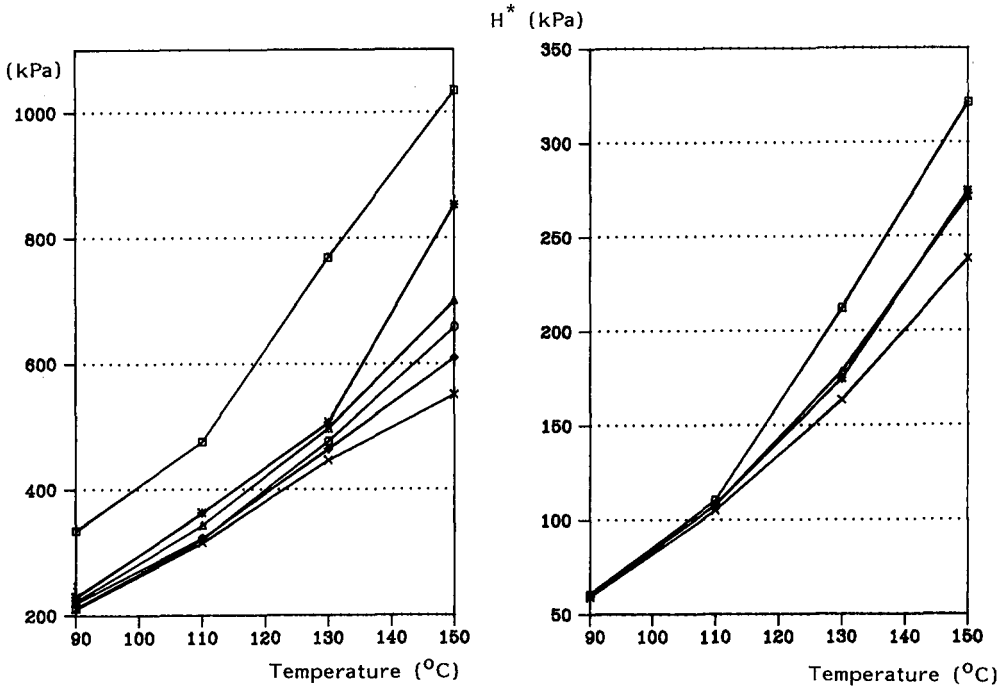

Fig. 1. H^* as a function of temperature for isooctane in equilibrium with six different oils: △ = oil A; × = oil B; □ = oil C; * = oil D; ◇ = oil E; ○ = oil F.

Fig. 2. H^* as a function of temperature for *m*-xylene in equilibrium with four different oils: △ = Oil A; × = oil B; □ = oil C; * = oil D.

lubricants with very high H^* values would reduce the amount of fuel dissolved in the lubricant film, and therefore the amount of unburned hydrocarbons found in the exhaust gas.

In Table III the observed H^* values for *n*-hexane and *n*-heptane are compared with results of other workers. Sugiyama *et al.* [1] measured the solubility of *n*-hexane and *n*-heptane in C_{28}–C_{36} *n*-alkane solvents, while Dent and Lakshminarayanan [5] suggested an extrapolation method for calculating the Henry's constant of *n*-alkanes in squalane ($C_{30}H_{62}$), based on measurements of Henry's constants for methane, ethane, propane and *n*-butane in squalane from Chappelow and Prausnitz [6]. The values of H^*, calculated by this method, are given in Table III. As the number of carbon atoms found in lubricant molecules is of the same magnitude as that for squalane, this is an acceptable comparison.

The H^* values for the lubricants (except lubricant C) are very close to the values obtained by other workers at 90°C. At 150°C the values of Dent and Lakshminarayanan [5] are slightly different from those found in this investigation, but this is probably caused by the uncertainty connected with the calculation method that they proposed.

Table IV gives the H^* values for the different categories of fuel components arranged according to increasing number of carbon atoms. The results showed, as

TABLE III

*H** VALUES (kPa) FOR *n*-HEXANE AND *n*-HEPTANE DISSOLVED IN DIFFERENT SOLVENTS

Alkane	Temperature (°C)	This study: lubricant				Sugiyama *et al.* [1]			Dent and Laksh-minarayanan [5]: $C_{30}H_{62}$
		A	B	C	D	$C_{28}H_{58}$	$C_{32}H_{66}$	$C_{36}H_{74}$	
n-Heptane	78	–	–	–	–	146	157	168	–
	84	–	–	–	–	178	192	206	–
	90	250	230	365	240	216	232	250	244
	96	–	–	–	–	260	281	301	–
	102	–	–	–	–	313	338	360	–
	110	377	353	553	414	–	–	–	346
	130	553	465	1009	577	–	–	–	462
	150	716	744	1507	781	–	–	–	599
n-Hexane	78	–	–	–	–	369	429	454	–
	84	–	–	–	–	468	507	540	–
	90	596	515	900	615	553	598	638	696
	96	–	–	–	–	652	705	752	–
	102	–	–	–	–	768	829	883	–
	110	774	726	1074	841	–	–	–	895
	130	1222	907	1300	1070	–	–	–	1243
	150	1374	1215	1526	1507	–	–	–	1740

expected, that the solubility increases with increasing number of carbon atoms. It can also be seen that aromatic compounds are more soluble than the corresponding paraffins and olefins with the same carbon number. An exception is cyclohexane, which is more soluble than both *n*-hexane and benzene.

n-Heptane is almost as soluble as isooctane, which indicates that a more branched structure results in a lower solubility.

CONCLUSIONS

These experiments have shown that GLC is suitable for determining Henry's constants for fuel components dissolved in lubricants for gasoline engines. This was verified by comparing the results with those given by other workers.

Most of the lubricants investigated gave Henry's constants that did not differ very much at lower temperatures (90°C). At higher temperatures (150°C), the differences were slightly larger. It was remarkable that of the two synthetic lubricants tested, one gave the highest and the other the lowest solubilities of all the oils tested. Henry's constant generally increased in proportion to the temperature.

The results showed, as expected, that the solubility increased with increasing carbon number of the fuel component. Aromatic components were more soluble in the

TABLE IV

H^* VALUES (kPa) ACCORDING TO MOLECULAR STRUCTURE OF THE FUEL COMPONENTS AND ARRANGED IN ORDER OF INCREASING CARBON NUMBER

Compound	Lubricant							
	90°C				150°C			
	A	B	C	D	A	B	C	D
Ether								
MTB	796	730	1011	1161	1521	1527	1987	2584
Olefins								
2-Methyl-2-butene	1401	1119	1817	1506	2655	2065	5433	2982
Trimethylpentene	188	177	257	191	604	529	1053	635
Paraffins								
Cyclohexane	343	334	487	355	926	823	1484	1083
n-Hexane	597	514	893	610	1366	1206	1512	1496
n-Heptane	248	233	365	244	724	745	1506	781
Isooctane	222	211	335	229	700	551	1034	853
Aromatics								
Benzene	411	388	385	429	1124	971	1524	1227
Toluene	160	148	153	160	537	482	638	572
o-Xylene	52	50	51	51	235	205	300	250
m-Xylene	61	59	61	60	271	238	321	274
p-Xylene	62	61	62	61	270	241	320	277
Ethylbenzene	68	67	68	69	287	252	342	294
n-Propylbenzene	31	30	30	31	160	143	207	166
Isopropylbenzene	39	38	40	39	186	162	234	193
Trimethylbenzene	24	24	24	24	135	119	161	135

lubricants than the corresponding paraffins and olefins with the same carbon number. Cyclic paraffins such as cyclohexane are an exception, as cyclohexane was more soluble than benzene.

REFERENCES

1 T. Sugiyama, T. Takeuchi and Y. Suzuki, *J. Chromatogr.*, 105 (1975) 265–272.
2 G. V. Filonenko and N. Korol, *J. Chromatogr.*, 119 (1976) 157–166.
3 J. Schramm, *Ph.D. Thesis*, Technical University of Denmark, Laboratory for Energetics, 1990 (in Danish).
4 J. Schramm and S. C. Sorenson, paper presented at the SAE International Congress and Exposition, Detroit, MI, 1989, paper 890622.
5 J. C. Dent and P. A. Lakshminarayanan, paper presented at the *SAE International Congress and Exposition, Detroit, MI, 1983*, paper 830652.
6 C. C. Chappelow and J. M. Prausnitz, *AIChE J.*, 20 (1974) 1097–1104.

Journal of Chromatography, 538 (1991) 249–257
Elsevier Science Publishers B.V., Amsterdam

CHROM. 22 859

Retention index monitoring of compounds of chemical defence interest using thermal desorption gas chromatography

JAMES R. HANCOCK*
Defence Research Establishment Suffield, Box 4000, Medicine Hat, Alberta T1A 8K6 (Canada)
and
GREGORY R. PETERS
Department of Chemistry, Queens University, Kingston, Ontario K7L 3N6 (Canada)
(First received June 19th, 1990; revised manuscript received October 3rd, 1990)

ABSTRACT

Retention index monitoring using thermal desorption gas chromatographic analysis was developed as a method for the verification of compounds of chemical defence interest in environmental matrices. Gas chromatography retention indices were determined by loading solid adsorbent packed sampling tubes initially with the target compounds and subsequently with a series of *n*-alkane probes. The resulting chromatographic performance and gas chromatography retention indices were shown to be independent of the tube loading method. A database of gas chromatography retention indices for chemical warfare agents and simulants was compiled and, in conjunction with simultaneous flame ionization and flame photometric detection, applied to the identification of triethyl phosphate, tributyl phosphate and diethyl malonate in water and soil samples.

INTRODUCTION

Sampling tubes packed with solid adsorbents are routinely used to sample organic compounds from a variety of matrices [1–7]. Analyte vapour, drawn through the sampling tube and concentrated by selective adsorption, may then be desorbed from the adsorbent by one of two methods: (i) thermal desorption, where the compounds are volatilized and swept from the adsorbent or (ii) solvent desorption where the analytes are extracted with a suitable solvent. When coupled to a gas chromatograph, thermal desorption offers greater sensitivity as all the analyte, on the adsorbent, may be introduced directly onto the column for analysis. Thermal desorption gas chromatographic (TD–GC) techniques typically only allow one analysis per tube, making it necessary to maximize the information from each GC analysis. GC retention index monitoring coupled with single or multiple detectors is an effective method for the tentative identification of analytes, when the retention index of the analyte has been determined prior to analysis. While this method is an effective

0021-9673/91/$03.50

screening procedure, confirmation of the identity of a detected analyte must be based on a technique like gas chromatography–mass spectrometry.

Standardization of GC retention information by determining retention indices relative to a homologous series of chemical probes was first proposed by Kováts in 1958 [8]. Samples are typically spiked with a mixture of probes (usually a series of *n*-alkanes) and the retention index for the component of interest calculated relative to the retention times of the neighbouring probes. This technique, initially designed for isothermal analysis, was subsequently refined for temperature programming, thus enabling the analysis of compounds of varying volatility in a single analysis [9]. Temperature programmed GC retention indices were calculated using Van den Dool's equation:

$$I_c = 100n\left[\frac{t_{R(c)} - t_{R(z)}}{t_{R(z+n)} - t_{R(z)}}\right] + 100z$$

where: c is the compound of interest, n is the difference in carbon number between the two *n*-akanes either side of the compound of interest, t_R is the retention time, z is the carbon number of the *n*-alkane immediately prior to compound c, and I_c is the GC retention index of compound c.

GC retention information in the form of GC retention indices have been reviewed recently [10,11] and databases for numerous classes of chemical compounds have been published. Generally GC retention indices for compounds of defence interest have been reported relative to *n*-alkanes [12–15] and recently relative to a series of alkyl bis(trifluoromethyl)phosphine sulphides [16,17]. Although given consideration as a technique for chemical warfare (CW) verification [18], application of retention indices during thermal desorption gas chromatography appears to be unique. The Defence Research Establishment Suffield (DRES) has developed the Minitube Air Sampling System (MASS), an integrated sampling and analysis system based on miniature solid adsorbent packed sampling tubes (minitubes) and TD–GC analysis [19]. This paper reports the use of GC retention index monitoring in conjunction with TD–GC for the analysis of compounds of chemical defence interest found on schedule [1] of the Annex to Article VI of the developing United Nations Chemical Weapons Convention (CWC). A database of GC retention indices of CW agents as well as some common simulants was created using four fused silica capillary columns of varying polarity. Application of TD–GC retention index monitoring in a verification role for the identification of analytes by headspace and purge and trap techniques was demonstrated using spiked environmental samples.

EXPERIMENTAL

Materials

Minitubes were constructed of borosilicate glass tubes 38 mm × 2 mm I.D. and packed with 15 mg of Tenax TA (Chrompack, Blenheim, Canada). A standard solution of *n*-alkane probes (200 ng/μl each), C_7–C_{20} and C_{22}–C_{32} (even numbers only), was prepared from individual standards (Alltech, Deerfield, IL, U.S.A.) in glass distilled hexane (BDH, Toronto, Canada).

The chemical warfare agents, their degradation products and methyl salicylate

were obtained from the DRES Organic Chemistry Laboratory. Dimethyl sulphoxide, diethyl malonate and glass-distilled acetone were purchased from BDH. Triethyl phosphate and tributyl phosphate were obtained from Fisher Scientific (Fair Lawn, NJ, U.S.A.).

Sample handling

A vapourizing unit was constructed from a GC injection port that had been modified to allow external temperature control and insertion of a minitube. The minitube was positioned at the outlet of the injector in order to minimize heat transfer to the tube during loading. Target compounds and retention index probes were injected into the vapourizing unit with a 10-μl syringe. A one minute transfer time from the injector to minitube, at a nitrogen flow rate of 75 ml/min, was used for each sample.

Air sampling was performed in a sealed plexiglass vapour chamber approximately 0.75 m^3 in volume. A 5-μl volume of the compound to be analyzed was placed in a heated glass dish and allowed to vapourize for 3 min while the air in the chamber was circulated using an electric fan. Air was then drawn through the minitube for 1.5 min at 50 ml/min. The retention index probes were subsequently loaded on the minitube using the vapourizing unit described above.

A 2-ml water sample spiked with 20 μg/ml triethyl phosphate was purged with nitrogen (75 ml/min) for 30 min and the volatilized analytes were trapped on a minitube. *N*-Alkane probes were then added and the minitube analyzed by TD–GC with simultaneous flame ionization (FID)–flame photometric (FPD) detection.

A 5-g sample of soil spiked with 4 μg/g diethyl malonate and 1 μg/g tributyl phosphate was warmed slightly for 5 min. A minitube was then held approximately 2–5 mm above the soil and the headspace air (100 ml) was drawn through the minitube using a syringe. *n*-Alkane probes were then added to the minitube using the vapourizing unit and analyzed by TD–GC with simultaneous FID–FPD monitoring. The spiked soil was also extracted with acetone (5 ml) for 15 min in an ultrasonic bath and an aliquot of this solution (1 μl) was loaded onto a minitube to verify the presence of these compounds.

Instrumental

GC analyses were performed with a HP 5890 (Hewlett-Packard, Avondale, PA, U.S.A.) gas chromatograph equipped for simultaneous FID and FPD detection. Four different megabore (15 m × 0.53 mm I.D.) fused-silica columns, DB-1, DB-5, DB-1701 and DBWAX (J&W Scientific, Rancho Cordova, CA, U.S.A.), were used for GC retention index monitoring. Each column was held at 50°C for 2 min followed by a ramp of 10°C/min to the upper temperature limit of the column. Minitubes loaded with analytes were desorbed on an automated thermal desorption unit (ATDU) at 240°C for 5 min. High-purity helium (Liquid Carbonic, Scarborough, Canada) was used as the carrier gas at a flow-rate of 6 ml/min. Five chromatographic analyses were carried out for each analyte on each column to determine GC retention index reproducibility. Data acquisition and handling were performed with a Nelson Analytical Model 6000 data system.

RESULTS AND DISCUSSION

Method validation

Minitubes were loaded using the vapourizing unit, as this method of loading followed by TD–GC analysis has been shown to produce chromatographic performance equivalent to traditional syringe injection techniques [19]. The *n*-alkane probes were then loaded onto the same minitube and the minitube analyzed by TD–GC. In order to validate the subsequent loading of minitubes with the *n*-alkanes, it was necessary to demonstrate that: (i) the secondary loading of the probes did not degrade chromatographic performance and (ii) that loading using the GC injector produced the same retention indices as actual vapour sampling. Fig. 1 illustrates the TD–GC analysis of a minitube that had been initially loaded with soman, triethyl phosphate, mustard, and methyl salicylate and subsequently loaded with the C_{10}–C_{12} *n*-alkane probes. It was evident from the chromatogram that subsequent loading of the probes did not affect the chromatographic resolution of the system. Peak shape and resolution were equivalent to syringe injection and previously published TD–GC data [19].

To demonstrate that retention indices obtained with the vapourizing loader were equivalent to those obtained by air sampling, a series of experiments were conducted with five simulants vapourized in a sealed chamber and the vapour collected under vapour sampling conditions. Table I lists the GC retention indices by both methods

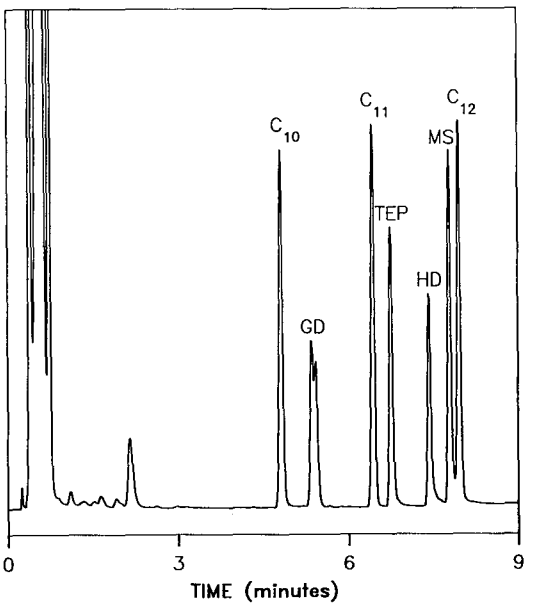

Fig. 1. TD–GC–FID chromatogram of soman (GD), triethyl phosphate (TEP), mustard (HD), methyl salicylate (MS) and C_{10}–C_{12} *n*-alkanes. Probes were added to minitube subsequent to initial loading analytes. Column conditions: 15 m × 0.53 mm I.D. DB-5, helium flow-rate of 6 ml/min, temperature program of 50°C (2 min), 10°C/min to 120°C. Desorption conditions: desorption temperature, 240°C and cycle time, 5 min.

TABLE I

COMPARISON OF RETENTION INDICES FROM VAPOUR SAMPLING AND DIRECT LOADING

Compound	Retention index (mean ± S.D., $n=5$)	
	Direct loading	Vapour chamber
Dimethyl sulphoxide	820.1 ± 0.4	820.5 ± 0.6
Diethyl malonate	1069.2 ± 0.1	1069.2 ± 0.1
Triethyl phosphate	1120.5 ± 0.2	1121.3 ± 0.2
Methyl salicylate	1188.8 ± 0.1	1188.6 ± 0.2
Tributyl phosphate	1647.4 ± 0.1	1647.9 ± 0.2

and clearly illustrates that the retention indices were independent of the loading method.

Compound database

Table II lists the GC retention indices calculated for fourteen compounds on four fused silica capillary columns of varying polarity using the HP 5890 GC. Sesquimustard [(2-chloroethylthio)ethyl 2-chloroethyl sulphide] and bis[(2-chloroethylthio)ethyl] ether were not included for the DBWAX column as they were not eluted by the upper temperature limit of that column. Error estimates for the indices were based on the standard deviation from five replicate analyses. The results obtained

TABLE II

GC RETENTION INDICES OF CHEMICAL DEFENCE RELATED COMPOUNDS

Compound	Retention index (mean ± S.D., $n=5$)			
	DB-1	DB-5	DB-1701	DBWAX
Nerve agents				
Sarin	789.1 ± 0.1	817.0 ± 0.4	954.5 ± 0.3	1296.6 ± 0.1
Soman	1011.6 ± 0.1	1038.0 ± 0.1	1178.7 ± 0.1	1478.4 ± 0.3
	1016.0 ± 0.1	1042.4 ± 0.1	1184.6 ± 0.1	1489.6 ± 0.3
Vesicants (and related impurities)				
1,4-Thioxane	856.8 ± 0.3	884.5 ± 0.1	966.8 ± 0.1	1333.8 ± 0.1
1,4-Dithiane	1027.5 ± 0.2	1067.7 ± 0.1	1163.5 ± 0.1	1611.6 ± 0.1
Mustard	1136.2 ± 0.1	1175.5 ± 0.1	1327.9 ± 0.3	1846.2 ± 0.4
Bis (2-chloroethyl) disulphide	1344.9 ± 0.2	1402.7 ± 0.1	1566.0 ± 0.1	2165.9 ± 0.1
2-Chloroethyl (2-chloroethoxy) ethyl sulphide	1426.0 ± 0.9	1476.0 ± 0.1	1659.4 ± 0.1	2274.2 ± 0.1
Sesquimustard	1632.0 ± 1	1694.0 ± 0.1	1923.1 ± 0.1	
Bis[(2-chloroethylthio)ethyl]ether	1921.0 ± 2	1987.8 ± 0.2	2240.7 ± 0.2	
Simulants				
Dimethyl sulphoxide	781.9 ± 0.3	829.2 ± 0.5	1043.1 ± 0.1	1506.7 ± 0.5
Diethyl malonate	1038.2 ± 0.1	1068.8 ± 0.1	1195.9 ± 0.1	1500.5 ± 0.4
Triethyl phosphate	1088.3 ± 0.1	1121.5 ± 0.2	1287.8 ± 0.1	1688.6 ± 0.8
Methyl salicylate	1175.5 ± 0.1	1203.2 ± 0.1	1306.6 ± 0.3	1801.8 ± 0.8
Tributyl phosphate	1615.6 ± 0.1	1638.7 ± 0.1	1817.7 ± 0.1	2157.7 ± 0.3

for the fourteen compounds were similar to those previously reported by D'Agostino and Provost [13] using on-column injection. Slight GC retention index differences were likely due to the differences in column diameter (0.32 mm *vs.* 0.53 mm) of variations in the thickness of the stationary phase (0.25 μm *vs.* 1.0 μm).

Simultaneous FID–FPD detection

Two detectors (FID and FPD) were operated in parallel by splitting the column effluent with a glass splitter and two short lengths (30 cm) of deactivated fused-silica column. The sections of deactivated column were then trimmed to bring the retention times of a reference peak (triethyl phosphate) to within 0.006 min of each other on the two detectors. The two detectors, operating in parallel, provided more specific and sensitive analysis of phosphorus and sulphur containing compounds with the added benefit of being able to determine retention indices using *n*-alkane probes. Fig. 2 illustrates the universal nature of the flame ionization detection and the specific response of the flame photometric detector in phosphorus and sulfur modes for a mixture of CW agents and simulants. All the compounds were detected by FID; only sarin, soman, triethyl phosphate and tributyl phosphate were detected by FPD in phosphorus mode and only the mustard peak was detected in sulfur mode. A small response (cross-talk) for mustard was observed on the phosphorus channel.

Water and soil samples

A sample of tap water (2 ml), spiked with triethyl phosphate (20 μg/g), was purged for 30 min with nitrogen and the volatiles trapped on a Tenax minitube. Fig.

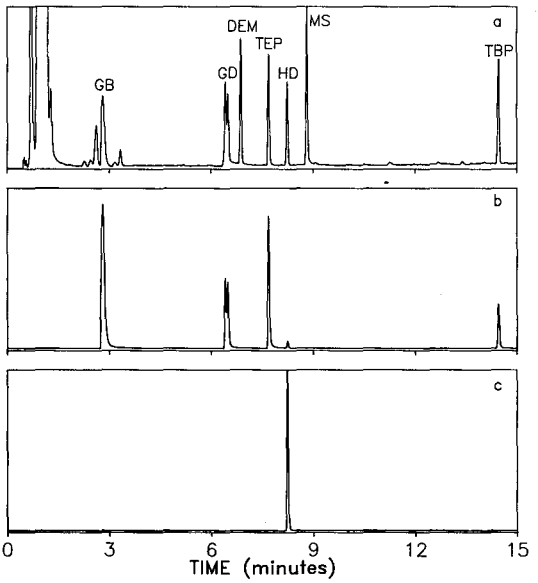

Fig. 2. TD–GC chromatograms of simultaneous detection by (a) FID, (b) FPD (phosphorus mode) and subsequent (c) FPD (sulfur mode) analysis of sarin (GB), soman (GD), diethyl malonate (DEM), triethyl phosphate (TEP), mustard (HD), methyl salicylate (MS) and tributyl phosphate (TBP). Column conditions: 15 m × 0.53 mm I.D. DB-5, helium flow-rate of 6 ml/min, temperature program of 50°C (2 min), 10°C/min to 180°C. Desorption conditions: desorption temperature, 240°C and cycle time, 5 min.

3 illustrates simultaneous thermal desorption flame photometric and flame ionization chromatograms. FPD (phosphorus mode) was used to detect triethyl phosphate at approximately the 250 pg level, while FID, operated in parallel, was used to determine the GC retention times of the *n*-alkane probes. A retention index of 1091.3 was calculated for triethyl phosphate, which was in good agreement with the previously determined value of 1088.3 (Table II). No peaks were detected in the chromatograms of the blanks run for this and subsequent samples.

The headspace above a soil sample (5 g), spiked with diethyl malonate (4 μg/g) and tributyl phosphate (1 μg/g), was sampled with a minitube and analyzed by TD–GC with simultaneous FID–FPD detection (Fig. 4). GC retention indices of 1038.4 and 1613.6 were determined for diethyl malonate and tributyl phosphate respectively. Diethyl malonate was easily detected, at approximately the 25 ng level, by FID and tributyl phosphate, while not detected by FID, was clearly visible, at approximately the 20 pg level with the FPD. Previous experience illustrated the limitations of headspace analysis for samples containing relatively non-volatile components. The soil was therefore also extracted with 5 ml of acetone and 1 μl of this extract was loaded onto a minitube for TD–GC analysis. Simultaneous FID–FPD chromatograms of the acetone extract of the soil are illustrated in Fig. 5. The peak for diethyl malonate was difficult to discern from the background chemical noise and tributyl phosphate could not be detected during FID analysis, while the FPD (phosphorus mode) chromatogram confirmed the presence of tributyl phosphate.

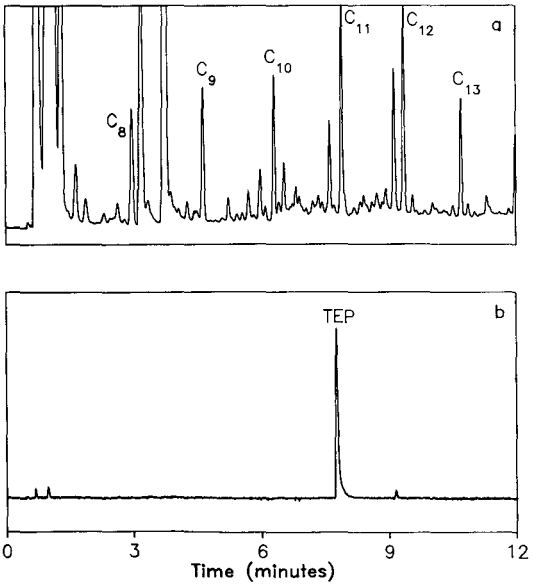

Fig. 3. TD–GC chromatograms of simultaneous detection by (a) FID and (b) FPD (phosphorus mode) of a water sample spiked with 20 μg/g triethyl phosphate (TEP) and subsequently loaded with *n*-alkane probes. Column conditions: 15 m × 0.53 mm I.D. DB-1, helium flow-rate of 6 ml/min, temperature program of 50°C (2 min), 10°C/min to 150°C. Desorption conditions: desorption temperature, 240°C and cycle time, 5 min.

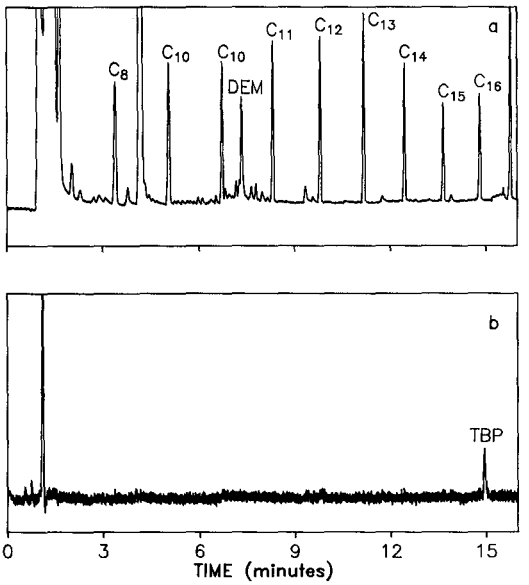

Fig. 4. TD–GC chromatograms of simultaneous detection by (a) FID and (b) FPD (phosphorus mode) of headspace above soil sample spiked with 4 μg/g diethyl malonate (DEM) and 1 μg/g tributyl phosphate (TBP). Column conditions: 15 m × 0.53 mm I.D. DB-1, helium flow-rate of 6 ml/min, temperature program of 50°C (2 min), 10°C/min to 190°C. Desorption conditions: desorption temperature, 240°C and cycle time, 5 min.

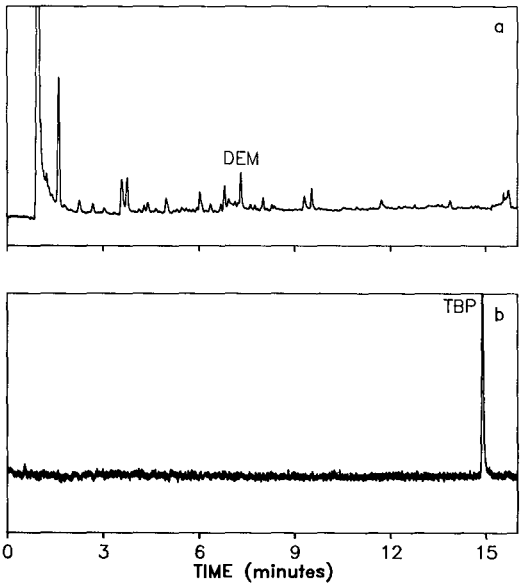

Fig. 5. TD–GC chromatograms of simultaneous detection by (a) FID and (b) FPD (phosphorus) mode of acetone extract of a soil sample spiked with 4 μg/g diethyl malonate (DEM) and 1 μg/g tributyl phosphate (TBP). Column conditions: 15 m × 0.53 mm I.D. DB-1, helium flow-rate of 6 ml/min, temperature program of 50°C (2 min), 10°C/min to 190°C. Desorption conditions: desorption temperature, 240°C and cycle time, 5 min.

CONCLUSIONS

Retention index monitoring using thermal desorption gas chromatographic analysis has been shown to be useful in the identification of compounds of chemical defence interest in environmental matrices. A database of GC retention indices for chemical warfare agents and simulants was compiled and, in conjunction with simultaneous flame ionization and flame photometric detection, applied to the identification of triethyl phosphate, tributyl phosphate and diethyl malonate in water and soil samples.

REFERENCES

1 J. Namiesnik and E. Kozlowski, *Chem. Anal. (Warsaw)*, 25 (1980) 999.
2 J. Namiesnik, L. Torres, E. Kozlowski and J. Mathieu, *J. Chromatogr.*, 208 (1981) 239.
3 A. Tangerman, *J. Chromatogr.*, 366 (1986) 205.
4 T. Noy, P. Fabian, R. Borchers, F. Janssen, C. Cramers and J. Rijks, *J. Chromatogr.*, 393 (1987) 343.
5 F. Bouchertall and J. C. Duinker, *Anal. Chim. Acta*, 185 (1986) 369.
6 J. Namiesnik, T. Gorecki, E. Kozlowski, L. Torres and J. Mathieu, *Sci. Total Environ.*, 38 (1984) 225.
7 J. F. Piecewicz, J. C. Harris and P. L. Levins, *Report EPA-600/7-79-216*, U.S. Environmental Protection Agency, Cambridge, MA, Sept. 1979.
8 E. Kováts, *Helv. Chim. Acta*, 41 (1958) 1915.
9 H. van den Dool and P. D. Kratz, *J. Chromatogr.*, 11 (1963) 463.
10 G. Tarjan, Sz. Nyiredy, M. Gyor, E. R. Lombosi, T. S. Lombosi, M. V. Budahegyi, S. Y. Meszaros and J. M. Takacs, *J. Chromatogr.*, 472 (1989) 1.
11 M. B. Evans and J. K. Haken, *J. Chromatogr.*, 472 (1989) 93.
12 P. A. D'Agostino and L. R. Provost, *J. Chromatogr.*, 331 (1985) 47.
13 P. A. D'Agostino and L. R. Provost, *J. Chromatogr.*, 436 (1988) 399.
14 P. A. D'Agostino, L. R. Provost and J. Visentini, *J. Chromatogr.*, 402 (1987) 221.
15 Z. Witkiewicz, M. Mazurek and J. Szulc, *J. Chromatogr.*, 503 (1990) 293.
16 *Air Monitoring as a Means for Verification of Chemical Disarmament, C.2, Development and Evaluation of Basic Techniques*, Part I, Ministry for Foreign Affairs of Finland, Helsinki, 1985.
17 A. Manninen, M.-L. Kuitunen and L. Julin, *J. Chromatogr.*, 394 (1987) 465.
18 *Air Monitoring as a Means for Verification of Chemical Disarmament, C.4, Further Development and Testing of Methods*, Part III, Ministry of Foreign Affairs of Finland, Helsinki, 1987.
19 J. R. Hancock, J. M. McAndless and R. P. Hicken, *J. Chromatogr. Sci.*, in press.

Journal of Chromatography, 538 (1991) 259–267
Elsevier Science Publishers B.V., Amsterdam

CHROM. 22 823

Gas chromatographic–mass spectrometric determination of oxolinic acid in fish using selected ion monitoring

KEIGO TAKATSUKI

Miyagi Prefectural Institute of Public Health and Environment, 4–7–2, Saiwai-cho, Miyagino-ku, Sendai, Miyagi 983 (Japan)

(Received May 29th, 1990)

ABSTRACT

A gas chromatographic–mass spectrometric (GC–MS) method is described for the determination of oxolinic acid in fish tissues. Oxolinic acid is reduced with sodium tetrahydroborate to permit GC analysis. The sample is homogenized with phosphate buffer (pH 6) and extracted with ethyl acetate. The extract is partitioned between sodium hydrogencarbonate solution and the aqueous phase is acidified and re-extracted with ethyl acetate. The residue from the ethyl acetate extract is dissolved in methanol and reduced with sodium tetrahydroborate. The reduction product is extracted with diethyl ether and analysed by GC–MS in the selected ion monitoring mode for the ions at *m/z* 204, 219 and 176. The detection limit is 0.001 mg/kg and the recoveries were 95.6% [relative standard deviation (R.S.D.) 7.7%] at 0.1 mg/kg and 72.9% (R.S.D. 13.3%) at 0.01 mg/kg fortification levels in fish.

INTRODUCTION

In recent years in Japan, fish for use as food have been artificially cultivated on a large scale in both fresh water and in sea water, and drugs are used to prevent and to treat disease. Oxolinic acid (1-ethyl-1,4-dihydro-6,7-methylenedioxy-4-oxo-3-quinolinecarboxylic acid) (Fig. 1, a), is an antimicrobial agent which is widely used in the cultivation of fish such as salmon, rainbow trout, sweetfish, carp, eel and yellowfish.

Drug residues in cultivated fish may cause problems with regard to human safety, and in Japan the Food Safety Law established a zero residual level for all

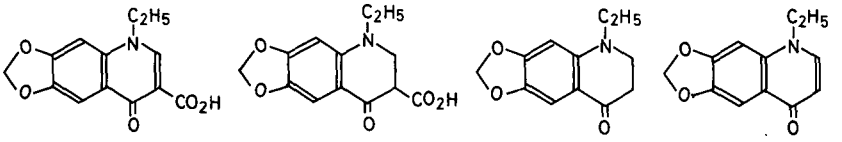

Fig. 1. Structures of (a) oxolinic acid, (b) reduction intermediate, (c) reduction product and (d) oxidation product of c.

0021-9673/91/$03.50

antimicrobial agents in foods in 1971. Hence routine screening for oxolinic acid residues in cultivated fish is necessary, but the methods of analysis available are very limited. Endo *et al.* [1] used the microbial assay of oxolinic acid in animal tissues, but this method lacks sensitivity and specificity. Kasuga *et al.* [2] reported a liquid chromatographic method, and the Japanese official method also uses a liquid chromatographic method, but its detection limit of 0.05 mg/kg is not sufficient and identification that relies solely on retention data is not specific enough to support regulatory action.

Gas chromatography–mass spectrometry (GC–MS) is the most reliable and sensitive technique for residue analysis, and we have been developing GC–MS methods for drug residue analysis. Methyl and *n*-butyl oxolinate were not suitable for GC because they are very polar and did not produce clear peaks on gas chromatograms [3]. We therefore tried other derivatives and found that sodium tetrahydroborate reduction of oxolinic acid smoothly gives a reduction product, 1-ethyl-1,2,3,4-tetrahydro-6,7-methylenedioxy-4-oxoquinoline (Fig. 1,c). This compound has good GC characteristics and gives a sharp, symmetrical peak on gas chromatograms. We therefore developed a GC–MS method with selected ion monitoring (SIM) using this reduction product for the determination of oxolinic acid residues in fish. This method is rapid, sensitive and is specific enough to support regulatory action, and is useful for daily screening and also for the identification of residual oxolinic acid.

EXPERIMENTAL

Materials and chemicals

Pesticide-grade and analytical-reagent grade chemicals were used as received. Pesticide-grade ethyl acetate, methanol, acetone and anhydrous sodium sulphate and analytical-reagent grade $NaH_2PO_4 \cdot 2H_2O$, NaOH, $NaHCO_3$, NaCl, $NaBH_4$ and HCl were obtained from Wako (Osaka, Japan). Pesticide-grade diethyl ether and methylene chloride (Wako) were used after alumina column chromatography just before use. Alumina was obtained from E. Merck (Darmstadt, F.R.G.) and a silica gel cartridge column (Sep-Pak silica) from Waters Assoc. (Milford, MA, U.S.A.). Oxolinic acid was obtained from Sigma (St. Louis, MO, U.S.A.).

Solutions were prepared as follows: for phosphate buffer solution (pH 6), 31.2 g of $NaH_2PO_4 \cdot 2H_2O$ were dissolved in 600 ml of water, the pH was adjusted to 6 by adding 1 M NaOH and the volume was made up to 1 l with water; for sodium hydrogencarbonate, 40 g of $NaHCO_3$ were added to 500 ml water and mixed and the supernatant was used; for 5 *M* HCl, 417 ml of HCl were added to 500 ml of water and the volume was made up to 1 l with water.

Standard solutions

A stock standard solution (100 mg/l) was prepared by dissolving 10.0 mg of oxolinic acid in 100 ml of methanol in a volumetric flask. Working standard solutions were prepared by diluting the stock solution with methanol to 0.1–1.00 mg/l. These solutions were stored in a refrigerator.

Instrumental

A Biotron BT 10 20 350D homogenizer (Biotrona, Kussnacht, Switzerland),

a Model 8-1-W wrist-action shaker (Yayoi, Tokyo, Japan) and a Model N-1 rotary evaporator (Tokyo Rikakikai, Tokyo, Japan) were used. A DB-5 capillary GC column (15 m × 0.25 mm I.D., film thickness 0.25 μm) (J&W Scientific, Folsom, CA) was used. A Model 5890 Series II gas chromatograph with a split/splitless injection port was coupled to a Model 5970B mass-selective detector (quadrapole mass spectrometer) and were operated using 59970 MS Chemistation computer software (Hewlett-Packard, Englewood, CO, U.S.A.). The capillary column (DB-5) was directly interfaced to the mass spectrometer ion source.

The operating conditions were as follows: splitless injection; purge on time, 2 min after injection; injection port temperature, 270°C; column temperature, 100°C, held for 2 min, increased to 200°C at 20°C/min, then to 270°C at 10°C/min; carrier gas, helium at a column head pressure of 5 p.s.i. (flow-rate 4.8 ml/min); transfer line temperature, 260°C; electron ionization, 70 eV; electron multiplier, 2600 V; selected ion monitoring, detection ions of *m/z* 204, 219 and 176.

Extraction and clean-up

A 10.0-g comminuted sample was homogenized with 20 ml of phosphate buffer solution (pH 6) in a 100-ml centrifuge tube for 5 min. The homogenizer shaft was washed with 40 ml of ethyl acetate and the washings were added to the centrifuge tube. The mixture was shaken for 10 min and centrifuged at 1000 *g* for 10 min. The upper ethyl acetate extract was pipetted into a 100-ml separating funnel. A 20-ml volume of ethyl acetate was added to the residue in the centrifuge tube and mixed again. The second ethyl acetate extract, separated by centrifugation at 1000 *g*, is added to the separating funnel. The combined ethyl acetate solution was extracted three times with sodium hydrogencarbonate solution (10, 10 and 5 ml) and the aqueous layer was collected in another 100-ml separating funnel.

A 6-ml volume of 5 *M* HCl was added to the hydrogencarbonate extract, mixed well and the pH was ascertained to be 1–2. If it was more basic, 5 *M* HCl was added to make the pH 1–2. After addition of 2 g of NaCl, the aqueous solution was re-extracted twice with ethyl acetate (30 and 20 ml) and the combined ethyl acetate extract was washed with 3 ml of phosphate buffer solution (pH 6). The pH of the washings must be 5–6; if it was more acidic, washing was repeated with a further 3 ml of phosphate buffer (pH 6). The ethyl acetate solution was dried over anhydrous Na_2SO_4, filtered into a 100-ml pear-shaped flask and evaporated to dryness using a rotary evaporator at 36°C. The residue was quantitatively transferred into a 10-ml test-tube with 1.0 and 0.5 ml of methanol.

Sodium tetrahydroborate reduction

A *ca.* 3-mg amount of $NaBH_4$ was added to the methanol solution and reacted at 20°C for 5 min with occasional swirling. After reaction, 2 ml of 0.1 *M* HCl were added and mixed well. The pH of this solution must be 2–3; if it was more basic, 0.1 *M* HCl was added to make the pH 2–3. The solution was allowed to stand at 20°C for 5 min, then 2 ml of water were added and the mixture was extracted three times with diethyl ether (2, 2 and 1 ml). The upper ether layer was transfered into a 10-ml erlenmeyer flask using a Pasteur pepette and dried over Na_2SO_4. The solution was filtered into a 20-ml pear-shaped flask and the solvent was evaporated to dryness using a rotary evaporator at 35°C. The residue was dissolved in 3 ml of methylene chloride.

A silica cartridge column was attached to a 5-ml syringe barrel and the above methylene chloride solution was transferred into this syringe. The flask was rinsed with 3 ml of methylene chloride and the rinsings were added to the syringe. The methylene chloride solution was forced gently through column by applying pressure on the syringe plunger. The eluate was discarded.Then 3 ml of methylene chloride–diethyl ether (1:1) were added to the syringe and eluted by gentle pressure. The eluate was collected in a 20-ml pear-shaped flask and the solvent was evaporated to dryness using a rotary evaporator at 35°C. The residue was dissolved in 1 ml of acetone and this solution was ready for injection into the GC–MS system. If GC–MS analysis does not follow immediately, the solutions must be stored under a nitrogen atmosphere in a refrigerator.

Preparation of standard solutions for calibration graph

Volumes of 1 ml of each working solution of 0.1–1.0 mg/l were pipetted into 10-ml test-tubes. A *ca.* 3-mg amount of $NaBH_4$ was added to each test-tube and reacted at 20°C for 5 min. After reaction, 2 ml of 0.1 *M* HCl were added and mixed well. The pH of this solution must be 2–3. If it was more basic, 0.1 M HCl was added to make the pH 2–3. The solutions were allowed to stand at 20°C for 5 min, then 2 ml of water were added and the solution was extracted three times with diethyl ether (2, 2 and 1 ml). The ether extract was dried over anhydrous Na_2SO_4, filtered into another 10-ml test-tube and the solvent was evaporated to dryness at 35°C with a gentle stream of nitrogen. The residue was dissolved in 1 ml of acetone and this solution was ready for injection into the GC–MS system. This solution must be stored under nitrogen in a refrigerator and must be prepared fresh each week.

Gas chromatographic–mass spectrometric analysis

The GC column was connected to the ion source of the mass spectrometer and the instrument parameters were adjusted. The quadrapole fields were calibrated using perfluorotributylamine as a standard.

A 2-μl volume of each standard solution (0.1–1.0 mg/l) for the calibration graph was injected into the GC–MS system and a calibration graph was constructed by plotting peak areas on the *m/z* 204 SIM chromatograms against amounts of oxolinic acid. A 2 μl sample solution was subsequently injected into the GC–MS system and the reduction product of oxolinic acid was identified from the retention time of the peaks in the *m/z* 204, 219 and 176 SIM chromatograms and from the intensity ratio of ions of *m/z* 219 and 176 to that of *m/z* 204. The amount of oxolinic acid in a sample solution was calculated by comparison of the peak area at *m/z* 204 with the calibration graph. The concentration of oxolinic acid in a sample was calculated by dividing the amount of oxolinic acid by the amount of the sample (10.0 g).

RESULTS AND DISCUSSION

Methyl or *n*-butyl oxolinate was not suitable for GC, so we tried other possible derivatives and found that sodium tetrahydroborate reduction of oxolinic acid proceeded smoothly to give a fluorescent product. The structure of this product was proved to be 1-ethyl-1,2,3,4-tetrahydro-6,7-methylenedioxy-4-oxoquinoline (Fig. 1, c) from the mass spectrum (Fig. 2) (M^+, *m/z* 219; $M^+ - CH_3$, *m/z* 204; $M^+ - CH_3 - CO$,

m/z 176). This compound (c) is considered to be formed by decarboxylation of an intermediate product (b) (Fig. 1, b), which is produced by Michael-type addition of hydride ion (H^-) to oxolinic acid (a). Compound c is smoothly eluted from GC columns, and gives a sharp, symmetrical peak at moderate temperatures, so it is well suited for GC analysis. We decided to use this reduction product (c) for the GC–MS determination of oxolinic acid residues.

Compound c gradually changed to another compound (d) when the diethyl ether solution was exposed to air at room temperature. This had a longer GC retention time analysis and its mass spectrum showed distinct ions at *m/z* 217 (M^+), 202 and 174, which indicated that the structure is a dehydrogenated product, 1-ethyl-1,4-dihydro-6,7-methylenedioxy-4-oxoquinoline (Fig. 1, d). This seems to be formed by air oxidation of c. Therefore, c must be analysed by GC–MS as quickly as possible, and the solutions must be stored under a nitrogen atmosphere in a refrigerator.

The detailed experimental conditions for this reduction were investigated with oxolinic acid solution. The time course of the reduction with sodium tetrahydroborate in methanol was followed by GC–MS-SIM. Fig. 3 shows the results, which indicate that the optimum reaction time was 5 min at 20°C. Reduction at ice-cooled temperature was fairly slow. After reduction, the reaction mixture was treated with HCl to decompose excess of sodium tetrahydroborate. When the amount of HCl was not sufficient to make the solution acidic, the yield of c decreased considerably. The pH of the reaction mixture after HCl addition is critical and should be carefully established with a pH test paper to be 2–3 in each reduction. The reaction time of acid treatment also affected the yield of c, and the optimum was 5 min at 20°C. The diethyl ether used for extraction of c must be column chromatographed on alumina just before use, because aged diethyl ether considerably lowered the yield. Compound c is very sensitive to oxidation, as described above.

The ions used for GC–MS-SIM detection are three distinct ions of c (Fig. 2), *i.e.*, those at *m/z* 204, 219 and 176. The injection volume is 2 μl in the splitless mode. Identification is based on the retention time and on the intensity ratio of the ions of *m/z* 219 and 176 to that of *m/z* 204. Sphone [4] pointed out that three ions are necessary for

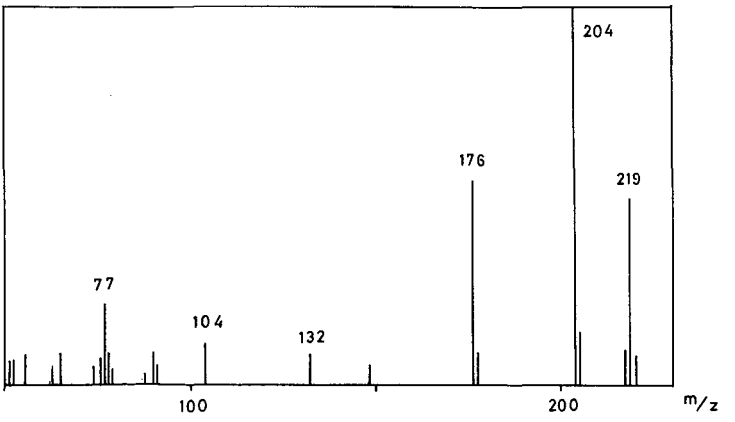

Fig. 2. Mass spectrum of the reduction product of oxolinic acid.

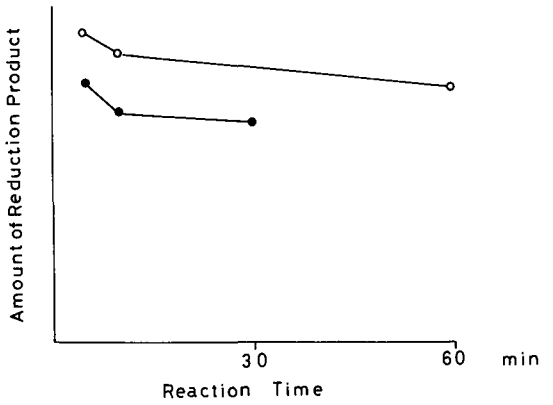

Fig. 3. Reaction time of sodium tetrahydroborate *vs.* yield of reduction product. ○ = 20°C; ● = ice-cooled.

the qualitative identification of an endogeneous drug residue by use of low-resolution MS.

Quantification was effected by comparing the peak area on the *m/z* 204 SIM chromatogram with a calibration graph. The calibration graph was constructed by plotting the peak areas on the *m/z* 204 SIM chromatogram of the reduction product of oxolinic acid against the amount of oxolinic acid. A straight-line graph was obtained in the range 0.2–2.0 ng with a correlation coefficient $\gamma = 0.9983$. The SIM chromatograms of c at 0.1 mg/l concentration are shown in Fig. 4. Fig. 5 shows the SIM

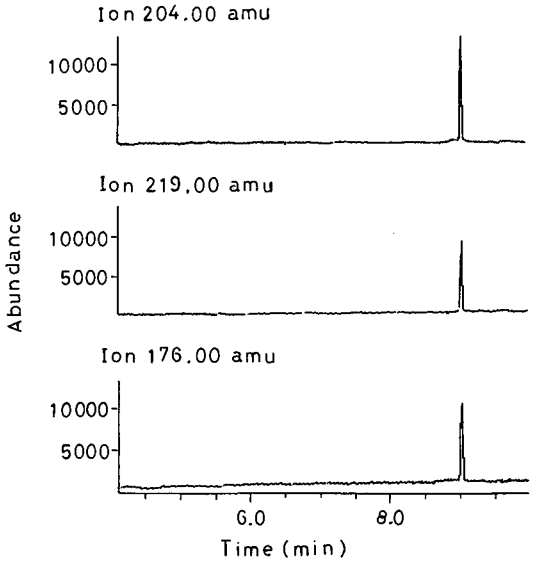

Fig. 4. SIM chromatograms at *m/z* 204, 219 and 176 of standard oxolinic acid reduction product (oxolinic acid, 0.2 ng).

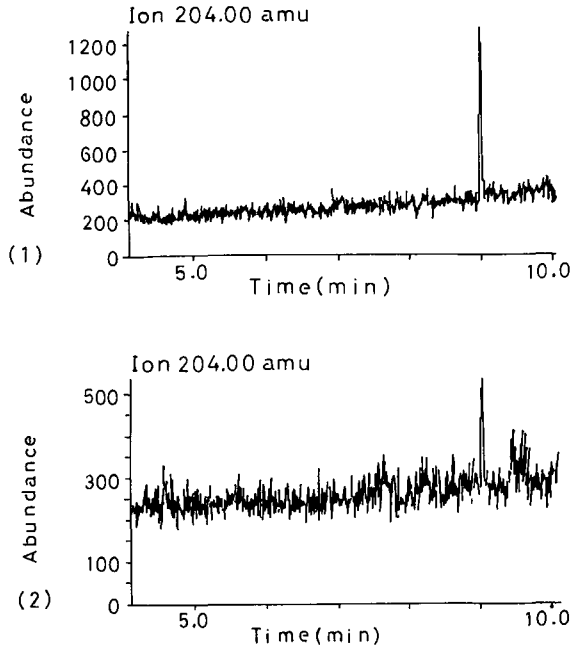

Fig. 5. SIM chromatograms at m/z 204 of standard oxolinic acid reduction product. (1) Oxolinic acid, 20 pg; (2) oxolinic acid, 6 pg.

chromatograms based on the ion of m/z 204 (most sensitive) at the detection limit concentration. A concentration of 0.003 mg/l was detectable with a standard solution, but 0.01 mg/l is the detection limit with the sample extract solution, which corresponds to 0.001 mg/kg in the sample.

We used the extraction solvent system reported by Browning and Pratt [5] for the determination of nalidixic acid. Oxolinic acid is amphoteric, so extraction with ethyl acetate after homogenization of the sample with phosphate buffer (pH 6) is necessary.

TABLE I

RECOVERY (%) OF OXOLINIC ACID ADDED TO SILVER SALMON

	Amount added (mg/kg)	
	0.1	0.01
	91.2	74.9
	97.6	64.9
	107.6	81.7
	89.6	60.8
	91.8	82.1
Mean	95.6	72.9
R.S.D.[a] (%)	7.7	13.3

[a] Relative standard deviation.

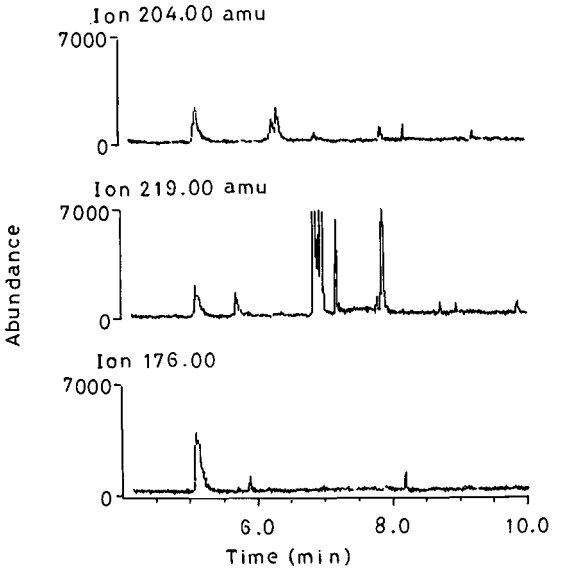

Fig. 6. SIM chromatograms at *m/z* 204, 219 and 176 of extract from silver salmon fortified with 0.01 mg/kg of oxolinic acid. The retention time of oxolinic acid reduction product is 9.028 min.

Kasuga *et al.* [2] also used this extraction solvent for the liquid chromatographic determination of oxolinic acid in fish and obtained a good extraction efficiency (94%).

The ethyl acetate extract from samples contained an oily substance and after sodium tetrahydroborate reduction many interfering peaks were observed in the SIM chromatograms, which made impossible to identify the peak of c. Extraction of oxolinic acid from the ethyl acetate solution with 0.1 *M* NaOH caused emulsion formation and interfering peaks were not completely eliminated. However, in extraction with sodium hydrogencarbonate solution, no emulsion was formed and interfering peaks were completely removed. Other drugs used for fish, such as tetracycline, ampicillin, sulphamonomethoxine, sulphadimethoxine and thiamphenicol, did not interfere in the determination of oxolinic acid with this procedure. Nalidixic and piromidic acid were reduced with $NaBH_4$ to give reduction products, which could be completely differentiated from that of oxolinic acid (c) by the retention times and SIM detection ions. After sodium tetrahydroborate reduction, the sample extract is passed through a silica gel cartridge column to remove high-boiling polar compounds for protection of the open-tubular GC column.

Recoveries were determined by adding oxolinic acid to blank silver salmon muscle tissue, which had been previously analysed with this method to confirm that no oxolinic acid was detected. Table I gives the results, and the SIM chromatograms are shown in Fig. 6. The detection limit is 0.001 mg/kg in muscle tissues.

This method is sensitive and reliable and the procedure is simple and rapid, and so is useful for both daily screening and qualitative identification of residual oxolinic acid. The application of this method to the determination of nalidixic and piromidic acid is in progress and will be reported later.

REFERENCES

1 T. Endo, K. Ogishima, H. Hayasaka, S. Kaneko and K. Ohshima, *Bull. Jpn. Soc. Sci. Fish.*, 39 (1973) 165.
2 Y. Kasuga, A. Sugitani and F. Yamada, *J. Food Hyg. Soc. Jpn.*, 23 (1982) 344.
3 H. Roseboom, R. H. A. Sovel, H. Lingeman and R. Bouwman, *J. Chromatogr.*, 163 (1979) 92.
4 J. A. Sphone, *J. Assoc. Off. Anal. Chem.*, 61 (1978) 1247.
5 R. S. Browning and E. L. Pratt, *J. Assoc. Off. Anal. Chem.*, 53 (1970) 464.

Journal of Chromatography, 538 (1991) 269–275
Elsevier Science Publishers B.V., Amsterdam

CHROM. 22 915

Determination of heroin and some common adulterants by capillary gas chromatography

ALBERT SPERLING
Special Testing and Research Laboratory, Drug Enforcement Administration, 7704 Old Springhouse Road, McLean, VA 22102 (U.S.A.)
(First received May 3rd, 1990; revised manuscript received October 9th, 1990)

ABSTRACT

A method has been developed for the simultaneous determination of heroin along with some of the commonly occurring adulterants that have been found in samples in recent years. The method utilizes simple sample dissolution along with an internal standard followed by capillary gas chromatography on a non-polar DB-1 column attached to a flame ionization detector. Column temperature programming was used along with a programmed temperature vaporizer in the injection port. Linearity studies were conducted on heroin base, heroin hydrochloride and several of the other drug adulterants. Excellent results were obtained and the method is applicable to a broad range and type of heroin sample.

INTRODUCTION

Forensic drug analysis always seems to present the analyst with new and unusual types of samples with which existing methods have had difficulty coping. Recently a new type of heroin sample has been appearing in our laboratory in which the sample is cut with a multitude of diluents and adulterants thereby rendering a once relatively simple analysis much more complex. In addition to the normally occurring components such as acetylcodeine, O^6- and O^3-monoacetylmorphines, codeine, morphine, papaverine and noscapine, a large number of other components have been occurring with some regularity. These include such drugs, in varying combinations, as caffeine, nicotinamide, phenobarbital, procaine, methaqualone, phenacetin, cocaine, acetylprocaine, lidocaine, diazepam, antipyrine, chloroquine, acetaminophen, quinine, N-phenyl-2-naphthylamine, phenolphthalein and occasional antihistamines along with sugars and inorganic salts such as calcium carbonate and sodium chloride.

While high-performance liquid chromatography (HPLC) methods [1–15] exist for the determination of heroin, they do not address the problem of quantitation of a large number of adulterants. Similarly HPLC screening techniques [16–22] do not address quantitation, although some authors [18,19] do list a comparison of UV response factors *vs.* electrochemical response factors. The same situation occurs in gas chromatography. Packed columns do not readily lend themselves to the analysis of these complex multicomponent mixtures. On the other hand, capillary columns are

0021-9673/91/$03.50

ideally suited to provide a simultaneous separation and quantitation of these multicomponent samples. There are capillary gas chromatography (GC) methods for the determination of heroin [23–27] as well as methods giving qualitative retention time data for a large number of drugs [28–37]. In addition, there is an extensive listing of retention time indices in the second edition of Clarke [38]. Again however, none of them deal with the quantitative aspects of samples that contain a large number of components.

Capillary GC in combination with a programmable temperature vaporizer (PTV) operated in the split mode was the technique used. The PTV allows a sample to be injected at low, or cold, temperatures which is then followed by a rapid rise in temperature to ensure immediate vaporization of all components. This eliminates mass discrimination effects as well as greatly reducing changes due to thermal breakdown of heat labile substances. Increased accuracy, precision and high resolution result from using this type of injection system. It can also allow pre-column separation of the solvent when used in the solvent purge mode. In standard injection systems, the syringe needle is exposed to high temperatures before the transfer of the sample into the injector which can result in selective volatilization as well as possible degradation and or adsorption. Poy and co-workers [39,40] showed excellent relative standard deviations with a PTV as compared to poorer results when using a standard hot split injection system. Schomburg and co-workers [41,42] showed excellent standard deviations of absolute and relative peak areas indicating high precision and accuracy. Loyola *et al.* [43] showed that the PTV gave the best accuracy and precision in his study and indicated that it provided better performance than the classical split injector technique.

This paper gives quantitative data on a selected number of drugs, in particular, those drugs which seem to occur most frequently in samples submitted to this laboratory. Excellent results were obtained.

EXPERIMENTAL

Instrumentation

A Perkin–Elmer Sigma 2000 gas chromatograph, equipped with a hydrogen flame ionization detector and interfaced with a Perkin–Elmer 7500 data system was used. The capillary column used was a fused silica, cross-linked and bonded DB-1 30 m × 0.25 mm I.D. with a 0.25 micron film thickness (J&W Scientific, Folsom, CA, U.S.A.). The carrier gas was hydrogen (zero grade) with an average gas velocity of 41 cm/s. The oven temperature program used started with an initial temperature of 200°C with a 1-min hold, then ramped at 12°C/min to 280°C followed by a final hold of 8 min. A PTV from Perkin–Elmer was used with an initial temperature of 75°C, held for 0.1 min then immediately ramped to 285°C. The detector temperature was held at 285°C. A split ratio of 25:1 was used for all injections.

Materials

Chloroform and methanol (Mallinckrodt) were reagent grade. All drugs were of pharmaceutical grade or better, with the exception of N-phenyl-2-naphthylamine. Caffeine was obtained from K&K Labs., procaine and tetracosane from Pfaltz and Bauer, nicotinamide from Eastman-Kodak, phenacetin from Dow Chemical, metha-

qualone from William B. Rorer, phenobarbital, cocaine hydrochoride and cocaine base from Merck & Co., heroin hydrochloride from Research Triangle, quinine hydrochloride from Mallinckrodt and heroin base was synthesized in our laboratory and is the DEA "house" standard. N-Phenyl-2-naphthylamine was obtained from Aldrich and was used as received.

Internal standard solutions

The internal standard solution for the linearity study was prepared by making a 0.1 mg/ml solution of tetracosane in chloroform. The internal standard solution for the quantitative analysis of the samples was prepared by making a 1.0 mg/ml solution of tetracosane in chloroform.

Preparation of drug stock solutions for linearity study

Three stock solutions were prepared for each drug, the second and third of which were dilutions of the first. The primary stock solutions of the drug standards were prepared by weighing 100 mg of each drug into separate 100 ml volumetric flasks, dissolving in a minimum amount of methanol and bringing to volume with chloroform. This solution was then diluted (1:10) into a second volumetric flask to produce the second stock solution and this in turn was further diluted (1:10) into a third volumetric flask to provide the third stock solution. Aliquots were then transferred from each of the three stock solutions for each drug, into separate glass stoppered tubes and evaporated to dryness. Aliquots of 1, 3, 5, 8 and 15 ml were transferred from the primary stock solution and 1-, 3-, 5- and 8-ml aliquots were transferred from the second and third stock solutions. The thirteen tubes for each drug were reconstituted with 1.0 ml of internal standard solution (0.1 mg/ml tetracosane in chloroform). Equal volumes of all solution were injected on the GC.

Quantitative analysis of the samples

A standard solution was prepared by weighing an amount of the appropriate standards into a 25-ml flask, dissolving in a minimum amount of methanol, adding 2.0 ml of internal standard solution (1 mg/ml tetracosane in chloroform) and diluting with chloroform. Generally 4–5 mg of standard is a suitable amount. In the case of nicotinamide approximately 10 mg is required, and for phenobarbital 8–10 mg is required. Quinine, which usually occurs as the hydrochloride, requires about 15–20 mg.

Preparation of the sample

The weight of sample to be used for the analysis depends on the concentrations of the particular components which are present. This may quickly be determined by performing a preliminary qualitative GC screening analysis on the material and estimating the concentrations based on their relative peak areas. An appropriate amount of sample, at least 100 mg, was weighed into a volumetric flask, mixed with a small amount of methanol and then brought to volume with chloroform. An aliquot was transferred to a 25-ml flask followed by the addition of 2.0 ml of internal standard solution (1.0 mg/ml) and diluted to a suitable volume. The final solution may be filtered if necessary.

RESULTS AND DISCUSSION

Good separation and quantitative results were achieved. Fig. 1 shows a chromatogram of a complex sample which was submitted to the laboratory. Linearity studies of the standards were conducted over a wide range of concentrations and correlation coefficients were calculated. These values along with the linearity ranges determined are listed in Table I.

Relative standard deviations were calculated from a sample that was injected repetitively eight times and the values are listed in Table II. Excellent results were obtained with values that ranged from 0.7 to 3.4%. This largest value was represented by nicotinamide indicating slightly less reproducibility for this component. Low levels of nicotinamide and quinine exhibited very poor reproducibility so care should be taken not to attempt an analysis below the stated limits. Results for heroin, caffeine and procaine compare favorably to quantitative results obtained by HPLC. These results are listed in Table III. Other components could not be quantitated by HPLC because of interferences with the peaks of interest.

It should be noted that while cocaine and N-phenyl-2-naphthylamine have virtually the same GC retention time, they have not been found to occur in combination with each other in any sample that has been analyzed to date. Noscapine and phenolphthalein are also a pair of compounds that co-elute under the existing temperature programming conditions. Although lowering the starting temperature as

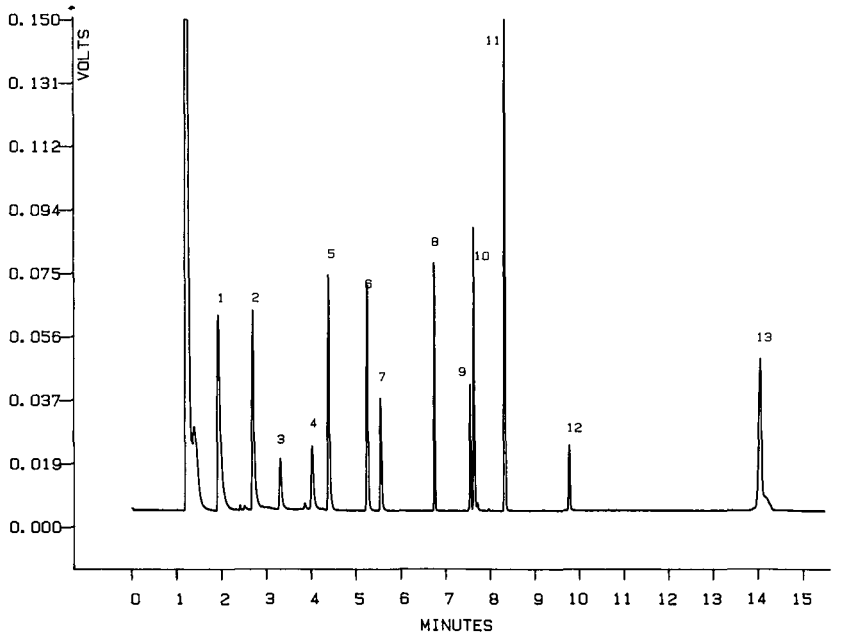

Fig. 1. Chromatogram of a complex heroin sample. Peaks: 1 = nicotinamide; 2 = phenacetin; 3 = caffeine; 4 = phenobarbital; 5 = procaine; 6 = methaqualone; 7 = N-phenyl-2-naphthylamine; 8 = tetracosane; 9 = acetylcodeine; 10 = O^6-monoacetylmorphine; 11 = heroin; 12 = papaverine; 13 = noscapine.

TABLE I

RESULTS FOR LINEARITY STUDY

Drug	Linearity range (μg on column)	Correlation coeff.
Heroin base	0.0008 – 0.6	0.9998
Heroin HCl	0.0008 – 0.6	0.9998
Cocaine base	0.0004 – 0.6	0.9998
Cocaine HCl	0.0008 – 0.3	0.9999
Caffeine	0.0004 – 0.6	0.9999
Nicotinamide	0.02 – 0.6	0.9999
N-Phenyl-2-naphthylamine	0.0012 – 0.2	0.9999
Methaqualone	0.0004 – 0.6	0.9999
Phenobarbital	0.002 – 0.6	0.9999
Procaine HCl	0.02 – 0.6	0.9993
Phenacetin	0.002 – 0.6	0.9994
Quinine HCl	0.04 – 0.6	0.9987

TABLE II

RESULTS OF ANALYSIS (8 REPETITIVE INJECTIONS)

R.S.D. = Relative standard deviation.

Drug	(%)	R.S.D. (%)
Nicotinamide	19.3	3.4
Phenacetin	11.7	1.8
Caffeine	4.5	1.0
Phenobarbital	5.0	2.2
Procaine	12.1	0.8
Methaqualone	7.0	0.7
N-Phenyl-2-naphthylamine	3.0	0.9
Heroin	16.2	0.8

TABLE III

COMPARISON OF GC AND HPLC RESULTS OF HEROIN, CAFFEINE AND PROCAINE

	Sample 1		Sample 2		Sample 3		Sample 4		Sample 5	
	GC	HPLC	GC	HPLC	GC	HPLC	GC	HPLC	GC	HPLC
Heroin	35.1	36.4	24.9	25.6	3.1	3.7	19.5	18.9	18.4	18.4
Caffeine	4.3	4.6	9.8	10.2			29.8	29.6	16.8	17.2
Procaine	9.8	9.5							2.6	2.7

well as the oven program rate will allow for some separation, for quantitative work it is necessary to treat the sample with a derivatizing agent. The preparation of a trimethylsilyl (TMS) derivative of phenolphthalein resolves the two peaks and allows for quantitation [27,44]. Similarly, in the quantitative analysis of O^6-monoacetylmorphine and acetylcodeine, the preparation of a TMS derivative of O^6-monoacetylmorphine is required for a satisfactory quatitation of both components [27,44].

The rationale for the presence of a noxious chemical like N-phenyl-2-naphthylamine in a heroin sample cannot be explained. The Aldrich catalog [45] describes the chemical as an irritant. One can speculate that it probably has some, if not a considerable degree of toxicity as well.

CONCLUSIONS

The nature of samples currently being examined are too complex for analysis by packed column gas chromatography, however capillary GC has been shown to be suitable for both qualitative and quantitative analysis of these samples. Excellent results were obtained with small relative standard deviations and a wide range of linearity for the compounds studied. Other drugs will be studied in future work.

REFERENCES

1 J. Albanbaur, J. Fehn, W. Furtner and G. Megges, *Arch. Kriminol.*, 162 (1978) 103; *C.A.*, 93 (1980) 1606j.
2 P. B. Baker and T. A. Gough, *J. Chromatogr. Sci.*, 19 (1981) 483.
3 J. D. Wittwer Jr., *Forensic Sci. Int.*, 18 (1981) 215.
4 M. Escribano Escribao and J. Boatella Riera, *Circ. Farm.*, 39 (1981) 431; *C.A.* 97 (1982) 1718e.
5 C. J. C. M. Laurent, H. A. N. Billiet and L. de Galan, *J. Chromatogr.*, 285 (1984) 161.
6 I. Lurie and S. Carr, *J. Liq. Chromatogr.*, 9 (1986) 2485.
7 J. Love and L. Pannell, *J. Forensic Sci.*, 25 (1980) 320.
8 I. Lurie and K. McGuinness, *J. Liq. Chromatogr*, 10 (1987) 2189.
9 H. A. Billiet, R. Wolters, L. de Galan and H. Huizer, *J. Chromatogr.*, 368 (1968) 351.
10 S. K. Soni and S. M. Dugar, *J. Forensic Sci.*, 24 (1979) 437.
11 P. C. White, I. Jane, A. Scott and B. E. Connett, *J. Chromatogr.*, 265 (1983) 293.
12 R. S. Schwartz and K. O. David, *Anal. Chem.*, 57 (1985) 1326.
13 H. Huizer, *J. Forensic Sci.*, 28 (1983) 40.
14 D. J. Reuland and W. A. Trinler, *J. Forensic Sci.*, 11 (1978) 195.
15 A. Fell, H. Scott, R. Gill and A. Moffat, *Chromatographia*, 16 (1982) 69.
16 K. D. Rehm and M. Steinigen, *Pharm. Ztg.*, 126 (1981) 99; *C.A.* 95 (1981) 49477m.
17 B. Wheals, *J. Chromatogr.*, 187 (1980) 65.
18 G. Musch, M. DeSmet and D. Masart, *J. Chromatogr.*, 348 (1985) 97.
19 I. Jane, A. McKinnon and R. Flanagan, *J. Chromatogr.*, 323 (1985) 191.
20 T. Daldrup, P. Michalke and W. Boehne, *Chromatogr. Newsl.*, 10 (182) 1.
21 G. Hoogewijs and D. L. Massart, *J. Pharm. Biomed Anal.*, 1 (1983) 321.
22 S. T. Chow, P. J. O'Neil, P. B. Baker and T. A. Gough, *J. Chromatogr. Sci.*, 21 (1983) 551.
23 H.-Y. Lim and S.-T. Chow, *J. Forensic Sci.*, 23 (1978) 319.
24 M. Prager, S. Harrington and T. Governo, *J. Assoc. Off. Anal. Chem.*, 62 (1979) 304.
25 F. van Vendeloo, J. Franke and R. de Zeeuw, *Weekbl. Sci. Ed.*, 2 (1980) 129.
26 T. Gough and P. Baker, *J. Chromatogr. Sci.*, 19 (1981) 227.
27 H. Neuman and M. Gloger, *Forensic Sci. Int.*, 22 (1983) 63.
28 W. Anderson and D. Stafford, *J. High Resolut. Chromatogr. Chromatogr. Commun.*, 6 (1983) 247.
29 B. Comparini, F. Centini and A. Pariali, *J. Chromatogr.*, 279 (1983) 609.
30 B. Perrigo, H. Peel and D. Ballantyne, *J. Chromatogr.*, 341 (1985) 81.
31 C. Lora-Tamayo, M. A. Rams and J. M. R. Chacon, *J. Chromatogr.*, 374 (1986) 73.
32 M. Chiarotti, A. Carnevale and N. DeGiovanni, *Forensic Sci. Int.*, 21 (1983) 245.

33 S. Alm, S. Jonson, H. Karlsson and E. Sundholm, *J. Chromatogr.*, 254 (1983) 179.
34 M. Japp, R. Gill and M. D. Osselton, *J. Forensic Sci.*, 32 (1987) 1574.
35 B. Pettitt, *J. High Resolut. Chromatogr. Chromatogr. Commun.*, 5 (1982) 45.
36 D. T. Chia and J. A. Gere, *Clin. Biochem.*, 20 (1987) 303.
37 P. Schepers, J. Witsbeek, J. P. Franke and R. A. de Zeeuw, *J. Forensic Sci.*, 27 (1982) 49.
38 A. Moffat, J. Jackson, M. Moss and B. Widdop (Editors), *Clarke's Isolation and Identification of Drugs in Pharmaceuticals, Body Fluids, and Post Mortem Material*, Pharmaceutical Press, London, 2nd ed., 1986, p. 1112–1120.
39 F. Poy, S. Visani and F. Terrosi, *J. Chromatogr.*, 217 (1981) 81.
40 F. Poy, *Chromatographia*, 16 (1982) 345.
41 G. Schomburg, H. Husmann, H. Behlau and F. Schulz, *J. Chromatogr.*, 279 (1983) 258.
42 G. Schomburg, H. Husmann, F. Schulz, G. Teller and M. Bender, *J. Chromatogr.*, 279 (1983) 259.
43 E. Loyola, M. Herraiz, G. Reglero and P. M. Alvarez, *J. Chromatogr.*, 398 (1987) 53.
44 M. Gloger, H. Neuman and V. Bissaria, Microgram, personal communication Aug., 1987).
45 *Catalog Handbook of Fine Chemicals*, Aldrich, Milwaukee, WI, U.S.A., 1988–89.

Journal of Chromatography, 538 (1991) 277–284
Elsevier Science Publishers B.V., Amsterdam

CHROM. 22 851

Collection of analytical data for benzodiazepines and benzophenones

Appendix

S. I. WESTON, M. JAPP*, J. PARTRIDGE and M. D. OSSELTON
Central Research and Support Establishment, Home Office Forensic Science Service, Aldermaston, Reading, Berkshire RG7 4PN (U.K.)
(First received June 13th, 1990; revised manuscript received September 25th, 1990)

ABSTRACT

An analytical database is presented for six benzodiazepines (clotiazepam, delorazepam, ethyl loflazepate, fludiazepam, haloxazolam and oxazolam) which are controlled in the U.K. Chromatographic, ultraviolet spectroscopic and mass spectrometric data are presented. Analytical data are also included for the benzophenones which have been prepared from the benzodiazepines.

INTRODUCTION

An earlier publication [1] detailed analytical data for twenty-seven of the thirty-three benzodiazepines which are controlled in the U.K. At the time of preparing the paper [1], six of the controlled benzodiazepines (clotiazepam, delorazepam, ethyl loflazepate, fludiazepam, haloxazolam and oxazolam) were unavailable for inclusion in the paper. Reference samples of these six drugs have now been obtained and an analytical database is presented as an appendix to the previous paper. Chromatographic properties have been measured including gas chromatography (GC) retention index (I) values, high-performance liquid chromatography (HPLC) capacity factors (k') and thin-layer chromatography (TLC) $R_F \times 100$ values. Ultraviolet (UV) spectroscopic data and mass spectrometric (MS) data are also given. Benzophenones have been prepared from the parent benzodiazepines and their GC, TLC and MS properties are also described.

EXPERIMENTAL

Materials

The benzodiazepines were from the drug collection of the Central Research and Support Establishment, Home Office Forensic Science Service. Benzophenones were prepared from the parent benzodiazepines by acid hydrolysis for 1 h followed by extraction into diethyl ether [2].

Methods

GC, HPLC, TLC and UV. The experimental conditions employed were identical to those described previously [1]. For HPLC and TLC, mixtures containing benzodiazepines and benzophenones, for which data had been obtained for the previous report, were run simultaneously with the six new benzodiazepines and their benzophenones. The measured capacity factors (k') and $R_F \times 100$ values of these new compounds were then corrected to standardise all data in the collection. For TLC of benzodiazepines, the $R_F \times 100$ values were corrected using the reference compounds described by Stead *et al.* [3].

For UV spectrophotometry, $E^{1\%}_{1cm}$ values were only calculated for those benzodiazepines which were completely soluble.

MS. The mass spectrometer was a VG Masslab Quadrupole 12-250 instrument interfaced to a PDP 11/73 data system.

Probe spectra of the benzodiazepines were collected over a mass range from 20 to 500 a.m.u. with a scan speed of 3 s per decade and a 0.1-s inter-scan delay.

GC–MS analysis of benzodiazepines and benzophenones was performed using a Hewlett-Packard 5890 gas chromatograph fitted with a DB1 narrow-bore capillary column (30 m × 0.25 mm I.D., 0.25 μm film thickness). Spectra were collected over a mass range from 20 to 500 a.m.u. with a scan speed of 1 s per decade and a 0.1-s inter-scan delay.

All other conditions were identical to those described previously [1].

RESULTS AND DISCUSSION

The chemical structures of the benzodiazepines are shown in Fig. 1. The benzophenones produced by acid hydrolysis of the parent benzodiazepines are listed alphabetically by chemical name in Table I and their chemical structures are shown in Fig. 2. Clotiazepam did not produce a benzophenone after acid hydrolysis; two products were obtained in minor quantities, detected by GC–MS (see Table VIII).

Table II lists the GC I values of the benzodiazepines and benzophenones on SE-30 equivalent narrow-bore and wide-bore capillary columns. Three of the benzodiazepines (ethyl loflazepate, haloxazolam and oxazolam) gave multiple peaks by decompositon and/or rearrangement. These benzodiazepines were not easily analysed by GC and concentrated solutions of the drugs were required for detection using a flame ionisation detector. The chromatograms obtained for ethyl loflazepate and haloxazolam were particularly complex. For ethyl loflazepate, the I values of the two major peaks only are given. Severe peak tailing was obtained for haloxazolam and the late eluting peak (I 2684) was very broad.

A list of HPLC k' values for benzodiazepines measured using four HPLC systems (A, B, C and D) is presented in Table III. Systems A and B (ODS-silica) contained 55% and 70% (v/v) methanol, respectively, to cover the wide range of polarities of benzodiazepines. System B was required to elute the more hydrophobic benzodiazepines, therefore only those benzodiazepines the k' values of which with system A were greater than 9 were eluted using system B. Haloxazolam and oxazolam each produced two peaks on the ODS-silica column; with the silica column only one peak was observed from each of these compounds. The multiple peaks obtained for haloxazolam and oxazolam are most likely due to decomposition, as pure samples of these drugs were received from the manufacturers.

Clotiazepam

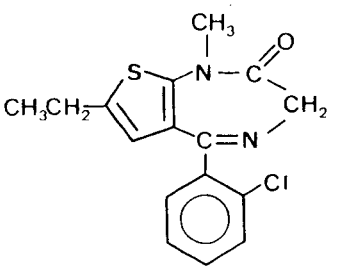

Fludiazepam

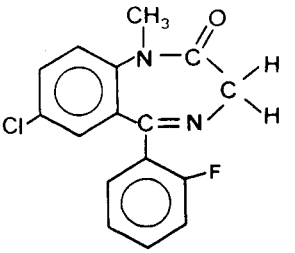

Delorazepam

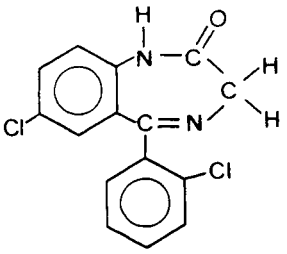

Haloxazolam

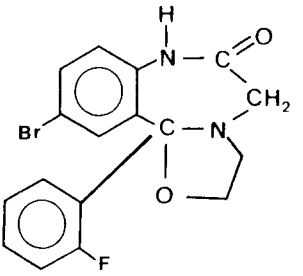

Ethyl loflazepate

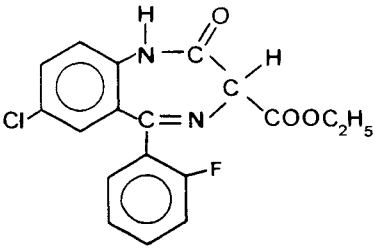

Oxazolam

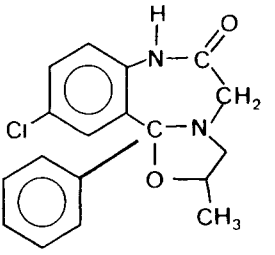

Fig. 1. Structures of benzodiazepines.

The TLC $R_F \times 100$ values for the benzodiazepines measured on three TLC systems are given in Table IV. The experimentally determined $R_F \times 100$ values have been corrected against the standard $R_F \times 100$ values of reference compounds [3] and it is the corrected values which are presented in Table IV. Haloxazolam and oxazolam gave multiple spots on the TLC plates and with system 3, tailing bands were obtained

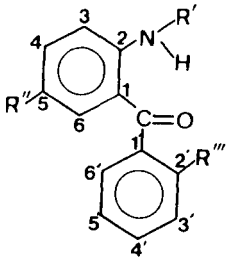

	R'	R''	R'''
ABFB :	H	Br	F
ACB :	H	Cl	H
ACFB :	H	Cl	F
ADCB :	H	Cl	Cl
MCFB :	CH_3	Cl	F

Fig. 2. Structures of benzophenones. For abbreviations see Table I.

for these compounds (probably due to decompositon). The benzodiazepines gave a yellow-brown or orange-brown colour with acidified iodoplatinate solution, except for ethyl loflazepate, which gave no reaction with this locating reagent.

For the benzophenones, the TLC $R_F \times 100$ values were measured on four TLC systems and the experimentally determined values are given in Table V. The reaction of the benzophenones to the Bratton–Marshall test [5] is also included.

Table VI contains ultraviolet absorption data for the benzodiazepines measured in acid, alkali and ethanol. The λ_{max} values and points of inflexion are presented and

TABLE I

BENZOPHENONES PRODUCED BY HYDROLYSIS OF BENZODIAZEPINES

Benzophenone	Abbreviation	Parent benzodiazepine
2-Amino-5-bromo-2'-fluorobenzophenone	ABFB	Haloxazolam
2-Amino-5-chlorobenzophenone	ACB	Oxazolam
2-Amino-5-chloro-2'-fluorobenzophenone	ACFB	Ethyl loflazepate
2-Amino-5,2'-dichlorobenzophenone	ADCB	Delorazepam
2-Methylamino-5-chloro-2'-fluorobenzophenone	MCFB	Fludiazepam
No benzophenone produced		Clotiazepam

TABLE II

GC RETENTION INDICES FOR BENZODIAZEPINES AND BENZOPHENONES ON SE-30 EQUIVALENT NARROW-BORE AND WIDE-BORE CAPILLARY COLUMNS

For compounds giving multiple peaks, minor peaks are shown in brackets.

Benzodiazepine or benzophenone	*I*	
	Narrow-bore capillary column	Wide-bore capillary column
2-Amino-5-bromo-2′-fluorobenzophenone (ABFB)	2079	2090
2-Amino-5-chlorobenzophenone (ACB)	2005	2028
2-Amino-5-chloro-2′-fluorobenzophenone (ACFB)	1987	2004
2-Amino-5,2′-dichlorobenzophenone (ADCB)	2128	2141
Clotiazepam	2513	2530
Delorazepam	2571	2593
Ethyl loflazepate	2442[a] (3010)	2439, 2935
Fludiazepam	2389	2408
Haloxazolam	2560[a] (2302[b], 2684[b])	2572[a] (2323[b], 2695[b])
2-Methylamino-5-chloro-2′-fluorobenzophenone (MCFB)	2060	2055
Oxazolam	2564 (2586)	2569 (2596)

[a] Peak tailing.
[b] Severe peak tailing.

for those benzodiazepines completely soluble in aqueous solution or ethanol, the $E^{1\%}_{1cm}$ values have been determined for the wavelengths of maximum absorbance.

The GC–electron ionisation (EI)-MS data for benzodiazepines and benzophenones are given in Tables VII and VIII, respectively, as listings of the eight most intense ions and relative intensities. Also included in Table VII is a similar listing for

TABLE III

HPLC CAPACITY FACTORS FOR BENZODIAZEPINES ON FOUR HPLC SYSTEMS

Systems: A = methanol–water–phosphate buffer (0.1 *M*) (55:25:20, v/v/v), ODS-Hypersil; B = methanol–water–phosphate buffer (0.1 *M*) (70:10:20, v/v/v), ODS-Hypersil; C = methanol (1000 ml) containing perchloric acid (100 μl), Spherisorb S5W; D = methanol–water–trifluoroacetic acid (997:2:1, v/v/v), Spherisorb S5W.

Benzodiazepine	*k′*			
	System A	System B	System C	System D
Clotiazepam	15.8	2.87	1.89	4.15
Delorazepam	6.46	–	0.85	1.04
Ethyl loflazepate	12.50	2.17	0.08	0.08
Fludiazepam	6.70	–	0.99	1.25
Haloxazolam	6.80, 10.75	2.13	2.19	5.40
Oxazolam	19.25, 22.95	3.48, 3.87	1.77	4.05

TABLE IV

TLC R_F × 100 VALUES FOR BENZODIAZEPINES ON THREE TLC SYSTEMS

Systems: 1 = cyclohexane–toluene–diethylamine (75:15:10, v/v/v), TLC plates pre-treated with methanolic KOH (0.1 *M*) [1]; 2 = chloroform–methanol (90:10, v/v), TLC plates pre-treated with methanolic KOH (0.1 *M*) [1]; 3 = chloroform–acetone (80:20, v/v).

Benzodiazepine	R_F × 100 value		
	System 1	System 2	System 3
Clotiazepam	33	70	53
Delorazepam	45	54	35
Ethyl loflazepate	0	58	50
Fludiazepam	23	70	51
Haloxazolam	3, 10	47, 66	44, 23 (12-32)[a]
Oxazolam	3, 11, 15	56,68	51[b]

[a] Broad tailing band.
[b] Tailing.

TABLE V

TLC R_F × 100 VALUES FOR BENZOPHENONES ON FOUR TLC SYSTEMS

Systems: 4 = toluene; 5 = toluene–isopropanol–ammonia (sp. gr. 0.880) (85:15:1, v/v/v); 6 = chloroform–methanol (90:10, v/v); 7 = chloroform–acetone (80:20, v/v). NR = No reaction. For abbreviations see Table I.

Benzophenone	R_F × 100 value				Reaction to Bratton–Marshall test
	System 4	System 5	System 6	System 7	
ABFB	20	63	70	63	Purple
ACB	16	63	70	64	Purple
ACFB	19	63	69	62	Purple
ADCB	21	63	70	63	Purple
MCFB	35	70	76	66	NR

TABLE VI

ULTRAVIOLET ABSORPTION DATA FOR BENZODIAZEPINES

Specific absorbance values are shown in parentheses after the corresponding λ_{max} value. ND = Not determined, insoluble.

Benzodiazepine	λ_{max} (nm) and specific absorbance measured in 0.1 *M* sulphuric acid	λ_{max} (nm) and specific absorbance measured in 0.1 *M* sodium hydroxide	λ_{max} (nm) and specific absorbance measured in absolute ethaol
Clotiazepam	214 (686), 261 (618), 302[a], 392 (153)	239, 351	212 (914), 243 (690), 319 (89)
Delorazepam	239, 286, 366	230, 274[a], 343	228 (1165), 257[a], 320
Ethyl loflazepate	ND	235 (852), 346 (70)	229 (1072), 318
Fludiazepam	240 (929), 283 (389), 364 (109)	233, 250[a], 312	229 (1086), 253[a], 316
Haloxazolam	243 (837), 286, 375	ND	247 (402)
Oxazolam	238 (930), 281 (272), 306[a], 369 (98)	ND	245 (422)

[a] Point of inflexion.

TABLE VII

MOLECULAR WEIGHTS AND EIGHT MOST INTENSE IONS OBSERVED USING EI CONDITIONS FOR BENZODIAZEPINES

Benzodiazepine	Molecular weight	*m/z* (% intensity)	
		Probe (EI)	Capillary GC (EI)
Clotiazepam	318	289 (100), 318 (56), 291 (42), 275 (32) 290 (23), 39 (22), 320 (20), 45 (16)	289 (100), 318 (64), 291 (38), 320 (24) 290 (24), 275 (23), 319 (16), 283 (15)
Delorazepam	305	275 (100), 269 (97), 277 (90), 304 (84) 303 (67), 276 (65), 306 (63), 305 (56)	275 (100), 269 (93), 304 (86), 277 (83) 36 (75), 303 (62), 276 (60), 306 (58)
Ethyl loflazepate	360	259 (100), 287 (54), 288 (46), 261 (38) 260 (28), 289 (23), 223 (17), 286 (14)	260[a] (100), 259 (100), 288 (74), 287 (67) 216 (67), 75 (62), 102 (49), 262 (38)
Fludiazepam	302	274 (100), 302 (81), 301 (81), 275 (46) 273 (41), 303 (40), 276 (35), 283 (33)	274 (100), 301 (85). 302 (79), 275 (48) 273 (44), 303 (40), 276 (38), 283 (33)
Haloxazolam	377	283 (100), 281 (100), 206 (33), 123 (24) 56 (17), 282 (16), 284 (15), 95 (12)	43[a] (100), 295 (50), 293 (50), 294 (42) 292 (36), 42 (26), 213 (13), 276 (12)
			305[a] (100), 303 (99), 304 (39), 209 (35) 182 (32), 183 (29), 306 (22), 181 (22)
			305[a] (100), 226 (78), 307 (49), 303 (49) 276 (36), 278 (34), 197 (31), 183 (27)
			210[a] (100), 333 (83), 335 (81), 183 (74) 211 (73), 291 (52), 290 (49), 289 (47)
Oxazolam	328	251 (100), 253 (42), 70 (33), 252 (19) 77 (18), 105 (17), 283 (11), 42 (11)	241[a] (100), 243 (36), 191 (29), 242 (23) 240 (23), 102 (23), 164 (20), 103 (19)
			251[a] (100), 70 (45), 253 (36), 42 (22) 77 (21), 41 (19), 105 (18), 252 (15)

[a] Decomposition product.

TABLE VIII

MOLECULAR WEIGHTS AND EIGHT MOST INTENSE IONS OBSERVED USNG EI CONDITIONS FOR BENZOPHENONES

For abbreviations of benzophenones, see Table I.

Benzophenone	Molecular weight	*m/z* (% intensity), capillary GC (EI)
ABFB	294	293 (100), 295 (97), 123 (88), 294 (79) 292 (67), 95 (63), 91 (34), 63 (34)
ACB	231	230 (100), 231 (74), 77 (54), 232 (43) 105 (30), 233 (25), 154 (22), 126 (17)
ACFB	249	249 (100), 248 (86), 123 (57), 95 (44) 154 (42), 250 (41), 251 (34), 126 (28)
ADCB	265	230 (100), 265 (52), 139 (40), 267 (34) 154 (34), 232 (33), 111 (33), 126 (25)
MCFB	263	263 (100), 246 (66), 211 (61), 262 (50) 265 (41), 95 (37), 123 (36), 264 (35)
Clotiazepam acid hydrolysis products		
1		111 (100), 264 (92), 139 (75), 279 (71) 244 (65), 229 (62), 228 (58), 152 (54)
2		255 (100), 284 (58), 256 (30), 283 (20) 241 (19), 198 (13), 77 (13), 285 (11)

benzodiazepines, from spectra obtained after sample introduction via the direct insertion probe.

Thermal degradation occurred during the capillary GC–MS analysis of some of the benzodiazepines [4]. The spectra of the decomposition products are also listed in Table VII. For ethyl loflazepate, haloxazolam and oxazolam, concentrated solutions of the drugs were required to obtain mass spectra. The GC–MS analysis of haloxazolam was especially complex and four spectra were obtained for the major components from this compound. For ethyl loflazepate, GC–MS analysis gave only one mass spectrum; the molecular ion of the parent compound (*m/z* 360) was not observed.

Also included in Table VIII are the relative intensities of the eight most intense ions for the two products from the acid hydrolysis of clotiazepam.

REFERENCES

1 M. Japp, K. Garthwaite, A. V. Geeson and M. D. Osselton, *J. Chromatogr.*, 439 (1988) 317.
2 H. Schütz, *Benzodiazepines, A Handbook, Basic Data, Analytical Methods, Pharmacokinetics and Comprehensive Literature*, Springer, Heidelberg, 1982.
3 A. H. Stead, R. Gill, T. Wright, J. P. Gibbs and A. C. Moffat, *Analyst (London)*, 107 (1982) 1106.
4 J. Zamecnik, J.-C. Ethier and G. A. Neville, *Can. Soc. Forens. Sci. J.*, 22 (1989) 233.
5 A. C. Bratton and E. K. Marshall, *J. Biol. Chem.*, 128 (1939) 537.

Journal of Chromatography, 538 (1991) 285–292
Elsevier Science Publishers B.V., Amsterdam

CHROM. 22 840

Computer simulations of displacement chromatography of systems with species-dependent saturation capacities

QIMING YU and DUONG D. DO*
Department of Chemical Engineering, The University of Queensland, Queensland 4072 (Australia)
(First received March 22nd, 1990; revised manuscript received September 11th, 1990)

ABSTRACT

Displacement chromatography of systems with Langmuir adsorption isotherms and species-dependent saturation capacities were analyzed and simulated with a general rate equation model. Conditions for the development of displacement train were derived and the effects of saturation capacity, initial slope and amount of the displacer on the displacement development were illustrated.

INTRODUCTION

Displacement chromatography has become an increasingly important column technique in the recovery and purification of biochemicals in large scale, because it is capable of producing concentrated products with high throughput. Recently, much effort has been devoted to the analyses of the column dynamics of displacement chromatography under ideal conditions [1–3] and non-ideal conditions [4–7]. These analyses provide useful guidelines for the design, scale up and optimization of displacement chromatography.

All the above mentioned studies have been restricted to systems with simple equilibrium isotherms. Standard Langmuir isotherms are used for adsorption and constant separation factors for ion exchange. It is generally required that the isotherm of the displacer lies above the isotherms of all solutes over the whole concentration range (Fig. 1D). The displacer has a higher affinity to the sorbent than all solutes, and it also has a higher or same saturation concentration [8]. For this reason, displacer components with small molecular weight are often used at high concentrations to effect the displacement.

The effects of species-dependent column capacities on the separation efficiencies in isocratic elution processes have been studied [9]. In this paper, the effects of species-dependent capacities on displacement development were analyzed. Langmuir adsorption kinetics with species-dependent saturation capacities and a general rate equation model, which includes axial dispersion, film diffusion, particle diffusion, and non-linear adsorption kinetics, were used to simulate the column dynamics in detail. Effects of saturation capacity, affinity, and amount of the displacer on the

0021-9673/91/$03.50

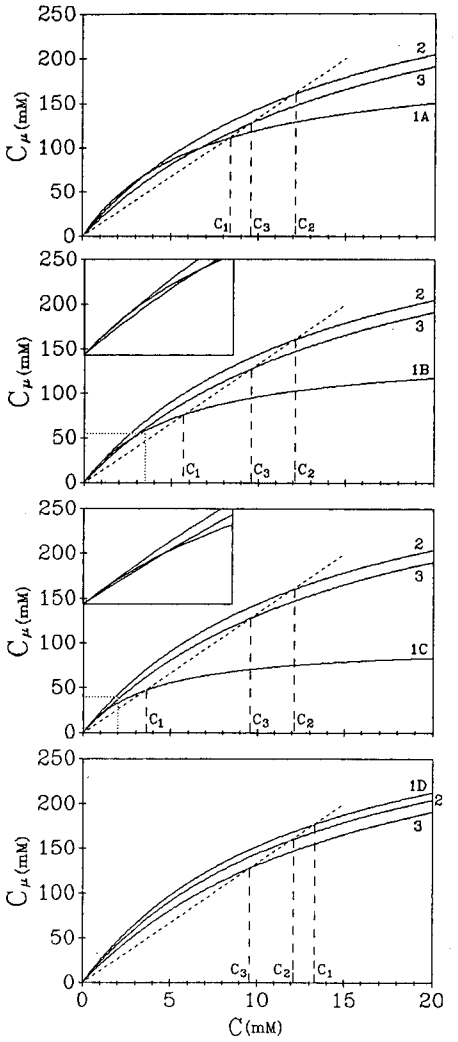

Fig. 1. Single component isotherms showing concentrations of fully developed displacement trains. All parameters are listed in Table I.

displacement train were illustrated with computer simulations. This study indicates that large molecules with low concentrations can also be used as displacers.

THEORETICAL ANALYSIS

Rate equation model and adsorption kinetics

A general rate equation model, which includes axial dispersion, film diffusion, particle diffusion, and adsorption kinetics, was used in the simulation of displacement chromatography. The details of the model description and solution procedure based

on the method of orthogonal collocation on finite elements were reported elsewhere [7], and the Langmuir adsorption kinetics with species-dependent saturation capacities were assumed in this study. The net rate of adsorption of solute i per unit solid volume of the stationary phase can be expressed as follows.

$$f(i) = k_a(i)C(i)\left(1 - \sum_{j=1}^{NC} \frac{C_\mu(j)}{C_{\mu s}(j)}\right) - k_d(i)\left(\frac{C_\mu(i)}{C_{\mu s}(i)}\right) \tag{1}$$

When the adsorption and desorption rates are faster than the diffusion rate, the local equilibrium prevails. The expression describing this local equilibrium is

$$C_\mu(i) = \frac{C_{\mu s}(i)b(i)C(i)}{1 + \sum_{j=1}^{NC} b(j)C(j)} \tag{2}$$

where $b(i) = k_a(i)/k_d(i)$.

Band concentrations and conditions of displacement development

In fully developed displacement bands, all the solute bands have the same concentration velocity. The band concentrations can be determined from the single component isotherms and the displacer concentration, as illustrated in Fig. 1, where the isotherm parameters are listed in Table I. The band concentration of species i displaced by the displacer 1 is given by:

$$C(i)_{BAND} = \frac{C_{\mu s}(i)}{C_{\mu s}(1)}C(1) - \left(\frac{1}{b(i)} - \frac{C_{\mu s}(i)}{C_{\mu s}(1)b(1)}\right) \tag{3}$$

Eqn. 3 indicates that the band concentration of a solute increases with the displacer concentration and is independent of its feed concentration. The necessary conditions for displacement development can be also derived from the above equation. They are

$$b(1)C_{\mu s}(1) > b(i)C_{\mu s}(i) \tag{4}$$

TABLE I

ISOTHERM PARAMETERS USED IN SIMULATION

Parameter	Value					
	1A	1B	1C	1D	2	3
k_a (1/s)	15	18	25	7.714	7	6
k_d (mM/s)	100	100	100	100	100	100
b (1/mM)	0.15	0.18	0.25	0.07714	0.07	0.06
$C_{\mu s}$ (mM)	200	150	100	350	350	350
$bC_{\mu s}$	30	27	25	27	24.5	21

$$\frac{C(1)}{C_{\mu s}(1)} > \frac{C(i)_{\mathrm{BAND}}}{C_{\mu s}(i)} + \left(\frac{1}{C_{\mu s}(i)b(i)} - \frac{1}{C_{\mu s}(1)b(1)}\right) \tag{5}$$

Eqn. 4 requires that the initial slope of the displacer must be higher than that of the solutes, while eqn. 5 gives the minimum displacer concentration to yield a band concentration of $C(i)_{\mathrm{BAND}}$ of the species i. This is equivalent to the classic condition that the chord slope of the displacer larger than the slope of the solute [2]. When $C(i)_{\mathrm{BAND}} = 0$, eqn. 5 gives the minimum displacer concentration for the onset of any displacement development of the solute i, and when $C(i)_{\mathrm{BAND}} \geqslant C_{\mathrm{f}}(i)$ a displacement factor higher than unity is achieved.

The third necessary condition for displacement development is a sufficient amount of displacer which maintains the displacer front in contact with the solutes. The minimum amount required can be determined from the slope and the chord slope of the displacer [3].

$$\Delta T_2 = \left(\frac{1-\varepsilon_b}{\varepsilon_b}\right)(1-\varepsilon_m)\left[\left(\frac{C_\mu}{C}\right)_1 - \left(\frac{dC_\mu}{dC}\right)_1\right] = \left(\frac{1-\varepsilon_b}{\varepsilon_b}\right)(1-\varepsilon_m)\left(\frac{b(1)C_{\mu s}(1)}{1+b(1)C(1)}\right)\left(\frac{C(1)}{C_{\mu s}(1)}\right) \tag{6}$$

Finally, from eqn. 3, the band concentrations are calculated from the affinity constants and the saturation capacities of the displacer and the solutes.

Same band concentrations can be obtained with different displacers (1A and 1B) under the following equivalent displacer condition, which is derived from eqn. 3.

$$\left(\frac{b(1\mathrm{A})C_{\mu s}(1\mathrm{A})}{1+b(1\mathrm{A})C(1\mathrm{A})}\right) = \left(\frac{b(1\mathrm{B})C_{\mu s}(1\mathrm{B})}{1+b(1\mathrm{B})C(1\mathrm{B})}\right) \tag{7}$$

Eqn. 7 implies that, under ideal conditions, if the chord slopes of the displacer 1A and 1B are the same, identical displacement trains can be formed. Under those conditions, the minimum amount of the displacer required can also be compared. From eqns. 6 and 7, if the initial slope of the displacer 1A is larger [$b(1\mathrm{A})C_{\mu s}(1\mathrm{A}) > b(1\mathrm{B})C_{\mu s}(1\mathrm{B})$], the minimum amount of the displacer required will be larger [$\Delta T_2(1\mathrm{A}) > \Delta T_2(1\mathrm{B})$]. This will also leads to a longer tailing in the regeneration step.

TABLE II

PHYSICAL PARAMETERS USED IN SIMULATION

Parameter	Value			Parameter	Value
	1A-1D	2	3		
C_f (mM)	3.3	4	4	u (cm^2/s)	0.004
D_p (cm/s)	$8 \cdot 10^{-7}$	$8.5 \cdot 10^{-7}$	$9 \cdot 10^{-7}$	L (cm)	25
				ε_b	0.35
				ΔT	2
				R_p (μm)	20
				ε_m	0.3

RESULTS AND DISCUSSION

In this section, detailed column dynamics of displacement chromatography were simulated to illustrate the effects of operational parameters. The physical parameters used in all the simulations are listed in Table II, unless otherwise stated.

The effects of displacer concentrations on the displacement development are similar to those in literature [5,6]. The effects of the affinity (b_1), saturation capacity ($C_{\mu s1}$), and initial slope ($b_1 C_{\mu s}$) were given in eqn. 3 and illustrated in Fig. 2a–c. For a given solute, its band concentration increases with decreasing $C_{\mu s1}$ and $b_1 C_{\mu s1}$ values. In Fig. 2a–c, both $C_{\mu s1}$ and $b_1 C_{\mu s1}$ were reduced and hence the displacement effect increases. In Fig. 2c, the solute 3 band is affected by the non-ideal effects (mass transfer resistances) where the band concentration is lower than that predicted by the ideal theory (eqn. 3).

The displacement effluent histories under the equivalent displacer conditions are shown in Fig. 3a–c. The initial slopes of the displacers in Fig. 3a and b are the same; hence the effluent histories are idential. In Fig. 3c, the initial slope of the displacer is

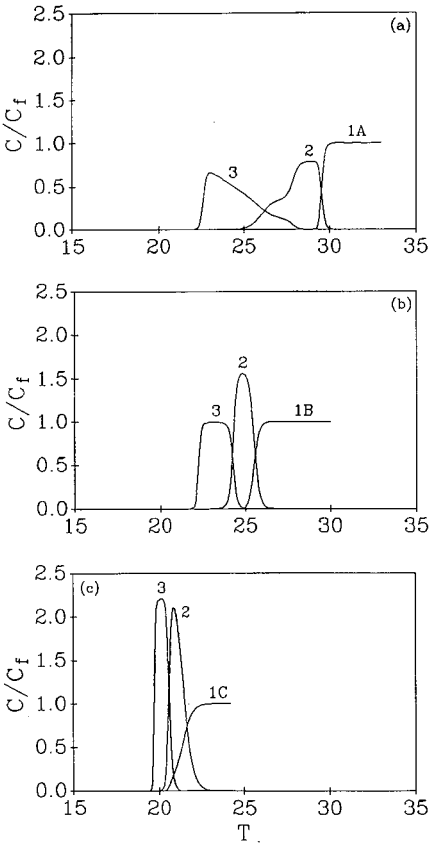

Fig. 2. Effect of displacer affinity on effluent histories. (a) $C_{\mu s} = 200$ mM; $b_1 = 0.15$ mM^{-1}; (b) $C_{\mu s} = 150$ mM, $b_1 = 0.18$ mM^{-1}; (c) $C_{\mu s} = 100$ mM, $b_1 = 0.25$ mM^{-1}.

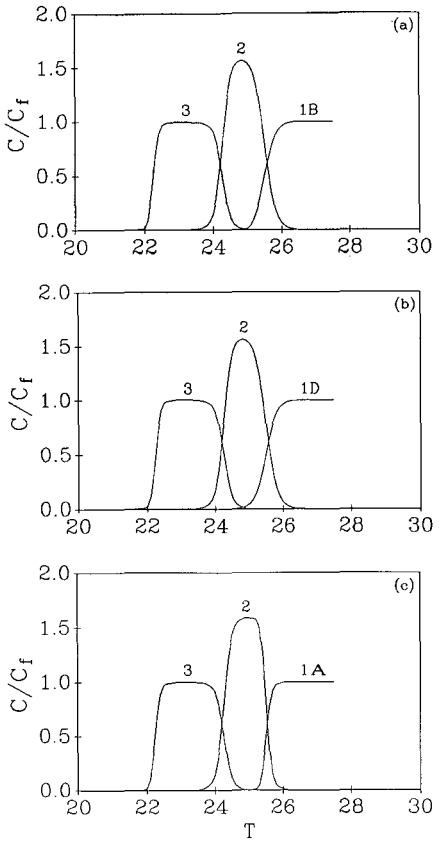

Fig. 3. Displacement under equivalent displacer conditions. (a) $C_{\mu s} = 150\,\mathrm{m}M$, $b_1 = 0.18\,\mathrm{m}M^{-1}$, $C_1 = 3.3\,\mathrm{m}M$; (b) $C_{\mu s} = 350\,\mathrm{m}M$, $b_1 = 0.077\,\mathrm{m}M^{-1}$, $C_1 = 7.7\,\mathrm{m}M$; (c) $C_{\mu s} = 200\,\mathrm{m}M$, $b_1 = 0.15\,\mathrm{m}M^{-1}$, $C_1 = 5.141\,\mathrm{m}M$.

larger than those used in Fig. 3a and b. The breakthrough curve of the displacer in Fig. 3c is slightly sharper. The band of solute 2, which is in contact with the displacer, is also slughtly sharper. On the other hand, the band of solute 3 is the same as those observed in Fig. 3a and b.

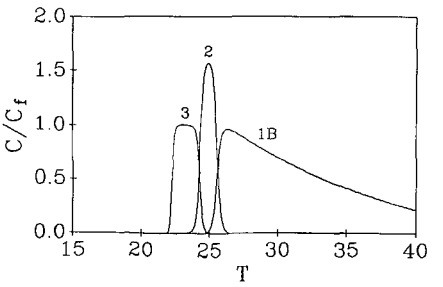

Fig. 4. Displacement under minimum amount of displacer. $\Delta T_2 = 9$.

Fig. 4 shows the displacement effluent histories when the minimum amount of the displacer (eqn. 6) is used. This minimum amount is needed to maintain the displacement bands as in Fig. 3a–c. A lesser amount of the displacer will cause the displacement bands to be degraded into elution peaks, while a larger amount only contributes to a longer regeneration time.

CONCLUSIONS

Displacement chromatography of systems with species-dependent saturation concentrations were analyzed and computer simulations with a general rate equation model were used to illustrate the effects of displacer saturation capacity and initial slope on the displacement dynamics.

Displacement can be developed only when the initial slope of the displacer is larger than those the solutes (eqn. 4), the displacer concentration is high enough (eqn. 5), and the displacer amount is large enough (eqn. 6). Under equivalent displacer conditions (eqn. 7), similar displacement profiles can be developed with different displacers and lower displacer concentration can be used if the displacer has a smaller saturation capacity. A displacer with a smaller initial slope will require less amount of the displacer and shorter regeneration time.

SYMBOLS

$b(j)$	Langmuir affinity constant of component $j(=k_a(j)/k_d(j))$
$C(j)$	concentration of component j in fluid phase
$C_\mu(j)$	concentration of component j in solid phase
$C_f(j)$	feed concentration of component j
$C_{\mu s}(j)$	saturation concentration of component j in solid phase
$D_p(j)$	effective diffusivity of component j
$f(j)$	net rate adsorption of component j per unit solid volume
$k_a(j)$	adsorption rate constant of component j
$k_d(j)$	desorption rate constant of component j
L	column length
NC	number of components
R_p	particle radius
t	time
T	dimensionless time $= tu/L\varepsilon_b$
u	superficial velocity
ΔT	dimensionless feed volume
ΔT_2	dimensionless amount of displacer
ε_b	bed void fraction
ε_m	particle porosity

ACKNOWLEDGEMENT

Support from Research Excellence Grant Scheme is gratefully acknowledged.

REFERENCES

1 F. Helfferich and D. B. James, *J. Chromatogr.*, 46 (1970) 1.
2 H. K. Rhee and N. R. Amundson, *AIChE J.*, 28 (1982) 423.
3 Q. Yu and N. H. L. Wang, *Sep. Purif. Methods*, 15 (1986) 127.
4 S. Golshan-Shirazi, B. Lin and G. Guiochon, *Anal. Chem.*, 61 (1989) 1960.
5 A. M. Katti and G. Guiochon, *J. Chromatogr.*, 449 (1988) 25.
6 M. W. Phillips, G. Subramanian and S. M. Cramer, *J. Chromatogr.*, 454 (1988) 1.
7 Q. Yu, T. S. Nguyen and D. D. Do, *Prep. Chromatogr.*, in press.
8 A. Nahum, *Ph.D. Thesis*, Yale University, New Haven, CT, 1981.
9 G. B. Cox and L. R. Snyder, *J. Chromatogr.*, 483 (1989) 95.

Journal of Chromatography, 538 (1991) 293–301
Elsevier Science Publishers B.V., Amsterdam

CHROM. 22 825

Properties and biomedical applications of packings with high-density coverage of C_{18} chemically bonded phase for high-performance liquid chromatography and solid-phase extraction[a]

BOGUSŁAW BUSZEWSKI[b]
Institute of Organic Chemistry, University of Tübingen, Auf der Morgenstelle 18, D-7400 Tübingen (F.R.G.)
(First received April 25th, 1990; revised manuscript received May 18th, 1990)

ABSTRACT

A series of packing materials with high-density coverage of chemically bonded C_{18} phases ($\alpha_{RP} \geqslant 2.8$ μmol/m^2) for high-performance liquid chromatography (HPLC) and clean-up solid-phase extraction columns were prepared. The resulting packings were characterized by different physico-chemical methods including porosimetric and elemental analysis, cross-polarization magic angle spinning NMR and HPLC. The packings prepared were used for the purification by solid-phase extraction, isolation and determination of various analytes present in different biological samples.

INTRODUCTION

In spite of the elaboration and successive introduction of new types of packings for reversed-phase high-performance liquid chromatography (RP-HPLC), *e.g.*, porous graphitic carbon, carbosil and polymers [1–3], packings with chemically bonded phases (CBP) have been increasingly used. This is a result of their physico-chemical properties and relatively greater stability under the conditions of the elution process. Moreover, the possibility of preparing packings with different functional groups, *e.g.*, NH_2, NO_2 or CN [4,5], has led to an increase in separation selectivity.

In order to improve the separation selectivity and the stability of the chemically bonded film formed on the siliceous support surface, a packing with high-density coverage was developed [6,7]. Using these packing materials, an increase in hydrophobic chain–chain and chain–solute interactions has been observed [8]. On the other hand, the influence of silanol groups is limited because these active groups are

[a] Presented at the *11th International Symposium on Biomedical Applications of Chromatography and Electrophoresis, Tallinn, April 24–28th, 1990.*

[b] Permanent address: Department of Chemical Physics, Faculty of Chemistry, Maria Curie Skłodowska University, PL-20 031 Lublin, Poland.

0021-9673/91/$03.50

effectively screened by long alkyl chains, so that interaction between residual silanols and polar solutes is almost impossible [8,9]. The reproducibility of the retention data and prolongation of the lifetime of these packings [10] are very important in routine clinical, biomedical, biochemical and pharmacological analysis.

Most of these applications relate to the separation of polar substances. Their separation using conventionally manufactured packing materials often gives repeatedly unsatisfactory results. Considering that clinical, biochemical and/or pharmaceutical analysis involves biological matrices, *e.g.* urine, blood, serum and tissue, which contain potentially interfering constituents, it is necessary to carry out an initial purification of these samples, without a quantitative or qualitative loss of the compounds to be determined. For this purpose, solid-phase extraction (SPE) on off-line clean-up columns can be ideal [11,12]. As a consequence, the purification and preconcentration of substances to be determined is possible, and a higher degree of analytical sensitivity can be obtained.

In this paper, the physico-chemical and chromatographic properties of packings with a high-density coverage of chemically bonded C_{18} phases are presented for analyses by RP-HPLC and SPE, using various biological samples as a test substances.

EXPERIMENTAL

Materials and reagents

Two types of silica gel, SG-7/G and SG-100, prepared in the Polymer Institute of Sciences (Bratislava, Czechoslovakia) [13,14], were used as the support for the preparation of chemically bonded phases (CPBs) for HPLC and clean-up SPE columns. The surface physico-chemical characteristics of the bare materials are given in Table I.

For chemical modification, momofunctional (MC_{18}), difunctional (DC_{18}) and/or trifunctional (TC_{18}) octadecylchlorosilanes (Wacker, Munich, F.R.G.) were used, and especially prepared morpholine was employed as an activator [15] (Riedel de Haën, Seelze, F.R.G.). All solvents, *e.g.*, toluene, benzene, hexane, methanol, acetonitrile and water (Merck, Darmstadt, F.R.G.), were of analytical-reagent grade.

Stainless-steel tubes (125 × 4.6 mm I.D.) were purchased from Grom and Stagroma (Herrenberg, F.R.G.).

TABLE I

PHYSICO-CHEMICAL PROPERTIES OF BARE SILICA GELS USED AS PACKING MATERIALS IN HPLC AND SPE COLUMNS

Type of silica	Fraction d_p (μm)	Porosity[a]			α_{SiOH}[b]	Use
		S_{BET}	V_p	D		
SG-7/G	7	361	2.1	20	5.21	HPLC
SG-100	43–65	196	2.1	>23	4.93	SPE

[a] S_{BET} = specific surface area (m^2/g); V_p = pore volume (cm^3/g); D = mean pore diameter (nm).
[b] α_{SiOH} = concentration of silanol groups ($\mu mol/m^2$).

TABLE II

CHARACTERISTICS OF PACKINGS WITH CHEMICALLY BONDED PHASES (CBP)

No. of packing	Type of packing	Type of CBP structure[a]	Coverage[b]		
			P_c	α_{RP}	α_{SiOH}
1	SG-7/G–$^{M}C_{18}$	M	15.23	2.20	2.97
2	SG-7/G–$^{M}C_{18}$	M	19.64	3.04	2.26
3	SG-7/G–$^{M}C_{18}$	M	25.53	4.25	0.82
4	SG-100–$^{M}C_{18}$	M	15.75	4.20	–
5	SG-100–$^{M}C_{18}$	M	8.46	2.02	–
6	SG-100–$^{M}C_{18}$	T	13.21	3.72	–

[a] M = monomeric structure of CBP; T = polymeric structure of CBP.

[b] P_c = measured carbon percentage (%); α_{RP} = degree of alkylsilyl ligand coverage (μmol/m^2); α_{SiOH} as in see Table I.

Chemical bonding procedure

The chemical surface modification was carried out in glass reactors under nitrogen. The method, mechanism and reaction conditions have been described previously [16,17]. The parameters characterizing the coverage density of prepared packings are listed in Table II.

Preparation of columns

A slurry of 2 g of the prepared HPLC phases in 35 ml of isopropanol was placed in an ultrasonic bath for 5 min and then filled into the column using 150 ml of methanol as a packing solvent. All HPLC columns were packed under a pressure of 50 MPa with a Shandon (Frankfurt, F.R.G.) packing pump according to the procedure described earlier [18].

The SPE columns were prepared by packing 2-ml plastic extraction tubes with the appropriate dry materials to a bed height of 2 cm.

Apparatus

The porosity parameters of the materials (S_{BET} = specific surface area, V_p = pore volume, D = mean pore diameter) were determined by low adsorption–desorption of liquid nitrogen using a Sorptomatic Model 1800 instrument (Carlo Erba, Milan, Italy).

The degree of alkylsilyl ligand coverage on the surface of the prepared packings was calculated from the carbon content, determined with a CHN Model 240 analyser (Perkin-Elmer, Norwalk, CT, U.S.A.).

Solid-state NMR measurements were performed on a Brucker MSL 200 spectrometer with samples of 200–300 mg in double-bearing rotors of ZrO_2. Magic angle spinning (MAS) was carried out at a spinning rate of 4 kHz. ^{29}Si cross-polarization (CP)-MAS NMR spectra were recorded with a pulse length of 5 μs together with a contact time of 5 ms and a pulse repetition time of 2 s. For ^{13}C CP-MAS NMR spectra a contact time of 12 ms was used. All NMR spectra were externally referenced to liquid tetramethylsilane; chemical shifts are given in parts per million (ppm).

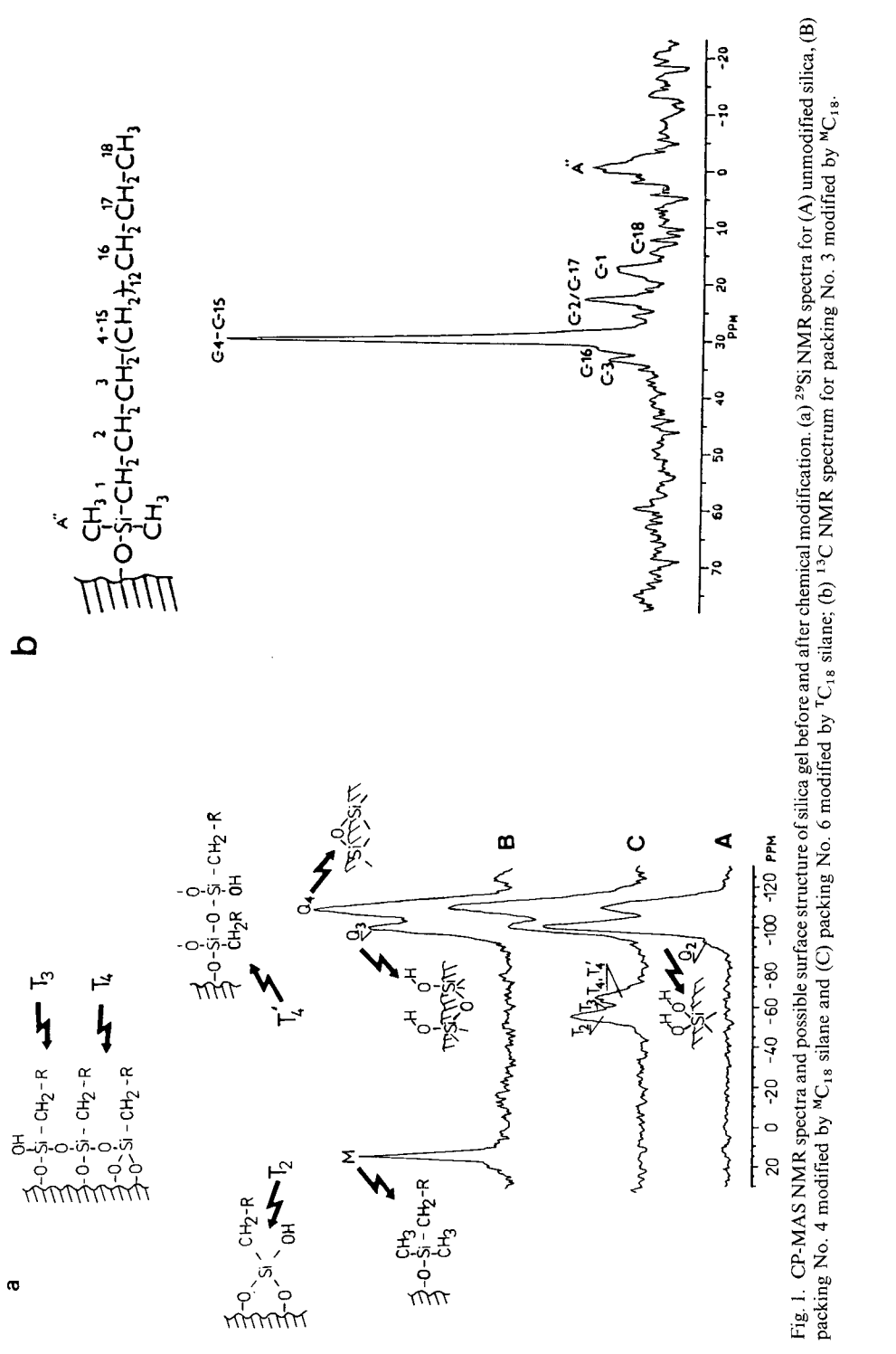

Fig. 1. CP-MAS NMR spectra and possible surface structure of silica gel before and after chemical modification. (a) ^{29}Si NMR spectra for (A) unmodified silica, (B) packing No. 4 modified by $^{M}C_{18}$ silane and (C) packing No. 6 modified by $^{T}C_{18}$ silane; (b) ^{13}C NMR spectrum for packing No. 3 modified by $^{M}C_{18}$.

RESULTS AND DISCUSSION

Characterization of CBP

In previous papers [9,10] it has been shown that by changing the preparation conditions of the chemically bonded phase (CBP) (specifically the molar ratios of individual reaction compounds), it is possible to obtain packing materials with a controlled density of coverage of CBP.

Table II presents the values characterizing the density of coverage of C_{18} CBP. From these data it appears that using silica with wide pores (Table I) as a support for CBP, packings with a high-density coverage were obtained ($\alpha_{RP} \geqslant 4.0$ μmol/m^2). Moreover, comparing α_{RP} and α_{SiOH} values, it can be seen that more than 85% of the surface-accessible silanol groups have been efficiently blocked by alkylsilyl ligands. Consequently, the packings obtained could be considered as homogeneously covered. This is confirmed by ^{29}Si and ^{13}C CP-MAS NMR spectra, as show in Fig. 1. These spectra also give information about the structure of the CBP formed during the chemical modification process [19,20].

Analysis of the example spectra shows that covalent siloxane bonds have been formed between the silica support surface and the chemical modifier (peak M in Fig. 1a, $\delta = +13$ ppm, and peak A″ in Fig. 1b, $\delta = +2.3$ ppm). Associated with the increase in α_{RP} values, there is a decrease in the individual silanol group content, *e.g.*, Q_2, $\delta = -91$ ppm; Q_3, $\delta = -100$ ppm; Q_4, $\delta = -108$ ppm [9,19,20]. Monofunctional silane gives pure monomeric structures of CBP with the creation of single $\equiv$Si–O–Si$\equiv$ bonds, but using trifunctional silane a polymeric network structure of CBP was obtained (peaks T_2, $\delta = -56$ ppm; T_3, $\delta = -60$ ppm; T_4 and T_4, $\delta = -66$ ppm) (Fig. 1a) [10,21]. These structures of CBP contain a relatively large population of the residual silanol groups.

HPLC applications

It is known that unblocked, residual silanol groups can play an important role in the elution process of solutes. This has been demonstrated by considerable differences in the capacity factor (k') values, low resolution (R_s) values and peak tailing (*i.e.*, higher asymmetry factor, f_{As}). The last effect is especially important during the routine analysis of polar substances, where the interactions between the analyte substances and the residual silanol groups is more apparent. Fig. 2 shows example chromatograms of five purines separated from blood serum, run on two columns filled with packings with different values of α_{RP}. The retention data (k') for all three columns are listed in Table III.

Comparing the k' values, it can be seen that changing the coverage density leads to a change in the separation selectivity, and that better separations are obtained using column No. 3 with $\alpha_{RP} = 4.25$ μmol/m^2 (Tables II and III). It can be seen that the residual silanol groups are well shielded by the dense film of CBP formed and therefore silanolophobic interactions are minimized. Moreover, when these packings are used for the determination of substances of biological origin, this leads to an increase in detection sensitivity (of about two orders of magnitude) and prolongation of the column lifetime. These are very important factors in routine analysis.

Fig. 3 presents the test proposed by Daldrup and Kardel [22] for substances characterized by their organic base nature, which were obtained on the packing with

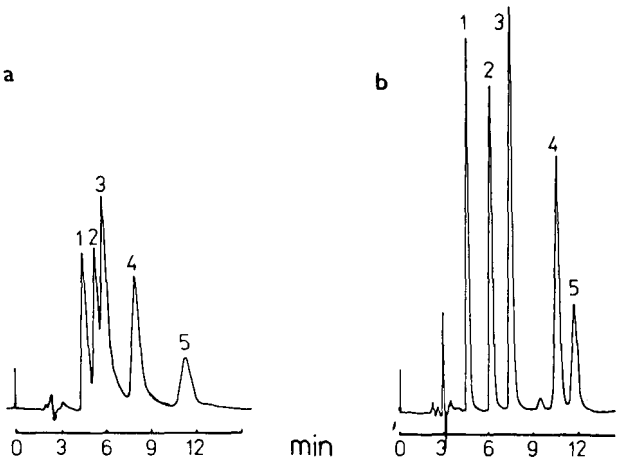

Fig. 2. Separation of purines (6.2 μg/μl) (theophylline and its metabolites) on columns packed with C_{18} chemically bonded phases. (a) $\alpha_{RP} = 2.20$ μmol/m^2; (b) $\alpha_{RP} = 4.25$ μmol/m^2. Peaks numbers as in Table III. Chromatographic conditions: column, 125 × 4.6 mm I.D.; mobile phase, acetonitrile–water (10:90) containing 0.1 *M* acetic acid; flow-rate, 0.9 ml/min; detection, UV (273 nm).

a high-density coverage (packing No. 3). The chromatogram shows that the peaks of individual substances are symmetrical and that the separation is characterized by a large peak capacity [23]. This gives a further important reason for using these packings in routine analysis, considering the higher sorption capacity and better mass transfer obtained.

Fig. 4 shows the separation with electrochemical detection of catecholamines isolated from human urine by means of the SPE clean-up column. The separation selectivity is high and the resolution of individual substances was obtained in a relatively short time (*ca.* 32 min).

SPE applications

Many factors determine the efficiency and effective application of SPE for the isolation and/or clean-up of substances in biological samples. The type of packing used, structure of CBP, the height of the packing bed and the appropiate choice of the

TABLE III

CAPACITY FACTORS OF PURINE BASES ISOLATED FROM HUMAN BLOOD SERUM

No. of peak	Substance	Capacity factor (k')		
		Column 1[a]	Column 2[a]	Column 3[a]
1	Theophylline	1.16	0.90	0.57
2	Theobromine	2.80	1.54	1.21
3	8-Methoxymethyltheophylline	3.02	1.79	1.59
4	7-(2-Hydroxymethyl)theophylline	3.88	2.47	2.63
5	Caffeine	5.07	3.87	2.98

[a] See Table II.

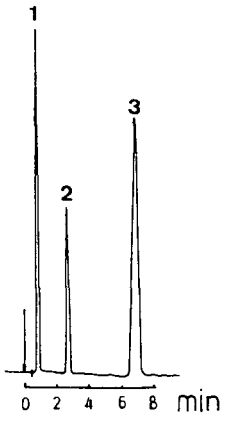

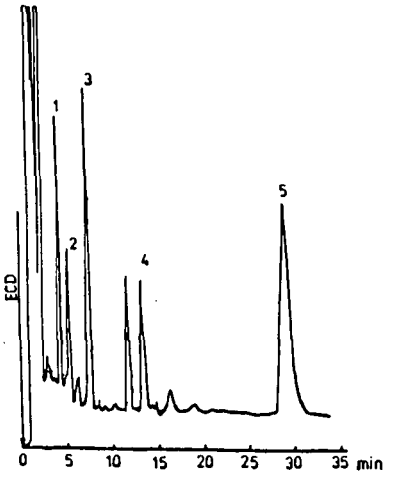

Fig. 3. Test mixture according to ref. 22 where 1 = diphenylhydramine chloride (0.5 μg/μl), 2 = 5-(*p*-methylphenyl)-5-phenylhydantoin (0.25 μg/μl) and 3 = diazepam (0.25 μg/μl). Chromatographic conditions: column, 60 × 4.6 mm I.D. with packing No. 3; mobile phase, 156 ml of acetonitrile + 340 ml of phosphate buffer (pH 2.3); flow-rate, 0.5 ml/min; detection, UV (220 nm).

Fig. 4. Separation of catecholamines isolated from human plasma, where 1 = noradrenaline (3.5 mmol/l), 2 = adrenaline (3.0 mmol/l), 3 = dihydroxybenzylamine (4.0 mmol/l), 4 = dopamine (4.2 mmol/l) and 5 = serotonin (3.5 mmol/l). Chromatographic conditions: column, 125 × 4.6 mm I.D. with packing No. 3; mobile phase, 50 m*M* sodium acetate + 20 m*M* acetic acid + 3.75 m*M* sodium octanesulphonate + 1 m*M* dibutanolamine + 0.134 m*M* ETDA + 950 ml of water + 50 ml of methanol; detection, electrochemical (working potential + 0.6 V, sensitivity 0.2 mA); flow-rate, 0.8 ml/min.

eluent are the main parameters [11,12,23]. However, these factors are closely connected with the chemical character of the analytes separated.

Fig. 5 shows example control chromatograms, demonstrating the efficiency of the SPE technique during isolation of 5-hydroxyindolacetic acid (5-HIAA) from human urine using an SPE column packed with material No. 4 (α_{RP} = 4.20 μmol/m^2; Table II). These results indicate that the determination of 5-HIAA without prior purification of the biological material is impossible when using electrochemical detection. Based on the adsorption effect, 5-HIAA was sorbed in the first step on the packing bed and then the 5-HIAA was displaced using an eluent with a higher elution strength. A recovery of 96 ± 2% was obtained.

Table IV lists the recoveries for two drugs, Melperone (M) and Paracetamol (P) isolated from individual standard solutions (SE) ($6.5 \cdot 10^{-6}$ g/ml) and also from various biological samples (RR) (M from rat brain, P from human urine) using the SPE clean-up columns packed with materials Nos. 4–6 (Table II).

On comparing the recoveries (in Table IV, it can be seen that for substances of basic character (M, pK_a = 9.6) a better recovery was obtained with the packing with a low concentration of alkylsilyl ligands on the support surface (material No. 4). This confirms that the recoveries of both SE and RR are due to small differences between them. Using the packing with a polymeric network structure of CBP in both instances did not guarantee reproducible recoveries. This is due to irreversible sorption of these substances, resulting from different interactions between the isolated solutes and the modified surface of the packings [8,9,21].

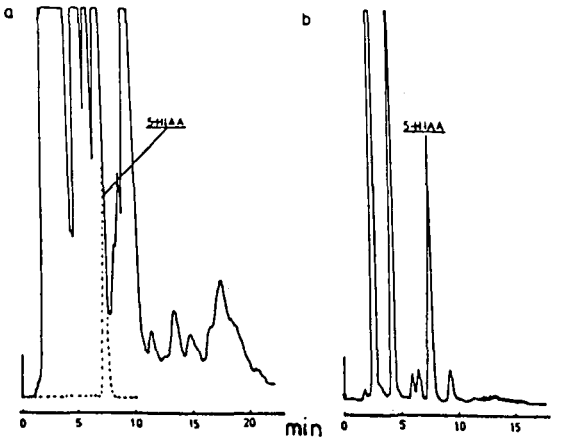

Fig. 5. Chromatograms illustrating the determination of 5-HIAA (167.3 μmol/l) in urine samples by HPLC with electrochemical detection. (a) Direct injection of an untreated urine sample; (b) injection of a purified urine sample using the SPE column with packing No. 4. Chromatographic conditions: column, 125 × 4.6 mm I.D. with packing No. 3; mobile phase, 0.08 *M* ammonium acetate–methanol (85:15%, v/v) (pH 4.5); flow-rate, 0.8 ml/min; detection, electrochemical (+0.55 V).

TABLE IV

COMPARISON OF RECOVERIES (%) AND RELATIVE STANDARD DEVIATIONS [R.S.D. (%)] FOR MELPERON AND PARACETAMOL ISOLATED FROM VALUES STANDARD SOLUTION (SE) AND BIOLOGICAL SAMPLES (RR)

No. of packing[a]	Melperone				Paracetamol			
	SE	R.S.D.	RR	R.S.D.	SE	R.S.D.	RR	R.S.D.
4	67.2	4.3	52.5	5.2	100.0	1.2	98.2	2.1
5	92.1	2.8	89.4	3.4	37.3	3.9	15.7	5.3
6	27.8	7.6	18.3	9.8	46.1	5.7	31.8	7.3

[a] See Table II.

ACKNOWLEDGEMENT

The author is grateful to the Alexander von Humboldt Foundation for a grant.

REFERENCES

1 J. H. Knox and B. Kaur, in P. R. Brown and R. A. Hartwick (Editor), *High Performance Liquid Chromatography*, Wiley, New York, 1989, Ch. 4, p. 189.
2 D. J. Pietrzyk, in P. R. Brown and R. A. Hartwick (Editors), *High Performance Liquid Chromatography*, Wiley, New York, 1989, Ch. 5, p. 223.
3 B. Buszewski and R. Leboda, *Chem. Stosow.*, 34 (1990) 191.
4 J. Nawrocki and B. Buszewski, *J. Chromatogr.*, 449 (1988) 1.
5 L. R. Sander and S. A. Wise, *CRC Crit. Rev. Anal. Chem.*, 18 (1987) 299.
6 K. Szabó, N. Le Ha, Ph. Schneider, P. Zeltner and E. sz. Kováts, *Helv. Chim. Acta*, 67 (1984) 2128.
7 B. Buszewski, A. Jurášek, J. Garaj, L. Nondek, I. Novák and D. Berek, *J. Liq. Chromatogr.*, 10 (1987) 2325.

8 R. K. Gilpin, *J. Chromatogr. Sci.*, 22 (1984) 371.
9 B. Buszewski, Z. Suprynowicz, P. Staszczuk, K. Albert, B. Pfleiderer and E. Bayer, *J. Chromatogr.*, 499 (1990) 305.
10 B. Buszewski and Z. Suprynowicz, *Anal. Chim. Acta*, 208 (1988) 199.
11 C. K. Lim, F. Li and T. J. Peters, *Int. Lab.*, 16 (1986) 60.
12 B. Tippins, *Int. Lab.*, 17 (1987) 28.
13 D. Berek and I. Novák, *U.S. Pat.*, 4 255 286 (1981) and 4 382 070 (1983).
14 L. Šoltes, I. Novák and D. Berek, *Czech. Pat.*, 234 100 (1983).
15 B. Buszewski, R. Lodkowski and J. Trocewicz, *J. High Resolut. Chromatogr. Chromatogr. Commun.*, 10 (1987) 527.
16 B. Buszewski and Z. Suprynowicz, *Chromatographia*, 22 (1987) 573.
17 B. Buszewski, L. Nondek, A. Jurášek and D. Berek, *Chromatographia*, 23 (1987) 442.
18 B. Buszewski, D. Berek, I. Novák and J. Garaj, *Chem. Listy*, 81 (1987) 552.
19 E. Bayer, K. Albert, J. Reiners, M. Nieder and M. Müller, *J. Chromatogr.*, 264 (1983) 197.
20 K. Albert, B. Evers and E. Bayer, *J. Magn. Reson.*, 62 (1985) 428.
21 B. Buszewski, *Chromatographia*, 29 (1990) 233.
22 T. Daldrup and B. Kardel, *Chromatographia*, 18 (1984) 81.
23 B. Buszewski, *J. Pharm. Biomed. Anal.*, 8 (1990) 645.

Journal of Chromatography, 538 (1991) 303–310
Elsevier Science Publishers B.V., Amsterdam

CHROM. 22 815

Separation of phenols and aromatic hydrocarbons from biomass tar using aminopropylsilane normal-phase liquid chromatography

CLAES BRAGE* and KRISTER SJÖSTRÖM
Royal Institute of Technology, Department of Chemical Technology, S-100 44 Stockholm (Sweden)
(First received November 22nd, 1989; revised manuscript received September 11th, 1990)

ABSTRACT

A quantitative procedure for the determination of selected phenols and aromatic hydrocarbons in biomass tar is described. Solid-phase extraction (SPE) through columns of amino-bonded silica stationary phase was used to separate tar samples into two fractions. These fractions were subjected to capillary gas chromatography using a DB-1 fused-silica column and a flame ionization detector. The efficiency of the method was determined by the use of synthetic and spiked tar samples. Excellent reproducibility and high recoveries were obtained for most of the target compounds. Compared with the traditional liquid–liquid extraction technique, the SPE technique eliminates the problems involved and provides higher overall recoveries in a shorter time.

INTRODUCTION

The production of fuel gases by pyrolysis and gasification of biomass for heating purposes and electricity generation are usually accompanied by the formation of various amounts of tar by-products which must be reduced prior to use. Tar reduction for these applications is usually accomplished by thermal and catalytic cracking or by cyclones in combination with wet or dry cleaning systems. The development of new analytical procedures for the determination of individual tar compounds is important in order to control operational parameters at gasification units and for monitoring emissions from full-scale gasifier plants, since several of the tar components have a strong environmental impact owing to their mutagenic and carcinogenic character. Various methods for the characterization of tar matrices have been published. Many of them are based on combinations of the following techniques: high-performance liquid chromatography (HPLC) [1–6], open-column liquid chromatography [4,8,9], capillary column gas chromatography (GC) [1,5,7–9], GC–mass spectrometry (MS) [1,5,6,8,10], solvent fractionation [5,7,8], liquid–liquid extraction (LLE) [1,4,6,8,9], ^{1}H NMR [6,9,12], ^{13}C NMR [6,12], MS–MS [11] and Fourier transform IR spectrometry [10]. The chemical composition of biomass tar varies, depending on the operational conditions, but it is generally very complex and can contain several hundred organic compounds belonging to many chemical classes. Owing to this complexity, a prefrac-

0021-9673/91/$03.50

tionation of the crude tar sample is a common starting point before detailed GC analysis is attempted.

Two conventionally used techniques for prefractionation are LLE and HPLC. These techniques, however, suffer from some disadvantages. Thus HPLC, successfully used in many applications, consumes too large solvent volumes to be useful for a rapid tar analysis method, and LLE when applied to tar samples is associated with the formation of emulsions and problems with the location of the phase boundary. In an attempt to overcome these problems, a quantitative analytical procedure was devised, based on capillary GC following prefractionation by solid-phase extraction (SPE) using micro columns, commercially packed with an amino-bonded silica phase. This technique allows the rapid determination of selected components present in biomass tar formed at high temperatures ($\geqslant 700$°C). To the best of our knowledge, the SPE technique using an amino-bonded sorbent has not previously been employed for this purpose, although amino phase columns have been successfully applied in the HPLC separation of coal-derived tar compounds into aromatic ring classes [3,7].

EXPERIMENTAL

Reagents and materials

Neutral aromatic reference compounds, dichloromethane, sodium sulphate and sulphuric acid were obtained from Merck (Darmstadt, F.R.G). SPE-NH_2 disposable extraction columns (100 mg packing, 40 μm, 60 Å) and 2-propanol were purchased from J. T. Baker (Phillipsburg, NJ, U.S.A.). N,O-bis(trimethylsilyl)trifluoroacetamide (BSTFA) was obtained from Supelco (Bellefonte, PA, U.S.A.). All phenolic reference compounds except 3,5-di-*tert.*-butylphenol and 2,6-di-*tert.*-butyl-4-methylphenol (Fluka, Buchs, Switzerland) were purchased from PolyScience (Niles, IL, U.S.A.). 4-Ethoxyphenol and 2-bromonaphthalene used as internal standards were obtained from Aldrich-Chemie (Steinheim am Albuch, F.R.G.) and Merck, respectively. All compounds and solvents were of very high purity (mostly $>99\%$) and used as received after being tested in blank procedures.

Gas chromatography and gas chromatography–mass spectrometry

Product analyses were carried out with a modified Packard Model 427 gas chromatograph (split injection) equipped with a flame ionization detector operated at 300°C. Separations were achieved on fused-silica capillary column (30 m $\times$ 0.25 mm I.D.) coated with 0.25-μm bonded and cross-linked DB-1 phase (J & W Scientific, Rancho Cordova, CA, U.S.A.). The column inlet pressure was 300 kPa using helium as a carrier gas. The splitting ratio was about 1:50. The injector temperature was 280°C. The oven temperature was programmed from 100 to 300°C at 5°C/min for the analysis of silylated phenols and at 8°C/min for aromatic hydrocarbons. Peak areas were measured with a Shimadzu (Kyoto, Japan) C-R4 A integrator. Two internal standards were used, *p*-ethoxyphenol for phenols and 2-bromonaphthalene for the aromatic compounds. The initial target compound identity was confirmed by GC–MS with subsequent quantitative GC runs based on comparison with retention times relative to those of the internal standards. Relative response factors (RF) for all target analytes were calculated from the equation $RF = A(\mathrm{s})C(\mathrm{is})/A(\mathrm{is})C(\mathrm{s})$, where A(s) is the area of the sample peak, C(is) the amount of internal standard added, A(is) the area of the

internal standard peak and $C(s)$ the amount of sample. Electron impact (EI) mass spectra were acquired with a Finnigan MAT 4500 quadrupole instrument at 70 eV, scanning from 40 to 300 u at 0.95 s per scan. The instrument was connected with an Incos 50 data system and a Varian Series 3700 gas chromatograph equipped with a fused-silica capillary column (30 m × 0.25 mm I.D.) coated with 0.25-μm DB-5 using helium as the carrier gas. The oven temperature was programmed at 5°C/min from 80 to 280°C with a 5-min final hold time.

Preparation of samples

Biomass tar was taken from a laboratory research pyrolysis unit operating at 900°C in the absence of a catalyst. The pyrolysis gas was quenched by passing it through a water condenser and a pair of cryogenic traps containing dry-ice–acetone (−81°C) and liquid nitrogen (−195°C) connected in series. The collected tarry aqueous mixture was washed from the condenser and traps with dichloromethane and small volumes of acetone. The washings were transferred into a separating funnel and the organic phase was run off and retained. The aqueous phase was acidified to pH 5 (sulphuric acid) and partitioned with dichloromethane. The organic phase and the combined dichloromethane extracts were dried by passing them through an anhydrous sodium sulphate column, quantitatively transferred into a volumetric flask and diluted to volume with dichloromethane. The total tar sample thus obtained was stored in a refrigerator until it was used.

Synthetic samples were prepared in dichloromethane from eighteen authentic compounds at three concentration levels as follows: synthetic sample 1 = 1.909 mg/ml (86–123 μg of each compound); synthetic sample 2 = 9.672 mg/ml (428–617 μg of each compound); and synthetic sample 3 = 32.060 mg/ml (1.22–2.47 mg of each compound). Spiked tar samples were prepared in dichloromethane from aliquots of the total tar sample by mixing with known amounts of authentic compounds.

Solid-phase extraction procedure

Each SPE amino column was conditioned prior to use by gravity feed elution of 0.5 ml of *n*-hexane. Aliquots of 1 ml of the tar extract were mixed with 100 μl of dichloromethane containing known amounts of 4-ethoxyphenol and 2-bromonaphthalene, serving as internal standards. From this mixture a 100-μl aliquot was withdrawn with a syringe and loaded onto the SPE column. Using gravity only, neutral compounds were eluted from the columns using four 100-μl aliquots of dichloromethane. Phenols were eluted with two 100-μl aliquots of dichloromethane–2-propanol (1:1, v/v) followed by three 100-μl aliquots of 2-propanol. To avoid cross-contamination and loss of sample components, the column tip was washed with small volumes of eluent following each fraction. Subsequently, the fractions were subjected to capillary GC after trimethylsilylation of the phenols (see *Derivatization*). Synthetic samples were similarly treated using the same sample volume. The adsorptive capacity of the sorbent was determined for phenol to be *ca.* 2% of the sorbent mass. The concentration of the tar mixture used in this study was *ca.* 26 mg/ml. This is equivalent to 2.6 mg applied to SPE columns. However, the best recoveries were obtained using a smaller sample size (less than 200 μg), as determined with synthetic samples.

Liquid–liquid extraction (LLE)

Aliquots of synthetic sample 3 (*ca.* 32 mg/ml) were mixed with internal standards and subjected to acid–base extraction in a glass-stoppered centrifugation tube. After extraction, the organic phases were dried over anhydrous sodium sulphate. The polar fraction was treated with BSTFA (see *Derivatization*) to convert the phenolic constituents into their trimethylsilyl derivatives prior to GC analysis.

Derivatization

Three different derivatization procedures were investigated for phenols: acetylation, methylation and silylation. For this study silylation was selected because of its simplicity and because the best GC resolution was obtained for isomeric compounds. The silylation was accomplished by reaction with an excess of BSTFA and dichloromethane as a cosolvent. The derivatization reaction was completed within 15–20 min at room temperature.

RESULTS AND DISCUSSION

The analytical procedure developed using capillary GC following SPE through amino phase columns was tested for selected phenols and aromatic hydrocarbons with

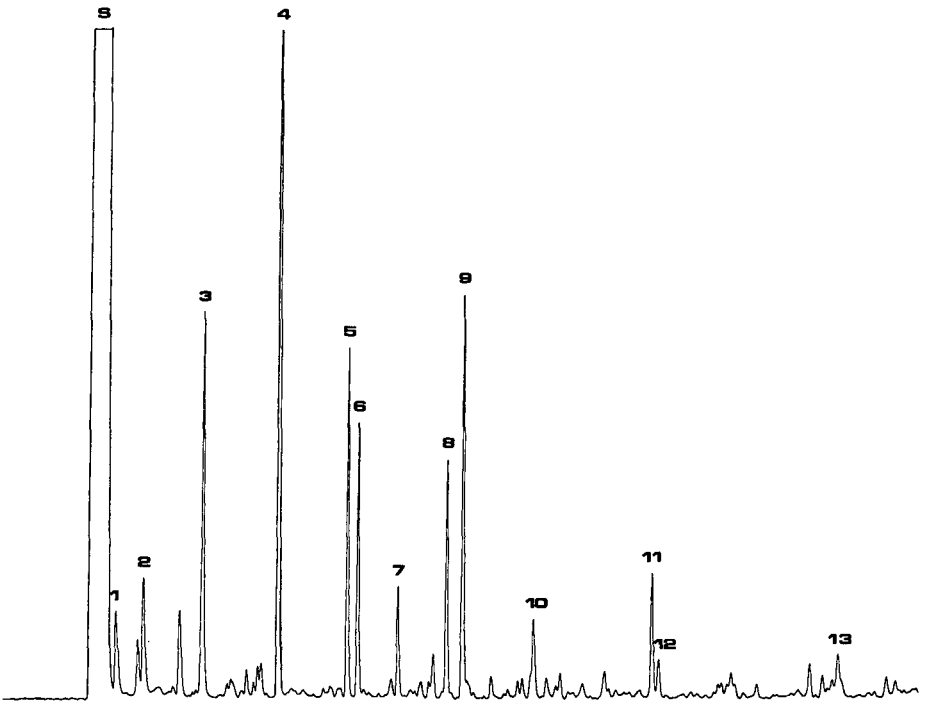

Fig. 1. Capillary GC of aromatic hydrocarbons. Peaks: 1 = toluene; 2 = *o*-xylene; 3 = indene; 4 = naphthalene; 5 = 2-methylnaphthalene; 6 = 1-methylnaphthalene; 7 = biphenyl; 8 = acenaphthylene; 9 = internal standard; 10 = fluorene; 11 = phenanthrene; 12 = anthracene; 13 = pyrene; S = solvent. Temperature programmed from 100 to 300°C at 8°C/min.

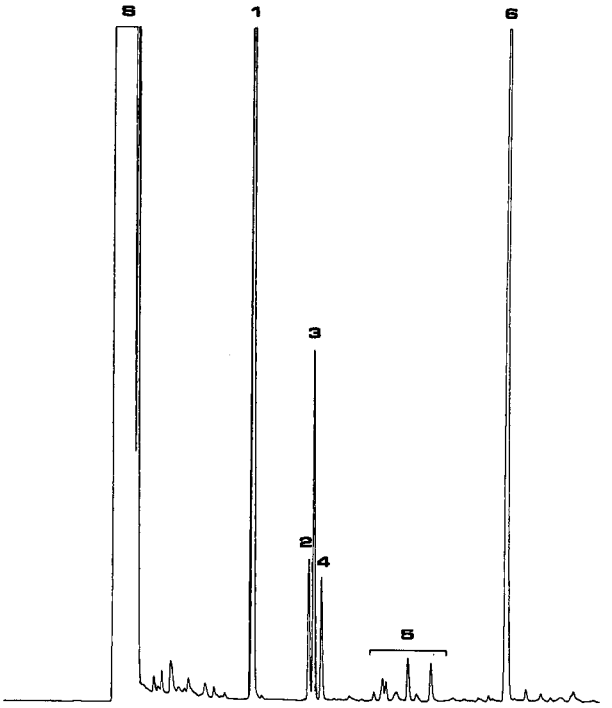

Fig. 2. Capillary GC of silylated phenolic compounds. Peaks: 1 = phenol; 2 = *o*-cresol; 3 = *m*-cresol; 4 = *p*-cresol; 5 = C_2-substituted phenols; 6 = internal standard; S = solvent. Temperature programmed from 100 to 220°C at 5°C/min.

TABLE I

REPRODUCIBILITY STUDY OF SPE AMINO COLUMNS FOR PRESEPARATION OF BIOMASS TAR

The number of SPE runs was 9. Eluted compounds were analysed by capillary GC in triplicate.

Compound	Mean value (μg)	Relative standard deviation (%)
Toluene	22.0	11.4
o-Xylene	36.6	9.4
Indene	131.7	0.6
Naphthalene	282.2	2.9
1-Methylnaphthalene	53.0	1.4
2-Methylnaphthalene	34.3	1.2
Biphenyl	13.5	1.7
Acenaphthylene	78.1	1.5
Fluorene	22.7	2.1
Phenanthrene	36.2	1.6
Anthracene	11.6	2.4
Pyrene	7.6	3.6
Phenol	156.4	1.0
o-Cresol	30.5	2.1
m-Cresol	60.3	1.0
p-Cresol	30.4	0.8

a high-temperature (800°C) biomass tar sample taken from a laboratory research pyrolysis unit. This type of tar contains only traces of amines and carboxylic acids which might interfere with the analysis of target compounds if present at higher concentrations. In order to obtain an adequate peak resolution for isomeric compounds, the phenols were converted into their trimethylsilyl analogues prior to GC analysis. Typical gas chromatograms of neutral and polar SPE fractions are shown in Figs. 1 and 2, respectively.

The reproducibility was evaluated by nine replicate analyses of a tar sample. Each SPE fraction was analysed in triplicate by GC. The average results given in Table I demonstrate that good precision was obtained for all compounds except toluene (*ca.* 11%) and *o*-xylene (*ca.* 9%).

The accuracy of the method was established by analysing alquots of synthetic samples containing seven phenols and eleven aromatic hydrocarbons at two concentration levels (1.9 and 9.7 mg/ml). Further recovery data were obtained from the analysis of a tar sample spiked with selected authentic compounds. The results from SPE were compared with those obtained by LLE traditionally used in much

TABLE II

COMPARISON OF THE RESULTS OF SPE AND LLE OF SYNTHETIC SAMPLES AND A SPIKED TAR SAMPLE

Eluted compounds were analysed by capillary GC in triplicate. Synthetic sample 1: concentration = 1.909 mg/ml, sample size ≈ 191 μg. Synthetic sample 2: concentration = 9.672 mg/ml, sample size ≈ 967 μg. Synthetic sample 3: concentration = 32.060 mg/ml, sample size ≈ 3.2 mg. Spiked tar sample: concentration = 3.184 mg/ml, sample size ≈ 318 μg.

Compound	Recovery (%)			
	SPE			LLE: Synthetic sample 3[d]
	Synthetic sample 1[a]	Synthetic sample 2[b]	Spiked tar sample[c]	
Phenol	94	86	–	68
o-Cresol	100	82	82	96
m-Cresol	101	85	–	94
p-Cresol	105	85	92	92
o-Ethylphenol	101	75	–	94
2,5-Xylenol	96	77	–	89
3,4-Xylenol	106	87	87	94
Toluene	108	92	–	86
o-Xylene	102	92	–	85
Naphthalene	94	75	–	80
2-Methylnaphthalene	88	85	98	86
1-Methylnaphthalene	92	78	93	86
Biphenyl	102	85	98	88
Acenaphthylene	93	65	–	85
Fluorene	76	85	–	88
Phenanthrene	77	105	–	109
Anthracene	79	86	–	92
Pyrene	85	116	–	100

[a,c] Average of two analyses.
[b,d] Average of three analyses.

quantitative work for the separation of polar and non-polar compounds. All recovery data are summarized in Table II.

From the measurements reported for sample 2 (high-concentration synthetic sample) an overall efficiency of 86% was obtained. Individual values ranged from 75 to 87% for phenols and from 65 to 116% for neutral compounds. The effects of using a smaller sample size (sample 1) are also illustrated in Table II. In this instance the overall recovery was 94%, an improvement of 8% over the high-concentration sample. Individual values were in the range 94–106% for phenols and 76–108% for neutral species. The results from the study performed with a spiked tar sample also showed good recovery (overall *ca.* 92%). In comparison, the overall efficiency for LLE (by means of three successive partitions) was 90%, with individual values in the range 68–96% for phenols and 80–109% for aromatic hydrocarbons. As is evident from the comparative results given in Table II, the overall recovery (94%) obtained by SPE (sample 1) agrees favourably with the results (90%) from LLE. Furthermore, the SPE recoveries were almost quantitative ($\geqslant 92\%$) for thirteen of the eighteen analytes compared with eight compounds for LLE. These data also show that the efficiency of the SPE procedure increased with a decrease in sample size, although this finding is most pronounced for phenols. Efficient separations using SPE are thus demonstrated. The tar used in this work also contains heavy tar components of low volatility such as pre-asphaltenes (constituting *ca.* 20 wt.-%), which are not analysable by GC but may interfere with the analysis, resulting in non-reproducibility of the results. To remove these components, solvent precipitation using *n*-alkane solvents is traditionally used. However, most of these components are effectively retained by the SPE amino-sorbent used in this work, and are thus separated from the target compounds. Owing to the highly polar nature of the amino-sorbent employed, phenols are expected to be very strongly retained. This is also true of the target compounds. However, we found that 2,6-di-*tert.*-butyl-4-methylphenol, reported to be present in pyrolytic biomass oil [10], and 3,5-di-*tert.*-butylphenol co-eluted with the aromatic hydrocarbons. This different behaviour may be due to the weakening of acidity caused by the inductive effects of the electron-repelling *tert.*-butyl groups in combination with steric hindrance which prevented effective interaction with the adsorbent. However, no *tert.*-butyl-substituted phenolic compounds were detected in the tar sample used in this study.

Summarizing the results, it may be concluded that the use of SPE for the analysis of high-temperature biomass tar circumvents the problems associated wtih LLE, thus providing a better alternative to this traditional preseparation technique.

CONCLUSIONS

An efficient method was developed for determination of selected phenols, alkylated aromatics and polycyclic aromatic hydrocarbons in biomass tar using SPE amino columns in combination with capillary column GC. The method was found to be rapid, highly reproducible and accurate, and is suggested as a better alternative to LLE, traditionally employed for chemical class separation prior to GC analysis.

ACKNOWLEDGEMENTS

Financial support for this work was provided by the Swedish Energy Agency (SEV). The authors are indebted to Professor Olle Lindström for his interest and to Mrs. Qizhuang Yu for assistance with the GC analysis.

REFERENCES

1 H. S. Hertz, J. M. Brown, S. N. Chesler, F. R. Guenther, L. R. Hilpert, W. E. May, R. M. Parris and S. A. Wise, *Anal. Chem.*, 52 (1980) 1650.
2 K. G. Lipard, *Chromatographia*, 13 (1980) 603.
3 S. Matsuzawa, P. Garrigues, O. Setokuchi, M. Sato, T. Yamamoto, Y. Shimizu and M. Tamura, *J. Chromatogr.*, 498 (1990) 25.
4 J. F. Schabron and R. J. Hurtubise, *Anal. Chem.*, 51 (1979) 1426.
5 K. C. Teo and A. P. Watkinson, *Fuel*, 66 (1987) 1123.
6 D. G. B. Boocock, R. K. M. R. Kallury and T. T. Tidweell, *Anal. Chem.*, 55 (1983) 1689.
7 S. Coulombe and H. Sawatzky, *Fuel*, 65 (1986) 552.
8 C. E. Rovere, P. T. Crisp, J. Ellis and P. Bolton, *Fuel*, 62 (1983) 1274.
9 H. Pakdel, C. Roy and K. Zeidan, in A. V. Bridgewater and J. L. Kuester (Editors), *Research in Thermochemical Biomass Conversion*, Elsevier Applied Science, Barking, 1988, pp. 573–584.
10 E. Churin, R. Maggi, P. Grange and B. Delmon, in A. V. Bridgewater and J. L. Kuester (Editors), *Research in Thermochemical Biomass Conversion*, Elsevier Applied Science, Barking, 1988, pp. 897–909.
11 S. Moore, S. Kaliaguine and M. J. Bertrand, in A. V. Bridgewater and J. L. Kuester (Editors), *Research in Thermochemical Biomass Conversion*, Elsevier Applied Science, Barking, 1988, pp. 280–293.
12 J. W. McKinley, G. Barrass and H. L. Chum, in A. V. Bridgewater and J. L. Kuester (Editors), *Research in Thermochemical Biomass Conversion*, Elsevier Applied Science, Barking, 1988, pp. 237–251.

Journal of Chromatography, 538 (1991) 311–321
Elsevier Science Publishers B.V., Amsterdam

CHROM. 22 810

Affinity partitioning of restriction endonucleases

Application to the purification of EcoR I and EcoR V

G. VLATAKIS and V. BOURIOTIS*

Enzyme Technology Division, Institute of Molecular Biology and Biotechnology, Foundation for Research and Technology, P.O. Box 1515, 711 10 Heraklion, Crete (Greece)

(First received May 11th, 1990; revised manuscript received August 10th, 1990)

ABSTRACT

Partitioning of restriction endonucleases between two liquid aqueous phases can be strongly influenced by group-specific ligands included in the two-phase system. Three restriction endonucleases, namely EcoR I, EcoR V and BamH I, were partitioned within an aqueous dextran–polyethylene glycol (PEG) system. The enzymes could be extracted into the upper PEG phase by using either triazine dyes or herring DNA as affinity ligands. The influence of the endogenous bacterial nucleic acids, concentration of polymer-bound dye and concentration of sodium chloride on the system were examined. A partial purification of EcoR I (up to 52-fold) and EcoR V (up to 37-fold) was achieved using a combination of affinity partitioning and ion-exchange chromatography, providing an extremely fast and economical method for the isolation of restriction endonucleases free from contaminating nuclease activities.

INTRODUCTION

Site-specific restriction endonucleases are widely used in the analysis of DNA molecules. The ability to cleave DNA at specific sequences is the fundamental technology responsible for the rapid development of genetic engineering. Today, more than 1000 restriction endonucleases have been identified from different bacterial sources [1].

Although several procedures have been published regarding their purification, most of them involve lengthy protocols, including precipitation with salts [2] followed by column chromatography on different media, such as phosphocellulose [2,3], hydroxylapatite [4], DEAE-cellulose [3,5], DNA–cellulose [2], Cibracron Blue F3G-A–agarose [6,7], heparin–agarose [8,9] and/or gel filtration [10].

However, recently a rapid two-step chromatographic procedure for the isolation of these enzymes [11] and an inexpensive scheme involving triazine dye adsorbents [12] have been reported.

Aqueous two-phase systems have been used for the purification of a vast number of biological macromolecules such as proteins, enzymes and nucleic acids [13]. These

0021-9673/91/$03.50

systems are obtained by dissolving two polymers in water at appropriate concentrations, *e.g.*, dextran and polyethylene glycol (PEG) [13,14]. The partitioning of proteins depends on a number of parameters, including concentration and molecular weight of the polymers, salt and buffer added to the system, pH and temperature [15]. Further, the partitioning of enzymes and other proteins can be selectively influenced by covalently binding of affinity ligands to one of the phase-forming polymers. This method, called affinity partitioning [16–18], has been widely used for the effective extraction of enzymes and for ligand–protein binding studies [19]. The most popular ligands in affinity partitioning are triazine dyes, which have been used for the affinity extraction of dehydrogenases, kinases and a number of other enzymes and proteins [20–23].

As we have demonstrated in previous work [12], various triazine dyes interact with restriction endonucleases and dye-ligand chromatography can be effectively used for the purification of these enzymes using three-step procedures.

This work was carried out to study the behaviour of restriction endonucleases in aqueous two-phase systems in the presence of dye ligands bound to PEG and to develop procedures which are economical and faster than those published previously. The influence of added non-specific DNA in the system was also examined.

EXPERIMENTAL

Materials

Yeast extract, tryptone and brain heart infusion were obtained from Difco (Detroit, MI, U.S.A.) and dextran T-500 (mol. wt. 500 000) and prepacked MonoS HR 5/5 (5 × 50 mm) cation-exchange high-performance liquid chromatographic (HPLC) column from Pharmacia (Uppsala, Sweden). DNA from herring testes, polyethyleneimine (PEI) and Nonidet P-40 (NP-40) were purchased from Sigma (St. Louis, MO, U.S.A.), agarose for gel electrophoresis and λDNA from Bethesda Research Labs. (Bethesda, MD, U.S.A.), polyethylene glycol PEG 6000 (mol. wt. 6000–7500) from Serva (Heidelberg, F.R.G.), DEAE-cellulose (DE52) from Whatman (Maidstone, Kent, U.K.) and the Procion dyes Blue MX-4GD and Navy H-ER (ICI, Manchester, U.K.) were provided by Dr. Y. D. Clonis (University of Patras, Greece). All other chemicals were of analytical-reagent grade.

Two-phase systems

Phase systems were prepared from stock solutions of the polymers in water. The PEG 6000 solution was 40% (w/w) and the dextran T-500 20% (w/w). The polymer solutions were weighed and mixed with salt, buffer, water and sample to the final weight, usually 4 g. All partitioning experiments were carried out at 4°C. Triazine dye derivatives of PEG were prepared according to Johansson [15]. The partition coefficient, K, is defined as the ratio of the concentrations of the component in the upper and lower phases. Enzyme concentrations were determined by measuring the activity expressed in units/μl. The concentration of herring DNA was determined photometrically at 260 nm (an absorbance of 1 corresponds to 50 μg/ml).

Crude extract preparation

Escherichia coli RY 13 (EcoR I) and *Escherichia coli* J62 pLG74 (EcoR V) were

grown at 37°C until the late log phase on a medium containing 5 g/l of yeast extract, 10 g/l of tryptone and 5 g/l of NaCl. *Bacillus amyloliquefaciens* (BamH I) was grown at 37°C until the late log phase on a medium containing 37 g/l brain heart infusion. All cell types after harvesting by centrifugation were dissolved in 20 m*M* Tris–HCl buffer (pH 7.4). The cells were disrupted with a French Press (SLM Instruments) and centrifuged at 4°C for 1 h at 100 000 *g*. With *Escherichia coli* RY 13 (EcoR I), the clarified crude extract was dialysed against buffer A [20 m*M* Tris–HCl (pH 7.4)–40% (v/v) glycerol] and stored at −20°C. With *Escherichia coli* J62 pLG74 (EcoR V), the clarified crude extract was treated with PEI in order to remove nucleic acids by precipitation [24]. Solid ammonium sulphate was added to the PEI supernatant to a final concentration of 75% of saturation. After centrifugation, the precipitate was dissolved in 20 m*M* Tris–HCl buffer (pH 7.4), dialysed against buffer A and stored at −20°C. In the case of *Bacillus amyloliquefaciens* (BamH I), the clarified crude extract was divided into two parts. One part was dialysed against buffer A and stored at −20°C. The other part, as with the EcoR V extract, was treated with PEI, precipitated with ammonium sulphate (75% of saturation), dialysed against buffer A and stored at −20°C.

Enzyme assays

Routine assays for locating EcoR I or EcoR V endonuclease activity during the chromatographic runs were performed as described elsewhere [12]. One unit of enzyme activity is defined as the amount of enzyme required to produce a complete digest of 1 μg of λDNA at 37°C for 1 h in a total volume of 50 μl. The purity of the final enzyme preparations with respect to non-specific nucleases was evaluated by the "overdigestion" and "cut–ligate–recut" tests [12]. Agarose gel electrophoresis of DNA fragments was performed as described earlier [12]. Protein determination was performed by the Bradford method using Coomassie Brilliant Blue G and bovine serum albumin as protein standard [25].

RESULTS AND DISCUSSION

Effect of sodium chloride

It is well known that the partitioning of DNA is strongly dependent on the salt composition of the system [26]. Therefore, the effect of NaCl on the partitioning of the restriction enzymes was studied in relation to the presence or absence of endogenous DNA.

A crude sample containing EcoR V was treated with PEI in order to remove nucleic acids whereas that containing EcoR I was not. Crude samples containing BamH I (treated and untreated with PEI) were also used.

Without the addition of NaCl, more than 90% of the enzyme EcoR V was in the lower phase, whereas 95% of the enzyme EcoR I was found in the upper phase. When the concentration of NaCl in the system is raised from 0 to 150 m*M*, the partitioning of EcoR V was affected only slightly, whereas the partitioning of EcoR I was changed dramatically and 95% of the enzyme was transferred into the lower phase (Fig. 1A).

Similar results were obtained with BamH I (Fig. 1B). Working with extract that had been treated with PEI (as with EcoR V), the partitioning of the enzyme was not affected by NaCl, whereas with the untreated extract the behaviour of the enzyme was similar to that of EcoR I.

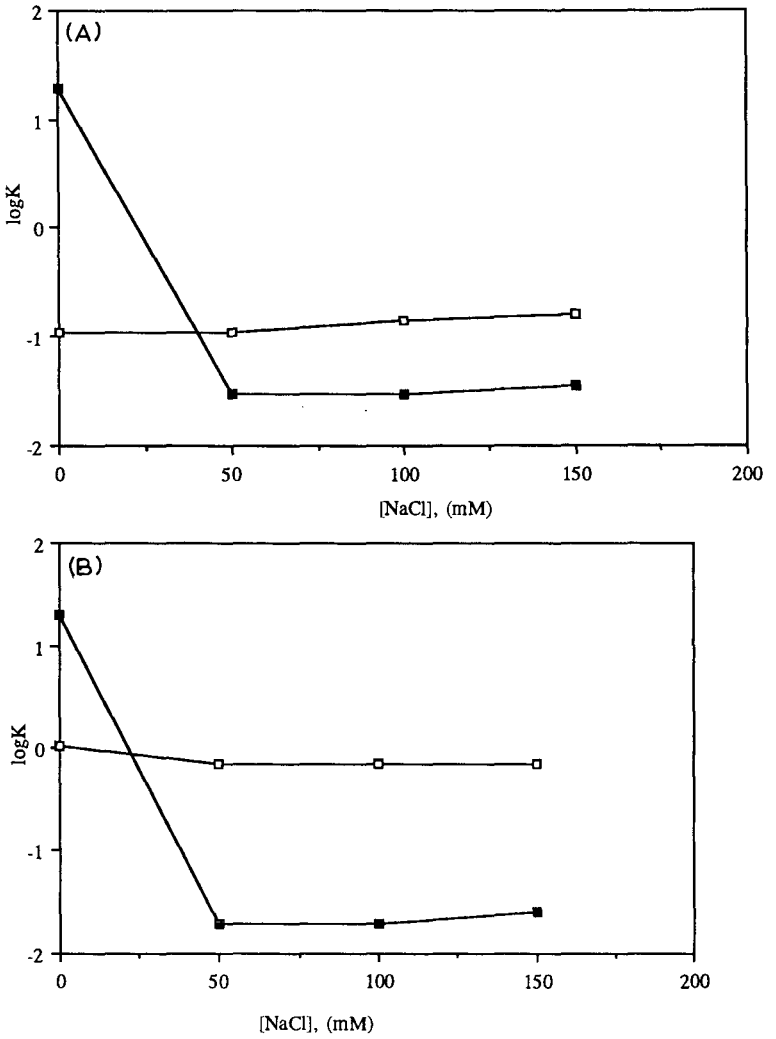

Fig. 1. Effect of NaCl on the partitioning of restriction endonucleases. System: 7.5% (w/w) dextran, 5.3% (w/w) PEG, 25 m*M* lithium phosphate buffer (pH 6.8) and increasing concentrations of NaCl. Temperature, 4°C. (A) Partitioning of the enzymes (□) EcoR V and (■) EcoR I. The crude sample containing EcoR V was treated with PEI in order to remove nucleic acids by precipitation. (B) Partitioning of the enzyme BamH I. Two crude samples were used, (□) after PEI treatment and (■) without PEI treatment.

From these results, we suggest that in the absence of endogenous DNA, NaCl has no effect on the partitioning of the restriction enzymes examined. However, in the presence of endogenous DNA, NaCl has an indirect effect on the partitioning, probably owing to the interaction of restriction enzymes with DNA.

In order to follow the partitioning of bacterial DNA, the phases of the systems were analysed by agarose gel electrophoresis. As expected, in systems without NaCl the DNA was detected in the upper phase, whereas in systems with NaCl it was detected in the lower phase (data not shown).

Effect of dye–PEG derivatives

A triazine dye, Procion Blue MX-4GD, which is known to interact with the restriction enzymes EcoR V and EcoR I [12], was coupled to PEG and further studied in affinity partitioning experiments. The dye–PEG was found to be effective in extracting the enzyme EcoR V into the PEG-rich phase with a maximum increase of 2 units in $\Delta \log K$, *i.e.*, the difference in the logarithm of the K values with and without dye-liganded polymer (Fig. 2). However, with EcoR I, the dye–PEG was not able to extract the enzyme into the upper phase. Even when 7% dye–PEG (of total PEG) was included in the system, 70% of the enzyme was still in the lower phase, whereas with 3% dye–PEG (of total PEG) less than 5% of EcoR V was found in the lower phase (Fig. 3A).

The influence of another PEG-bound dye, Procion Navy H-ER, on the partitioning of the enzyme BamH I is shown in Fig. 3B. Similarly the dye–PEG was able to extract BamH I into the upper phase only if the nucleic acids had been removed from the crude extract. However, with EcoR I, at higher NaCl concentrations the dye–PEG can more effectively extract the enzyme into the upper phase (Fig. 4), suggesting that there is a salt-dependent competition between the dye and bacterial DNA for binding to restriction endonucleases.

Effect of non-specific DNA

All the sequence-specific DNA-binding proteins exhibit a non-specific binding to any DNA. Further, immobilized non-specific DNA (calf thymus DNA, salmon sperm DNA, etc.) has been used for the isolation of several restriction endonucleases [2]. In an effort to study the affinity partitioning of restriction endonucleases in aqueous two-phase systems, we used as a ligand non-specific DNA (herring testes DNA).

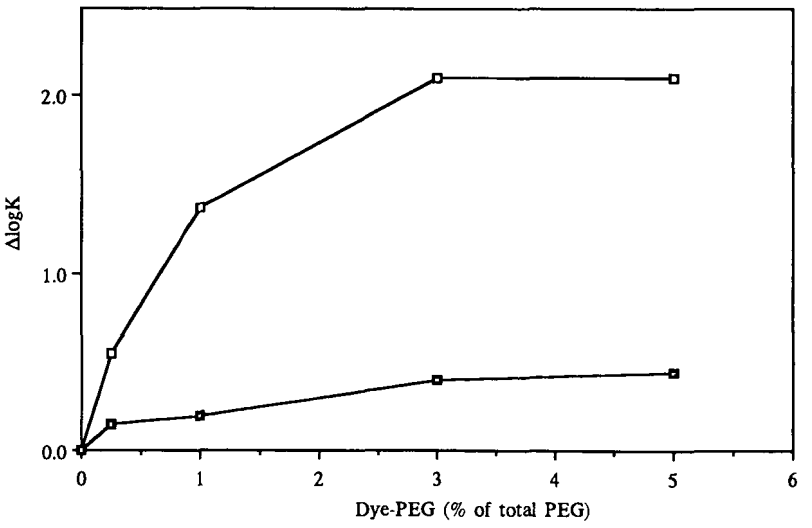

Fig. 2. Change in the partition coefficient of the enzyme EcoR V as a function of PEG-bound Procion Blue MX-4GD concentration. (■) Protein; (□) EcoR V. System: 7.5% (w/w) dextran, 5.3% (w/w) PEG, 25 mM lithium phosphate buffer (pH 6.8). Temperature, 4°C.

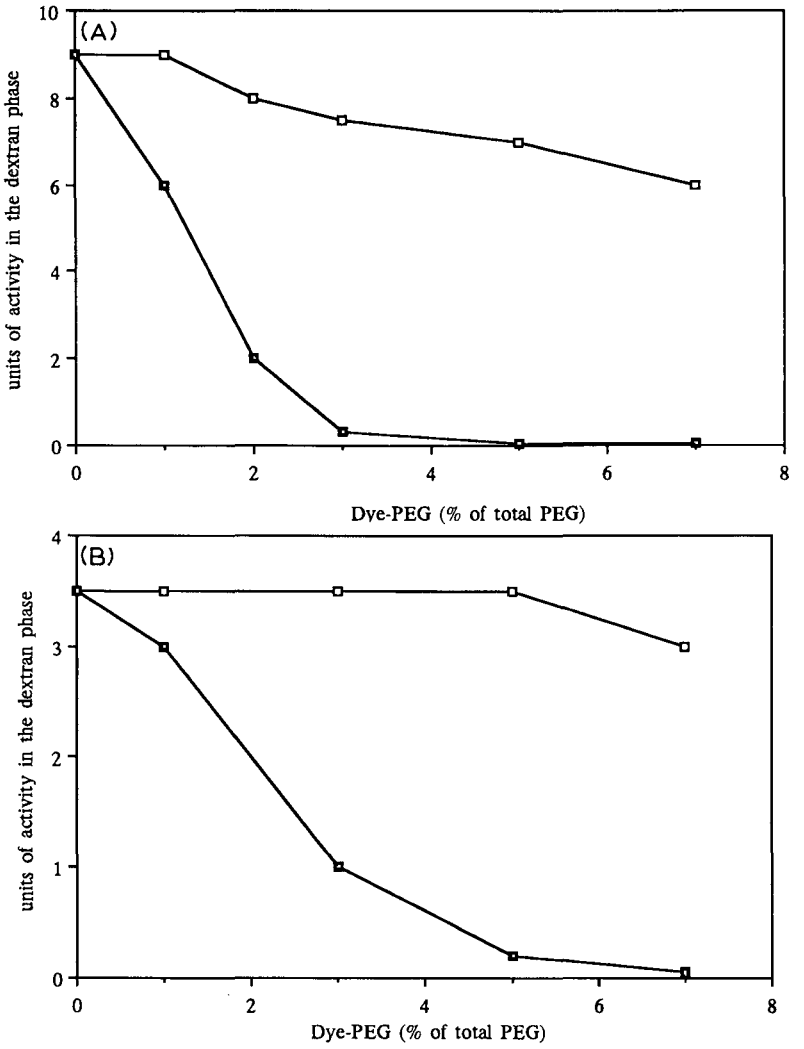

Fig. 3. Effect of dye–PEG derivatives on the partitioning of restriction endonucleases. The same system was incorporated as in Fig. 2, containing 50 m*M* NaCl. Temperature, 4°C. (A) Activity of the enzymes (■) EcoR V and (□) EcoR I remaining in the dextran phase after the addition of increasing amounts of PEG-bound Procion Blue MX-4GD. The crude sample containing EcoR V was treated with PEI. (B) Activity of the enzyme BamH I remaining in the dextran phase after the addition of increasing amounts of PEG–bound Procion Navy H-ER. Crude sample (■) after PEI treatment and (□) without PEI treatment.

As expected, the partitioning of herring DNA is influenced by the salt composition of the system. The DNA is totally transferred into the lower phase when 100 m*M* NaCl is included in the system, as shown in Fig. 5.

In order to examine the influence of non-specific DNA on the partitioning of restriction endonucleases, increasing amounts of herring DNA were added to a two-phase system containing a crude sample of EcoR V (treated with PEI). In Fig.

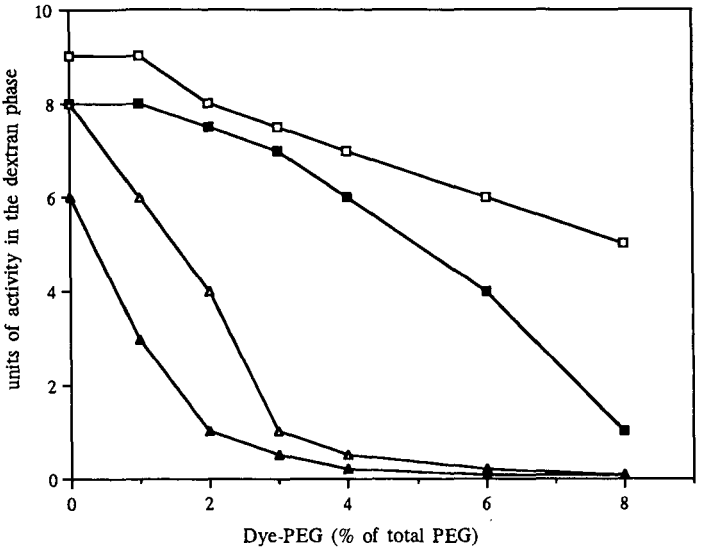

Fig. 4. Activity of the enzyme EcoR I remaining in the dextran phase after the addition of increasing amounts of PEG-bound Procion Blue MX-4GD. The experiment was performed at four different NaCl concentrations: (□) 50; (■) 100; (△) 200; (▲) 300 m*M*. The same system was incorporated as in Fig. 2. Temperature, 4°C.

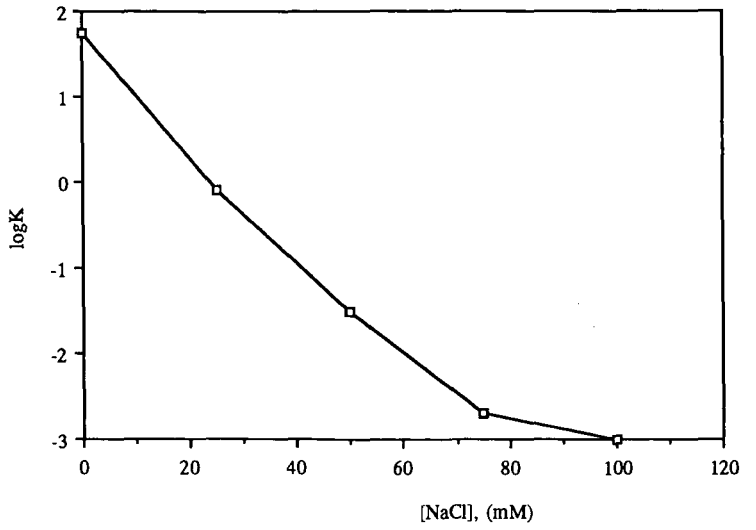

Fig. 5. Effect of NaCl on the partitioning of herring testes DNA. The same system was incorporated as in Fig. 2. Temperature, 4°C.

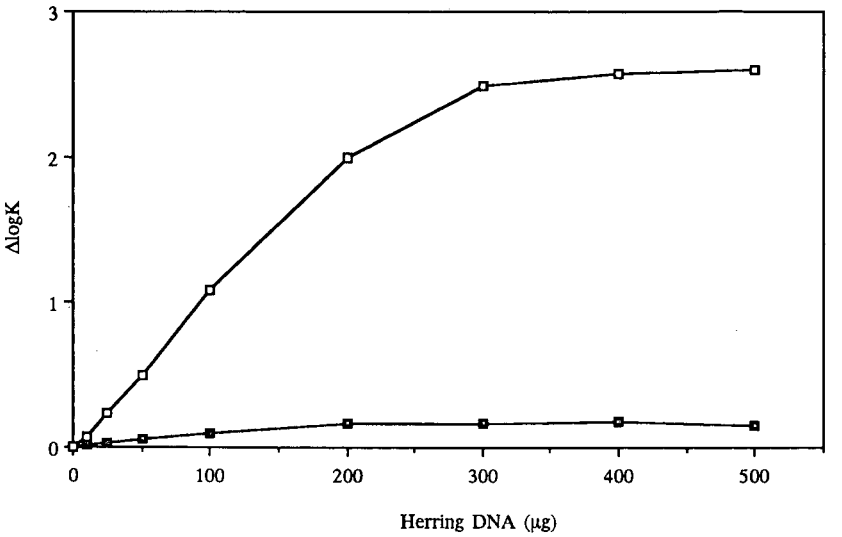

Fig. 6. Change in the partition coefficient of the enzyme EcoR V as a function of increasing concentration of herring testes DNA. (■) Protein; (□) EcoR V. The same system was incorporated as in Fig. 2. Temperature, 4°C.

6 it is shown that herring DNA not bound to PEG is able to extract the enzyme EcoR V into the PEG-rich phase with a maximum increase in $\Delta \log K$ of 2.5 units.

The affinity extraction of the enzyme EcoR V using non-specific DNA as an affinity ligand is illustrated in Fig. 7. The enzyme binds to herring DNA and follows its partitioning within the extraction steps. Using this simple scheme the enzyme can be extracted into the lower phase, in less than 1 h, with a 92% recovery and 4.7-fold purification.

Purification of EcoR I

Restriction endonuclease EcoR I was purified from an extract of *Escherichia coli* RY 13 cells prepared as described under Experimental. Crude extract (0.5 ml; 5.2 mg of total protein; 40 000 units) was included in the initial two-phase system (No. 0). The composition of the system (4 gram) was 7.5% (w/w) dextran, 5.3% (w/w) PEG, 25 m*M*

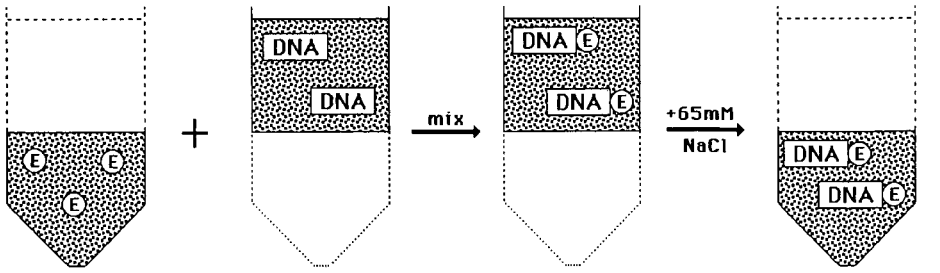

Fig. 7. Scheme for the affinity extraction of the enzyme EcoR V using non-specific DNA as an affinity ligand. The same system was incorporated as in Fig. 2. Temperature, 4°C.

lithium phosphate buffer (pH 6.8) and 50 m*M* sodium chloride. The partitioning was carried out at 4°C using gentle mixing for 30 s and centrifugation for 3–5 min at low speed (1000 *g*). Results from this experiment and from the following partitioning steps are given in Table I. The lower phase of systen 0, containing 90% of the enzyme, was washed by equilibration with pure upper phase of the same composition as above but containing 2% Procion Blue MX-4GD-PEG (of the total PEG amount), giving system No. 1. During the washing step, some dye-binding proteins were extracted into the upper phase, leaving 81% of the target enzyme in the lower phase. As shown in Fig. 4, the enzyme at low concentration of NaCl is not extracted by the dye into the upper phase. Subsequently, the upper phase of system 1 was replaced with a pure upper phase containing Procion Blue MX-4GD-PEG (6% of the total amount of PEG) and 490 m*M* NaCl, yielding system No. 2 (with a final concentration of 300 m*M* NaCl). In system No. 2 the PEG-bound triazine dye was now able to extract the enzyme in the upper phase with an 83% recovery and 4.3-fold purification.

The upper phase of system No. 2 (2.2 ml) was diluted with 10 ml of 20 m*M* Tris–HCl buffer (pH 7.4) containing 10% (v/v) glycerol. The solution was loaded onto a DEAE-cellulose column (8 ml) previously equilibrated in dilution buffer. The column was washed with buffer (40 ml) followed by a linear gradient of 0–0.8 *M* NaCl (80 ml) in dilution buffer. Fractions with EcoR I activity corresponding to *ca* 0.2 *M* NaCl in the gradient were pooled and stored at 4°C.

The final enzyme preparation was subjected to the "overdigestion" test and up to 100 U EcoR I did not produce any non-specific cleavage products after 6 h incubation with 1 μg of λDNA at 37°C, *i.e.*, after 600-fold overdigestion. In the "cut–ligate–recut" test, after more than 10-fold overdigestion of λDNA with EcoR I more than 90% of the DNA fragments could be ligated and recut with this enzyme.

Several purification methods related to the isolation of restriction endonuclease EcoR I have been reported previously [2,4,27]. However, all the procedures involve two or three chromatographic steps and 3–4 days are required for the completion of the preparation.

The purification method presented here is a rapid two-step procedure involving affinity partitioning in aqueous two-phase systems and ion-exchange chromatography with DEAE-cellulose. The whole preparation was completed within 1 day and with 54% recovery. The resulting enzyme preparation was purified 52-fold free from contaminating nuclease activities and is therefore suitable for commercial exploitation.

Purification of EcoR V

Restriction endonuclease EcoR V was purified from an extract of *Escherichia coli* J62 pLG74 cells prepared as described under Experimental. Crude extract (1 ml; 15 mg of total protein; 70 000 units) was included in the initial two-phase system (No. 0). The composition of the system (8 gram) was 7.5% (w/w) dextran, 5.3% (w/w) PEG and 25 m*M* lithium phosphate buffer (pH 6.8). The partitioning was carried out at 4°C using gentle mixing for 30 s and centrifugation for 3–5 min at low speed (1000 *g*). Results from this experiment and from the following partitioning steps are given in Table II. The lower phase of system 0, containing 86% of the enzyme, was equilibrated with pure upper phase [of the same composition as above but containing 2.5% Procion Blue MX-4GD-PEG (of the total PEG amount)], giving system No. 1. To the upper

TABLE I

PURIFICATION SCHEME FOR THE ISOLATION OF EcoR I USING THE DYE PROCION BLUE MX-4GD AS PEG-BOUND AFFINITY LIGAND

Purification step	Total protein (mg)	Total activity (units)	Purification factor	Yield (%)
Crude extract	5.2	40 000	1	100
Affinity partitioning				
System 0, lower "phase"	3.02	36 000	1.55	90
System 1, lower "phase"	1.8	32 400	2.34	81
System 2, upper "phase"	0.35	27 000	10	67.5
DE-52 column	0.054	21 600	52	54

phase of system 1 (in which the dye–PEG extracts the target enzyme), 0.5 g of a solid mixture of K_2HPO_4 and $NaH_2PO_4 \cdot 2H_2O$ (1:1.3, w/w) was added, giving a PEG–salt two-phase system (No. 2). The enzyme was recovered into the lower (salt-rich) phase and dialysed against 20 m*M* Tris–HCl buffer (pH 7.4) containing 7 m*M* 2-mercapto-ethanol, 50 m*M* NaCl, 10% (v/v) glycerol and 0.1% (v/v) NP-40 (buffer B). The solution (3 ml) from the latter preparation was applied to a MonoS cation-exchange HPLC adsorbent (50 × 5 mm I.D.; 1 ml) which had been previously equilibrated in buffer B. The column was washed with 4 ml of irrigating buffer and then developed with a linear gradient of NaCl (15 ml total volume; 50–400 m*M*) in buffer B at a flow-rate of 1 ml/min. Fractions with EcoR V activity corresponding to *ca.* 0.15 *M* NaCl in the gradient were pooled and stored at 4°C. The final enzyme preparation was subjected to the "overdigestion" test and up to 100 U of EcoR V did not produce any non-specific cleavage products after incubation for 6 h with 1 μg of λDNA at 37°C, *i.e.*, after 600-fold overdigestion. In the "cut–ligate–recut" test, after more than 10-fold overdigestion of λDNA with EcoR V more than 90% of the DNA fragments could be ligated and recut with this enzyme.

A method for the purification of EcoR V has been described previously [12]. It involves three chromatographic steps based on dye-ligand chromatography and 3–4

TABLE II

PURIFICATION SCHEME FOR THE ISOLATION OF EcoR V USING THE DYE PROCION BLUE MX-4GD AS PEG-BOUND AFFINITY LIGAND

Purification step	Total protein (mg)	Total activity (units)	Purification factor	Yield (%)
Crude extract	15	70 000	1	100
Affinity partitioning				
System 0, lower "phase"	7.2	60 000	1.78	86
System 1, upper "phase"	4.3	55 000	2.74	78
System 2, lower "phase"	3.8	51 000	2.88	73
Mono S column	0.23	40 000	37.3	57

days are required for the completion of the preparation. Similarly to EcoR I, the preparation presented above was completed within 1 day and with 57% recovery. The resulting enzyme preparation was purified 37-fold free from contaminating nuclease activities and is therefore suitable for commercial exploitation.

CONCLUSIONS

Restriction endonucleases can be isolated free from non-specific endonucleases using a combination of affinity partitioning and ion-exchange chromatography. Triazine dyes bound to PEG and free endogenous and herring DNA can be effectively employed as affinity ligands in aqueous two-phase systems. Bacterial DNA affects the partitioning of restriction endonucleases and this property can be exploited for their effective isolation. Owing to the extreme partitioning of DNA, several other DNA-binding proteins could potentially also be effectively extracted.

REFERENCES

1 R. J. Roberts, *Nucleic Acids Res.*, 17 (1989) 347.
2 R. A. Rubin and P. Modrich, *Methods Enzymol.*, 65 (1980) 96.
3 L. Y. Fuchs, L. Covarrubias, L. Escalante, S. Sanchez and F. Bolivar, *Gene*, 10 (1980) 39.
4 P. J. Greene, L. H. Heyneker, F. Bolivar, R. L. Rodriguez, M. C. Betlach, A. A. Covarrubias, K. Beckman, D. J. Russell and H. W. Boyer, *Nucleic Acids Res.*, 5 (1978) 2373.
5 D. I. Smith, R. F. Blattner and J. Davies, *Nucleic Acids Res.*, 3 (1976) 343.
6 J. George and J. G. Chirikjian, *Nucleic Acids Res.*, 5 (1978) 2223.
7 K. Baski, L. D. Rogerson and W. G. Rushizky, *Biochemistry*, 17 (1978) 4136.
8 T. A. Bickle, V. Pirrotta and R. Imber, *Nucleic Acids Res.*, 4 (1977) 2561.
9 A. Q. Farooqui, *J. Chromatogr.*, 184 (1980) 335.
10 K. Baski and G. W. Rushizky, *Anal. Biochem.*, 99 (1979) 207.
11 V. Bouriotis, A. Zafeiropoulos and Y. D. Clonis, *Anal. Biochem.*, 160 (1987) 127.
12 G. Vlatakis, G. Skarpelis, I. Stratidaki, Y. D. Clonis and V. Bouriotis, *Appl. Biochem. Biotechnol.*, 15 (1987) 201.
13 P.-Å. Albertsson, *Partition of Cell Particles and Macromolecules*, Almqvist and Wiksell, Stockholm, 2nd ed., 1971.
14 G. Johansson, A. Hartman and P. A. Albertsson, *Eur. J. Biochem.*, 33 (1973) 379.
15 G. Johansson, *Methods Enzymol.*, 104 (1984) 356.
16 V. P. Shanbhag and G. Johansson, *Biochim. Biophys. Acta*, 61 (1974) 1141.
17 S. D. Flanagan, S. H. Barondes and P. Taylor, *J. Biol. Chem.*, 251 (1976) 858.
18 P. Hubert, E. Dellacherie, J. Neel and E. E. Baulieau, *FEBS Lett.*, 65 (1976) 169.
19 S. D. Flanagan and S. H. Barondes, *J. Biol. Chem.*, 250 (1975) 1484.
20 G. Kopperschläger and G. Johansson, *Anal. Biochem.*, 124 (1982) 117.
21 G. Johansson and M. Andersson, *J. Chromatogr.*, 291 (1984) 175.
22 G. Kopperschläger and G. Lorenz, *Biomed. Biochim. Acta*, 44 (1985) 517.
23 G. Birkenmeier, E. Usbeck and G. Kopperschläger, *Anal. Biochem.*, 136 (1984) 264.
24 V. Pirrota and T. Bickle, *Methods Enzymol.*, 65 (1980) 89.
25 S. Read and D. Northcote, *Anal. Biochem.*, 116 (1981) 53.
26 P.-Å. Albertsson, *Biochim. Biophys. Acta*, 103 (1965) 1.
27 P. A. Luke and S. E. Halford, *Gene*, 37 (1985) 241.

Journal of Chromatography, 538 (1991) 323–330
Elsevier Science Publishers B.V., Amsterdam

CHROM. 22 808

Identification of trichothecenes by frit-fast atom bombardment liquid chromatography–high-resolution mass spectrometry

R. KOSTIAINEN*
Food and Environmental Laboratory of Helsinki, Helsinginkatu 24, 00530 Helsinki (Finland)
and
K. MATSUURA and K. NOJIMA
Jeol Ltd., 1–2 Musashino, 3-Chome, Akishima, Tokyo 196 (Japan)
(Received August 17th, 1990)

ABSTRACT

Frit-fast atom bombardment liquid chromatography–mass spectrometry (LC–frit-FAB-MS) provides a specific and reliable method for the identification of trichothecenes without derivatization. The frit-FAB spectra exhibit an abundant glycerol adduct ion, a protonated molecule and fragment ions formed by the losses of functional groups in various combinations. The use of high-resolution mass spectrometry in LC–frit-FAB-MS provides improved selectivity in the monitoring and makes the determination of the elemental compositions of the ions possible. The measured mass values with resolution 8000 were typically within 5 mmu of the calculated values. Sensitivity in the range of hundreds of picograms per microlitre was achieved with resolution 8000 using selected ion monitoring in the detection of trichothecenes.

INTRODUCTION

Trichothecenes are serious contamination problem in foods and feeds [1–5]. They are naturally produced by a variety of fungi, which can be formed rapidly in grain and feed during harvest, transport and storage. Because of their extreme toxicity [3,6] and natural occurrence, several identification methods have been developed. Trichothecenes are often detected as their derivatives by gas chromatography (GC) [7–9] and GC–mass spectrometry (MS) [5,9–12]. Trichothecenes have been identified without derivatization by desorption chemical ionization tandem mass spectrometry (DCI-MS–MS) in relative pure samples [13–18]. In spite of the high specificity of MS–MS, the separation power of the DCI probe is very poor and the total specificity of DCI-MS–MS may not suffice in the determination of trichothecenes in complex matrices.

The recently introduced thermospray (TSP) LC–MS [19] has been used in the identification of trichothecenes without derivatization [20–23]. Trichothecenes form a very abundant ammonium adduct ion with minimum fragmentation under TSP

0021-9673/91/$03.50

conditions. LC–TSP-MS provides good sensitivity by monitoring the ammonium adduct ion of trichothecenes, but the lack of fragmentation leads to a reduced reliability of the identification and makes the structure characterization very difficult. The fragmentation can be improved by using MS–MS [23], but accurate mass measurements are not possible for daughter ions using triple quadrupole mass spectrometers, which have been used in most applications of tandem MS.

The recently introduced dynamic fast atom bombardment (FAB) LC–MS often produces spectra with molecular weight information and structure-characteristic fragmentation [24–27]. The method with low-resolution MS has been applied in the analysis of many organic compounds, such as bile acids [25,26], peptides [27,28], medicines [29], amino acids [30], antibiotics [31] and oligosaccharides [32], but only a few studies have been made using the high-resolution mode [33,34]. This paper describes the use of the high-resolution mode in the identification of some trichothecenes by LC–MS using the frit-FAB interface described in detail previously [25,26].

EXPERIMENTAL

The measurements were made with a Jeol JMS-SX102 high-resolution mass spectrometer with a JMA-DA6000 data system connected to an LC system by a Jeol frit-FAB interface. The ionization chamber temperature was 50°C, the xenon particle energy 4 keV, the emission current 10 mA, the accelerating voltage 8 kV and the magnetic field scanning range m/z 70–700 (3 s per scan). In order to increase the evacuation speed of the ion source, a liquid nitrogen trap was provided.

The eluent delivery was provided by two high-pressure pumps (Hewlett-Packard 1090 LC) coupled with an automated gradient controller. The pump used in the post-column addition of glycerol was a Jasco Familio-300 S. Samples were introduced into the LC system using an autoinjector with a 20-μl loop. The column used was ODS

TABLE I

THE TRICHOTHECENES STUDIED

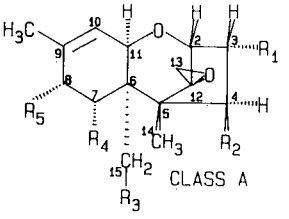

No.	Compound	R_1	R_2	R_3	R_4	R_5
1	T-2 toxin (T-2)	OH	OAc[a]	OAc	H	$OCOCH_2CH(CH_3)_2$
2	HT-2 toxin (HT-2)	OH	OH	OAc	H	$OCOCH_2CH(CH_3)_2$
3	Triacetoxyscirpenol (TAS)	OAc	OAc	OAc	H	H
4	Diacetoxyscirpenol (DAS)	OH	OAc	OAc	H	H
5	Monoacetoxyscirpenol (MAS)	OH	OH	OAc	H	H
6	Deoxynivalenol (DON)	OH	H	OH	OH	=O

[a] OAc = Acetyl.

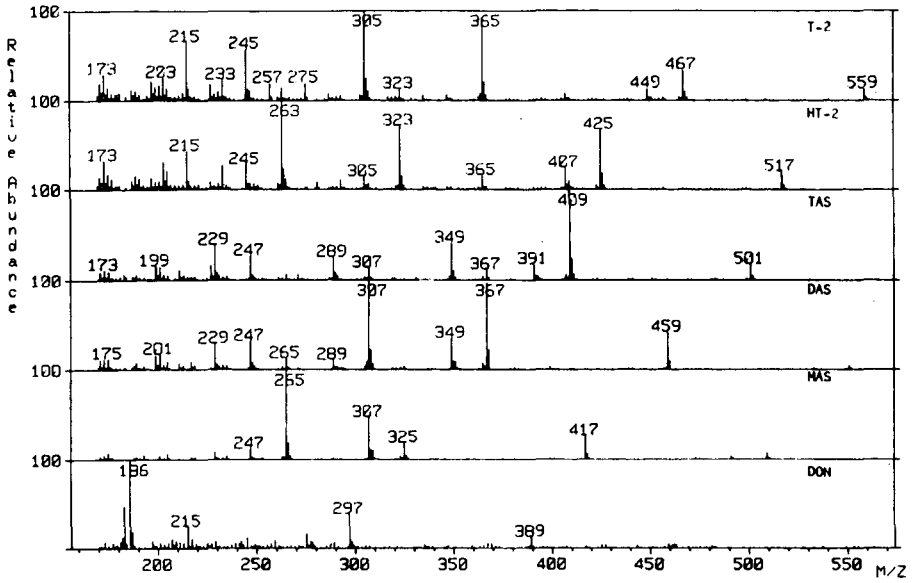

Fig. 1. Frit-FAB-MS spectra of the trichothecenes studied. Amount of trichothecenes introduced on-column, 2 μg (100 ng/μl; 20-μl injection).

(15 cm × 4.6 mm I.D.) (Nomura Kagaku). The trichothecenes were separated by means of a gradient at a flow-rate of 1.0 ml/min. Mobile phase A was water and B was methanol, with a gradient from 30% to 80% B from 0 to 15 min. Glycerol (4%) in methanol was added by means of a post-column at a flow-rate of 250 μl/min. Polyethylene glycol (0.02%) in the methanol solution including glycerol was used as a calibrant in the high-resolution measurements. The effluent from the column was split by a pneumatic splitter and the flow into the frit was 5 μl/min.

All the trichothecenes (Table I) were obtained from Sigma and dissolved in methanol. Glycerol was purchased from Waeko and polyethylene glycol (PEG) from Kanto.

RESULTS AND DISCUSSION

All the frit-FAB spectra of the trichothecenes (Fig. 1) exhibit an abundant glycerol adduct ion $[M+H+92]^+$ and a protonated molecule $[M+H]^+$ from which molecular weights can be reliably determined. Fragment ions are formed by the losses of functional groups as neutral species (water, acetic acid, formaldehyde and isovaleric acid) in various combinations (Table II). The most abundant fragment ions are formed by the loss of isovaleric acid and/or by successive losses of units of acetic acid. The loss of water in the case of TAS, which does not include any hydroxy group, probably occurs from the acetoxy group. This suggests the possibility that the ions $[M+H-H_2O]^+$ are partly formed by the loss of water from the acetoxy or isovaleroyloxy groups in the other trichothecenes.

Ion series of *m/z* 367, 307 and 247 in the spectrum of TAS are possibly formed by the losses of 0, 1 or 2 units of acetic acid combined with the loss of ketene or by the

TABLE II

ION SPECIES OF THE TRICHOTHECENES STUDIED

Compound	Ion species (m/z)[a]
T-2	559 = $[M+H+92]^+$, 467 = $[M+H]^+$, 449 = $[M+H-18]^+$, 407 = $[M+H-60]^+$, 365 = $[M+H-102]^+$, 323 = $[M+H-102-42]^+$ or $[M+H-60-84]^+$, 305 = $[M+H-102-60]^+$, 275 = $[M+H-102-60-80]^+$, 263 = $[M+H-102-60-42]^+$ o $[M+H-60-60-84]^+$, 257 = $[M+H-102-60-30-18]^+$, 245 = $[M+H-102-60-60]^+$ 233 = $[M+H-102-60-30-42]^+$ or $[M+H-60-60-30-84]^+$, 227 = $[M+H-102-60-60-18]^+$, 215 = $[M+H-102-60-60-80]^+$
HT-2	517 = $[M+H+92]^+$, 425 = $[M+H]^+$, 407 = $[M+H-18]^+$, 365 = $[M+H-60]^+$, 323 = $[M+H-102]^+$, 305 = $[M+H-102-18]^+$, 293 = $[M+H-102-30]^+$, 281 = $[M+H-102-42]^+$ or $[M+H-60-84]^+$, 263 = $[M+H-102-60]^+$, 245 = $[M+H-102-60-18]^+$, 233 = $[M+H-102-60-30]^+$, 215 = $[M+H-102-60-30-18]^+$
TAS	501 = $[M+H+92]^+$, 409 = $[M+H]^+$, 391 = $[M+H-18]^+$, 367 = $[M+H-42]^+$, 349 = $[M+H-60]^+$, 307 = $[M+H-60-42]^+$, 289 = $[M+H-60-60]^+$, 247 = $[M+H-60-60-42]^+$, 229 = $[M+H-60-60-60]^+$
DAS	459 = $[M+H+92]^+$, 367 = $[M+H]^+$, 349 = $[M+H-18]^+$, 307 = $[M+H-60]^+$, 289 = $[M+H-60-18]^+$, 265 = $[M+H-60-42]^+$, 247 = $[M+H-60-60]^+$, 229 = $[M+H-60-60-18]^+$
MAS	417 = $[M+H+92]^+$, 325 = $[M+H]^+$, 307 = $[M+H-18]^+$, 265 = $[M+H-60]^+$, 247 = $[M+H-60-18]^+$, 229 = $[M+H-60-18-18]^+$
DON	389 = $[M+H+92]^+$, 297 = $[M+H]$

[a] 18 = H_2O; 30 = CH_2O; 42 = CH_2CO; 60 = CH_3COOH; 84 = $(CH_3)_2CHCHCO$; 102 = $(CH_3)_2CHCH$; 92 = $CH_2OHCHOHCH_2OH$.

substitution reaction with water. In an earlier study, the respective ions were shown to be formed by the losses of functional groups with the loss of ketene in the collision-activated dissociation (CAD) of ammonium adduct ions [13]. This suggests the possibility that the ion series of m/z 367, 307 and 247 in the frit-FAB spectrum of TAS and the respective ions in the spectra of the other trichothecenes are partly formed via a similar pathway.

The fragmentation in the frit-FAB spectra is higher than in the TSP spectra obtained in previous studies [20–22], but is very similar to the CAD spectra of ammonium adduct ions [13] and to the isobutane desorption chemical ionization (DCI) [16,35] spectra of the trichothecenes reported earlier. It might be only in this instance that the amount of energy transferred into the internal energy of the molecule is nearly the same in DCI as in frit-FAB. However, the conclusion cannot be generalized, as the exothermicity of the proton transfer reaction determines the amount of fragmentation in isotubtane CI, but in addition to exothermicity many other factors affect the fragmentation in the frit-FAB mode.

Fig. 2 shows mass chromatograms of the studied trichothecenes recorded by LC–frit-FAB-MS with whole mass range scanning and resolution 1000 from the standard sample (100 μg/ml). All the studied trichothecenes separated well with relatively symmetrical and narrow peaks (peak width 0.5–1 min) under the chosen LC conditions, although post-column addition of the glycerol causes peak broadening.

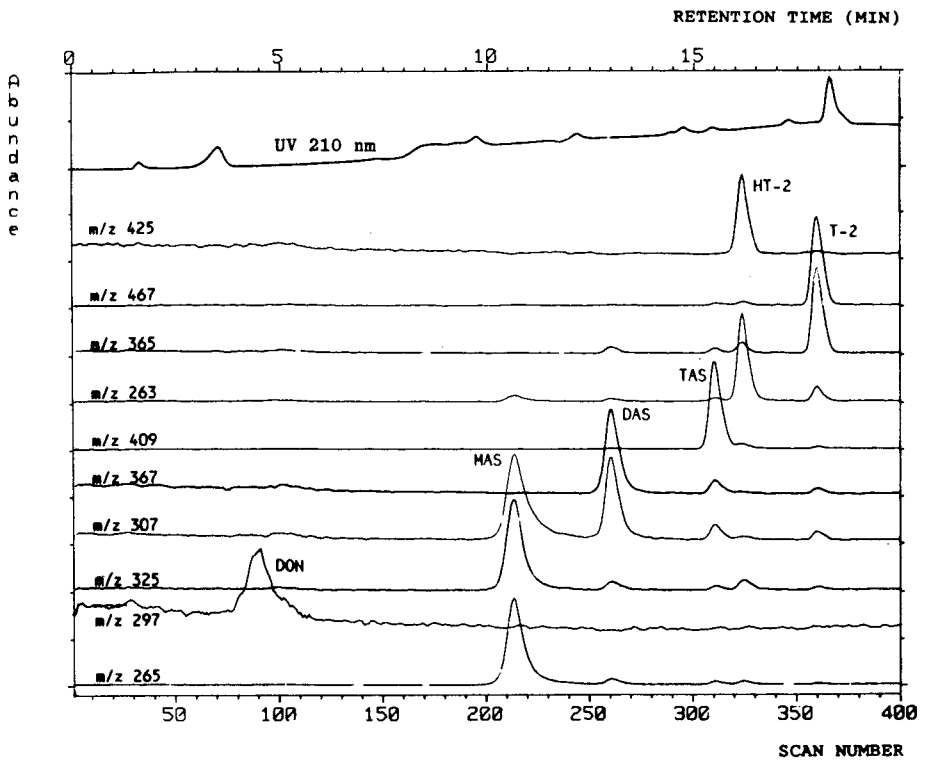

Fig. 2. Mass chromatograms of the trichothecenes studied, recorded by LC–frit-FAB-MS with resolution 1000 from the standard sample. Amount of trichothecenes introduced on-column, 2 μg (100 ng/μl; 20-μl injection). The scan range was from *m/z* 70 to 700.

The specificity of the method can be improved by using high-resolution MS. Fig. 3 shows mass chromatograms of the protonated molecules of the studied trichothecenes recorded with resolution 8000 from the standard sample (10 μg/ml) using selected ion monitoring and a multi-grouping technique: the monitored mass values *m/z* 297.134 (DON), 325.165 (MAS), 367.176 (DAS) and 371.228 (PEG; lock mass) were changed after 14.5 min to *m/z* 409.186 (TAS), 425.216 (HT-2), 467.228 (T-2) and 459.281 (PEG; lock mass). The mass window used in the lock mass monitoring was 200 mmu. Stable lock ion current profiles show good stability of the LC–frit-FAB-high-resolution MS. The detection limits with resolution 8000 using selected ion monitoring were about 5 μg/ml for DON and MAS and slightly less than 1 μg/ml for the other trichothecenes.

The use of high resolution in LC–frit-FAB-MS also allows the determination of elemental compositions of the ions from the components represented in the LC peaks. Table III presents accurate mass measurements of the protonated molecules and some fragment ions of the studied trichothecenes with resolution 8000. The measurements were made with column injection from the standard samples including trichothecenes (100 μg/ml). The measured mass values are typically within 5 mmu of the calculated values. The results are accurate enough for a reliable determination of the elemental compositions of the ions.

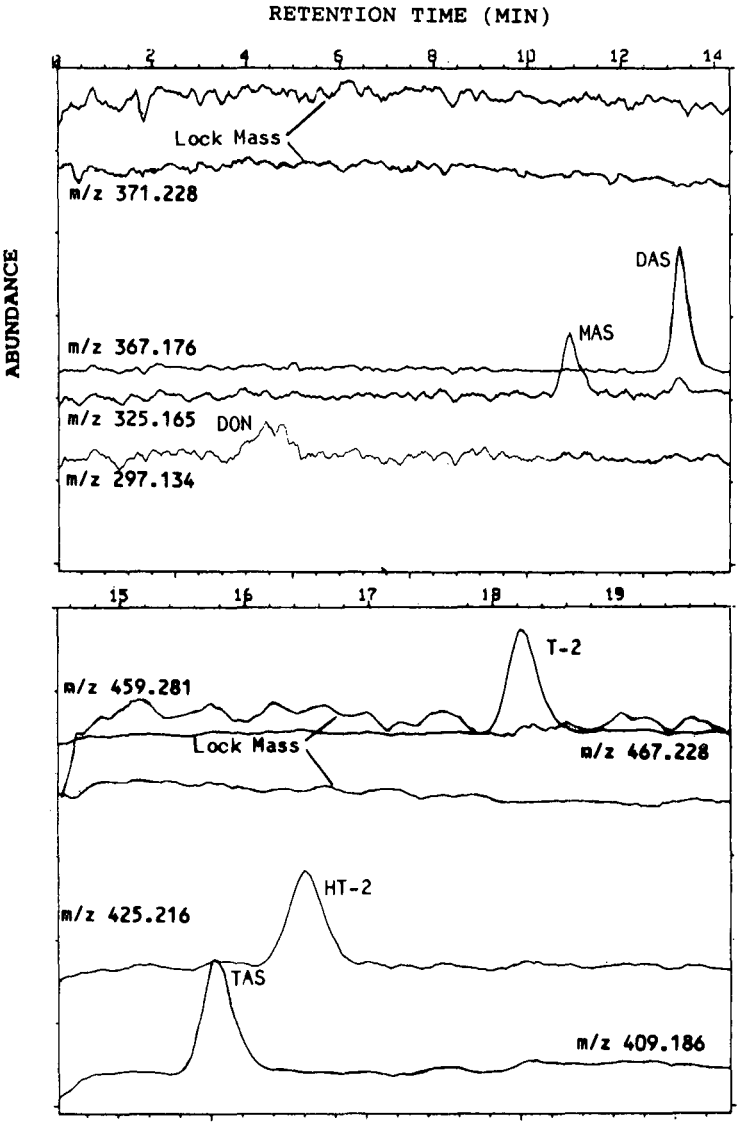

Fig. 3. Selected ion current profiles of the protonated molecules of the thichothecenes studied, recorded by LC–frit-FAB-MS with resolution 8000 using selected ion monitoring and the multi-grouping technique from the standard solution. Amount of trichothecenes introduced on-column, 200 ng (10 ng/μl; 20-μl injection).

CONCLUSIONS

LC–frit-FAB-MS is well suited to the identification of trichothecenes at concentration levels higher than hundreds of picograms per microlitre. The selectivity of the detection can be increased by using high-resolution mass spectrometry, which

TABLE III

ELEMENTAL COMPOSITIONS AND ACCURATE MASSES OF SOME IONS OF THE TRICHOTHECENES STUDIED, OBTAINED BY FRIT–FAB LC–MS

The resolution was 8000 and the scan range was from m/z 150 to 550. Trichothecenes were separated with an ODS C_{18} column and the standard sample concentration was 100 μg/ml.

Compound	Measured mass	mmu	Elemental composition
T-2	467.2140	−14.2	$C_{24}H_{35}O_9$
T-2	365.1581	− 2.0	$C_{19}H_{25}O_7$
T-2	305.1449	6.0	$C_{17}H_{21}O_5$
HT-2	425.2260	8.5	$C_{22}H_{33}O_8$
TAS	409.1823	− 4.0	$C_{21}H_{29}O_8$
DAS	367.1758	0.1	$C_{19}H_{27}O_7$
DAS	349.1707	5.7	$C_{19}H_{25}O_6$
DAS	307.1516	− 3.0	$C_{17}H_{23}O_5$
MAS	325.1607	− 4.4	$C_{17}H_{25}O_6$
MAS	307.1584	3.8	$C_{17}H_{22}O_5$
MAS	265.1486	4.6	$C_{15}H_{21}O_4$
DON	297.1412	7.4	$C_{15}H_{21}O_6$

also allows accurate mass measurements of the components represented in the LC peaks.

ACKNOWLEDGEMENTS

This work was supported by the Magnus Ehrnrooth and Oskar Öflunds Foundations.

REFERENCES

1 Y. Ueno, in K. Miller (Editor), *Toxicological Aspects of Food*, Elsevier Applied Science, Barking, 1987, p. 150.
2 Y. Ueno, in P. Krogh (Editor), *Mycotoxins in Food*, Academic Press, London, 1988, pp. 123–147 and 217–249.
3 T. Yoshizawa, in Y. Ueno (Editor), *Trichothecenes —Chemical, Biological and Toxicological Aspects (Developments in Food Science*, Vol. 4), Kodansha and Elsevier, Tokyo, 1983, p. 195.
4 E. Karppanen, A. Rizzo, S. Berg, E. Lindfors and R. Aho, *J. Agric. Sci. Finl.*, 57 (1985) 195.
5 R. Kostiainen and S. Nokelainen, *J. Chromatogr.*, 513 (1990) 31.
6 K. C. Erlich and K. W. Daigle, *Biochim. Biophys. Acta*, 923 (1987) 206.
7 C. E. Kientz and A. Verweij, *J. Chromatogr.*, 355 (1986) 229.
8 H. D. Rood, Jr., W. B. Buck and S. P. Swanson, *J. Agric. Food Chem.*, 36 (1988) 74.
9 R. M. Black, R. J. Clarke and R. W. Read, *J. Chromatogr.*, 388 (1987) 365.
10 R. Kostiainen and A. Rizzo, *Anal. Chim. Acta*, 204 (1988) 233.
11 J. D. Rosen, R. T. Rosen and T. G. Hartman, *J. Chromatogr.*, 355 (1986) 241.
12 C. J. Mirocha, S. V. Pathre, R. J. Pawlosky and D. W. Hewetson, in R. J. Cole (Editor), *Modern Methods in the Analysis and Structural Eludiation of Mycotoxins*, Academic Press, Orlando, FL, 1986, p. 353.
13 R. Kostiainen and A. Hesso, *Biomed. Environ. Mass Spectrom.*, 15 (1988) 79.
14 R. Kostiainen, *Biomed. Environ. Mass Spectrom.*, 16 (1988) 197.
15 R. Kostiainen, *Biomed. Environ. Mass Spectrom.*, 18 (1988) 116.
16 R. Kostiainen, A. Rizzo and A. Hesso, *Arch. Environ. Contam. Toxicol.*, 18 (1989) 356.
17 T. Krishnamurthy and E. W. Saver, *Anal. Chem.*, 59 (1987) 1272.
18 T. Krishnamurthy and E. W. Saver, *Biomed. Environ. Mass Spectrom.*, 15 (1988) 13.

19 C. R. Blakey and M. L. Vestal, *Anal. Chem.*, 55 (1983) 750.
20 R. D. Voyksner, W. M. Hagler, Jr., and S. W. Swanon, *J. Chromatogr.*, 394 (1987) 183.
21 P. Sakkers, E. Rajakylä and K. Laasasenaho, *J. Chromatogr.*, 384 (1987) 391.
22 T. Krishnamurthy, D. J. Beck, R. K. Isensee and B. B. Jarvis, *J. Chromatogr.*, 469 (1989) 209.
23 T. Krishnamurthy, D. J. Beck and R. K. Isensee, *Biomed. Environ. Mass Spectrom.*, 18 (1989) 287.
24 A.Hosoi, *Jpn. Pat. Appl.*, 83-209854, 1983.
25 Y. Ito, T. Takeuchi, D. Ishii, M. Goto and T. Mizuno, *J. Chromatogr.*, 346 (1985) 161.
26 Y. Ito, T. Takeuchi, D. Ishii, M. Goto and T. Mizuno, *J. Chromatogr.*, 358 (1986) 201.
27 R. Caprioli, T. Fan and J. S. Cottrell, *Anal. Chem.*, 58 (1986) 2949.
28 R. M. Caprioli, *Spectra*, 12 (1989) 4.
29 P. Kokkonen, W. M. A. Niessen, U. R. Tjaden and J. Van Der Greef, *J. Chromatogr.*, in press.
30 A. E. Ashcroft, J. R. Chapman and J. S. Cottrell, *J. Chromatogr.*, 394 (1987) 15.
31 T. Takeuchi, S. Watanabe, N. Kondo, D. Ishii and M. Goto, *J. Chromatogr.*, 435 (1988) 482.
32 Y. Ito, T. Takeuchi, D. Ishii, M. Goto and T. Mizuno, *J. Chromatogr.*, 391 (1987) 296.
33 R. Pesch, *Application Data Sheet*, No. 3, Finnigan MAT, San Jose, CA, 1988.
34 R. Owen, *FAB Application Note*, VG Tritech, Manchester, 1987.
35 R. Kostiainen, T. Kotiaho and A. Hesso, in M. Rautio (Editor), *Systematic Identification of Mycotoxins: B5: Selected Trichothecenes, Aflatoxins and Related Mycotoxins, Mass Spectrometric Analysis*, Ministry for Foreign Affairs of Finland, Helsinki, 1986, p. 53.

Journal of Chromatography, 538 (1991) 331–339
Elsevier Science Publishers B.V., Amsterdam

CHROM. 22 806

Determination of β-carbolines in foodstuffs by high-performance liquid chromatography and high-performance liquid chromatography–mass spectrometry

JUNKO ADACHI* and YASUHIKO MIZOI
Department of Legal Medicine, Kobe University School of Medicine, Kobe 650 (Japan)
TAKEAKI NAITO
Kobe Women's College of Pharmacy, Kobe 658 (Japan)
KENJI YAMAMOTO and SATOSHI FUJIWARA
Department of Legal Medicine, Kobe University School of Medicine, Kobe 650 (Japan)
and
ICHIYA NINOMIYA
Kobe Women's College of Pharmacy, Kobe 658 (Japan)
(First received February 5th, 1990; revised manuscript received August 6th, 1990)

ABSTRACT

A high-performance liquid chromatographic method combined with fluorimetric detection is described for the determination of β-carboline (norharman) and 1-methyl-β-carboline (harman). The analysis of foodstuffs for the identification of β-carbolines is facilitated by clean-up of samples using Bond Elut PRS cartridges. Recoveries were excellent. Further, a high-performance liquid chromatographic–mass spectrometric method was also developed for their identification. The concentrations of β-carboline among the foodstuffs and alcoholic beverages varied greatly. Also, norharman and harman were observed in uncooked foodstuffs, whereas acetaldehyde was found in most fermented food. The toxicological implication of β-carbolines in foodstuffs is discussed.

INTRODUCTION

β-Carboline (norharman) and 1-methyl-β-carboline (harman) have been prepared by the reaction of tryptophan with some aldehydes under an oxidative condition. It is well known that these β-carbolines inhibit monoamine oxidase [1] and benzodiazepine receptor binding [2]. In addition, β-carbolines, which are not mutagenic *per se*, have been reported to possess co-mutagenic activity [3,4] as carcinogens such as aniline and *o*-toluidine are mutagenic in the presence of β-carbolines. β-Carbolines have been found to be present in tryptophan pyrolysate, cigarette smoke condensate [5], cooked foods [6] and mushrooms [7]. As the concentrations of β-carbolines are so low that their extraction is extremely difficult, an analytical procedure for foodstuffs has not yet been established.

This paper describes a simple solid-phase method for the extraction of

0021-9673/91/$03.50

norharman and harman from foodstuffs and alcoholic beverages followed by analysis by high-performance liquid chromatography (HPLC) and high-performance liquid chromatography–mass spectrometry (LC–MS).

EXPERIMENTAL

Materials

L-Tryptophan, propionaldehyde, norharman and harman were purchased from Sigma. 1-Ethyl-1,2,3,4-tetrahydro-β-carboline-3-carboxylic acid, which was readily prepared from L-tryptophan and propionaldehyde as described by Brossi *et al.* [8], was heated at 240°C in the presence of 10% palladium–carbon without solvent for 30 min and yielded 1-ethyl-β-carboline, to be used as an internal standard (I.S.). The methanol used was of HPLC grade (Wako). Perchloric acid was obtained from Koso Chemicals. All other chemicals were of analytical-reagent grade.

Foodstuffs and alcoholic beverages were purchased from local groceries. Propylsulphonic acid (PRS) solid-phase extraction cartridge and the vacuum manifold used (Vac-Elut) were purchased from Analytichem International.

Sample preparation

For alcoholic beverages, a 10–20-ml aliquot was diluted to 30–50 ml with distilled water, and for vinegar and soy sauce a 1.0-ml aliquot was similarly diluted to 10 ml. Amounts of 3–5 g of solid samples (all powder except for miso, which is a soybean paste) were homogenized with 0.6 *M* perchloric acid followed by centrifugation, the supernatant being used for analysis. Each sample was poured into a beaker containing 60 ng of the internal standard, mixed and adjusted to pH 1.5 by the addition of 2 *M* hydrochloric acid. Solid-phase extraction cartridges (Bond Elut) of 3-ml capacity, containing propylsulphonic acid-derivatized silica (PRS) packing material, were positioned in a ten-cartridge-capacity Vac Elut system. The pressure was adjusted to 5–10 mmHg and each cartridge was conditioned by washing with 2 × 3 ml of methanol followed by 2 × 3 ml of 0.1 *M* hydrochloric acid. Before complete desiccation of the cartridge, the acidified sample was applied to the cartridge and drawn through, then washed with 6 ml of water. The cartridge was rinsed with 3 ml of 0.4 *M* phosphate buffer (pH 9.1). Up to this point, all the washings and unadsorbed portions of the samples were discarded. Clean 8-ml glass collection tubes were inserted into the vacuum manifold and β-carbolines were eluted with 3 ml of methanol–0.2 *M* phosphate buffer (pH 8.8) (1:1). A 5-μl volume of the eluate was injected directly into the HPLC system.

Chromatography

HPLC was performed on a Yanaco, L-4000W instrument using a stainless-steel column (150 × 4.6 mm I.D.) packed with Cosmosil C_{18}-P (5 μm) (Nacalai Tesque). The flow-rate was kept constant at 0.6 ml/min at ambient temperature. The compounds were detected with a fluorescence monitor (Shimadzu RF 535) equipped with a xenon lamp. The excitation wavelength was 300 nm (band width 13 nm) and the emission wavelength was 433 nm (band width 15 nm). The mobile phase was methanol–0.1 *M* potassium phosphate buffer (0.1 *M* KH_2PO_4 adjusted with H_3PO_4) (pH 3.0) (32:68, v/v).

Quantitation

Calibration graphs for norharman and harman were constructed by plotting peak-height ratios (norharman/I.S. and harman/I.S.) against concentration. The standard solutions consisted of 5–50 ng/ml of norharman, 10–100 ng/ml of harman and 20 ng/ml of I.S. The calibration graphs were linear over the concentration range studied. The concentrations of norharman and harman were determined from the peak-height ratio of each sample by reference to the calibration graphs. Their recoveries from the sample extracts were determined by comparison of the peak heights obtained after injection of a sample extract spiked with a known concentration. The recoveries of norharman and harman varied from 90 to 100%.

LC–MS

A liquid chromatograph–tandem quadrupole mass spectrometer (Shimadzu LC–MS-QP1000) equipped with a Vestec thermospray (TSP) interface was used for recording mass spectra and selected ion monitoring. The mobile phase, methanol–(0.1 *M* ammonium formate + 0.1 *M* formic acid) (pH 3.4) (23:77, v/v), was delivered by a syringe pump (Shimadzu LC-6A) at a flow-rate of 1.0 ml/min. Samples were injected with a Rheodyne Model 7125 injector fitted with a 100-μl loop. The exit temperature of the vaporizer was 140°C and the block temperature of the ionization chamber was 250°C. Positive-ion TSP mass spectra were obtained. Typical conditions for TSP-MS were scan range *m/z* 150–400 in 2 s, electron multiplier voltage 2450 V and preamplifier gain $7 \cdot 10^7$ V/A. The lower scan range limit of *m/z* 150 was used to avoid any background interference from ammonium formate.

Determination of ethanol and acetaldehyde concentrations

A 1-ml volume of each alcoholic beverage was diluted to 100 ml with distilled water and a 1.0-ml aliquot of this, 0.5 ml of vinegar and soy sauce and 0.5 g of miso were used as samples for ethanol determination. A 1.0-ml aliquot of each liquid sample and 1.0 g of miso were used as samples for acetaldehyde determination. A 6-ml volume of 0.6 *M* perchloric acid and each sample were mixed thoroughly and the mixtures were centrifuged at 1665 *g* for 10 min at 4°C. Volumes of 2 ml of the clear acidic supernatants were placed in vials and the headspace gas in each vial was analysed using a Perkin-Elmer F45 headspace analyser according to an earlier method [9].

RESULTS

Extraction

Four sorbents (C_8, C_{18}, SCX and PRS) of solid-phase extraction cartridges were evaluated for extraction of norharman and harman from applied samples. PRS yielded the cleanest and highest recoveries, whereas using a C_8, C_{18} or SCX cartridge many co-eluting peaks from beer samples appeared in the chromatogram.

Chromatography

Fig. 1 shows the HPLC of norharman, harman and I.S. in standards and a brandy sample. Two different columns packed with TSK gel ODS-80Tm (250 × 4.6 mm I.D.) and Cosmosil $5C_{18}$-P were evaluated for the separation of norharman and harman. With the TSK gel ODS-80Tm, the analysis of each sample took about

30 min, whereas only 10 min were necessary to achieve a good separation among the compounds analysed using $5C_{18}$-P, as shown in Fig. 1. The limit of detection of each β-carboline was 2 pg. The reproducibility of sake analyses (n = 5) was 2% (relative standard deviation) for norharman and 1.5% for harman.

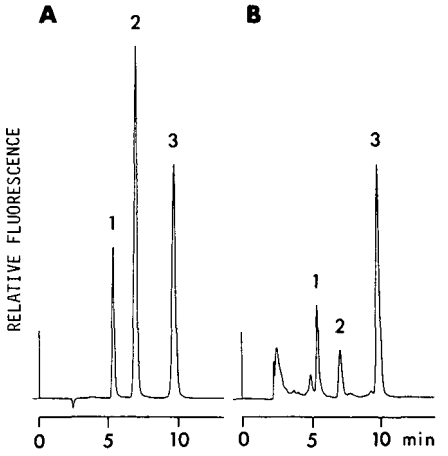

Fig. 1. High-performance liquid chromatograms of β-carbolines. (A) Standard mixture; (B) brandy sample. Peaks: 1 = norharman; 2 = harman; 3 = 1-ethyl-β-carboline (internal standard). A 5-μl volume of the eluate from the extraction cartridge was injected and the amounts injected in a brandy sample were 22 pg of norharman and 9 pg of harman.

LC–MS

The TSP ionization mass spectra of norharman and harman extracted from sake are displayed in Fig. 2. The mass spectra were identical with those obtained from standards. Formation of the MH^+ ion of either norharman and harman was observed as a base peak under TSP ionization conditions. The total ion chromatogram and mass chromatograms of norharman and harman obtained in the analysis of a standard mixture and an extract of sake are illustrated in Fig. 3. Peaks representing norharman as MH^+ were seen at m/z 169 at a retention time (R.T.) of 5.8 min and from harman as MH^+ at m/z 183 at an R.T. of 8.5 min. Hence LC–MS analysis provided a definitive structural identification. The amounts injected to obtain the data in Figs. 2 and 3 were calculated to be 0.27 μg for norharman and 2.3 μg for the harman.

Concentrations of β-carbolines

Table I gives the concentrations of norharman and harman in various alcoholic beverages. Generally, a small amount of β-carbolines was observed. The highest concentrations of both norharman and harman were obtained in sake A, which was brewed in a rural district. Sake and wine contained larger amounts of harman than beer and whisky. The norharman concentration was high in beer, whereas it was lower and similar in sake, wine and whisky. The concentration of harman was higher than that of norharman in sake and wine.

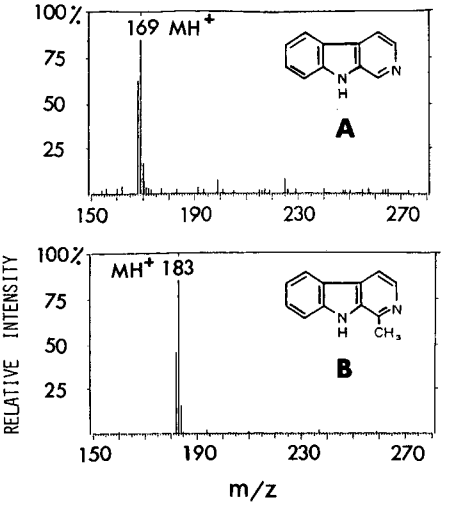

Fig. 2. Thermospray ionization mass spectra of β-carbolines from sake. (A) Norharman; (B) harman. A 5-μl volume of the eluate from the extraction cartridge was injected and the amounts injected were 0.27 μg of norharman and 2.3 μg of harman.

Concentrations of norharman and harman in various foodstuffs are given in Table II. Wide variations existed in the concentrations of β-carbolines among the foodstuffs. Both norharman and harman were highest in vinegar A (made from wheat), whereas norharman was lowest in vinegar D (made from corn) and harman

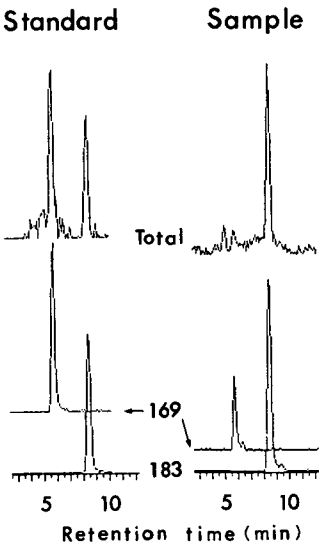

Fig. 3. Total ion chromatograms and mass chromatograms of β-carbolines from a standard mixture and sake sample obtained using thermospray LC–MS. The MH^+ ions of norharman (mol. wt. 168) and harman (mol. wt. 182) were obtained at *m/z* 169 and 183, respectively. A 5-μl volume of the eluate from the extraction cartridge was injected and the amounts injected in a sake sample were 0.27 μg of norharman and 2.3 μg of harman.

TABLE I

CONCENTRATIONS OF NORHARMAN AND HARMAN IN ALCOHOLIC BEVERAGES

Values are means ± S.D.

Sample[a]	*N*	Norharman (ng/ml)	Harman (ng/ml)
Sake	6	0.2 ± 0.2	4.1 ± 4.0
Wine	5	0.5 ± 0.2	8.5 ± 14
Beer	8	2.7 ± 0.7	1.7 ± 0.7
Whisky	5	1.2 ± 1.1	2.1 ± 2.6
Shochu	2	0.1 ± 0	0.1 ± 0
Brandy	1	0.5	0.2
Sake A	1	67	590
Liqueur	1	26	85

[a] Brand names were as follows. Sake: Hakutsuru, Kikumasamune, Umenishiki, Sawanotsuru, Yamatokotsuchi, Nadagiku. Wine: Kirin Wine Club White, Kirin Wine Club Red, Kirin Wine Club Rosé, Zeller Schwarze Katz, Piat d'Or. Beer: Kirin Lager, Asahi Super Dry, Kirin Light Beer, Suntory Malt's, Sapporo Hardy, Kirin Fine Pilsner, Coors, Budweiser. Whisky: Suntory Red, Nikka Pure Malt, Hi Nikka Whisky, Torys, Glenfiddich. Shochu: Iichiko, Kumesen. Brandy: Remy Martin VSOP. Sake A: Akitanishiki. Liqueur: Kurisake.

TABLE II

CONCENTRATIONS OF NORHARMAN, HARMAN, ETHANOL AND ACETALDEHYDE IN VARIOUS FOODSTUFFS

Each value represents a single determination.

Sample[a]	Source	Norharman (ng/ml or g)	Harman (ng/ml or g)	Ethanol (mg/ml or g)	Acetaldehyde (μg/ml or g)
Vinegar					
A	Wheat	96	730	0.57	15
B	Rice	22	56	2.1	3.1
C	Grape	5.6	35	13	70
D	Corn	1.9	15	1.2	1.9
Soy sauce					
A	Soybean	71	250	21	13
B	Soybean	15	130	24	14
Miso					
A	Soybean	8.2	35	0.11	8.3
B	Rice	15	0.9	2.8	13
C	Barley	45	9.6	4.4	6.9
Soybean protein	Soybean	3.0	0.8		
Soybean flour	Soybean	10	4.7		
Corn starch	Corn	3.6	0.9		
Rye flour	Rye	39	12		

[a] Brand names were as follows: vinegar A, Mitsukan; vinegar B, Mitsukan; vinegar C, Bodegas Reserva 25; vinegar D, Tamanoi Su; soy sauce A, Kikkoman; soy sauce B, Higashimaru; miso A, Oucho; miso B, Toyama Kouji miso; miso C, Ehime Inaka miso; soybean protein, Meiji protein powder; soybean flour, Fukumoto; corn starch, Nisshoku; rye flour, Mukai.

was lowest in corn starch. In general, fermented products from grain contained a relatively large amount of β-carbolines.

Concentrations of ethanol and acetaldehyde

Table II gives the concentrations of ethanol and acetaldehyde in foodstuffs. The highest level of ethanol was found in soy sauce B and the lowest in miso A. The highest level of acetaldehyde was found in vinegar C (made from grape) and the lowest in vinegar D (made from corn). Table III shows the amount of acetaldehyde contained in alcoholic beverages. The acetaldehyde concentration was highest in a liqueur and lowest in a shochu.

TABLE III

CONCENTRATIONS OF ETHANOL AND ACETALDEHYDE IN ALCOHOLIC BEVERAGES

Each value represents a single determination.

Sample[a]	Ethanol % (v/v)	Acetaldehyde (μg/ml)
Sake A	16	30
Sake B	16	13
Wine A	14	31
Beer A	4.5	13
Whisky A	43	24
Shochu A	25	5.5
Brandy A	40	51
Liqueur A	14	55

[a] Brand names were as follows: sake A, Akitanishiki; sake B, Sawanotsuru; wine A, Kirin Wine Club Red; beer A, Kirin Fine Pilsner; whisky A, Suntory Red; shochu A, Iichiko; brandy A, Remy Martin VSOP; liqueur A, Kurisake.

DISCUSSION

As β-carbolines containing an amino group are not easily volatilized, direct analysis by gas chromatography–MS is difficult and a derivatization reaction such as amidation is necessary [6,10]. We have reported here for the first time the analysis of norharman and harman directly and qualitatively using LC–MS. The MH^+ ion of either norharman or harman was demonstrated as a base peak. We identified the molecular weights of the compounds extracted from sake by the use of LC–MS. The HPLC system reported here gave a good separation of norharman and harman. No peak-interfering norharman or harman appeared in the liquid chromatogram (Fig. 1). Previously, the concentration of harman in alcoholic beverage was determined by HPLC [10], but the sensitivity was not reported, which precludes any comparison with the present method. The proposed method has the advantage of yielding extracts more simply and faster than liquid–liquid extraction [5,6,10], because the alkaline eluate of the solid-phase extraction cartridge through which food samples passed could be injected onto the HPLC column.

Although pancreatic or liver cancer is predominant in habitual drinkers and

alcoholic patients, it is not yet clear whether the direct action of alcohol or a very small amount of some substance contained in alcoholic beverages having mutagenic or carcinogenic activity could cause the cancer. The alcoholic beverages tested in this study were shown to contain β-carbolines, although the amount was very small. No relationship was found between the alcohol content and β-carboline concentration of alcoholic beverages. Our results for the concentration of harman in wine were in agreement with that obtained by Bosin and Faull [10], although the concentration in beer did not coincide with their result, which was much higher. As alcoholic patients consume large amounts of alcoholic beverages, it follows that relatively large amounts of β-carbolines would be ingested. In addition, acetaldehyde, a metabolite of ethanol, may have a possible role in forming β-carbolines endogenously in alcoholic patients. Accordingly, β-carbolines might also be involved in promoting cancer in alcoholic patients to some extent.

The content of norharman in the charred part of broiled bread, beef and sardines was reported to be 18–158 ng/g and that of harman 6–52 ng/g [6]. It was shown that cigarette smoke contained large amounts of norharman and harman, whereas tobacco leaf contained only 1% of the amount in smoke. The concentration of norharman in smoke was about 12 μg/g and that of harman was 4 μg/g [5]. In comparing the concentrations of β-carbolines between cigarette smoke and the present foodstuffs tested, the former was much greater than the latter. Norharman and harman must be formed during pyrolysis of tryptophan; however, even non-heated foodstuffs were observed to contain β-carbolines in the present study. This is the first report showing the existence of norharman in uncooked food. In addition, we showed that acetyldehyde, possibly formed from ethanol added to a condiment as a preservative, was present in most foodstuffs. However, no relationship between concentrations of ethanol and acetaldehyde or acetaldehyde and β-carbolines can be derived. As the involvement of not only acetaldehyde, but also tryptophan, in the formation of β-carbolines was considered, foodstuffs with high tryptophan contents should contain larger amounts of β-carbolines than alcoholic beverages.

In conclusion, this study has established a simple and sensitive method for determining norharman and harman, which have a co-mutagenic activity to produce human cancer, and found them not only in alcoholic beverages but also in some uncooked foods.

ACKNOWLEDGEMENTS

The authors thank Mrs. Junko Iida and Mr. Shingo Makioka, Shimadzu, Kyoto Analytical Applications Laboratory, for technical assistance.

REFERENCES

1 W. M. McIsaac and V. Estevez, *Biochem. Pharmacol.*, 15 (1966) 1625.
2 H. Rommelspacher, C. Nanz, H. O. Borbe, K. J. Fehske, W. E. Muller and U. Wollert, *Eur. J. Pharmacol.*, 70 (1981) 409.
3 M. Nagao, T. Yahagi, M. Honda, Y. Seino, T. Matsushima and T. Sugimura, *Proc. Jpn. Acad.*, 53B (1977) 34.
4 K. Wakabayashi, T. Yahagi, M. Nagao and T. Sugimura, *Mutat. Res.*, 105 (1982) 205.
5 E. H. Poindexter and R. D. Carpenter, *Phytochemistry*, (1962) 215.

6 T. Yasuda, Z. Yamaizumi, S. Nishimura, M. Nagao, Y. Takahashi, H. Fujiki, T. Sugimura and K. Tsuji, *Proc. Japan. Soc. Biomed. Mass Spectrom.*, 3 (1978) 97.
7 T. Takeuchi, K. Ogawa, H. Iinuma, H. Suda, K. Ukita, T. Nagatsu, M. Kato, H. Umezawa and O. Tanabe, *J. Antibiot.*, 26 (1973) 162.
8 A. Brossi, A. Focella and S. Teitel, *J. Med. Chem.*, 16 (1973) 418.
9 T. Okada and Y. Mizoi, *Jpn. J. Alcohol Drug Depend.*, 17 (1982) 141.
10 T. R. Bosin and K. F. Faull, *Alcoholism: Clin. Exp. Res.*, 12 (1988) 679.

Journal of Chromatography, 538 (1991) 341–354
Elsevier Science Publishers B.V., Amsterdam

CHROM. 22 771

Factors affecting selectivity in micelle exclusion chromatography of inorganic anions

TETSUO OKADA
Faculty of Liberal Arts, Shizuoka University, Shizuoka 422 (Japan)
(First received April 17th, 1990; revised manuscript received August 21st, 1990)

ABSTRACT

Selectivity in micelle exclusion chromatography is influenced by a number of factors, such as adsorption ability of stationary phases, mobile phase additives, pH of mobile phases and the charge density of micelles. These effects on the retention behaviour of inorganic anions are discussed on the basis of a model that permits the determination of partition coefficients of analytes. If needed, the acid–base equilibrium of an analyte can be involved in the model. A derived equation allows the evaluation of the individual contributions of the neutral and the ionic species to the total partition and the determination of the dissociation constant of the analyte in a micellar solution. Stationary phases of low adsorption ability offer unique selectivity and precise partition coefficients.

INTRODUCTION

Micellar mobile phases, which are often substituted for organic solvents in the reversed-phase chromatography of organic compounds [1–10], provide some advantages, such as non-toxicity, non-flammability, unique selectivity, high sensitivity in fluorimetric detection [11,12] and improvement of baseline drift in gradient elution chromatography with electrochemical detection [13], over hydro–organic or aqueous mobile phases. However, micellar mobile phases do not necessarily improve the chromatographic resolution. On the contrary, peak broadening due to slow kinetics of micellar partitioning was pointed out as a disadvantage. Adding organic solvents and/or raising the temperature for overcoming this problem were investigated [4–6]. Khaledi *et al.* [6], for example, reported that a mixture of an organic solvent and a surfactant showed a higher elution strength than expected from the individual elution strengths, and systematically enhanced the selectivity. However, we cannot say that micellar mobile phases are useful because of their separation abilities. The unique selectivity and the facility to evaluate the partition behaviour of solutes are important features of micellar mobile phases. From this point of view, the retention and partition behaviour of organic compounds have been well investigated using various micellar mobile phases [5–10].

In spite of its uniqueness and usefulness, only a few reports have appeared which describe the applicability of micellar mobile phases to inorganic chromatography. Mullins and Kirkbright [14,15] studied the reversed-phase chromatographic separa-

0021-9673/91/$03.50

tion of inorganic anions with cationic micellar mobile phases. However, the chromatographic selectivity was reported to be the same as that of anion-exchange or ion-interaction chromatography. This is due to the strong adsorption ability of the stationary phase; the retention was principally controlled by the partition to the stationary phase. Although they determined partition coefficients for some inorganic anions according to Armstrong's model [1], these values may involve much ambiguity, as will be indicated later. Okada [16,17] developed micelle exclusion chromatography in which size-exclusion chromatographic stationary phases of low adsorption ability were used in place of the usual non-polar stationary phases, and showed that the selectivity of inorganic chromatography can be effectively modified using micellar mobile phases. In micelle exclusion chromatography, the retention of analytes is mainly controlled by the partition of analytes to micellar phases rather than by that to the stationary phase.

In previous work, Okada [16], indicated factors that affect the selectivity of micelle exclusion chromatography, and inferred that some of them affected the partition either to the micellar phase or to the stationary phase, and some influenced both. Actual retention was thought to be determined by a subtle balance of these effects. In this paper, these factors, that is, the adsorption ability of the stationary phase, mobile phase additives, pH of mobile phases and the charge density of micelles, are quantitatively discussed on the basis of a model derived to interpret the retention behaviour of analytes.

EXPERIMENTAL

The chromatographic system consisted of a Tosoh CCPM computer-controlled pump, a Rheodyne injection valve equipped with a 100-μl sample loop, a column oven (CO-8000; Tosoh), a JASCO 875-UV UV–visible detector, a JASCO Model 830-RI refractive index detector and a conductimetric detector (CM-8000; Tosoh). Separation columns were Asahipak GS-300H, GS-310H and GS-320H [250 mm × 7.6 mm I.D., packed with poly(vinyl alcohol) gel with a variety of degrees of saponification, particle size 9 μm]. A Toa Model CM-20S conductimeter was used to determine critical micelle concentrations (CMC) of ionic and mixed ionic–non-ionic micelles. The temperature was maintained at 25°C. The flow-rate was 1 ml/min.

Hexadecyltrimethylammonium bromide (HTAB) of analytical-reagent grade and polyoxyethylene(23)dodecyl ether [POE(23)D; the number in parentheses refers to the average number of repeating oxyethylene units] of amino acid analysis grade were purchased from Nacalai Tesque. Hexadecyltrimethylammonium chloride (HTAC) was prepared by replacing bromide in HTAB solutions with an anion-exchange resin (Dowex 1-X4) in the Cl^- form. POE(23)D solutions were deionized with a mixed-bed ion-exchange resin column.

Standard solutions of inorganic anions were prepared by dissolving potassium salts, which were dried at 110°C under vacuum, in water. Distilled, deionized water was used throughout.

RESULTS AND DISCUSSION

Basic aspects of micelle exclusion chromatography

Fig. 1 represents a scheme of operative equilibria for the micelle exclusion chromatographic retention of an anion (A^-) with an alkylammonium micellar mobile phase: V_e, V_i and V_s denote the volume of the external solvent into which micelles permeate, the volume of the inner solvent into which micelles do not permeate but monomeric surfactants do permeate, and the volume of the stationary phase, respectively; K_{MW}, K_{SW} and K_d represent the partition coefficients of analytes between the micellar and the external solvent phase, between the inner solvent and the stationary phase and between the inner and the external solvent phase, respectively. K_d can be regarded as unity for small analytes such as simple inorganic anions which can permeate the entire inner pores of the stationary phase without restriction. Anionic analytes are partitioned both to the micellar phase and to the stationary phase by electrostatic interactions similarly to anion exchange.

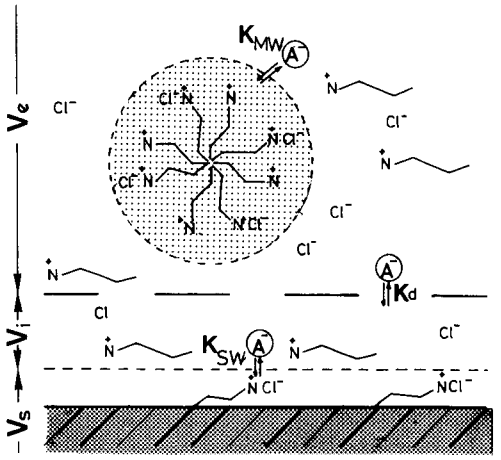

Fig. 1. Schematic representation of operative equilibria in micelle exclusion chromatography. Symbols are given in the text.

We can derive the following equation that describes the retention behaviour of analytes in micelle exclusion chromatography, if a pseudo-phase model is applicable to micelles [1,16]:

$$1/(V_r - V_e) = [(K_{KW} - 1)\bar{v}C_m + 1]/(V_i + V_sK_{SW}) \quad (1)$$

where $\bar{v}$, C_m and V_r represent the partial molal volume of micelles, the concentration of micelles (which is equal to the difference between the concentration of the surfactant used in the mobile phase and the CMC) and the retention volume of the analyte, respectively. Armstrong and Nome [1] reported a similar equation for interpreting the retention of organic compounds in reversed-phase chromatography with micellar

mobile phases. V_i will be negligibly small for the usual reversed-phase columns, but should be taken into account in micelle exclusion chromatography. According to eqn. 1, we can calculate K_{MW} and K_{SW} values from plots of $1/(V_r - V_e)$ *vs.* C_m. An analyte that is not retained on the stationary phase ($K_{SW} = 0$) will be eluted between V_e and $V_e + V_i$. The stationary phases employed in this study are weak adsorbents in comparison with the usual reversed-phase materials. However, the adsorption of surfactants is not negligible when discussing the retention behaviour of anions. Adsorbed surfactants act as anion-exchange sites and widen the effective elution window, as can be envisaged from eqn. 1. However, large K_{SW} values diminish the uniqueness in the selectivity, as shown later, because the partition to the micellar phase becomes less important.

It should be noted that V_e is used instead of the void volume of the stationary phase. The stationary phases used in this study exclude molecules with molecular weights >40 000. The aggregation number of an HTA^+ micelle was reported to be 78 [18]; although the molecular sieve effects depends not only on the molecular weights but also on the molecular shapes, HTAC micelles are thought to permeate part of the stationary phase. Fig. 2 shows the change in the elution volume of HTAC micelles with concentration (C_{HTAC}). The elution time decreases with increasing C_{HTAC}, and becomes constant when C_{HTAC} reaches 0.01 *M*. The constant elution time can be regarded as the intrinsic elution time of HTAC micelles. On the other hand, the monomeric surfactants mainly determine the elution times of HTAC solutions, when C_{HTAC} is lower than 0.01 *M*. This phenomenon depicts the dynamic aspect of the micellar system.

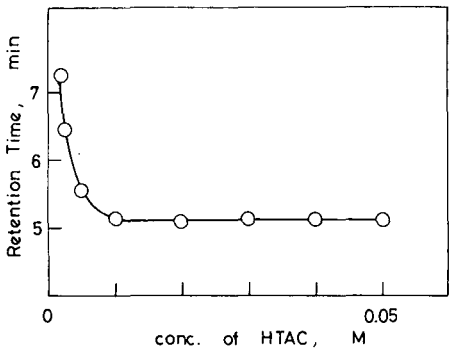

Fig. 2. Variation in the retention times of HTAC micelles with concentration. Stationary phase, GS-320H.

Adsorption ability of the stationary phase

The poly(vinyl alcohol) stationary phases used in this study have variable adsorption ability. The amounts of HTAC adsorbed on these stationary phases are listed in Table I together with other column parameters. GS-320H is the weakest and GS-300H is the strongest adsorbent. Fig. 3 shows a comparison of chromatograms obtained with these three stationary phases. The usual elution order of anions in anion-exchange or ion-interaction chromatography is $IO_3^- < NO_2^- < NO_3^- < I^-$ [16]. This order cannot be changed by varying the anion-exchange capacity, the structure of anion-exchange sites or the concentration of non-micellar mobile phases.

TABLE I

ADSORPTION ABILITY AND OTHER PARAMETERS OF STATIONARY PHASES

Stationary phase	Amount of HTAC adsorbed (mmol per column)	V_e (ml)	V_i (ml)	V_s (ml)
GS-300H	0.76[a]	5.7	1.4	4.3
GS-310H	0.66[a]	5.7	2.2	3.5
	0.96[b]			
	1.09[c]			
	1.20[d]			
GS-320H	0.21[a]	5.1	1.9	4.4

[a,b,c,d] Adsorption measured using 0.01 *M* HTAC solutions containing 0, 0.1, 0.2 and 0.3 *M* NaCl, respectively.

However, in micelle exclusion chromatography, the elution order varies with the adsorption ability of the stationary phases and the concentrations of micelles in the mobile phase. The selectivity obtained with GS-320H especially is very unusual, *i.e.*, I^- is eluted most rapidly and the elution order of NO_2^- and NO_3^- is also reversed.

Partition of analytes to the stationary phase is governed by electrostatic interactions similarly to the usual anion exchange. According to the Donnan–Gibbs theory, an ion-exchange equilibrium constant (K_{IE}) between univalent anions, A and B, is given by the following equation [19]:

$$A(b) + B(f) \rightleftharpoons A(f) + B(b)$$

$$\ln K_{IE} = P(\bar{v}_A - \bar{v}_B)/RT + \ln(\gamma_A/\gamma_B)_{(b)} - \ln(\gamma_A/\gamma_B)_{(f)} \quad (2)$$

where P, R and T represent the swelling pressure of the resin, the gas constant and absolute temperature, respectively, $\bar{v}_A$ *and* $\bar{v}_B$ are the partial molal volumes of A and B,

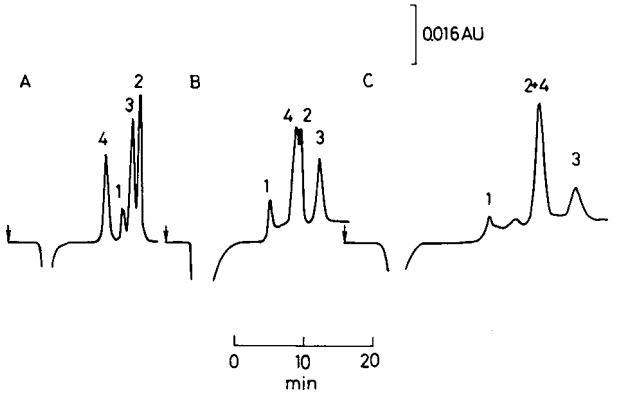

Fig. 3. Comparison of micelle exclusion chromatograms of anions. Stationary phase: (A) GS-320H; (B) GS-310H; (C) GS-300H. Mobile phase, 0.05 *M* HTAC for GS-300H and GS-310H, 0.013 *M* HTAC for GS-320H. Peaks: (1) IO_3^- (10 ppm); (2) NO_2^- (5 ppm); (3) NO_3^- (5 ppm); (4) I^- (10 ppm). Detection, UV (220 nm). Other conditions are given in the text.

γ_A and γ_B are the activity coefficients of A and B and (b) and (f) denote bound and free anions, respectively. Eqn. 2 shows that ions with small hydrated volumes will be more strongly bound by the resin as P increases. Therefore, such analytes become more distributable to the stationary phase with increasing P than ions of large hydrated volumes. In this study, an increase in the swelling pressure is roughly related to an increase in the adsorption ability of the stationary phases. K_{SW} values for NO_2^- and NO_3^- determined with varying C_{HTAC} in the mobile phase are listed in Table II. A $K_{SW}(NO_3^-)/K_{SW}(NO_2^-)$ ratio becomes large with increasing adsorption ability of the stationary phase; partitioning of NO_3^- is more enhanced than that of NO_2^-. This effect obviously diminishes the uniqueness in the selectivity. This result shows that the use of the stationary phase of low adsorption ability is essential to obtain unique selectivity.

TABLE II

COMPARISON OF K_{SW} VALUES OBTAINED FOR THREE STATIONARY PHASES

Stationary phase	K_{SW}[a] (relative value)	
	NO_2^-	NO_3^-
GS-300H	28 (0.25)	110 (1)
GS-310H	17 (0.26)	66 (1)
GS-320H	6.4 (0.44)	14 (1)

[a] K_{SW} values were determined on the basis of eqn. 1 by varying the concentration of HTAC in the mobile phase.

Effect of mobile phase additives

Most mobile phase additives affect the partitioning of analytes both to micelles and to the stationary phase. As reported previously [16], organic solvents, for example, decrease the amount of surfactants adsorbed on the stationary phase by lowering the permittivity and increasing the hydrophilicity of mobile phases. These effects lower the K_{SW} values and decrease the retention. In addition, organic solvents permeate to the micelles, stabilize the monomeric surfactants in solutions and finally prevent micellization [20], thus lowering the K_{MW} value and increasing the retention. The actual retention of analytes is determined by a subtle balance of both effects. Although effects of organic solvents are important from fundamental and practical viewpoints, a quantitative discussion is not included in this paper because of its extreme difficulty.

Addition of salts also affects partitioning both to the stationary phase and to micelles. Mass action reduces the partitioning to both phases; both K_{MW} and K_{SW} become small. On the other hand, the salting-out effect promotes the adsorption of surfactants and enhances K_{SW} values. The changes in the amounts of adsorbed HTAC on GS-310H with sodium chloride concentration are given in Table I. However, it was found in ion-interaction chromatography that the mass action effect was more important than the salting-out effect [21] in the determination of the retention. The salting-out effect also influences the micellization and lowers the CMC. This effect is negligible, however, because the increase in the micelle concentration is marginal.

TABLE III

K_{MW} AND K_{SW} VALUES OBTAINED FOR SOLUTIONS OF VARIOUS SALINITY USING GS-310H AS THE STATIONARY PHASE

[NaCl] (M)	NO_2^-		NO_3^-		I^-	
	K_{MW}	K_{SW}	K_{MW}	K_{SW}	K_{MW}	K_{SW}
0.05	74.3	6.89	189	19.6	850	68.1
	(1.7)[a]	(0.09)	(10)	(0.7)	(73)	(5.0)
	$r = 0.999$[b]		$r = 0.999$		$r = 1.000$	
0.1	37.8	3.86	100	11.6	615	53.9
	(2.3)	(0.13)	(3.7)	(0.3)	(26)	(2.0)
	$r = 0.998$		$r = 1.000$		$r = 1.000$	
0.15	29.8	2.82	76.8	8.65	438	40.4
	(1.4)	(0.04)	(2.2)	(0.13)	(21)	(1.6)
	$r = 0.998$		$r = 1.000$		$r = 1.000$	
0.2	23.6	2.34	56.6	7.14	341	35.1
	(0.4)	(0.33)	(2.3)	(0.13)	(18)	(1.5)
	$r = 0.999$		$r = 0.999$		$r = 1.000$	
0.3	16.2	1.55	43.1	5.17	226	25.1
	(0.7)	(0.01)	(1.6)	(0.08)	(4.4)	(0.3)
	$r = 0.999$		$r = 1.000$		$r = 1.000$	

[a] Standard deviations in parentheses (n = 5–9).
[b] r = Correlation coefficient of plots based on eqn. 1.

K_{MW} and K_{SW} values for NO_2^-, NO_3^- and I^- determined in 0.05–0.3 M sodium chloride solutions are given in Table III, together with standard deviations. K_{MW} values, which are not affected by the adsorbed surfactant concentration in the stationary phase, are decreased by the mass action of Cl^-. Despite the increase in the amount of surfactant adsorbed, the K_{SW} values decrease with increasing salt concentration. This indicates that mass action is the primary factor determining the retention change induced by adding salts.

Decreases in K_{SW} and K_{MW} values by adding salts to the mobile phase bring about an advantage. The determination of precise K_{MW} values will be of fundamental importance in analytical, solution and micellar chemistry. Micellar chromatography generally facilitates the determination of a K_{MW} value, which is calculated from the ratio of the slope to the intercept of the $1/(V_r - V_e)$ *vs.* C_m plot. In this instance, the standard deviation of the K_{MW} value is calculated on the basis of the theory of the method of least squares. A Jacobian matrix (**J**) can be derived from eqn. 1:

$$\mathbf{J} = [\partial f(C_{m_j})/\partial K_{MW},\ \partial_f(C_{m_j})/\partial I]_n \tag{3}$$

$$f(C_{m_j}) = [(K_{MW} - 1)\bar{v}C_{m_j} + 1]I$$

$$I = 1/(K_{SW}V_s + V_i)$$

where n represents the number of measurements. The standard deviation (σ) of the K_{MW} is given by

$$\sigma = \left\{\sum_j S_j^2 r^2 / I^2 \bar{v}^2 \left[\sum_j C_{m_j}^2 \sum_j S_j^2 - \left(\sum_j C_{m_j} S_j\right)^2\right](n-2)\right\}^{1/2} \tag{4}$$

$$S_j = (K_{MW} - 1)\bar{v} C_{m_j} + 1$$

where r^2 represents the residual sum of squares. Ambiguity of K_{MW} originates from deviations of both the slope and the intercept, and increases as the intercept (I) approaches the origin. This indicates that large intercepts, which result from low K_{SW} values, are required for the determination of reliable K_{MW} values. As shown in Table III, except for accidental errors, a near-zero intercept is generally accompanied by a large standard deviation.

Further, lack of distinction of the CMC of a surfactant employed in a mobile phase causes serious errors. Partitioning of analytes to micellar phases has been regarded as the primary separation mode in micellar chromatography. However, some studies have shown that retention behaviour is not necessarily changed at the CMC determined in water [7,22]. This may be caused by a difference between the CMC measured in water and that in a chromatographic system. This ambiguity in the CMC also becomes serious as the intercept approaches the origin. Negative intercepts, which obviously have no physical meaning, were often observed for plots based on eqn. 1 or equivalent equations when analytes show large K_{SW} values [16,17]. This is due to the lack of distinction of CMC in the chromatographic system and the near-zero intercept of the plot. From these viewpoints, a stationary phase of low adsorption ability should be used to study micellar partitioning on the basis of K_{MW} values. The adsorption abilities of the stationary phases used in this study were not low enough for the purpose. However, addition of salts to the mobile phases lowers the K_{SW} values (in other words, it increases the intercept), and makes it possible to discuss K_{MW} values precisely and systematically.

Some workers studied partitioning of ions by applying an ion-exchange model to micellar systems [23]. Also, Hux and Cantwell [24] derived an equation that describes the ion-exchange distribution (or partition) coefficients ($= K_{SW}$) for a univalent anion:

$$K_{SW} = \sigma_0 K_{IE} A_{Sp} \cdot 10^3 / 2Fc \tag{5}$$

where σ_0 is the surface charge density, F is the Faraday constant, c is the ionic strength of the bulk solution and A_{Sp} is the specific surface area of the ion exchanger. If the ionic distribution to micelles obeys an ion-exchange model, and the ion-exchange equilibrium constant at the micellar surface is not affected by the ionic strength of the bulk solution, an equivalent equation can be derived:

$$K_{MW} = \sigma_0^m K_{IE}^m A_{Sp}^m \cdot 10^3 / 2Fc \tag{5a}$$

where the superscript m denotes a micelle. In this case, the K_{MW} values are proportional to the reciprocal of the ionic strength of the bulk solution (c). Ionic micelles usually imbibe most of the counter ions; for example, 80% of Br^- are bound by HTAB micelles [20]. Thus, in the presence of large excess of an added salt, the concentration of the salt dominates the ionic strength of the solution. In fact, this consideration is

applicable to the K_{MW} values listed in Table III. The relationships between K_{MW} values and $1/c$ are as follows:

$$K_{MW}(NO_2^-) = 3.4(1/c) + 5.6 \, (r = 0.998)$$
$$K_{MW}(NO_3^-) = 8.7(1/c) + 14.7 \, (r = 0.999)$$
$$K_{MW}(I^-) = 57.7(1/c) + 44.3 \, (r = 0.998)$$

The K_{MW} value for I^- determined in a 0.05 *M* sodium chloride solution was omitted from this relationship, because it includes much ambiguity. Non-zero intercepts of these relationships arise because the concentrations of the monomeric surfactants and the micelles were not involved in ionic strength. Except for this point, this result justifies the applicability of an ion-exchange model to micellar systems.

K_{MW}/K_{SW} ratios tend to decrease with increasing sodium chloride concentration. This indicates that mass action decreases both K_{MW} and K_{SW} values almost equally but that, on the other hand, the salting-out effect increases only the K_{SW} values. Thus, adding a salt permits us to discuss systematically changes in K_{MW}, but diminishes the unique selectivity.

pH of mobile phases

The pH of the mobile phase also affects the retention behaviour of weak acids. Arunyanart and Cline Love [4] investigated the effects of pH on the retention behaviour in micellar reversed-phase chromatography using a model developed for cyclodextrin mobile phases [25]. They assumed intrinsic capacity factors for neutral and ionic species to derive equations describing the retention behaviour. This model has some advantages, but simultaneously involves some disadvantages; for example, 1:1 stoichiometry between a surfactant molecule in micelles and an analyte was assumed, and individual contributions of neutral or ionic species to the total partition to micelles cannot be evaluated. Okada [26] modified eqn. 1 and derived the following equation to describe the retention behaviours of analytes involving acid–base equilibria:

$$1/(V_r - V_e) = [(K_{MW}^T - 1)\bar{v}C_m + 1]/(V_s K_{SW}^T + V_i) \quad (6)$$

$$K_{MW}^T = \alpha_1 K_{MW1} + \alpha_0 K_{MW0} = \alpha_1(K_{MW1} - K_{MW0}) + K_{MW0} \quad (7)$$

$$K_{SW}^T = \alpha_1 K_{SW1} + \alpha_0 K_{SW0} = \alpha_1(K_{SW1} - K_{SW0}) + K_{SW0} \quad (8)$$

where α_1 and α_0 are the fractions of ionic and neutral species with respect to the total concentration of the analyte, and partition coefficients accompanied by subscripts 0 and 1 are for neutral and ionic species, respectively.

In this study, the retention of NO_2^- was influenced by the pH of the mobile phase. To evaluate the effect of pH on the retention of NO_2^-, it was assumed that HNO_2 was not distributable to the micellar phase. In such a case, K_{MW}^T can be simply replaced by $\alpha_1 K_{MW1}$. The dissociation constant of an ionizable compound at the micellar surface is known to be different from its intrinsic value. It is known that, if the surface potential (ψ) is the only factor affecting an acid–base equilibrium, the apparent

K_a value in a micellar systems (K^m) can be related to the intrinsic K_a value (K_a^i) as follows [27]:

$$pK_a^m - pK_a^i = -F\psi/2.3RT$$

A low permittivity at the micellar surface also influences K_a^m values, although this effect is not contained in the above equation. Before eqn. 6 is applied to HNO_2, the dissociation constant in HTAC solutions should be determined. The dissociation constant (K_a^m) can be determined from a plot of $1/K_{MW}^T$ *vs.* $[H^+]$ in mobile phases according to

$$1/K_{MW}^T = [H^+]/K_{MW1}K_a^m + 1/K_{MW1} \quad (9)$$

This equation can be derived from $K_{MW}^T = \alpha_1 K_{MW1}$. For NO_2^- in 0.1 *M* sodium choride medium, the following relationship was found between $1/K_{MW}^T$ and $[H^+]$:

$$1/K_{MW}^T = 45.6[H^+] + 0.0266 \, (r = 0.991)$$

K_a^m for NO_2^- was calculated as $5.8 \cdot 10^{-4}$ from this relationship. This value is close to $7.1 \cdot 10^{-4}$, the K_a^i value in aqueous solution. A positive surface potential of HTAC micelles decreases pK_a, but the low dielectric constant at the micellar surface leads to an increase in pK_a. These opposite effects results in the above K_a value for HNO_2.

Substituting α_1, which can be calculated from K_a^m and $[H^+]$, in eqns. 7 and 8 permits us to calculate K_{MW} and K_{SW} values for both NO_2^- and HNO_2. Fig. 4 shows the changes in K_{MW}^T and K_{SW}^T with α_1. According to eqn. 7 and 8, the intercepts of these plots are equal to K_{MW0} and K_{SW0} and the slopes correspond to $K_{MW1} - K_{MW0}$ and $K_{SW1} - K_{SW0}$. Although both linear relationships included relatively large deviations, approximate partition coefficients can be calculated as $K_{MW0} \approx 0$, $K_{MW1} = 38$, $K_{SW0} = 9.8$ and $K_{SW1} = 3.9$. The assumption that HNO_2 is not partitioned into micelles proves to be reasonable. Surprisingly, HNO_2 is more strongly retained on the

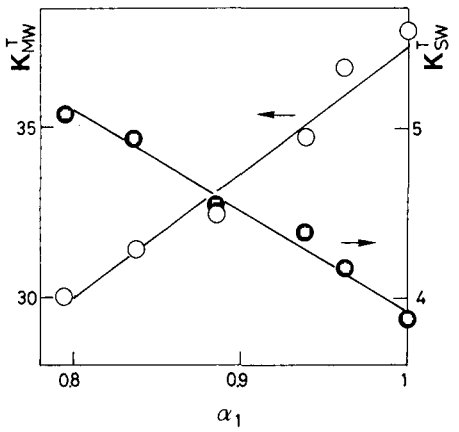

Fig. 4. Plots of (○) K_{MW}^T and (●) K_{SW}^T for NO_2^- *vs.* α_1. Stationary phase, GS-310H.

stationary phase than NO_2^-. Although the details have not been elucidated, specific interactions of HNO_2 with the stationary phase matrix may occur.

The change in the retention of nitrite with the pH of mobile phases containing 0.01 *M* HTAC is plotted as circles in Fig. 5. If the specific retention of HNO_2 did not exist, the retention of nitrite should decrease with decreasing pH, as shown by the broken line. However, the interaction of HNO_2 with the stationary phase leads to the opposite dependence of the retention on pH, *i.e.*, the retention increase with decreasing pH. The disagreement clearly indicates that the specific retention of HNO_2 should be taken into account. In fact, the experimental data are well explained by the calculation using the partition coefficients reported above, as shown by the solid line in Fig. 5.

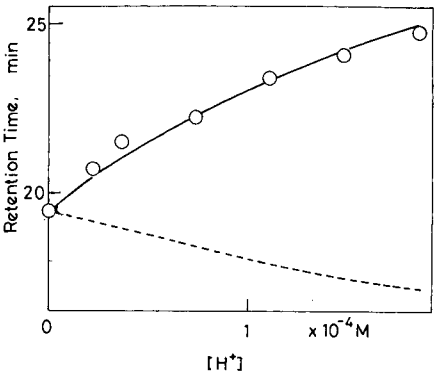

Fig. 5. Change in the retention of NO_2^- with $[H^+]$. ○, Experimental values obtained with mobile phases containing 0.01 *M* HTAC; solid line, calculated on the basis of eqns. 6–8; broken line, calculated by assuming the absence of the specific retention of HNO_2 ($K_{SWO} = 0$). Stationary phase, GS-310H.

Charge density of micelles

The effect of the charge density on the selectivity in ion-exchange resins has been theoretically and experimentally investigated [28,29]. In this study, we can discuss this effect by varying the charge density of micelles instead of an ion-exchange resin, *i.e.*, mixed micelle formation of HTAC and POE(23)D allowed us to change systematically the charge density of micelles (σ_0^m). In a particular mixed micellar system, heterogeneous mixed-micelle formation has been reported [30]. However, HTAC and POE(23)D are expected to form homogeneous mixed micelles [31], and permit the systematic evaluation of the effect of σ_0^m on K_{MW} values.

In this study, CMCs of mixed micelles were determined conductimetrically. Fig. 6 shows examples of changes in the specific equivalent conductance (Λ) with the concentration of HTAC in HTAC–POE(23)D mixed micelles. The applicability of conductimetric measurements was limited because of the extremely low CMCs of POE(23)D-rich micelles. However, as ambiguity of low CMC values does not cause serious errors in K_{MW} values, the CMCs of POE(23)D-rich micelles were assumed to be zero. This assumption led only a 2% error even for K_{MW} values determined for HTAC-rich micelles such as HTAC–POE(23)D (10:1) mixed micelle. It is known that

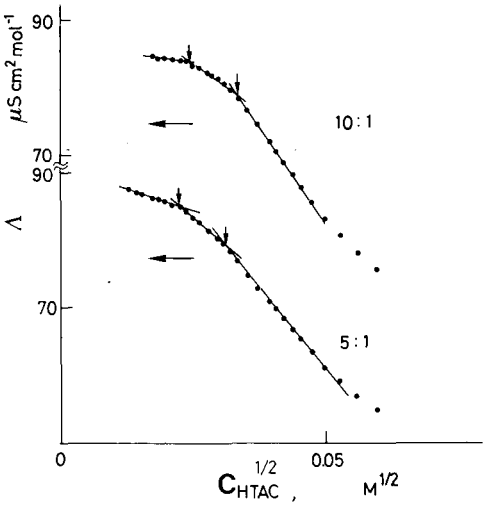

Fig. 6. Conductimetric determination of CMC of HTAC–POE(23)D (10:1 and 5:1) mixed micelles. Small arrows represent break points.

conductimetric and surface tension measurements on HTAB–POE(23)D mixed micelles give two breakpoints [31], which are due to the micellization and the transition of the spherical micelles to the asymmetric micelles. The same phenomena can be seen in Fig. 6. In this study, it was assumed that both spherical and asymmetric mixed micelles would show identical partition behaviour. This assumption is reasonable because the partitioning of anionic compounds to micelles is strongly attributed to the electrostatic attraction; on the other hand, there may be a difference in partition behaviour between these two micelles when the partitioning is determined by dissolving analytes in the micelle cores.

Fig. 7 shows the changes in K_{MW} values with ratio of HTAC concentration to the

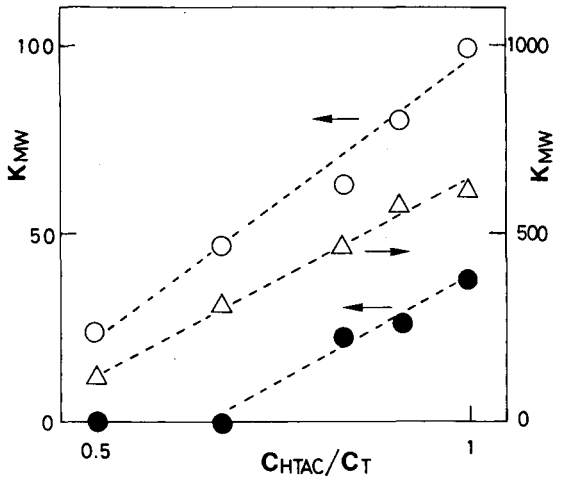

Fig. 7. Changes in K_{MW} values with C_{HTAC}/C_T. ○, NO_3^-; ●, NO_2^-; △, I^-. K_{MW} values were determined with GS-310H as the stationary phase.

total surfactant concentration [C_T, sum of the concentrations of HTAC and POE(23)D]. All mobile phases contained 0.1 M sodium chloride. When C_T is much higher than the CMC, the composition of the surfactants in micelles is the same as that of the surfactants initially mixed in the mobile phases.

According to eqn. 5a, if the changes in the A_{Sp}^{m} values of mixed micelles and in K_{IE}^{m} values are negligibly small, a linear relationship between K_{MW} and σ_0^m exists. K_{MW} values decrease almost linearly with decreasing C_{HTAC}/C_T, as shown by the broken lines in Fig. 7. Partitioning of NO_2^- to mixed micelles cannot be detected when the concentration of POE(23)D increases up to $1/3C_T$.

In conclusion, the usefulness of micelle exclusion chromatography lies in the unique selectivity and the facility for the evaluation of K_{MW} values. In order to employ these features efficiently, K_{SW} values should be kept as low as possible by using a stationary phase of low adsorption ability and adding optimum amounts of salt to the mobile phase. It is believed that micellar chromatography will continue to make significant contributions to micellar chemistry.

ACKNOWLEDGEMENTS

The author thanks Asahi Chemicals for generous gifts of separation columns. This work was supported in part by a Grant-in-Aid for Scientific Research (Grant No. 01740333) from the Ministry of Education, Science, and Culture, Japan.

REFERENCES

1 D. W. Armstrong and F. Nome, *Anal. Chem.*, 53 (1981) 1662.
2 D. W. Armstrong and G. Y. Stine, *Anal. Chem.*, 55 (1983) 2317.
3 J. P. Berry and S. G. Weber, *J. Chromatogr. Sci.*, 25 (1987) 307.
4 Arunyanart and L. J. Cline Love, *Anal. Chem.*, 57 (1985) 2837.
5 M. G. Khaledi, *Anal. Chem.*, 60 (1988) 876.
6 M. G. Khaledi, J. K. Strasters, A. H. Rodgers and E. D. Breyer, *Anal. Chem.*, 62 (1990) 130.
7 J. S. Landy and J. G. Dorsey, *Anal. Chim. Acta*, 178 (1985) 179.
8 M. F. Borgerding, F. H. Quina, W. L. Hinze, J. Bowermaster and H. M. McNair, *Anal. Chem.*, 60 (1988) 2520.
9 E. Pramauro, C. Minero, G. Saini, R. Graglia and E. Pelizzetti, *Anal. Chim. Acta*, 212 (1988) 171.
10 E. Pramauro and E. Pelizzetti, *Anal. Chim. Acta*, 154 (1983) 153.
11 L. J. Cline Love, R. Weinberger and P. Yarmchuk, in K. L. Mittal and A. Lindman (Editors), *Surfactants in Solution*, Plenum Press, New York, 1984, p. 1139.
12 A. Sanz-Medel, R. F. D. L. Campa and J. I. G. Alonso, *Analyst (London)*, 112 (1987) 493.
13 M. G. Khaledi and J. G. Dorsey, *Anal. Chem.*, 57 (1985) 2191.
14 F. G. P. Mullins and G. F. Kirkbright, *Analyst (London)*, 109 (1984) 1217.
15 F. G. P. Mullins, in P. A. Williams and M. J. Hudson (Editors), *Recent Developments in Ion-Exchange*, Elsevier, London, 1987, p. 87.
16 T. Okada, *Anal. Chem.*, 60 (1988) 1511.
17 T. Okada, *Anal. Chem.*, 60 (1988) 2116.
18 L. J. Cline Love, J. G. Habata and J. G. Dorsey, *Anal. Chem.*, 56 (1984) 1132A.
19 R. W. Grimshaw and C. E. Harland, *Ion-Exchange: Introduction to Theory and Practice*, Chemical Society, London, 1975.
20 A. Berthod, I. Girard and C. Gonnet, *Anal. Chem.*, 58 (1986) 1362.
21 P. G. Rigas and D. J. Pietrzyk, *Anal. Chem.*, 58 (1986) 2226.
22 V. Castro and J.-P. Canselier, *J. Chromatogr.*, 363 (1986) 139.
23 F. H. Quina and H. Chaimovich, *J. Phys. Chem.*, 83 (1979) 1844.
24 R. A. Hux and F. F. Cantwell, *Anal. Chem.*, 56 (1984) 1258.

25 D. Sybilska, J. Debowski, J. Jurczak and J. Zubowski, *J. Chromatogr.*, 286 (1984) 163.
26 T. Okada, *Anal. Chim. Acta*, 230 (1990) 9.
27 E. Pelizzetti and E. Prmauro, *Anal. Chim. Acta*, 169 (1985) 1.
28 G. E. Boyd, B. A. Soldano and O. D. Bonner, *J. Phys. Chem.*, 58 (1954) 456.
29 D. T. Gjerde and J. S. Fritz, *J. Chromatogr.*, 176 (1979) 199.
30 M. Abe, N. Tsubaki and K. Ogino, *J. Colloid Interface Sci.*, 107 (1985) 503.
31 M. Olteanu and I. Mandru, *J. Colloid Interface Sci.*, 106 (1985) 247.

Journal of Chromatography, 538 (1991) 355–364
Elsevier Science Publishers B.V., Amsterdam

CHROM. 22 811

Fractionation of potassium isotopes in cation-exchange chromatography

K. KAWADA and T. OI*
Department of Chemistry, Sophia University, 7-1 Kioicho, Chiyodaku, Tokyo 102 (Japan)
M. HOSOE
Department of Geoscience, National Defence Academy, 1-10-20 Hashirimizu, Yokusuka, Kanagawa 239 (Japan)
and
H. KAKIHANA
Department of Chemistry, Sophia University, 7-1 Kioicho, Chiyodaku, Tokyo 102 (Japan)
(First received March 30th, 1990; revised manuscript received September 5th, 1990)

ABSTRACT

Ion-exchange chromatography of potassium was carried out to study the potassium isotope effect in aqueous ion-exchange systems. The heavier isotope, ^{41}K, was found to be preferentially fractionated into the resin phase. This trend was independent of the type of cation-exchange resin (strongly or weakly acidic), the kind of potassium salt (chloride or lactate), the kind of replacement ion for K^+ (Ca^{2+} or Sr^{2+}) and the operating temperature (25 or 70°C). The values of the single-stage separation factor minus 1 obtained were $1.25 \cdot 10^{-5} - 3.48 \cdot 10^{-5}$. It was inferred that the ion association in the resin phase increases the separation factor and that in the solution phase decreases it.

INTRODUCTION

The use of ion-exchange chromatography for isotope separations of metals was first attempted by Taylor and Urey [1] in 1938. Since then, there has been and still is a continuing interest not only in investigating basic isotope effects observed in ion-exchange reactions but also in finding practical chemical chromatographic methods for isotope separation based on the effects. Elements whose isotope separation by ion-exchange chromatography has been studied include lithium [2], boron [3], carbon [4], nitrogen [5], magnesium [6], sulphur [7], calcium [8], zirconium [9] and uranium [10].

In previous papers [11,12], we reported the results of the chromatographic separation of rubidium isotopes. The heavier isotope, ^{87}Rb, was retained more strongly than ^{85}Rb by cation-exchange resins, and this tendency was independent of the type of resin, the kind of rubidium salt and the operating temperature, within the experimental conditions studied. On the other hand, it has been reported by other workers [2] that with lithium isotopes, the heavier isotope, ^{7}Li, was preferentially

0021-9673/91/$03.50

TABLE I

EXPERIMENTAL CONDITIONS AND LOCAL ENRICHMENT FACTOR AND SINGLE-STAGE SEPARATION FACTOR VALUES OBTAINED

Parameter	Run No.					
	K01	K02	K03	K04	K05	K06
Cation-exchange resin	Strongly acidic	Strongly acidic	Weakly acidic	Strongly acidic	Strongly acidic	Weakly acidic
Temperature (°C)	25.0 ± 0.2	25.0 ± 0.2	25.0 ± 0.2	25.0 ± 0.2	70.0 ± 0.2	70.0 ± 0.2
Resin bed height (cm)	410.7	404.5	202.5	408.6	405.0	200.4
Operating manner	Reverse	Band	Reverse	Reverse	Band	Reverse
[band length (cm)]	breakthrough	(25.0)	breakthrough	breakthrough	(30.8)	breakthrough
Potassium feed solution[a]	0.101 *M* KCl	0.104 *M* KL	0.102 *M* KCl	0,101 *M* KCl	0.103 *M* KL	0.108 *M* KCl
Eluent[a]	0.049 *M* $CaCl_2$	0.050 *M* CaL_2	0.050 *M* $CaCl_2$	0.052 *M* $SrCl_2$	0.051 *M* SrL_2	0.048 *M* $SrCl_2$
Flow-rate ($cm^3\ cm^{-2}\ h^{-1}$)	11.51	9.87	13.72	10.65	11.34	11.03
($cm^3\ h^{-1}$)	(9.04)	(7.75)	(10.77)	(8.36)	(8.90)	(8.66)
Band velocity (cm^{-1})	1.01	0.87	0.89	0.97	1.06	0.72
R_{local}^{max}	1.0085	1.0065	1.0097	1.0092	1.0027	1.0039
R_{local}^{min}	–	0.9953	–	–	0.9954	–
$10^5\varepsilon$	2.52	2.35[b]	3.48	2.52	1.25[c]	2.49

[a] L = lactate.

[b] Average of values from the front part ($2.64 \cdot 10^{-5}$) and the rear part ($2.07 \cdot 10^{-5}$) of the band.

[c] Average of values from the front part ($1.33 \cdot 10^{-5}$) and the rear part ($1.16 \cdot 10^{-5}$) of the band.

fractionated into the solution phase, *i.e.* the direction of the isotope effect in ion-exchange chromatography for lithium is the opposite of that for rubidium. It is therefore of interest to investigate whether the potassium isotope effect in ion-exchange chromatography is similar to that of rubidium or that of lithium. To clarify this point, we carried out a series of chromatographic experiments on potassium isotope separation. In this paper, we report the results of such experiments and analyse them on the basis of a theory on isotope distribution between two phases [13,14]. Naturally occurring potassium consists of two stable isotopes, ^{39}K (93.2581 atom% [15]) and ^{41}K (6.7302%), and a radioactive isotope, ^{40}K (0.0117%), the half-life of which is $1.24 \cdot 10^9$ years.

To the best of our knowledge, the only previous work on potassium isotope fractionation under aqueous ion-exchange conditions was that by Taylor and Urey [1]. They used zeolites as ion exchangers and reported that the heavier isotope, ^{41}K, was preferentially fractionated in the exchanger phase. Unfortunately, no value of the single-stage separation factor, S, was given. This paper is the first to report S values for potassium isotopes in aqueous ion-exchange systems. For mixed solvent systems, Schmidhalter and Schumacher [16] reported the potassium isotope effect between K^+ and KL^+, where L is a macrocyclic polyether. Using an elution chromatographic technique, they obtained S values of 1.00074–1.00118. In their systems, ^{41}K was enriched in the complex species.

Although obtaining exact magnitudes of isotope effects under aqueous conditions provides fundamental data for chemical isotope separation practice, its significance is of course not limited to that field of science. For instances, isotope effects could be used for elucidating geochemical cycles and interactions [17,18] and for understanding the hydration states of metal ions in aqueous solutions [19].

EXPERIMENTAL

Reagents

The ion-exchange resins used were a highly porous, strongly acidic cation-exchange resin, Asahi LS-6 (100–200 mesh), and a porous, weakly acidic cation-exchange resin, Diaion WK-13 (65–170 mesh). All reagents were of analytical-reagent grade and were used without further purification.

Chromatographic process

Six chromatographic experiments were carried out, four with the strongly acidic and two with the weakly acidic cation-exchange resin. The experimental conditions are summarized in Table I. In the experiments with the strongly acidic resin, two Pyrex glass chromatographic columns (210 cm × 1 cm I.D.) with water-jackets were connected in series with a PTFE tube (1 mm I.D.) so that the total resin bed height was *ca.* 400 cm, whereas in the experiments with the weakly acidic resin, only one column was used. Chromatography was operated either in a band displacement manner or in a reverse breakthrough manner; the chromatographic procedure in this work is basically the same used previously [12] except that Sr^{2+} in addition to Ca^{2+} was used as the displacement ion for K^+. The effluent from the columns was collected and portioned into fractions of 5 cm^3.

Analysis

The potassium concentration in each fraction of the effluents was determined flame photometrically using a Daini Seikosha SAS-727 atomic absorption spectrometer after appropriate dilution with pure water. For selected fractions of each experiment [mostly fractions near the end(s) of the potassium band], the $^{39}K/^{41}K$ isotopic ratios were measured, the procedure for which was briefly as follows.

For each fraction, an aliquot containing about $5 \cdot 10^{-5}$ mol of potassium was treated to prepare the sample for mass spectrometry. The aliquot was passed through a chromatographic column packed with an anion-exchange resin (Dowex 1-X8) in the OH^- form. To the effluent from the column, which was in fact an aqueous potassium hydroxide solution, was added hydriodic acid, yielding a potassium iodide solution. This solution was evaporated until the concentration of potassium iodide became about 0.05 *M* and was subjected to the $^{39}K/^{41}K$ isotopic ratio measurement. Only Teflon or polyethylene ware was used in the mass sample preparation in order to minimize potassium contamination.

The $^{39}K/^{41}K$ ratio of a mass sample was measured with the double-filament surface ionization technique using a Finnigan MAT 261 mass spectrometer. The filament unit for the $^{39}K/^{41}K$ measurement consisted of two filaments, one a vaporizing filament and the other an ionization filament, both being made of rhenium ribbon. A 1-μl volume of the mass sample was loaded on the vaporizing filament and dried. Ionization was performed by passing a heating electric current through the ionization filament. When the ion beam intensities of $^{39}K^+$ and $^{41}K^+$ became sufficiently high, about 1 h after initiation of heating, the ^{39}K and ^{41}K mass peaks were repeatedly recorded. The mass scanning was repeated eight times in a block and ten blocks were recorded as one measurement. The measuring time was about 1 h, hence the total time spent for one measurement was about 2 h. The $^{39}K/^{4}K$ ratio of a block was calculated by averaging all the peak-height ratios in the block and that of the mass sample was calculated as an average of the $^{39}K/^{41}K$ ratios of the ten blocks.

In the present work, no attempt was made to measure $^{40}K/^{39}K$ or $^{40}K/^{41}K$ isotopic ratio.

RESULTS AND DISCUSSION

Examples of chromatograms and ^7Li isotopic molar fractions obtained are shown in Figs. 1–3. Fig. 1 presents the analytical results of run K01 using the strongly acidic resin and operated in the reverse breakthrough manner, Fig. 2 those of run K02 using the same resin and operated in the band displacement manner and Fig. 3 those of run K03 using the weakly acidic resin and operated in the reverse breakthrough manner. In each figure, the solid step-like line shows the potassium concentration profile and the open circles the ^{41}K istopic molar fractions. It is clearly seen that the heavier isotope, ^{41}K, is enriched in the rear part of the chromatogram, that is, it is preferentially fractionated into the resin phase. This trend is also observed in all the other experiments conducted, and is the same as that observed for the rubidium isotopes [11,12]; it is independent of the type of cation-exchange resin (strongly acidic *vs.* weakly acidic; run K01 *vs.* K03), of the kind of anions in the solution phase (Cl^- *vs.* lactate ion; run K01 *vs.* K02), of the kind of replacement ion for K^+ (Ca^{2+} *vs.* Sr^{2+}; run K01 *vs.* K04) and of the operating temperature (25°C *vs.* 70°C; run K02 *vs.* K05 and run K03 *vs.* K06).

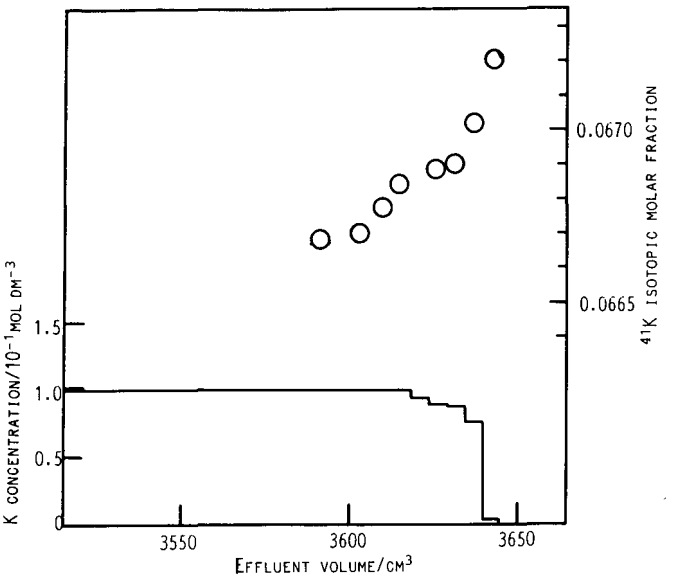

Fig. 1. Chromatogram and the ^{41}K isotopic molar fractions in run K01. Experimental conditions are summarized in Table I. The solid step-like line denotes the total potassium concentration and the open circles the ^{41}K isotopic molar fractions. The ^{41}K molar fraction of the feed solution is 0.06667.

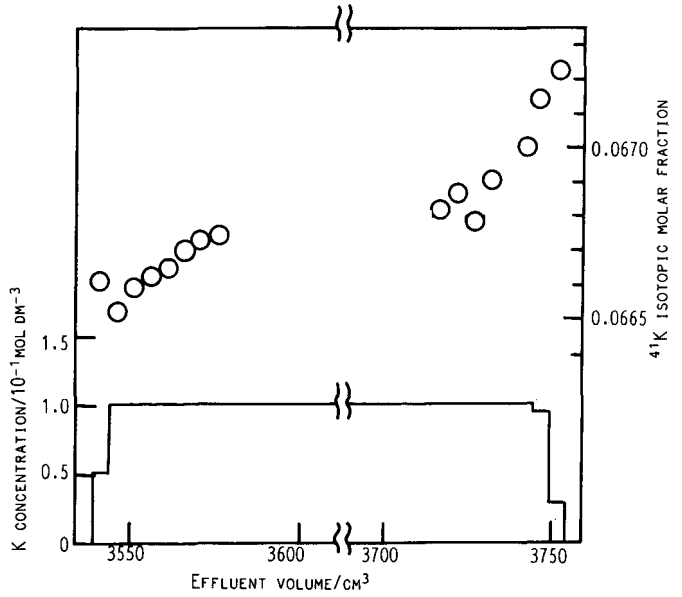

Fig. 2. Chromatogram and the ^{41}K isotopic molar fractions in run K02. Experimental conditions are summarized in Table I. The solid step-like line denotes the total potassium concentration and the open circles the ^{41}K isotopic molar fractions. The ^{41}K molar fraction of the feed solution is 0.06682.

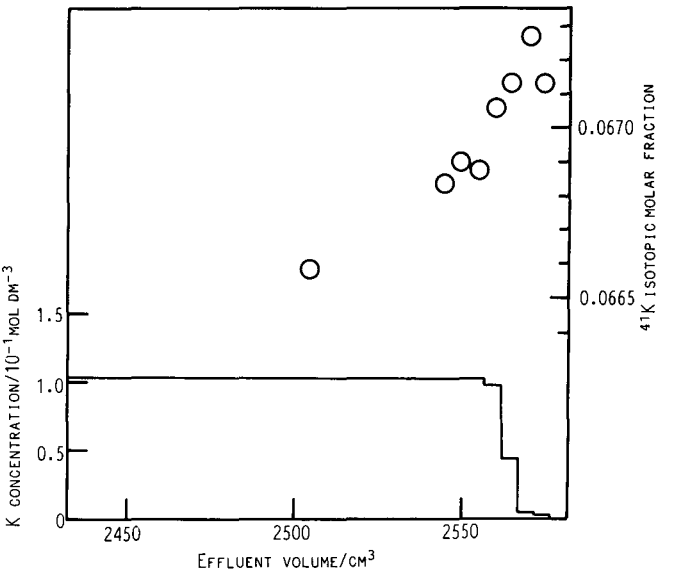

Fig. 3. Chromatogram and the ^{41}K isotopic molar fractions in run K03. Experimental conditions are summarized in Table I. The solid step-like line denotes the total potassium concentration and the open circles the ^{41}K isotopic molar fractions. The ^{41}K molar fraction of the feed is 0.06667.

For each of the experiments, the maximum degrees of enrichment and/or depletion achieved expressed as the maximum and/or minimum of the local enrichment factor, R_{local}, defined as

$$R_{local} = ([^{41}K]/[^{39}K])_{fraction}/([^{41}K]/[^{39}K]_{feed} \quad (1)$$

were calculated. In eqn. 1, [A] denotes the concentration of isotope A and the subscripts fraction and feed denote that the quantities refer to those of a fraction of the effluent and those of the feed solution, respectively. The results are given in Table I. R_{local}^{max} and R_{local}^{min} are the maximum degrees of enrichment and depletion, respectively. The highest R_{local}^{max} was achieved in run K03.

For each of the experiments, the single-stage separation factor, S ($= \varepsilon + 1$), defined as

$$S = (\overline{[^{41}K]}/\overline{[^{39}K]})/([^{41}K]/[^{39}K]) \quad (2)$$

where the quantities with overbars refer to those in the resin phase and the quantities without overbars to those in the solution phase, was calculated using the equation [20]

$$\varepsilon = \Sigma [\, | R_i - R_0 \, | f_i]/[R_0(1 - R_0)Q] \quad (3)$$

where R_0 is the ^{41}K isotopic molar fraction in the feed solution, R_i that in the ith fraction, f_i the amount of potassium in the ith fraction, Q the total exchange capacity of

the resin for potassium and the summation is taken over all the fractions that are enriched or depleted in ^{41}K. The ε values obtained are listed in Table I; they are generally of the order of 10^{-5} and the maximum is obtained for the system with the weakly acidic cation-exchange resin at 25°C. The following may be deduced from a comparison of these values:

(1) In the systems with the strongly acidic resin, the magnitude of the potassium isotope effect depends on the kind of anions in the solution phase. Cl^- yielded a larger ε value than the lactate ion (run K01 *vs.* K02).

(2) For the common potassium chloride feed solution, the weakly acidic cation-exchange resin (exchange group COO^-) gave a larger ε value than the strongly acidic resin (exchange group SO_3^-) (run K01 *vs.* K03).

(3) The potassium isotope effect in ion-exchange chromatography is independent of the kind of replacement ions for the K^+ (run K02 *vs.* K04), as is generally expected.

(4) The effect is temperature dependent, being larger at a lower temperature (run K02 *vs.* K05 and run K03 *vs.* K06).

These observations are qualitatively consistent with what had been observed for the rubidium isotopes [11,12], except for point (3), which was not examined for the rubidium isotopes.

In addition to the separation factor, parameters such as the HETP and the migration length required to obtain the desired degree of enrichment are essential in evaluating the feasibility of a certain chromatographic isotope enrichment system. These parameters are strongly dependent on such operating conditions as flow-rate, temperature and uniformity of packing. Unfortunately, the present experiments were not designed for obtaining values of the parameters with high accuracy; the migration lengths are too short and the maximum degrees of enrichment achieved are too low for this purpose, and a series of experiments in which only one of the experimental conditions is taken as a variable were not carried out. Although it is possible to evaluate the feasibility of the present systems based on theories of isotope separation by displacement chromatography [21,22], such an evaluation is merely an exercise in calculations and will convey no practical importance. In the following, we limit our discussion to the separation factors and extract information on fundamental potassium isotope effects underlying them.

Analysis of the observed potassium isotope effect on the basis of an isotope two-phase distribution theory

The theory of isotope distribution between two phases [13,14] correlates S with the isotopic reduced partition function ratios (RPFRs) and the molar fractions of the species in a separation system. An application of the theory to the present systems yields the following expression for S [12–14]:

$$\ln S = \ln S_{\text{phase}} + \ln \bar{S}_{\text{hydra}} + \ln [\bar{x} + (1 - \bar{x})\bar{S}_{\text{asso}}] - \ln [x + (1 - x)S_{\text{asso}}] \quad (4)$$

where

$$S_{\text{phase}} = \bar{f}_{\text{n,0}}/f_{\text{n,0}} \quad (5)$$

$$\bar{S}_{\text{hydra}} = \bar{f}_{\text{n,0}}/\bar{f}_{\text{n,0}} \quad (6)$$

$$S_{\text{asso}} = f_{n,1}/f_{n,0} \tag{7}$$

$$\bar{S}_{\text{asso}} = \bar{f}_{\bar{n},0}/\bar{f}_{\bar{n},0} \tag{8}$$

and x and $\bar{x}$ are the molar fractions of the simple hydrated K^+ ion in the solution phase and in the resin phase, respectively. In eqns. 5–8, $f_{p,q}$ and $\bar{f}_{p,q}$ ($p = n$ or $\bar{n}$, $q = 0$ or 1) are the $^{41}K/^{39}K$ isotopic RPFRs of the species, $K^+(H_2O)_pL_q^-$, in the solution phase and in the resin phase, respectively, n and $\bar{n}$ the hydration numbers in the solution phase and in the resin phase, respectively, L^- the ion-association partner anion and q the number of anions ion-associated to a K^+.

S_{phase} is the separation factor due to the phase change, that is, the separation factor obtained when the simple hydrated species, $K^+(H_2O)_n$, is transferred from the solution phase to the resin phase without any change in the hydration circumstances. $\bar{S}_{\text{hydra}}$ is the separation factor originating from a change in the hydration number from n to $\bar{n}$ in the resin phase. It is usually considered that n is larger than $\bar{n}$ [23]. Therefore, ln $\bar{S}_{\text{hydra}}$ is negative. S_{asso} is the separation factor resulting from the ion association in the solution phase and $\bar{S}_{\text{asso}}$ is that in the resin phase.

In run K01, both the solution and the resin phases can be regarded as strong electrolyte solutions and no ion association is viable in either phase, *i.e.*, $x = \bar{x} = 1$. Eqn. 4 is then simplified to

$$\ln S(\text{K01}) = \ln S_{\text{phase}}(\text{K01}) + \ln \bar{S}_{\text{hydra}}(\text{K01}) \tag{9}$$

ln S(K01) is positive and ln S_{hydra}(K01) is negative, so that ln S_{phase}(K01) is positive, that is, the RPFR of the simple hydrated species is larger in the resin phase than in the solution phase, so the magnitude of ln S_{phase}(K01) is larger than that of ln S_{hydra}(K01).

In run K02, the situation in the resin phase is the same as that in run K01. In the solution phase, however, part of potassium ions are expected to be ion-associated with lactate ions. Thus, $\bar{x}$ is equal to unity but x is not. Eqn. 4 is simplified in this instance to

$$\begin{aligned} \ln S(\text{K02}) &= \ln S_{\text{phase}}(\text{K01}) + \ln \bar{S}_{\text{hydra}}(\text{K01}) - \ln [x + (1 - x)S_{\text{asso}}(\text{K02})] \\ &= \ln S(\text{K01}) - \ln [x + (1 - x)S_{\text{asso}}(\text{K02})] \end{aligned} \tag{10}$$

Substituting $2.52 \cdot 10^{-5}$ for ln S(K01) and $2.35 \cdot 10^{-5}$ for ln S(K02), we obtain $\ln[x + (1 - x)S_{\text{asso}}(\text{K02})] = 0.17 \cdot 10^{-5}$. We have at present no estimate for the x value, but the value of ln S_{asso}(K02) is evidentally at least $0.17 \cdot 10^{-5}$. A positive value of ln S_{asso}(K02) means $f_{n,1} > f_{n,0}$, that is, the RPFR of the ion-associated species is larger than that of the simple hydrated species. Assuming that the effects of the hydration and the ion association on ln$f$ are additive, which is good as a first approximation, this result is reasonable and consistent with the formation of the outer-sphere ion-associated species. The fact that S(K01) is larger than S(K02) means that the ion association in the solution phase reduces the overall single-stage separation factor.

In run K03, the ion association between K^+ and COO^- is expected in the resin phase but not in the solution phase. A similar consideration to K02 yields the expression

$$\ln S(\text{K03}) = \ln S_{\text{phase}}(\text{K03}) + \ln \bar{S}_{\text{hydra}}(\text{K03}) + \ln [\bar{x} + (1 - \bar{x})\bar{S}_{\text{asso}}(\text{K03})] \tag{11}$$

TABLE II

COMPARISON OF SINGLE-STAGE SEPARATION FACTOR VALUES BETWEEN POTASSIUM AND RUBIDIUM ISOTOPES AT 25°C

Heavier isotopes (^{41}K and ^{87}Rb) are preferentially fractionated into the resin phase.

Cation-exchange resin	Anion in solution phase	Ln S for	
		$^{41}K/^{39}K$	$^{87}Rb/^{85}Rb$
Strongly acidic	Cl^-	$2.52 \cdot 10^{-5}$	$5.2 \cdot 10^{-6}$
Strongly acidic	Lactate	$2.35 \cdot 10^{-5}$	$3.5 \cdot 10^{-6}$
Weakly acidic	Cl^-	$3.48 \cdot 10^{-5}$	$11.4 \cdot 10^{-6}$

Because of the difference in resin used in runs K01 and K03, $S_{phase}(K03)$ is not necessarily equal to $S_{phase}(K01)$ nor $\bar{S}_{hydra}(K03)$ to $\bar{S}_{hydra}(K01)$. However, it will not be a very poor approximation to put

$$\ln S_{phase}(K03) + \ln \bar{S}_{hydra}(K03) = \ln S_{phase}(K01) + \ln \bar{S}_{hydra}(K01) \qquad (12)$$

Assuming the equality in eqn. 12, we obtain $\ln [\bar{x} + (1 - \bar{x})\bar{S}_{asso}(K03)] = \ln S(K03) - \ln S(K01) = 3.48 \cdot 10^{-5} - 2.52 \cdot 10^{-5} = 0.94 \cdot 10^{-5}$. Like the x value in run K02, we have no estimate for the $\bar{x}$ value in this instance. Hence $0.94 \cdot 10^{-5}$ can be considered to be the possible minimum value of $\ln \bar{S}_{asso}(K03)$. A positive $\ln \bar{S}_{asso}(K03)$ value means that the RPFR of the ion-associated species is larger than that of the simple hydrated species in the resin phase. This result is reasonable in the light of the outer-sphere ion-associated species and is consistent with the result obtained in the previous paragraph. The fact that $S(K03)$ is larger than $S(K01)$ means that the ion association in the resin phase increases the overall separation factor.

The difference in replacement ion for K^+ is not included in eqn. 4, which explains why runs K01 and K04 give the same S value. This fact in turn indicates the high reliability of the S values obtained in this work.

TABLE III

COMPARISON OF VARIOUS S VALUES BETWEEN POTASSIUM AND RUBIDIUM ISOTOPES

For the definition of each kind of S, see the text.

Parameter	K	Rb
$\ln S_{phase}$:sign	+	+
$\ln \bar{S}_{hydra}$:sign	+	+
$\lvert S_{phase} \rvert > \lvert \bar{S}_{hydra} \rvert$?	Yes	Yes
$\ln S_{phase} + \ln \bar{S}_{hydra}$	$2.52 \cdot 10^{-5}$	$5.2 \cdot 10^{-6}$
$\ln S_{asso}$: sign	+	+
value (min.)	$0.17 \cdot 10^{-5}$	$1.7 \cdot 10^{-6}$
$\ln \bar{S}_{asso}$: sign	+	+
value (min.)	$0.94 \cdot 10^{-5}$	$6.2 \cdot 10^{-6}$
S: temperature dependence	Normal	Normal

Comparison of potassium and rubidium isotope effects

Single-stage separation factor values obtained for the potassium and rubidium [11,12] isotope separation systems are compared in Table II. Information on various kinds of S for the two alkali metals, such as S_{phase} and S_{asso}, is summarized in Table III. These tables show that the signs of every corresponding isotope effect are the same, but that the magnitudes differ for the two metal ions. It is interesting to question whether such a correspondence can be extended to the light alkali metals, sodium and lithium. An answer to this will be given in a future paper.

CONCLUSION

Major findings of the present study are as follows.

(i) The heavier isotope, ^{41}K, was preferentially fractionated into the resin phase. This trend is independent of the type of cation-exchange resin (strongly acidic or weakly acidic), of the kind of potassium salts used in the feed solutions (potassium chloride or potassium lactate), of the kind of replacement ions for K^+ (Ca^{2+} or Sr^{2+}) and of the operating temperature (25 or 70°C).

(ii) The ε values were $2.52 \cdot 10^{-5}$, $2.35 \cdot 10^{-5}$ and $3.48 \cdot 10^{-5}$ for the potassium chloride–strongly acidic resin, potassium lactate–strongly acidic resin and potassium chloride–weakly acidic resin systems, respectively, at 25°C. The ε values for the second and third systems were $1.25 \cdot 10^{-5}$ and $2.49 \cdot 10^{-5}$, respectively, at 70°C. Thus, the potassium isotope separation effect showed the normal temperature dependence.

(iii) It was inferred that the ion association in the solution phase reduces the separation factor and that in the resin phase increases it, and that the RPFR value of the ion-associated species is larger than that of the simple hydrated species both in the solution phase and in the resin phase.

REFERENCES

1 T. I. Taylor and H. C. Urey, *J. Chem. Phys.*, 6 (1938) 429.
2 Z. Hagiwara and Y. Takakura, *J. Nucl. Sci. Technol.*, 6 (1969) 326.
3 M. Aida, Y. Fujii and M. Okamoto, *Sep. Sci. Technol.*, 21 (1986) 643.
4 K. A. Piez and H. Eagle, *J. Am. Chem. Soc.*, 78 (1956) 5284.
5 F. H. Spedding, J. E. Powell and H. J. Svec, *J. Am. Chem. Soc.*, 77 (1955) 1393 and 6125.
6 T. Oi, S. Yanase and H. Kakihana, *Sep. Sci. Technol.*, 22 (1987) 2203.
7 T. E. Eriksen, *Acta Chem. Scand.*, 26 (1972) 980.
8 B. E. Jepson and G. C. Shockey, *Sep. Sci. Technol.*, 19 (1984) 173; 22 (1987) 1029.
9 K. Kogure, M. Nomura and M. Okaoto, *J. Chromatogr.*, 259 (1983) 480; K. Kogure, M. Kakihana, M. Nomura and M. Okamoto, *J. Chromatogr.*, 325 (1985) 195.
10 M. Seko, T. Miyake, K. Inada and K. Takeda, *Nucl. Technol.*, 50 (1980) 178.
11 M. Hosoe, T. Oi, K. Kawada and H. Kakihana, *J. Chromatogr.*, 435 (1988) 253.
12 M. Hosoe, T. Oi, K. Kawada and H. Kakihana, *J. Chromatogr.*, 438 (1988) 225.
13 H. Kakihana and M. Aida, *Bull. Tokyo Inst. Technol.*, 116 (1973) 39.
14 H. Kakihana, *J. Chromatogr.*, 102 (1974) 47.
15 IUPAC, *Pure Appl. Chem.*, 56 (1984) 6.
16 B. Schmidhalter and E. Schumacher, *Helv. Chim. Acta*, 65 (1982) 1687.
17 A. J. Spivack, M. R. Palmer and J. M. Edmond, *Geochim. Cosmochim. Acta*, 51 (1987) 1939.
18 M. Nomura, T. Kanzaki, T. Ozawa, M. Okamoto and H. Kakihana, *Geochim. Cosmochim. Acta*, 46 (1982) 2403.
19 M. Kakiuchi, *Z. Naturforsch., A*, 43 (1988) 449.
20 H. Kakihana and T. Kanzaki, *Bull. Tokyo Inst. Technol.*, 90 (1969) 77.
21 Y. Fujii, M. Aida, M. Okamoto and T. Oi, *Sep. Sci. Technol.*, 20 (1985) 377.
22 H. Kakihana and T. Oi, *J. Chromatogr.*, 483 (1989) 179.
23 D. A. Lee, *J. Phys. Chem.*, 64 (1960) 187.

Journal of Chromatography, 538 (1991) 365–372
Elsevier Science Publishers B.V., Amsterdam

CHROM. 22 803

Determination of trace elements by ion chromatography

I. Beryllium

M. BETTI*
Institute of Instrumental Analytical Chemistry, CNR, c/o Department of Chemistry, University of Pisa, Via Risorgimento 35, 56126 Pisa (Italy)
and
S. CAVALLI
Dionex Italiana srl, Via Grigna 9, 20155 Milan (Italy)
(First received May 1st, 1990; revised manuscript received September 7th, 1990)

ABSTRACT

A method for the determination of beryllium by ion-exchange chromatography followed by post-column derivatization with 4,5-dihydroxy-3-(8-hydroxy-3,6-disulpho-1-naphthylazo)naphthalene-2,7-disulphonic acid (Beryllon II) and spectrophotometric detection at 625 nm is described. With injection of 50 μl of the sample, the calibration graph was linear from 50 to 5000 μg/l of beryllium with a detection limit (3σ) of 42 μg/l. The detection limit for direct injection of a 500-μl volume is 2 μg/l. Typical relative standard deviations of 0.9–0.2% and 1.5–2.0% for 10 mg/l and 10 μg/l beryllium standards, respectively, were obtained. Freedom from interference from nine cations investigated is reported. The method was applied successfully to the determination of low levels of beryllium in environmental samples.

INTRODUCTION

Beryllium can be considered as a trace element, which occurs naturally in the earth's crust and in surface waters at μg/g and ng/l levels, respectively [1,2]. This element is used as a hardening agent in alloys, as a moderator in atomic energy reactors and as a compact fuel element for rockets [3].

The most significant feature of the biological activity of beryllium is the highly toxic character of the element and its compounds. Inhalation of beryllium can cause beryllosis, a serious disease which leads to weight loss, dyspnea, cough, chest pains, fatigue and general weakness [4].

Owing to its toxicological importance and unknown physiological activity, the development of a method to determine beryllium accurately at low levels in environmental and biological samples has attracted attention. Different methods based on atomic absorption [5,6], spectrophotometry [7,8] and spectrofluorimetry [9,10], etc., have been reported. Photometric and fluorimetric methods, predominantly based on coloured complex formation, are more popular owing to their simplicity.

0021-9673/91/$03.50

Some methods, although sensitive, suffer from interferences and pretreatment of the sample is generally required before determination [5–10].

The use of modern ion-exchange chromatographic techniques for trace metal determination is now well established, as is evident from the steady increase in the number of papers in this area reviewed recently [11,12]. However, few of these papers have dealt with the determination of the trace amounts of beryllium. Noda *et al.* [13] demonstrated the feasibility of gel permeation chromatography for the separation of mixed-ligand complexes of several beryllium(II) β-diketonates. Biswanath and Desay [14] separated beryllium as β-isopropyltropolone complexes on a reversed-phase column. Kondratjonok and Schwedt [15] recently found that the optimum separation conditions for beryllium ions on a polymer-coated cation-exchange column (polybutadiene–maleic acid on silica) are an eluent based on pyridine-2,6-dicarboxylic and citric acid with conductivity as the detection mode. With these methods quantitative separation and accurate determination of beryllium can be carried out, but a simpler method based on widely used instrumentation is required. As ion chromatographic (IC) techniques are potentially cost effective, as recently shown for anions and cations [13,16], and are suitable for studying metals and their speciation [13,17], we decided to develop a simpler and accurate method for low-level beryllium determination by IC.

This paper describes the use of ion-exchange chromatography followed by post-column derivatization using 4,5-dihydroxy-3-(8-hydroxy-3,6-disulpho-1-naphthylazo)naphthalene-2,7-disulphonic acid (Beryllon II) and spectrophotometric detection to determine beryllium at the μg/l level. Experimental conditions and analytical figures of merit including linear dynamic range, column efficiency and interferences are discussed. Results for the determination of beryllium in environmental certified reference materials are also presented.

EXPERIMENTAL

Instrumentation

A Dionex (Sunnyvale, CA, U.S.A.) Model 4500i ion chromatograph system equipped with a pressurized post-column reagent delivery module (RDM) and a UV–VIS detector (VDM II, Dionex) were employed. A Dionex AI-450 data system was used for data collection and processing and a Varian (Australia) DMS-300 spectrophotometer for spectrophotometric measurements.

The separations were carried out on an IonPac CS3 cation-exchange column (250 mm × 4.6 mm I.D.) used in conjunction with an IonPac CG3 guard column (50 mm × 4.6 mm I.D.).

The eluent and the post-column reagent solution (PCR) were mixed with the aid of a T-piece, positioned at the exit of the analytical column, followed by a packed-bed reaction coil of 100-μl volume.

Injections of 50, 100, 200 and 500 μl of the sample were performed.

Reagents and standards

Hydrochloric acid, glycine, sodium chloride and sodium hydroxide were Suprapur grade materials (Merck). Beryllon II [4,5-dihydroxy-3-(8-hydroxy-3,6-disulpho-1-naphthylazo)naphthalene-2,7-disulphonic acid] was obtained from Novachimica.

Ultra-pure water (18 MΩ/cm resistivity at 25°C) obtained treating doubly distilled water (Carlo Erba) in a UHQ system (Elga, U.K.), was used throughout.

Working standards were prepared by serial daily dilution of stock solutions, containing 1000 mg/l of Be(II), Ca(II), Mg(II), Cu(II), Ni(II), Al(III), Mn(II), Co(II), Cr(III) and Mo(VI) obtained from Merck.

National Bureau of Standards (NBS) Standard Reference Material SRM 1643b (water) was obtained from the NBS (Washington, DC, U.S.A.) and MESS-1 and BCSS-1 (Estuarine Sediment Reference Materials) from the National Research Council of Canada (Ottawa, Canada).

All standards, samples and reagents were prepared and stored in polyethylene containers previously cleaned and conditioned following a procedure for trace element determination [18].

Eluent solution

The final choice for the eluent solution was 190 m*M* hydrochloric acid, which was prepared fresh daily and used at a flow-rate of 1 ml/min.

Post-column reagent (PCR) solution

The PCR solution consisted of 0.01% (w/v) Beryllon II in glycine–sodium chloride–sodium hydroxide buffer at pH 12.6. The PCR solution was prepared daily by dissolving 100 mg of Beryllon II in 1 l of the above buffer. This buffer was obtained mixing 350 ml of a solution which was prepared by dissolving 7.507 g of glycine (the buffer substance) and 5.84 g of sodium chloride in 1 l of water, with 650 ml of 1 *M* sodium hydroxide solution. The PCR flow-rate varied between 0.2 and 1.5 ml/min, as will be explained in the following section.

RESULTS AND DISCUSSION

Complexing reagents for beryllium

Beryllium belongs to Group IIA of the Periodic System, but only complex ions of it are known [19]. Apart from fluoride, stable complexes are primarily obtained with ligands containing O and N donor atoms. Such ligands of analytical interest are hydroxy acids, β-diketones (acetylacetone), chromotropic acid azo derivatives (Beryllon II, III and IV), anthraquinone derivatives (quinalizarin) and triphenylmethane derivatives [20]. Among these dyes, Beryllon II, which is the product of coupling chromotropic acid with diazo H-acid, 4,5-dihydroxy-3-(8-hydroxy-3,6-disulpho-1-naphthylazo)naphthalene-2,7-disulphonic acid, is soluble in water. It turns red in acidic solution and violet in alkaline solution. In the pH range 11.5–14 it forms blue complexes with Be, Ca, Mg, Al, Cu, Co, Ni, Mn, Mo and Cr [21]. When performing normal colorimetric procedures, many of these interferences with beryllium determination must usually be eliminated by the addition of EDTA [19,20]. If this is not sufficient, beryllium has to be separated by extraction with acetylacetone [20] or by means of ion-exchange [22].

Detection conditions

Studies on the absorption of the PCR solution mixed with the eluent with and without the addition of beryllium were performed.

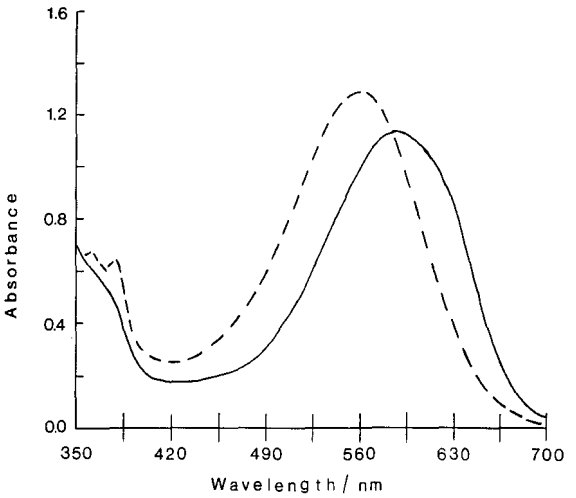

Fig. 1. Absorption spectra of the PCR–eluent mixture from the chromatographic cell without (dashed line) and with (solid line) the addition of 10 mg/l of beryllium.

The effluent from the spectrophotometric cell of the ion chromatograph was collected and a known amount of beryllium added. The spectrum of the effluent without the addition of beryllium (Fig. 1, dashed line) showed a maximum absorption at 560 nm, as reported for Beryllon II in alkaline solutions [19,20].

When adding beryllium to the effluent solution, the spectrum which was measured *vs.* the PCR–eluent mixture presented the maximum absorption of the Be–Beryllon II complex at 626.5 nm (Fig. 1, solid line). pH values about 2 units lower and higher than 12.6 caused a decrease in the sensitivity of the beryllium determination. In this investigation a wavelength of 625 nm was used.

Separation conditions

The feasibility of beryllium separation on a low-capacity divinylbenzene–styrene sulphonated copolymer cation-exchange column [23], using hydrochloric acid as eluent, was investigated. Six different concentrations of hydrochloric acid between 50 and 220 mM at a flow-rate of 1 ml/min for the elution of a 10 mg/l beryllium standard were tested.

For all the mobile phase concentrations, the column efficiency, N, using 10 mg/l of beryllium was evaluated. A comparison of the data obtained shows that there was no statistical difference, at the 99% confidence interval, using the different concentrations for the mobile phase, thus indicating that the beryllium peak has similar column efficiencies ($N = 1120 \pm 50$), irrespective of the eluent concentration used.

The retention time of beryllium ions was found to be linearly dependent ($r = -0.99982$) on the eluent concentration. For concentrations below 100 mM the retention times were unacceptably long. In order to minimize the analysis time and avoid overlap with potential interferent ions (*i.e.*, Mg^{2+}), 190 mM was found to be the best concentration for the hydrochloric acid mobile phase.

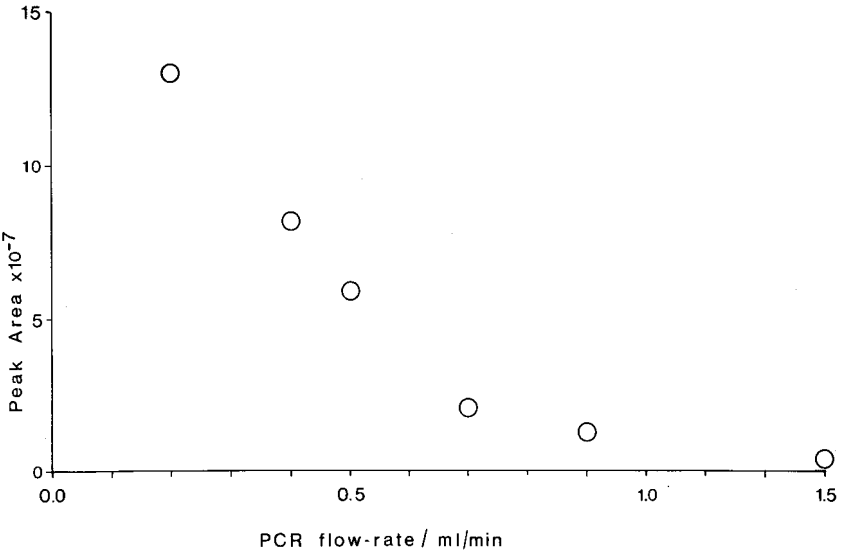

Fig. 2. Effect of the PCR flow-rate on the analytical response (peak area) of 10 mg/l of beryllium. Injection volume 50 μl.

Effect of PCR flow-rate on the peak area of beryllium

The effect of the PCR flow-rate on the response of beryllium while keeping the eluent flow-rate constant was investigated. As shown in Fig. 2, the chromatographic response (peak area) was found to be dependent on the PCR flow-rate. An excellent linearity ($r = -0.99998$) was obtained in the range 0.2–0.5 ml/min. On increasing the PCR flow-rate, the peak area decreased. This behaviour could be used for increasing the dynamic range, so that high concentrations can be determined without diluting the sample.

Linearity and detection limit

For a PCR flow-rate of 0.2 ml/min, excellent linearity ($r = -0.99998$) over two orders of magnitude from 50 to 5000 μg/l (5.5–556 μM) of beryllium, on injecting 50-μl samples, was found. The linear range can be extended using the PCR flow-rate (as mentioned above) or using smaller injection volumes, thus avoiding sample dilution in some instances. The detection limit, calculated by using the definition of three times the standard deviation (3σ), was 42 μg/l on injection of 50 μl. Concentrations lower than 1 μg/l (0.1 μM) can be determined by increasing the injection volume, or by means of the on-line preconcentration technique.

Reproducibility

Using two different PCR flow-rates (0.4 and 0.2 ml/min) and 190 mM hydrochloric acid as the eluting agent, data on the reproducibility of the peak area and the retention time were obtained by performing ten injections of 50 μl of a 10 mg/l beryllium standard solution on four separate occasions.

The relative standard deviations (R.S.D.) for the peak area varied from 0.20 to

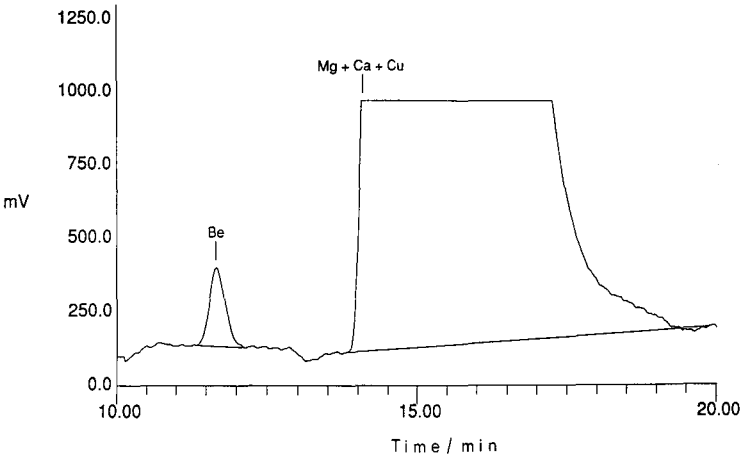

Fig. 3. Chromatogram obtained on injecting 200 μl of a solution containing 40 μg/l of beryllium together with 10 mg/l of Mg(II), Ca(II) and Cu(II).

0.73% for a 0.4 ml/min PCR flow-rate and from 0.44 to 0.90% for a 0.2 ml/min PCR flow-rate. The R.S.D. values for the retention time varied from 0.13 to 0.40% and from 0.10 to 0.33% for PCR flow-rates of 0.4 and 0.2 ml/min, respectively. Thus, both peak area and retention time data were indicative of a stable and reproducible system.

Interferences

Beryllon II, at alkaline pH, is not a specific spectrophotometric reagent for beryllium. Therefore, interferences are possible if other species elute at similar retention times to beryllium. This was investigated by analysing a solution containing 0.5 mg/l of beryllium and increasing amounts of interferents from 10 to 100 mg/l. The interferents tested were Mg(II), Ca(II), Cu(II), Ni(II), Al(III), Mn(II), Cr(III), Mo(VI) and Co(II). It was found that using 190 m*M* hydrochloric acid as mobile phase only three cations, Mg(II), Ca(II) and Cu(II), had retention times in the vicinity of beryllium, *viz.*, 14.3, 14.8 and 15.9 min, respectively. However, they could not interfere in the determination of beryllium even at the highest concentration ratio tested, as shown in Fig. 3, where the chromatogram obtained for a sample containing 40 μg/l of beryllium together with 10 mg/l of Mg(II), Ca(II) and Cu(II) is illustrated.

Real sample analysis

The method investigated was used to determine beryllium in three different certified reference materials: NBS SRM 1643b (trace metals in water) and National Research Council of Canada MESS-1 and BCSS-1 (estuarine sediment reference materials for trace elements).

The chromatograms obtained for SRM 1643b (a) before and (b) after the addition of 50 μg/l of beryllium are shown in Fig. 4.

In order to leach the total metal concentration, the estuarine sediment samples were treated with nitric acid by refluxing for 2 h, following the procedure described by Langston [24].

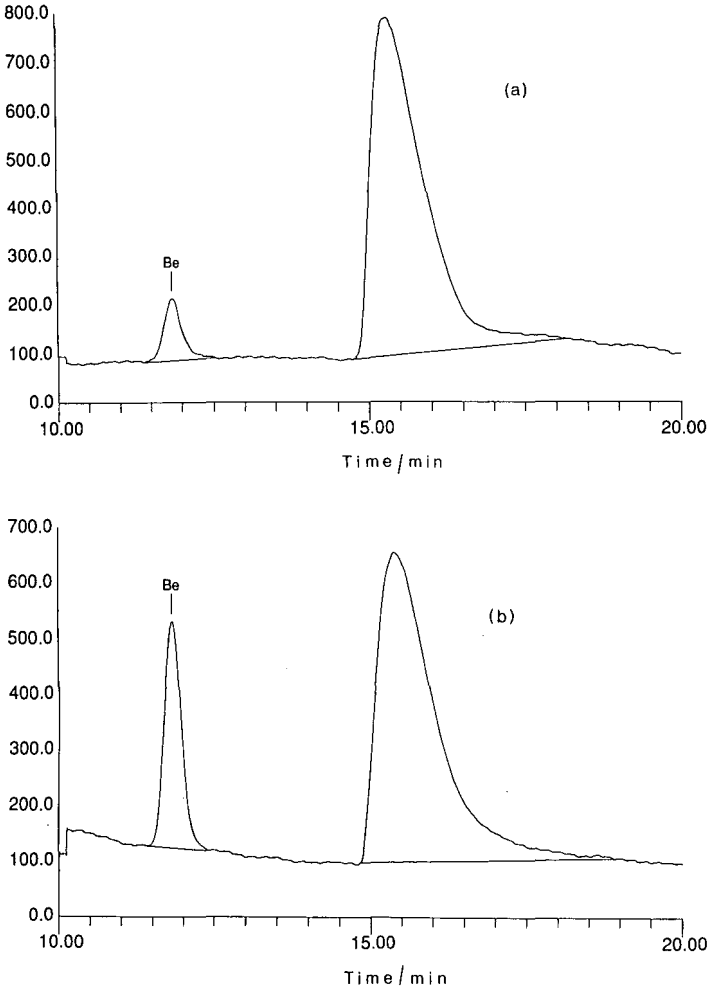

Fig. 4. Chromatograms obtained for direct injection of 200 μl of SRM 1643b (a) before and (b) after the addition of 50 μg/l of beryllium.

TABLE I

RECOVERY OF BERYLLIUM IN CERTIFIED REFERENCE MATERIALS

Sample	Certified Be content ± S.D. (ng/g)	Concentration determined ± S.D. (n = 10) (ng/g)	Recovery (%)
SRM 1643b	19	19.2 ± 0.36	101
MESS-1	1900 ± 200	1879 ± 20	98
BCSS-1	1300 ± 300	1307 ± 20	100.5

For all three reference materials tested, the beryllium concentrations obtained using the standard addition method were found to concur with the certified values, as reported in Table I.

CONCLUSIONS

A simple, rapid and accurate method based on ion-exchange chromatography with post-column derivatization has been developed to determine beryllium in the μg/l–mg/l range. The possibility of obtaining lower detection limits by means of on-line preconcentration techniques is under investigation.

REFERENCES

1 U. Forstner and G. T. W. Wittmann, in E. D. Goldberg (Editor), *Metal Pollution in the Aquatic Environment*, Springer, Berlin, 1983, pp. 87 and 134.
2 W. Salomons and U. Forstner, *Metals in Hydrocycle*, Springer, Berlin, 1984, p. 141.
3 F. A. Patty, *Industrial Hygiene and Toxicology*, Vol. II, Interscience, New York, 1962, pp. 1020–1030.
4 M. B. Jacobs, *The Analytical Toxicology of Industrial Inorganic Poisons*, Interscience, New York, 1967, pp. 388–398.
5 X. Q. Shan, Z. Yian and Z. M. Ni, *Anal. Chim. Acta*, 217 (1989) 271.
6 R. Kuroda, S. Nagao, Y. Hayashibe and K. Oguma, *J. Trace Microprobe Tech.*, 7 (1989) 47.
7 Y. L. Zhu and J. X. Shao, *Analyst (London)*, 114 (1989) 97.
8 P. Kaur and V. K. Gupta, *Fresenius Z. Anal. Chem.*, 334 (1989) 447.
9 F. Capitan, E. Manzano, A. Navalon, J. L. Vilchez and L. F. Capitan-Valley, *Analyst (London)*, 114 (1989) 969.
10 K. Soroka, R. S. Vithanage, D. A. Philips, B. Walker and P. K. Dasgupta, *Anal. Chem.*, 59 (1987) 629.
11 G. Nickless, *J. Chromatogr.*, 313 (1985) 129.
12 P. K. Dasgupta, *J. Chromatogr. Sci.*, 27 (1989) 422.
13 H. Noda, K. Saitoh and N. Suzuki, *Chromatographia*, 14 (1981) 189.
14 M. Biswanath and S. R. Desai, *Analyst (London)*, 114 (1989) 969.
15 B. Kondratjonok and G. Schwedt, *Fresenius Z. Anal. Chem.*, 337 (1988) 332.
16 V. Cheam and A. S. Y. Chau, *Analyst (London)*, 112 (1987) 993.
17 *The Alternative to AAS and ICP*, Dionex, Sunnyvale, CA, 1985, LPN 32631.
18 M. Betti, M. P. Colombini, R. Fuoco and P. Papoff, *Mar. Chem.*, 17 (1985) 313.
19 F. A. Cotton and G. Wilkinson, *Advanced Inorganic Chemistry*, Interscience, New York, 1973.
20 E. Upor, M. Mohai and G. Y. Novak, *Photometric Methods in Inorganic Trace Analysis*, Elsevier, Amsterdam, 1985.
21 F. D. Snell, *Photometric and Fluorimetric Methods of Analysis–Metals*, Wiley, New York, 1978, p. 667.
22 S. Majee and J. Das, *Indian J. Chem.*, 27A (1988) 983.
23 C. A. Pohl, personal communication, 1986.
24 W. J. Langston, *Estuarine Coastal Shelf Sci.*, 23 (1986) 239.

Journal of Chromatography, 538 (1991) 373–383
Elsevier Science Publishers B.V., Amsterdam

CHROM. 22 816

Identification of individual diacylglycerols by adsorption thin-layer chromatography of their coordination complexes

V. P. PCHELKIN* and A. G. VERESHCHAGIN

Laboratory of Lipid Metabolism, Institute of Plant Physiology, Academy of Sciences, Botanicheskaya 35, Moscow 127276 (U.S.S.R.)

(First received June 5th, 1989; revised manuscript received June 15th, 1990)

ABSTRACT

Diacylglycerols (DAGs) obtained by glycerolysis of a mixture of cocoa butter, poppy seed and linseed oils were separated by preparative thin-layer chromatography (TLC) into their positional isomers. An isomerically pure model mixture of *rac*-1,2-DAGs was further separated into eleven fractions using adsorption TLC of coordination complexes of unsaturated DAG species with silver ions on an analytical scale. The mobility of the separate TLC zones of this mixture, which included residues of stearic (St), palmitic (P), oleic (O), linoleic (L) and linolenic (Le) acids, was compared with that of standard *rac*-1,2-DAG zones. The comparison demonstrated that the model mixture was composed of the following individual DAG species: StO-, PO-, OO-, OL-, LL-, OLe-, LLe- and LeLe-glycerols, in addition to SS-, SL- and SLe-glycerols in which S is St or P. The different mobilities of these DAG species can be accounted for by the differences in the relative polarities of the Ag^+ complexes of O, L and Le, which were found to be 1.03, 2.46 and 5.45, respectively. There was a strong negative correlation between the mobility and the polarity of the DAG species.

INTRODUCTION[a]

Fractionation of a model mixture of diacylglycerols (DAGs) by reversed-phase thin-layer chromatography (RP-TLC) has been reported previously [1]. The distribution of individual fatty acid residues between DAG molecular species was found to be close to random (see below), and therefore this mixture could include as many as fifteen DAG species. Because of this complexity, the complete separation of the mixture into individual species of DAGs was not achieved, and so a new attempt was made to identify them. In order to increase the separation selectivity of DAGs, we

[a] Major abbreviations: DAGs and TAGs = di- and triacylglycerols, respectively; FAMEs = fatty acid methyl esters; St, P, O, L, Le, S, U = residues of stearic, palmitic, oleic, linoleic, linolenic, saturated and unsaturated fatty acids, respectively; e = number of olefinic bonds in a DAG molecule; Δe = difference in e values between two adjacent DAG zones; n and N = number of major fatty acid and DAG molecular species in their mixtures, respectively; Ag^+-TLC = adsorption TLC on silver nitrate-impregnated silica gel; RP-TLC = reversed-phase TLC; $hR_F = 100R_F$; $hR_{1,3\text{-LL}} = 100R_{1,3\text{-LL}}$ = mobility of a DAG zone in relation to that of *rac*-1,3-LL.

0021-9673/91/$03.50

tested other modes of TLC which differ from RP-TLC in the mechanism of lipid fractionation, in particular adsorption TLC of the coordination complexes of unsaturated lipids with silver ions (Ag^+-TLC). To identify DAGs in the model mixture, we compared their Ag^+-TLC mobilities with those of standard DAGs of a relatively simple species composition. In this paper we report the results of the identification and discuss the separation selectivity of individual DAGs differing in their unsaturation.

EXPERIMENTAL

Materials

Purification of solvents and the preparation of the DAG model mixture and a mixture of trimethylborate and methanol were performed as described previously [1,2]. Mobile phases for TLC contained 10 ppm butylated hydroxytoluene and 0.9 ppm DL-α-tocopherol (Serva, Heidelberg, Germany) as antioxidants. Bromine, silver nitrate, boric acid, urea, glycerol (all analytical-reagent grade), *p*-toluenesulphonic acid (pure) and LSL_{254} silica gel (5–40 μm) with 13% gypsum (Chemapol, Prague, Czechoslovakia) were used as received. Glass plates with a permanent adsorbent layer were prepared as described previously [3] except that water, not toluene, was used to suspend the mixture of glass powder and silica gel.

Preparation of DAG standards

Fatty acid methyl esters (FAMEs) obtained by methanolysis of cocoa butter and poppy seed oil [1] were dissolved in 22% (w/v) methanolic urea solution and the resulting urea complexes of stearic (St), palmitic (P), oleic (O) and linoleic (L) acid methyl esters were precipitated by fractional crystallization at different temperatures [4]. Linolenic acid (Le) methyl ester was prepared from linseed oil as described previously [5]. The FAMEs thus obtained were used to prepare seven mixtures, in which the number of major FAME species (*n*) was two or three, as follows: (1) P + O; (2) St + O; (3) St + P + L; (4) St + P + Le; (5) O + L; (6) O + L + Le; (7) L + Le. The fatty acid composition of each FAME preparation was determined by gas chromatography (GC) [6].

Standard DAGs were synthesized by the modified method of Markley [7]. Each of the seven FAME mixtures (2 mmol) was mixed with glycerol (1 mmol), *p*-toluenesulphonic acid (2 mmol) and 10 ml of toluene, and incubated for 1 h at 118°C. The reaction mixture was used to isolate the sum of DAG isomers, *rac*-1,2- plus -1,3-DAGs [1], from which *rac*-1,2-DAGs used as standards were prepared [2].

Isolation of positional isomers of DAGs

For the preparative isolation of DAG positional isomers, 40 mg of the above standards were applied as a band on a starting line of a silica gel and boric acid layer (19:1; 200 × 200 × 0.5 mm) and separated for 1.5 h in a chamber for ascending TLC [1] using chloroform–acetone (98:2, v/v) as the mobile phase [8]. Layers were sprayed with a 0.001% aqueous solution of Rhodamine 6G, and the *rac*-1,2- and -1,3-DAG zones (R_F = 0.3 and 0.5, respectively) were revealed under UV radiation (254 nm). Each DAG isomer was eluted from the adsorbent for 1 h in an extractor [9] with

chloroform–methanol–trimethyl borate (2:1:0.1, v/v/v). The isomeric purity of the DAGs was determined by known methods [1]. Isomers of DAGs dissolved in benzene were stored in the cold in sealed ampoules [4].

Ag^+-TLC of DAGs

Prior to Ag^+-TLC, a plate with a permanent adsorbent layer (10 × 20 cm) was sprayed with a 1% (w/v) methanolic solution of silver nitrate [10,11]. As a result, the layer acquired about 5% (w/w) of silver nitrate. At the starting line of this plate, 20–50 μg of *rac*-1,2- or -1,3-DAGs were applied, and DAGs were separated for 3–23 h by continuous TLC [12] using a silver nitrate-saturated mixture of chloroform and isopropanol (99:1, v/v) as the mobile phase. Silver ions were removed from the adsorbent with water and the dry plate was held for 30 min in the presence of bromine vapour. DAG zones were revealed as described previously [3], and their mobility was expressed as $(hR_{1,3\text{-LL}})_j$ using $x \pm s$, where x is the arithmetic mean of individual measurements of mobility and s is the absolute standard deviation of these measurements. The relative intensity of DAG zones obtained during the analysis of a given standard mixture was assessed visually. Other methods were the same as those used previously [1,2].

RESULTS AND DISCUSSION

Composition of DAG positional isomers in the products of glycerolysis

A DAG model mixture was obtained by glycerolysis, and therefore it was a mixture of DAG positional isomers [1]. Previously we did not consider the role of these isomers in the analysis of the DAG composition by RP-TLC, because under these conditions they did not differ from each other in their TLC mobility [1]. However, in adsorption TLC such a separation within a given DAG molecular species does take place; this was first demonstrated by Barrett *et al.* [13] in the Ag^+-TLC of synthetic *rac*-1,3- and -1,2-DAGs. Therefore, before discussing the Ag^+-TLC fractionation of the DAG model mixture, it is necessary to consider the qualitative and quantitative composition of its positional isomers.

Evidently, the random DAG model mixture (see below) obtained by glycerolysis of esters of fatty acids A and B (where A = B and also A ≠ B) contains non-symmetrical positional isomers, *i.e.*, *sn*-1,2-(AB) and *sn*-2,3-(AB) stereoisomers; their sum, according to the IUPAC nomenclature [14], is referred to as *rac*-1,2-AB. In turn, the natural *sn*-1,2-(AB) stereoisomers include the positional isomers of fatty acid residues, *i.e.*, *sn*-1-A,2-B- and *sn*-1-B,2-A-glycerols. Similarly, *sn*-2,3-(AB) stereoisomers, which do not occur in nature, include *sn*-2-A,3-B- and *sn*-2-B,3-A-glycerols. Together with *rac*-1,2-AB, the DAG model mixture also contains symmetrical isomers, *i.e.*, *sn*-1-A,3-B- and *sn*-1-B,3-A-glycerols; the sum of these stereoisomers is designated as *rac*-1,3-AB.

During adsorption TLC, *rac*-1,2- and -1,3-AB completely separate from each other (see above), regardless of the presence of silver ions in the mobile phase, whereas resolution within a given positional isomer does not occur [11]. Thus, synthetic *rac*-1,2-DAGs do not differ from natural *sn*-1,2-DAGs in their TLC mobility. Therefore, only a *rac*-1,2-DAG mixture was used as a model mixture in this study. This mixture was isolated from the glycerolysis products by preparative adsorption TLC on

boric acid-containing silica gel, because the presence of this acid enhances the difference in TLC mobility between the positional isomers [8]. Non-symmetrical and symmetrical DAG isomers thus obtained proved to be chromatographically pure.

Determination of the number of zones formed during Ag^+-TLC of the rac-1,2-DAG model mixture

Fatty acid residues present in the DAG model mixture vary in their unsaturation

TABLE I

IDENTIFICATION OF INDIVIDUAL DAG SPECIES IN SEPARATE Ag^+-TLC ZONES OF DAG STANDARDS AND RELATIVE POLARITIES OF COORDINATION COMPLEXES OF THESE DAG SPECIES (p_{DAG})

$hR_{1,3\text{-LL}}$ of DAG zones ($x \pm s$)	Possible DAG species composition (mol%)[a] and visual evaluation of their relative contents[b] in standards 1–7							DAG identification (*e* values)	p_{DAG}[c]
	1	2	3	4	5	6	7		
700 ± 9	49 +++	53 +++	63 +++	57 +++	–	–	–	SS (0)	0 0 0
488 ± 7	[2] +	35 +++	[2] +	–	–	–	–	StO (1)	1.03 1 1
344 ± 8	40 +++	[2] +	–	–	–	–	–	PO (1)	1.03 1 1
250 ± 6	9 ++	7 ++	–	–	–	46 +++	–	OO (2)	2.06 2 2
147 ± 9	–	[3] +	31 +++	[3] +	2 +	–	–	SL (2)	2.46 2.1 1.9
94 ± 6	–	–	–	–	12 ++	9 ++	[2] +	OL (3)	3.49 3.1 2.9
60 ± 4	–	–	4 ++	–	86 +++	–	3 +	LL (4)	4.92 4.2 3.8
33 ± 3	–	–	–	35 +++	–	–	–	SLe (3)	5.45 4.4 5.1
20 ± 3	–	–	–	–	–	35 +++	[8] ++	OLe (4)	6.48 5.4 6.1
10 ± 2	–	–	–	–	–	3 +	25 +++	LLe (5)	7.91 6.5 7.0
3 ± 1	–	–	–	5 ++	–	7 ++	62 +++	LeLe (6)	10.90 8.8 10.2

[a] Calculated from the data of DAG fatty acid composition in Table II. Figures in square brackets are the content of minor DAGs.

[b] –, +, ++, and +++ represent visual evaluation of the relative intensities of DAG zones.

[c] Top, middle and bottom figures are p_{DAG} values calculated by using p_i, p_i' and p_i'', respectively.

(number of olefinic bonds, *e*) from 0 to 3 [1]. Therefore, DAG species with $e = 0$–6 can be assumed to be present in this mixture. On the basis of this assumption, it could be expected that during Ag^+-TLC of the model mixture seven *e* fractions of DAGs would be formed, because during the Ag^+-TLC of FAMEs only separation according to *e* has been observed [11], each zone differing from the adjacent zone by one *e* unit (*i.e.*, $\Delta e = 1$). In reality, however, the total number of zones formed during this separation turned out to be eleven instead of seven (*cf.*, Table I). Thus, the DAG separation was not limited by the $\Delta e = 1$ rule, and hence many adjacent Ag^+-TLC zones did not differ from each other in their *e* values (*i.e.*, $\Delta e = 0$). At the same time this number (eleven) was less than the possible total number of DAG molecular species in the model mixture (fifteen [1]); therefore, some zones seem to be heterogeneous, *i.e.*, to contain more than one DAG molecular species.

The same number of zones (eleven) was observed after Ag^+-TLC of the *rac*-1,3-DAG mixture. These isomers always exceeded the corresponding *rac*-1,2-DAG molecular species in their relative mobility. For example, the latter was equal to 100 for *rac*-1,3-LL compared with 60 for *rac*-1,2-LL. In the studies described below, the only *rac*-1,3-DAG species used was *rac*-1,3-LL, which served as a standard in the calculation of the relative mobility of individual *rac*-1,2-DAG molecular species ($hR_{1,3\text{-LL}}$; see Experimental).

Standards for the identification of individual rac-1,2-DAG molecular species in separate Ag^+-TLC zones

In order to determine the *rac*-1,2-DAG molecular species composition in each of the eleven Ag^+-TLC zones obtained, all of them were compared with respect to their mobility with various *rac*-1,2-DAG standards (see Experimental). These standards were synthesized by catalysed transesterification of FAMEs and glycerol in toluene [7], because this reaction could be carried out at a lower temperature than the glycerolysis without the solvents used earlier for preparing the model mixture [1]. Thus, both the mixture and the standards were the products of transesterification, differing from each other only in the number of fatty acid molecular species used for the synthesis. Hence, the possible DAG molecular species composition can be described in both instances in terms of the same distribution theory, *viz.*, the theory of random distribution [1].

According to this theory, the distribution of fatty acid residues between the products of glycerolysis, including DAGs, occurs in such a way that the probability of formation of a given DAG molecular species is determined on the one hand by the molar content of its component fatty acids in the original FAME mixture, and on the other by the number of a given fatty acid residue (one or two) in this species. Finally, the calculation of the random distribution is based on the assumption that all DAGs are formed by a completely random esterification of each hydroxyl group, and the rate of this reaction does not depend on the nature of fatty acid residues.

The qualitative composition, *i.e.*, the possible total number of major DAG molecular species (*N*) in each *rac*-1,2-AB standard, disregarding AB and BA positional isomers (see above), is made up of monoacid (*n*) and diacid [$n(n-1)/2$] DAG molecular species, and so is equal to $N = n(n+1)/2$ [1]. The fatty acid composition of both the standards and the original FAME mixtures is shown in Table II. Both lipid classes appear to be generally similar in this respect, each standard including 3–5 fatty acid species. However, only the major species (*n*), *i.e.*, those exceeding 6% of the total,

TABLE II

FATTY ACID COMPOSITION OF ORIGINAL FAME MIXTURES AND RESULTING DAG STANDARDS

Standards		Fatty acid composition (mol%)				
No.	Class	St	P	O	L	Le
1	FAMEs	4.0	69.8	26.2	–	–
	DAGs	3.1	67.0	29.9	–	–
2	FAMEs	68.8	2.9	25.8	2.5	–
	DAGs	69.3	3.2	25.3	2.2	–
3	FAMEs	48.4	23.8	0.6	27.2	–
	DAGs	49.6	27.8	2.1	20.5	–
4	FAMEs	44.0	26.4	1.2	1.8	26.6
	DAGs	44.0	30.1	1.2	2.2	22.5
5	FAMEs	–	1.1	6.8	92.1	–
	DAGs	–	0.7	6.9	92.4	–
6	FAMEs	–	0.5	65.3	6.2	28.0
	DAGs	–	0.8	67.4	7.0	24.8
7	FAMEs	–	–	3.0	16.3	80.7
	DAGs	–	–	5.2	16.2	78.6

were used to calculate N. In the standards 1, 2, 5 and 7 (where $n = 2$) $N = 3$, and in those with $n = 3$ (3, 4 and 6) $N = 6$. Thus, the N value in each standard was much less than $N = 15$ ($n = 5$) in the DAG model mixture [1]. Therefore, the molecular species composition in a given standard could be relatively easily determined and in turn used for identifying individual DAG species in the model mixture.

The quantitative composition, *i.e.*, the random concentration of each molecular species in the DAG standards (A_1, A_2, ..., A_N%), can be calculated by using the concentrations of individual fatty acid residues in these standards (a, b, ..., %). For each monoacid DAG species $A_1 = a^2/100$, and for the diacid species $A_2 = 2ab/100$, the factor of 2 being used in this equation to take into account both positional isomers AB and BA of diacid DAGs. DAG contents below 2%, *i.e.*, below the usual sensitivity limit when using the Ag^+-TLC technique, were disregarded and the remaining ones approximated to the nearest unit percent.

The results of the "random" calculation of both qualitative and quantitative DAG molecular species composition in the standards 1–7 and the data on the Ag^+-TLC mobility of the latter are shown in Table I. It can be seen that the standards as a whole formed eleven TLC zones, as was also the case with the original DAG model mixture (see above), whereas the number of major zones in each standard varied from three to five.

Identification of individual DAG species

Using the data in Tables I and II, let us consider the identification procedure for DAGs present in each of these zones, beginning with the TLC zone characterized by the lowest mobility ($hR_{1,3\text{-LL}} = 3 \pm 1$) and referred to below as zone 3. It can be seen that this zone can be found in the standards containing Le (Nos. 4, 6 and 7), although it is only in standard 7 that this zone is the predominant one because of its high Le

content. Thus, zone 3 contains only the LeLe species characterized by the maximum *e* number ($e = 6$) possible for our model mixture.

Zone 10 adjoining the LeLe can only be found in standards 6 and 7, which, unlike all the other standards, include both L and Le. On the transition from standard 6 to standard 7 there is a rise in the L level from 7.0 to 16.2%, and an increase in the zone 10 content (from + to + + +). At the same time, this zone is absent from standards 3 and 4, which contain only one or other of the two polyenic fatty acids. Therefore, this zone cannot be composed of monoacid DAGs (LL or LeLe); it can contain only a single DAG species, *viz.*, LLe, the only possible combination of L and Le.

The next zone, 20, is present mainly in standard 6, characterized by an elevated content of O and Le. Therefore, it may represent either OLe or OO. The first possibility is more likely because there is a positive correlation between the relative intensity of zone 20 in standards 6 and 7 and their O content. The latter hypothesis is improbable as zone 20 is absent from standards 1 and 2, which must certainly contain diolein. Therefore, we conclude that zone 20 includes only OLe.

Zone 33 occurs only in standard 4, in which saturated (S) fatty acids account for 85% of its total fatty acids whereas the unsaturated (U) fatty acids are composed predominantly of Le. In addition to zone 33 this standard contains only trace amounts of LeLe and also a highly non-polar zone 700 present also in standards 1 and 2 (SS, see below). Therefore, zone 33 can include only SLe, where S is either P or St.

Zone 60 is the major component in standard 5, where L accounts for 92% of total fatty acids. Therefore, this zone can include only a single individual DAG species, *i.e.*, LL. As regards zone 94, it can be detected only in the standards devoid of S (Nos. 5–7). Therefore, DAGs in this zone can only be of the UU type, *i.e.*, either OL or OO. However, the latter hypothesis should be discarded owing to the absence of zone 94, together with zone 20 (see above), in standard 1. It is inferred that zone 94 is composed of the diacid OL species.

A high concentration of zone 147 was found only in standard 3, which contains mainly S and L. Obviously, DAGs of this zone have nothing to do either with the SS type (because of the absence of this zone in standard 1, see above) or with the UU type, as LL is located in zone 60, and the presence of OO can be excluded because of the low O content in standard 3. It is therefore evident that zone 147 is composed only of SL.

Zone 250 was found in standard 6 and thus should belong to the UU type (see above). We believe that this zone includes only the monoacid OO species because all the other UU DAGs have already been identified. Moreover, O makes up to 67% of the total fatty acids in standard 6. Diolein occurs also in standards 1 and 2, which have a higher O content than any other standard except 6.

Zones 344 and 488 are present almost exclusively in standards 1 and 2, respectively. It is evident that these DAGs do not belong to either the UU or the SS type (see above), and should therefore represent only the SU DAGs. We consider that zones 344 and 488 are composed of PO and StO, respectively. This conclusion is based mainly on the fatty acid composition of standards 1 and 2 (Table II). Moreover, in standard 3, in which the St content is 1.3 times higher than that of P and the calculated StO and PO concentrations are 2.5 and 0.8 mol-%, respectively, there is the clear zone 488 (StO) whereas zone 344 (PO) cannot be observed.

Finally, standards 1–4 have one more zone, 700, which exceeds any other zone in its mobility. All UU and SU DAGs having already been identified (see above), this

zone should contain only SS species, which are known not to form coordination complexes and therefore cannot be separated by Ag^+-TLC [11].

Hence Ag^+-TLC makes it possible to identify in standards 1–7 eight individual DAGs, *viz.*, StO, PO, OO, OL, LL, OLe, LLe, and LeLe, *i.e.*, all UU and SO species possible. It follows also from our data that these standards contain SS, SL and SLe components. Their species composition cannot be determined by Ag^+-TLC (see above); the maximum number of individual DAG species in these components is 3, 2 and 2, respectively. The eleven zones found in standards 1–7 coincided in their TLC mobilities with the respective zones of the model mixture [2]. The data for DAG identification in this mixture can be considered to be accurate because the fatty acid composition of DAGs used as standards was established unambiguously (see above). Therefore, the GC and mass spectrometric identification of DAGs in separate zones were not carried out.

It can be expected that Ag^+-TLC will be suitable for determining the species composition of DAG radicals of highly unsaturated polar glycerolipids of plant origin because they are usually characterized by low levels of S and SS ($\leqslant 20$ and $\leqslant 4\%$, respectively), and of SL and SLe. At the same time, complete identification of DAGs in mixtures with similar S contents to our model mixture would require the combination of Ag^+-TLC with some other chromatographic techniques.

Selectivity of DAG separation by Ag^+-TLC

The comparison of the fatty acid composition of DAG species identified above with their mobility on Ag^+-TLC fractionation makes it possible to assess the selectivity of this separation. From Table I it can be seen that at $\Delta e \geqslant 1$ these species always separate from each other (A-type separation). This rule has been demonstrated repeatedly for both DAGs and other neutral lipids [15].

At the same time, when separating DAGs with $e = 1$–4, it has been established that their mobility depends not only on e, but also on other factors, because in this instance there was a separation of DAG species with $\Delta e = 0$ (B-type separation, see above). In this instance there were three modes of separation: mode B_1 involves the resolution of UU DAGs with the same e value (*e.g.*, LL and OLe), mode B_2 the separation of UU DAGs from respective SL and SLe DAGs with strongly asymmetric structures (*e.g.*, OL from SLe, and OO from SL) and mode B_3 the separation of SO DAGs differing in the length of their unsaturated acyl residues (StO and PO).

We are unaware of any B_1- and B_3-mode fractionation experiments performed so far, but the B_2-mode separation has been reported [16,17]. For example, when DAGs obtained by hydrolysis of animal lecithins were fractionated using a mixture of chloroform and ethanol (96:4) as the mobile phase, the hR_F values of OL and SLe were 58 and 44 and those of OO and SL were 75 and 64, respectively [17]. These data are close to our results (Table I).

Relationship between the selectivity of Ag^+-TLC separation of individual DAG species and the relative polarity of their coordination complexes[a]

The data in Table I suggest that in the course of separation according to modes

[a] The term relative polarity of coordination complexes of unsaturated DAG species with silver ions means the affinity of these complexes to the highly polar stationary phase of the Ag^+-TLC system [11]. This term is referred to subsequently simply as "polarity (of lipids)".

A and B the elution order of individual DAG species is inversely proportional to their relative polarity (p_{DAG}). To test this suggestion we had to calculate the p_{DAG} value. To this end we assumed that p_{DAG} values are additive, being similar in this respect to TAG polarity values reported earlier [18]. From this viewpoint, the value of p_{DAG} is equal to the sum of polarities of fatty acid residues (p_i) forming a given DAG species:

$$p_{DAG} = \sum_i (n_i p_i) \tag{1}$$

where n_i is the number of ith fatty acid residues in this species. In turn, p_i values were calculated from the mobilities of disaturated DAGs (SS) and Ag^+ complexes of monoacid diunsaturated DAGs (UU), OO, LL and LeLe (Table I). By substituting these data in the equation

$$p_i = \ln [(hR_{1,3\text{-LL}})_{SS}/(hR_{1,3\text{-LL}})_{UU}] \tag{2}$$

obtained empirically, it was shown that the p_i values of O, L and Le residues are 1.03, 2.46 and 5.45, respectively.

It was of interest to compare these values with those obtained earlier when separating Ag^+ complexes of other neutral lipid classes, *viz.*, FAMEs and TAGs [18,19]. FAMEs were separated by countercurrent distribution between *n*-hexane and 0.2 *M* silver nitrate in aqueous methanol (9:1) [20]. In this experiment, on transition from O ($e = 1$) to L ($e = 2$) and from O to Le ($e = 3$), the affinity of the ith FAME to the polar phase of the system, *i.e.*, its p_i value, did not increase 2- and 3-fold, respectively, but increased to a much greater extent. In the opinion of Scholfield *et al.* [20], this relationship occurs because on the formation of coordination complexes every olefinic bond of L and Le polarizes the adjoining one, the degree of such polarization being directly proportional to the number of methylene groups located between the interacting double bonds. Thus, the qualitative relationships between O, L and Le residues as regards their polarity found by these authors [20] were similar to those found in our work; however, they failed to obtain quantitative data to characterize this parameter.

The hypothesis of Scholfield *et al.* [20] was confirmed by Gunstone and Padley [18], who attempted for the first time to assess semiquantitatively the "complexing power" (p_i') between the O, L and Le residues on the one hand and the silver ions on the other on Ag^+-TLC of natural TAGs including these residues (see above). In further discussion we assume that the p_i' values are directly proportional to the polarity of the fatty acid residues. According to Gunstone and Padley [18], $p_S' = 0, p_O' = 1, p_L' = 2 + a$ and $p_{Le}' = 4 + 4a$, where $a < 1$ is some fraction. Let $a = 0.1$, then $p_L' = 2.1$ and $p_{Le}' = 4.4$.

Finally, when using Ag^+-TLC to separate FAMEs, Grynberg and Ceglowska [19] introduced the concept of "relative force of complex formation" of an ith fatty acid residue (f.c.$_i$). This concept was similar to that of Gunstone and Padley's "complexing power", but its calculation was based on the results of TLC rather than on an arbitrary assumption:

$$\text{f.c.}_i = p_i'' = [(1 - R_F)_i - (1 - R_F)_S]/[(1 - R_F)_O - (1 - R_F)_S] \tag{3}$$

It follows from eqn. 3 that p''_O is always equal to 1. As regards p''_L and p''_{Le}, it has been shown that in a mobile phase similar to that used in our work (chloroform–methanol [19]) they were equal to 1.9 and 5.1, respectively.

It can be seen that p'_i and p''_i are close to the respective p_i values (see above). At the same time, there is a considerable difference between p'_L and p''_L and between p'_{Le} and p''_{Le} values, f.c.$_i$ being even lower than the number of olefinic bonds in the L residue.

Using p_i and eqn. 1, we calculated p_{DAG} values for all DAG molecular species (see Table I). These values were used to verify our initial suggestion (see above) by the correlation coefficients r between p_{DAG} and $hR_{1,3\text{-LL}}$. The results of this calculation are given in Table III. It can be seen that there is a strong negative correlation between these parameters ($r = -0.804$; $p > 99\%$). Thus, as regards A, B_1 and B_2 separation modes, our suggestion was fully justified. At the same time, the B_3-mode separation between StO and PO could not be explained from this viewpoint, because these species did not differ from each other in their p_{DAG} values.

A similar correlation ($p > 99\%$) was found after replacing p_i in eqn. 1 with p'_i and p''_i (Table I). Nevertheless, it was of interest to compare the values of p_i, p'_i and p''_i as regards their accuracy. To this end they were used to calculate not only the polarity of free DAGs but also that of individual species of other lipid classes, *viz.*, DAG acetates and TAGs; the Ag^+-TLC mobility data of the latter (hR_F) were obtained earlier [15–17,21,22]. The polarity of these species calculated by substituting p_i, p'_i and p''_i into eqn. 1 was used to calculate correlation coefficients between p and hR_F (Table III). It

TABLE III

CORRELATION BETWEEN RELATIVE POLARITIES OF COORDINATION COMPLEXES OF INDIVIDUAL SPECIES BELONGING TO DIFFERENT NEUTRAL LIPID CLASSES AND Ag^+-TLC MOBILITY OF THESE COMPLEXES

$-r \cdot 1000$ values calculated using $hR_{1,3\text{-LL}}$ (Table I) and hR_F values found by other workers [15–17,21,22].

Lipid class	Polarity values of unsaturated fatty acid residues used for calculating lipid polarity according to eqn. 1			Ref.
	p_i	p'_i	p''_i	
DAGs	804	821	779	This work
	983[a]	968[a]	989[a]	16
	997	988	976	17
	946[a]	921[a]	893[a]	15
	998	993	984	15
DAG acetates	956	969	920	21
	991	995	980	15
	987	993	970	15
	977	962	944[a]	15
TAGs	989	979	966	21
	944	835[a]	830[a]	21
	980	975	966	22
	962	951	932	15
	809[a]	802[a]	818[a]	15

[a] Accurate at the $95\% < p < 99\%$ level; other r values are accurate at the $p > 99\%$ level.

can be seen that all correlations are accurate at $p > 95\%$. At the same time, when using p_i, p_i' and p_i'' values, the correlation at $p > 99\%$ was observed in eleven, ten and nine cases, respectively. Thus, the relative polarity of unsaturated fatty acid residues on Ag^+-TLC is most accurately reflected by the p_i values.

The correlation between p and R_M values, which were calculated from R_F values [23], was similar to that described above (data not shown).

In conclusion, it should be stressed that the relationship between the polarity of an individual DAG species and its Ag^+-TLC mobility is logarithmic (see eqns. 1 and 2). Therefore, it can be suggested that there is some connection between the polarity of the DAG molecule and its chemical potential (μ), as $\ln(1/R_F - 1)$ is a member of the well known equation

$$\Delta\mu_X = RT\ln[(1/R_{F_A} - 1)/(1/R_{F_B} - 1)] \quad (4)$$

where $\Delta\mu_X$ is the difference between the μ values of A and B homologues, differing in the presence of an X group in B, R is the universal gas constant and T is the absolute temperature [23]. It must be recognized that eqn. 4 can be applied only to liquid–liquid systems. However, when separating FAME coordination complexes in such systems, *i.e.*, by reversed-phase partition chromatography [24] and countercurrent distribution [20], there was the same polarity relationship between O, L and Le residues as that described above.

REFERENCES

1 V. P. Pchelkin and A. G. Vereshchagin, *J. Chromatogr.*, 209 (1981) 49.
2 V. P. Pchelkin and A. G. Vereshchagin, *Appl. Biochem. Microbiol. (USSR)*, 24 (1989) 667.
3 V. D. Tsydendambaev, A. V. Zhukov and A. G. Vereshchagin, *J. Chromatogr.*, 132 (1977) 195.
4 A. V. Zhukov, I. M. Davydova and A. G. Vereshchagin, *J. Chromatogr.*, 51 (1970) 155.
5 J. D. Nadenicek and O. S. Privett, *Chem. Phys. Lipids*, 2 (1968) 409.
6 A. G. Vereshchagin, *Fiziol. Biokhim. Kul't. Rast.*, 4 (1972) 645.
7 K. S. Markley, in K. S. Markley (Editor), *Fatty Acids, Part 5*, Interscience, New York, 1968, p. 3503.
8 A. E. Thomas, III, J. E. Sharoun and H. Ralston, *J. Am. Oil Chem. Soc.*, 42 (1965) 789.
9 A. V. Zhukov and A. G. Vereshchagin, *J. Am. Oil Chem. Soc.*, 53 (1976) 1.
10 L. J. Morris, *Chem. Ind. (London)*, 27 (1962) 1238.
11 L. J. Morris, *J. Lipid Res.*, 7 (1966) 717.
12 J. G. Kirchner, *Thin Layer Chromatography*, Interscience, New York, 1967.
13 C. B. Barrett, M. S. Dallas, Jr., and F. B. Padley, *J. Am. Oil Chem. Soc.*, 40 (1963) 580.
14 The Nomenclature of Lipids, *Hoppe-Seyler's Z. Physiol. Chem.*, 358 (1977) 617.
15 A. Kuksis, in H. Mangold (Editor), *CRC Handbook of Chromatography: Lipids*, CRC Press, Boca Raton, FL, 1984, p. 381.
16 L. M. G. van Golde, W. A. Pieterson and L. L. M. van Deenen, *Biochim. Biophys. Acta*, 152 (1968) 84.
17 L. M. G. van Golde, V. Tomasi and L. L. M. van Deenen, *Chem. Phys. Lipids*, 1 (1967) 282.
18 F. D. Gunstone and F. B. Padley, *J. Am. Oil Chem. Soc.*, 42 (1965) 957.
19 H. Grynberg and K. Ceglowska, *Rev. Fr. Corps Gras*, 17 (1970) 89.
20 C. R. Scholfield, E. R. Jones, R. O. Butterfield and H. J. Dutton, *Anal. Chem.*, 35 (1963) 1588.
21 W. W. Christie, *Lipid Analysis*, Pergamon Press, Oxford, 1973, pp. 238, 248.
22 C. Litchfield, *Analysis of Triglycerides*, Academic Press, New York, London, 1972, p. 57.
23 R. Block, R. LeStrange and G. Zweig, *Paper Chromatography*, Academic Press, New York, 1952, p. 16.
24 A. G. Vereshchagin, *J. Chromatogr.*, 17 (1965) 382.

Journal of Chromatography, 538 (1991) 385–391
Elsevier Science Publishers B.V., Amsterdam

CHROM. 22 802

Improvement of resolution in the capillary electrophoretic separation of catecholamines by complex formation with boric acid and control of electroosmosis with a cationic surfactant

TAKASHI KANETA, SHUNITZ TANAKA and HITOSHI YOSHIDA*
Department of Chemistry, Faculty of Science, Hokkaido University, Kita-ku, Sapporo 060 (Japan)
(Received August 22nd, 1990)

ABSTRACT

In order to improve the resolution of catecholamines, the control of both the electroosmotic and the electrophoretic mobilites were carried out. The former was controlled by the addition of borate ion and a change in pH. The control of the latter was carried out by addition of a cationic surfactant. Ten catecholamines were sufficiently separated.

INTRODUCTION

Capillary electrophoresis (CE) [1–3] is used to separate mixtures of ionic species. Many attempts have been made to improve the resolution of CE. The factors governing the resolution of CE include the electrophoretic mobilities of sample species and the electroosmotic mobility, the diameter and length of the capillary and the applied voltage. The electroosmotic and electrophoretic mobilities are most important factors for achieving a higher separation resolution in CE.

The conventional technique for the control of electrophoretic mobilities is the selection of the pH of the background electrolyte. For the separation of ionic species such as weak acids or bases, the pH should be selected near the dissociatioa constant (pK_a) of the species. Then the separation can be easily accomplished on the basis of the difference in their values [4–6].

Another approach is the use of a complex formation reaction. For example, amino acid enantiomers have been separated by using ligand exchange with copper(II)–aspartame complexes [7]. Addition of cyclodextrin to the background electrolyte allowed the separation of optical isomers of catecholamines [8]. Micellar electrokinetic capillary chromatography (MECC) is also an effective technique for controlling the mobilities and improving the resolution [9,10]. The utility of MECC combined with complex formation has been reported, *e.g.*, for the separation of catecholamines [11] and oligonucleotides [12].

The electroosmotic flow, which is another important factor with regard to

0021-9673/91/$03.50

resolution, is generated by the negative charge on the inner wall of the glass capillary, resulting from the dissociation of silanol groups. The electroosmotic velocity is dependent on several factors, which include the origin of the capillary, the nature and concentration of background electrolyte and their pH. One of the methods for controlling the electroosmotic mobility is to add surfactants to the background electrolyte [5,13–15]. It is effective not only for the suppression of electroosmotic flow but also for its reversal. Tsuda obtained flow reversal by using cetyltrimethylammonium ion [15]. Huang *et al.* [5] reported the separation of a six-component carboxylic acid mixture using the tetradecyltrimethylammonium ion.

In this work, to improve the resolution of catecholamines, the control of both the electroosmotic and the electrophoretic mobilities was investigated. The effective mobilities of catecholamines could be controlled by complex formation with borate ion. The control of electroosmotic flow was performed by the addition of cationic surfactants to the background electrolyte. The electroosmotic mobility decreased with increasing concentration of surfactant and the length of its alkyl chain. The electroosmotic flow was reversed by a cationic surfactant with a longer alkyl chain. Using a background electrolyte containing borate buffer and a cationic surfactant, ten components of catecholamines were sufficiently separated.

EXPERIMENTAL

Apparatus

A fused-silica capillary tube (70 cm × 100 μm I.D.) was obtained from Gasukuro Kogyo (Tokyo, Japan). A high-voltage power supply of a Shimadzu (Kyoto, Japan) IP-1B isotachophoretic analyser was used. A Model CV^4 variable-wavelength absorbance detector (ISCO, Lincoln, NE, U.S.A.) was employed. Detection was carried out by measuring the absorbance at 217 nm on the column at a position 20 cm from the negative end of the capillary tube. A sample was injected by moving the injection end of the capillary to the sample reservoir and raising it higher than the other end for a constant time. The electroosmotic velocity was measured by the peak of methanol or toluene. A new capillary was flushed with 0.1 *M* potassium hydroxide solution overnight before the experiments, and according to the study by Lauer and McManigill [16], a 15-min flush with water followed by a 15-min flush with operating buffer was applied new experiments. When the experiments were completed, the capillary was flushed and filled with 0.1 *M* potassium hydroxide solution. All investigations were performed at room temperature.

Reagents

All reagents were of analytical-reagent grade and used without further purification. Epinephrine (EP), isoproterenol (IP), 3,4-dihydroxyphenylalanine (Dopa) and vanillylmandelic acid (VMA) were obtained from Wako (Osaka, Japan), metanephrine (MN) and normetanephrine (NM) from Nacalai Tesque (Kyoto, Japan), dopamine (DA) and 3,4-dihydroxybenzylamine (DBA) from Aldrich (Milwaukee, WI, U.S.A.) and norepinephrine (NE) and deoxyepinephrine (DEP) from Sigma (St. Louis, MO, U.S.A.). The solutions were stored in a refrigerator. Decyltrimethylammonium bromide (DeTAB), dodecyltrimethylammonium bromide (DoTAB) and tetradecyltrimethylammonium bromide (TTAB) were purchased from Tokyo Kasei Kogyo (Tokyo, Japan).

RESULTS AND DISCUSSION

Control of effective mobilities of catecholamines

The effective mobilities of catecholamines are too close for them to be separated. Therefore, the resolution cannot be improved simply by controlling the pH (8–10) of the background electrolyte containing ammonium chloride. Previously, we have reported the utility of complex formation with boric acid for the separation of catecholamines on CE [17]. By adding boric acid to the background electrolyte, the retention time of each solute is increased as they react with boric acid to form borate complexes with no charge or a negative charge, except for MN and NM. The resolution increased with increasing concentration of boric acid.

When borate buffer containing 100 m*M* potassium hydroxide was used as the background electrolyte, the retention times of catecholamines and the electroosmotic flow were varied under the influence of the pH, as shown in Fig. 1. The retention time of electroosmotic flow became shorter with increasing pH and hardly changed above

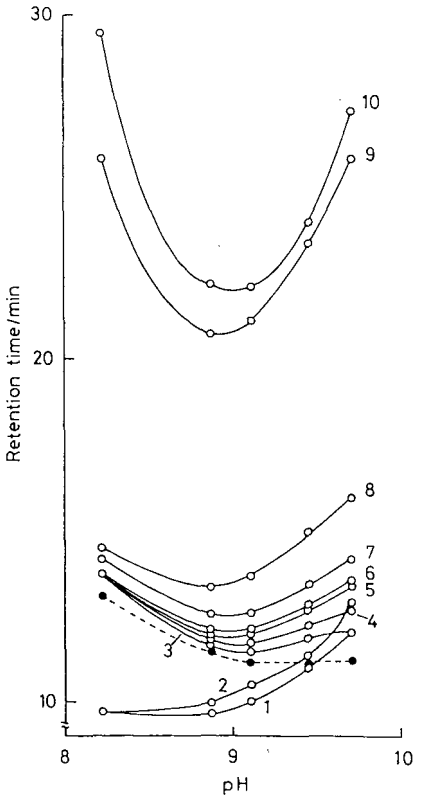

Fig. 1. Effect of pH of borate buffer on retention times of catecholamines: (1) MN; (2) NM; (3) DEP; (4) DA; (5) DBA; (6) IP; (7) EP; (8) NE; (9) Dopa; (10) VMA. The dashed line represents electroosmotic flow; buffer solution, 100 m*M* KOH–boric acid; separation tube, 700 mm × 100 μm I.D.; length of the tube used for separation, 500 mm; total applied voltage, *ca.* 10 kV; current, 100 μA; detection wavelength, 217 nm; concentration of test mixture, 0.5 m*M* of each catecholamines; injection time, 10 s.

pH 9.1; the retention times of catecholamines also became shorter up to pH 9.1. Above pH 9.1, the retention times of catecholamines increased with increasing pH. The reason may be that catecholamines may be dissociated via the amino group and complexed with borate efficiently to produce anions of higher charged states, except MN and NM, which exist as cations. Therefore, as shown in Fig. 1, pH 9.0–9.5 was suitable for the separation of the ten catecholamines.

Fig. 2 illustrates the electropherogram obtained with 100 m*M* potassium hydroxide–200 m*M* boric acid solution (pH 9.1). The resolution of catecholamines was improved better than when using ammonia buffer. It seems reasonable to assume that sample ions except for MN and NM migrated in the opposite direction to the electroosmotic flow. However, the separation of DBA and IP was not sufficient even under these condition. In order to improve the resolution further, the control of the electroosmotic flow was investigated.

Control of electroosmotic flow

In CE, the resolution between a pair of adjacent components is calculated as follows, as shown by Jorgenson and Lukacs [1]:

$$R_S = 0.177\ (m_{eff1} - m_{eff2})[V/D(m_{av} + m_{eo})]^{1/2} \quad (1)$$

where R_S is the resolution, V is the applied voltage, D is the diffusion coefficient, m_{av} is the average mobility of the two components and m_{eff1}, m_{eff2} and m_{eo} are the effective mobilities of the two components and the electroosmotic mobility, respectively. From the above equation, the resolution becomes better when the sum of the electroosmotic mobility and the average electrophoretic mobility is smaller. If the value of electroosmotic mobility is the same as, but of the opposite sign to, the average

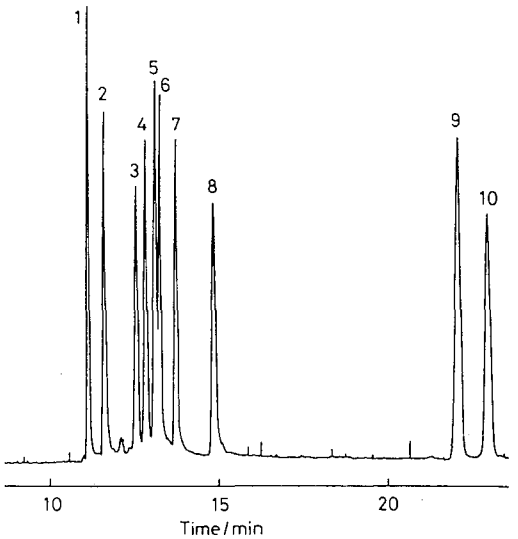

Fig. 2. Electropherogram of test mixture of catecholamines. pH of buffer solution, 9.1. Solutes and other conditions as in Fig. 1.

electrophoretic mobility of sample ions and $m_{eff1} \neq m_{eff2}$, two components will migrate in the opposite direction to each other.

To control the electroosmotic flow, electrically neutral surfactants such as poly(vinyl alcohol) (PVA), Triton X-100 and hydroxyethylcellulose have usually been used in isotachophoresis [13] and CE [14]. These surfactants suppress the electroosmotic flow by adsorption on the capillary inner wall or by increasing the viscosity of the solution. In our study, the electroosmotic flow was suppressed slightly by the addition of PVA or Triton X-100 at the final concentration of 0.01–0.1%, but not sufficiently to improve the resolution. Especially PVA was complexed with borate, and it made the solution very viscous. Nevertheless, the effect of suppressing the electroosmotic flow was small.

Control of electroosmotic flow by a cationic surfactant

Addition of cationic surfactants such as the long-chain ternary alkylammonium type would result in the suppression or reversal of the electroosmotic flow. Depending upon the concentration of the surfactant, the inner wall of the capillary can have varying degrees of negative or positive charge or be neutral. We therefore investigated the influence of three cationic surfactants with different lengths of the alkyl chain, DeTAB, DoTAB and TTAB. Huang *et al.* [5] have reported the effect of TTAB on electroosmosis in low pH buffer. However, the effect will be different in alkaline media. In fact, in alkaline media, with increasing concentration of cationic surfactant the electroosmotic velocity was changed more than in acidic media. The silica surface of the capillary tube probably become more negatively charged in alkaline media owing to the dissociation of the silanol groups. Therefore, addition of a cationic surfactant in alkaline media will have a much greater effect on the electroosmotic flow than in a more acidic medium, where the silanol group are not as fully dissociated.

Fig. 3 shows the effect on the electroosmotic mobility, m_{eo}; m_{eo} is positive when

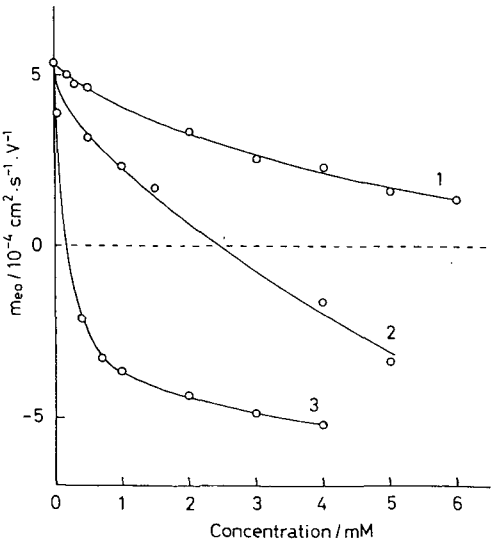

Fig. 3. Effect of concentration of cationic surfactants on electroosmotic mobility: (1) DeTAB; (2) DoTAB; (3) TTAB. pH of buffer solution, 9.1; other conditions as in Fig. 1.

the solution flows from the anode to the cathode. As the alkyl chain increases, the change in electroosmotic flow increased and a reversed electroosmotic flow was observed at a lower concentration of cationic surfactant with a longer alkyl chain. Reversed electroosmotic flow was observed at less than the critical micellar concentration with both DoTAB and TTAB. However, the increase in the concentration of the cationic surfactant makes the conductivity of the background electrolyte larger. To minimize the increase in the conductivity, it will be effective for a cationic surfactant with a longer alkyl chain to be used at a lower concentration for the control of electroosmotic velocity. Fig. 4 shows the electropherogram of catecholamines with buffer containing 0.1 m*M* TTAB (its critical micellar concentration is about 3 m*M*). Each peak was extended slightly, but the resolution between DBA and IP increased and the ten catecholamines could be sufficiently separated under these conditions. The electroosmotic mobility in Fig. 4 was $3.9 \cdot 10^{-4}$ cm^2 V^{-1} s^{-1} and in Fig. 2 $5.3 \cdot 10^{-4}$ cm^2 V^{-1} s^{-1}.

To improve the resolution in CE, it is important to be able to control both the electrophoretic mobilities of sample ions and the electroosmotic mobility. Control of the electrophoretic mobilities of many sample ions can be achieved by using not only the adjustment of the pH of the background electrolyte but also complex formation. Complex formation makes it possible to change the charge of sample ions and then to increase the differences between the effective mobilities of sample ions. Many catecholamines exist as positively charged species even in a background electrolyte of pH *ca.* 9. However, on complex formation with borate ion they are converted into the negatively charged species. Therefore, the direction of migration of catecholamines is changed to the opposite direction of the electroosmotic flow and the resolution is improved. Further, the control of the electroosmotic velocity can be achieved by the addition of a cationic surfactant. Cationic surfactants with long chains such as tetraalkylammonium salts were effective for achieving changes at less than the critical micellar concentration. A longer chain surfactant is preferred because the electroosmotic flow can be suppressed at lower concentration, and the influence on the constitution of the background electrolyte, *i.e.*, the increase in the conductivity and the association of ions, can be reduced. Addition of a longer aklyl chain cationic surfactant is one of the easiest techniques for controlling the electroosmotic flow to improve the resolution of CE.

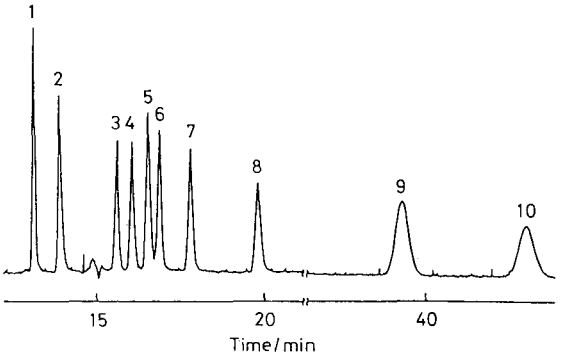

Fig. 4. Electropherogram of test mixture of catecholamines. Buffer. 100 m*M* KOH–200 m*M* boric acid containing 0.1 m*M* TTAB (pH 9.1). Solutes and other conditions as in Fig. 1.

REFERENCES

1 J. W. Jorgenson and K. D. Lukacs, *Anal. Chem.*, 53 (1981) 1298.
2 J. W. Jorgenson and K. D. Lukacs, *J. Chromatogr.*, 218 (1981) 209.
3 J. W. Jorgenson and K. D. Lukacs, *Science (Washington, DC)*, 222 (1983) 266.
4 W. G. Kuhr and E. S. Yeung, *Anal. Chem.*, 60 (1988) 2642.
5 X. Huang, J. A. Luckey, M. J. Gordon and R. N. Zare, *Anal. Chem.*, 61 (1989) 766.
6 S. Terabe, T. Yashima, N. Tanaka and M. Araki, *Anal. Chem.*, 60 (1988) 1673.
7 P. Gozel, E. Gassmann, H. Michelsen and R. N. Zare, *Anal. Chem.*, 59 (1987) 44.
8 S. Fanali, *J. Chromatogr.*, 474 (1989) 441.
9 S. Terabe, K. Otsuka, K. Ichikawa, A. Tsuchiya and T. Ando, *Anal. Chem.*, 56 (1984) 111.
10 S. Terabe, K. Otsuka and T. Ando, *Anal. Chem.*, 57 (1985) 834.
11 R. A. Wallingford and A. G. Ewing, *J. Chromatogr.*, 441 (1988) 299.
12 A. S. Cohen, S. Terabe, J. A. Smith and B. L. Karger, *Anal. Chem.*, 59 (1987) 1021.
13 J. C. Reijenga, G. V. A. Aben, Th. P. E. M. Verheggen and F. M. Everaerts, *J. Chromatogr.*, 260 (1983) 241.
14 S. Terabe, H. Utsumi, K. Otsuka, T. Ando, T. Inomata, S. Kuze and Y. Hanaoka, *J. High Resolut. Chromatogr. Chromatogr. Commun.*, 6 (1986) 666.
15 T. Tsuda, *Nippon Kagaku Kaishi*, 7 (1986) 937.
16 H. H. Lauer and D. McMannigill, *Anal. Chem.*, 58 (1986) 166.
17 S. Tanaka, T. Kaneta and H. Yoshida, *Anal. Sci.*, 6 (1990) 467.

Journal of Chromatography, 538 (1991) 393–402
Elsevier Science Publishers B.V., Amsterdam

CHROM. 22 822

Isotachophoresis as an on-line concentration pretreatment technique in capillary electrophoresis

D. S. STEGEHUIS, H. IRTH, U. R. TJADEN* and J. VAN DER GREEF

Center for Bio-Pharmaceutical Sciences, Division of Analytical Chemistry, University of Leiden, P.O. Box 9502, 2300 RA Leiden (The Netherlands)

(First received July 4th, 1990; revised manuscript received September 14th, 1990)

ABSTRACT

One of the major disadvantages of capillary electrophoresis (CE) is its limited loadability. Therefore, the on-line coupling of isotachophoresis (ITP) and CE was studied with regard to its potential for the improvement of the minimum concentration that can be measured by CE. Based on the concentrating and separating power of ITP, detection limits could be lowered by at least two orders of magnitude. Especially for biological samples containing proteins, it appeared that in non-treated capillaries the electromigration characteristics are hardly influenced when isotachophoretic pretreatment is applied. The potential of ITP–CE coupling is illustrated by the analysis of *o*-phthaldialdehyde and fluorescein isothiocyanate derivatives of a number of amino acids.

INTRODUCTION

Capillary electrophoresis (CE) is a highly efficient miniaturized separation technique with remarkable resolving power. The technique is based on differences in electrophoretic mobilities. Typical capillary dimensions are between 20 and 100 μm in diameter and a length of 50–100 cm, resulting in a volume of a few microlitres. As a consequence, the loadability of the system is limited to injection volumes of 1–30 nl. This poor loadability is a severe drawback in CE and puts high demands on the detection. Although impressive detection limits in the (sub)attomole range [1–6] have been reported, the corresponding measurable sample concentrations are still too high (10^{-7}–10^{-6} mol/l) to allow trace-level determinations of, *e.g.*, drugs in plasma.

Another limitation of CE is the poor performance in the analysis of complex biological matrices. For bioanalysis based on CE, a sample pretreatment for concentration and isolation of the analyte is essential. Isotachophoresis (ITP) is a capillary separation technique also based on the differences in electrophoretic mobilities [7–9], but this technique has the advantage of much higher loadability, *e.g.*, microlitres instead of nanolitres in CE. In addition, ITP is a concentration technique for trace components and a dilution technique for major constituents of the sample. The combination of these features makes ITP in principle an ideal technique for sample treatment. The use of ITP for sample pretreatment in CE has already been described [10–14]. Especially the extended study of Kaniansky and Marak [10] gives

0021-9673/91/$03.50

a good impression of the potential of combined ITP–CE. The diameters used in their study were 300 μm for both ITP and the CE capillary. Although, owing to the heat generation in the capillary, such large diameters are in principle not favourable in CE, the results achieved were impressive.

In contrast to the previous techniques [10–14] in which the ITP preconcentration and CE separation were performed in capillaries with identical dimensions, we have developed a coupled system which involves two separate capillaries with optimum dimensions for each process. Using this approach it is easier to use smaller diameters for the CE capillary allowing higher voltages without disturbing the plug flow of electroosmosis.

The degree of the concentration effect of ITP can be derived [15] from the Kohlrausch equation:

$$C_L/C_A = [\mu_L/(\mu_L + \mu_R)][(\mu_A + \mu_R)/\mu_A] \quad (1)$$

where C_L is the molarity of the leading buffer, C_A the analyte concentration and μ the electrophoretic mobility (the subscript R refers to the counter ion). From this equation it can be seen that the final concentration of the analyte is proportional to the molarity of the leading buffer. Thus the equation can be written as

$$C_A = C_L K \quad (1a)$$

where K is a proportionality factor. In the case of similar mobilities, K will have a value of about 1. Eqn. 1a clearly demonstrates the tremendous concentration potential of ITP. The result of the ITP process is that major components are diluted but also, much more important, that trace compounds are concentrated.

In this paper, the coupling of an ITP system with a CE system enabling the determination of level concentrations that cannot be determined by direct injection in CE is described.

EXPERIMENTAL

Materials

Sodium borate and barium hydroxide were purchased from Merck (Darmstadt, F.R.G.). N-(2-acetamido)-2-aminoethanesulphonic acid (ACES) from Serva (Heidelberg, F.R.G.), aspartic acid (Asp), glutamic acid (Glu), glycine (Gly), histidine (His), threonine (Thr), alanine (Ala), valine (Val), lysine (Lys), arginine (Arg), fluorescein isothiocyanate (FITC) and *o*-phthaldialdehyde (OPA) from Aldrich (Steinheim, F.R.G.) and mercaptoethanol from Fluka (Buchs, Switzerland). The OPA reagent was a mixture of 100 mg of OPA, 100 μl of mercaptoethanol and 10 ml of borate buffer (5 mmol/l, pH 9.5) and was made freshly every day.

Equipment

The ITP system was a commercial system (Isotachophor; LKB, Bromma, Sweden). The fused-silica capillary used for CE was obtained from SGE (North Melbourne, Australia). The UV detector used for the detection of the OPA derivatives in CE was a variable-wavelength instrument (Spectroflow 757; Kratos, Ramsey, NJ,

U.S.A.), equipped with a laboratory-made on-capillary detection cell with a volume of 8 nl. Detection of the FITC derivatives was based on laser-induced fluorescence (LIF) using an air-cooled argon-ion laser (Model 161 C; Spectra Physics, San Jose, CA, U.S.A.) lasing at 488 nm.

A 100-kV power supply was used for both ITP and CE (Gamma, Model RR 100–1.5 P; High Voltage Research, Coimex, Hattem, The Netherlands). Electropherograms were registered on a flat-bed recorder (Model 40; Kipp & Zonen, Delft, The Netherlands).

Coupling of ITP and CE

The ITP system was modified by inserting a fused-silica capillary into the ITP PTFE capillary as close as possible to the UV cell. In this way the ITP system is hardly influenced by the coupling to CE. Also, the CE part of the coupled system continues to perform like a separate CE system. The only difference for the CE system is that the electrode of the leading electrolyte buffer vial of the ITP system, which is connected with earth, is acting as the CE anode (Fig. 1). For such a set-up a reversible power supply is advantageous.

Isotachophoresis

In the ITP sample pretreatment mode, 5 mmol/l borate buffer (pH 9.5) was used as the leading buffer and 5 mmol/l ACES (pH 10.0) as the terminating buffer. The ACES buffer was adjusted to pH 10 with barium hydroxide to avoid interference from carbonate from the air because of the alkaline pH. After thorough cleaning of the system by rinsing with sodium hydroxide, hydrochloric acid and ethanol, samples of 1–50 μl can be injected into the ITP system with a 100-μl injection syringe. A voltage of about 8 kV was applied over the capillary (61 cm × 500 μm I.D.). ITP was stopped when the zone of interest reached the detector.

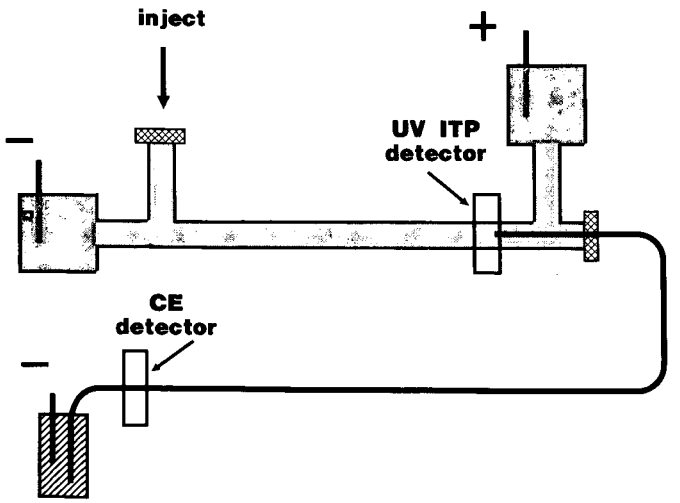

Fig. 1. Scheme of coupled ITP–CE system.

Injection into capillary electrophoresis system

Injection into the CE system was effected by electrokinetic injection, positive displacement injection or by a combination of both techniques depending on the concentration and the number of analytes.

Electrokinetic injection

After a sample zone has reached the beginning of the CE capillary, the high voltage of the ITP system is switched off. Then the power supply of the CE system is switched on for 5 s at 5 kV, whereafter the ITP capillary is flushed with the leading buffer in the direction of the ITP injection port. This is done by sucking with an injection syringe through the ITP injection port. The high voltage is raised to the running voltage of 25 kV during the cleaning in order to prevent back-migration of the analytes.

Positive displacement injection

After the compounds of interest have reached the beginning of the CE capillary, a few microlitres of the terminating buffer are injected into the ITP system. This causes a positive displacement of the sample zones passing the entrance of the CE capillary, During flushing of the ITP capillary the high voltage is switched on in order to prevent back-migration as described for electrokinetic injection.

Capillary electrophoresis

After the injection is completed the electrophoretic run is started, applying 25 kV over the 75 cm × 50 μm I.D. capillary. The electrophoresis is performed in a continuous buffer system using the leading buffer of the ITP system.

o-Phthaldialdehyde derivatization

From a mixture of amino acids containing Asp, Glu, Gly, His, Thr, Ala, Val, Lys and Arg, several dilutions were made, varying from 10 μg/ml to 1 mg/ml. To 100 μl of these dilutions, 100 μl of OPA reagent were added, then the mixture was vortex mixed for 3 s and immediately injected. The serum samples that were analysed were derivatized without any prior sample pretreatment. Volumes of 100 μl of serum were mixed with 100 μl of borate buffer (pH 9.5, 0.02 mol/l) and 100 μl of OPA reagent. The extra borate buffer was added to compensate for the strong buffer capacity of the serum.

Fluorescein isothiocyanate derivatization

To 50 μl of a Phe solution with a concentration of 5 μg/ml, 100 μl of FITC solution (1 mg/ml) in borate buffer (0.01 mol/l, pH 9.5) were added. The derivatization mixture was allowed to stand for overnight in order to complete the reaction.

RESULTS AND DISCUSSION

Fig. 1 shows the scheme of the coupled ITP–CE system. The fused-silica CE capillary was inserted into the ITP capillary as close as possible to the detector cell without affecting the optical path. This can easily be seen during insertion by observing the baseline of the UV detector. It should be realized that, by inserting an open CE

capillary, the possibility of hydrodynamic flow and thus during ITP a real electroosmotic flow has been created. This can be circumvented by the use of a CE capillary with an inside diameter such that the ratio of the diameters of the ITP and CE capillary is at least 10. Care should be taken that no hydrodynamic forces caused by differences in liquid levels will initiate a flow in the capillaries. Using an ITP PTFE capillary of I.D. 500 μm and an CE fused-silica capillary of I.D. 50 μm, it appeared that the electroosmotic flow through the CE capillary during the ITP run can be neglected.

Apparently this manner of coupling results in an inflexible system, but in practice it appeared to improve the reliability of the complete system considerably. Injections into the CE system are done without moving the CE capillary, a buffer vial or a sample vial. Only the buffer or the sample itself is flushed through the system while the capillaries remain in a constant configuration with respect to each other.

Two modes of injection are predominantly used in CE, *viz.*, hydrodynamic and electrokinetic injection. Positive displacement injection is in fact a hydrodynamic mode of injection by the displacement of a well defined liquid volume. The reproducibility, characterized by the relative standard deviation (R.S.D.), was 4.2% (n = 5), which is superior to that of electrokinetic injection with an R.S.D. of 7.6% (n = 5). The reproducibility of electrokinetic injection is also significantly improved, because all injections are made from an environment of constant molarity resulting from the ITP process.

In practice, it appeared that a combination of electrokinetic injection and positive displacement offers the best performance. In fact, most of the time both methods are used in combination because by inserting the syringe into the ITP system in order to flush the ITP system, a small displacement injection is made. In principle this is the minimum injection that always has to be made. This volume can be increased by either injecting some buffer to increase the displacement or by doing an electrokinetic injection.

In order to study the characteristics of the ITP system, OPA derivatives of different amino acids were used as test compounds. In Fig. 2 the isotachopherogram of

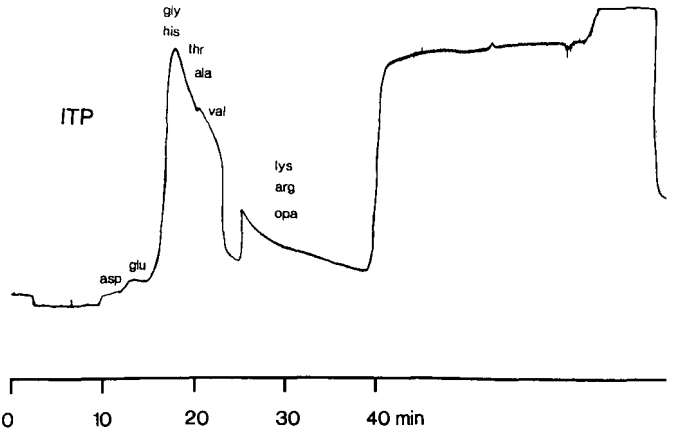

Fig. 2. Isotachopherogram of a test mixture of OPA-derivatized amino acids. Injection: 25 μl of an amino acid mixture with each amino acid at a concentration of about 1 ng/ml Applied voltage: 8 kV. Detection: UV absorbance at 254 nm. For other conditions, see text.

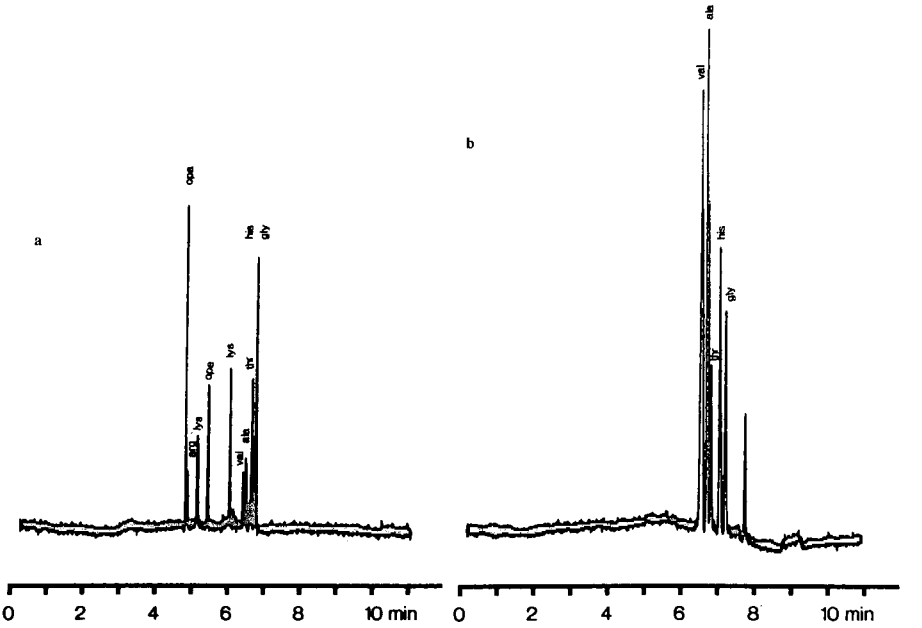

Fig. 3. (a) Single capillary electropherogram of some OPA-derivatized amino acids. Electrokinetic injection (5 kV, 5 s) of a test mixture with each amino acid at a concentration of about 100 ng/ml. Applied voltage: 25 kV. Detection: UV absorbance at 234 nm. For other conditions, see text. (b) Coupled ITP–CE of OPA-derivatized amino acids. ITP injection: 25 ml of a test mixture with each amino acid at the concentration of about 1 ng/ml. Injection in CE electrokinetic (5 kV, 5 s). Applied voltage: in ITP 8 kV and in CE 25 kV. For other conditions, see text.

such a mixture is depicted. Amino acids with an extra amino group, *e.g.*, Arg and Lys, migrate much more slowly than the other acids, probably because at the pH chosen these acids have electrophoretic mobilities that are even slower than the terminating buffer, implying that migration is not based on ITP but on CE, as recently suggested by Beckers and Everaerts [16]. From the time scale, it can be concluded that the ITP run is time consuming, which is caused by the length of the applied capillary and the molarity of the buffers. It must be emphasized that the time window in which the amino acids occur corresponds to an extremely small volume. Starting with amino acid concentrations of 10 μmol/l and applying a leading buffer of 10 mmol/l, in principle ITP will result in an effective volume reduction of a factor of 1000. With an applied injection volume of 25 μl this means that each component will have a volume of about 25 nl. On the other hand, this also explains the limited quality of the ITP trace, as the detection volume is large in comparison with the small zones. Owing to these small dimensions it is possible to inject the complete mixture of all components into the CE system, although of course a split injection is made. The splitting ratio is determined by the ratio of the cross-sectional areas of the ITP capillary and the CE capillary.

The following calculation illustrates the concentration effect of the total system, including the split during injection into the CE capillary. According to eqn. 1, ITP of an analyte solution (1 μmol/l) in a leading buffer concentration of 5 mmol/l results in

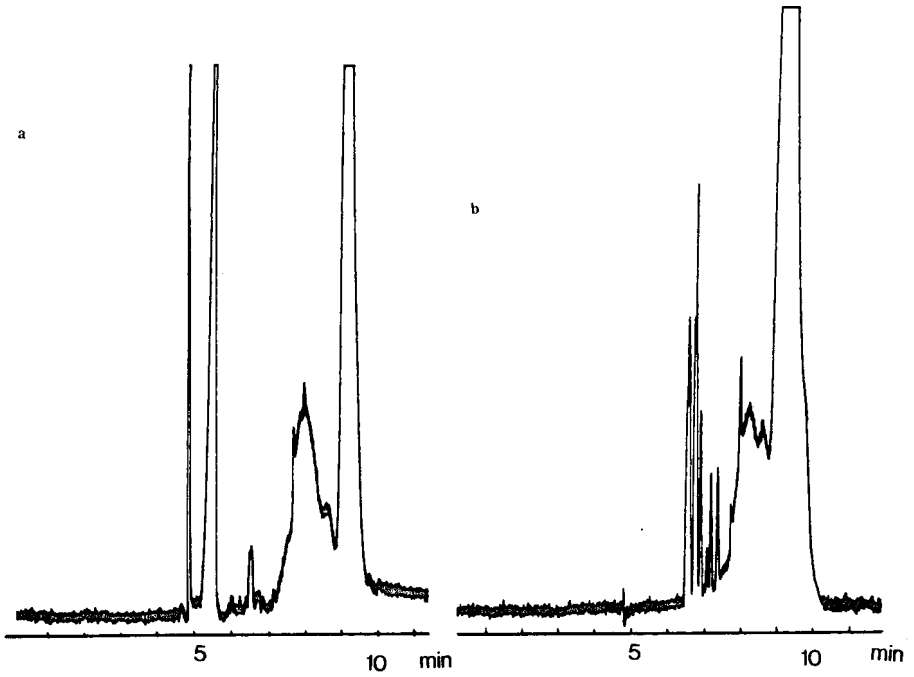

Fig. 4. (a) Single capillary electropherogram of an OPA-derivatized sample of serum spiked with some amino acids. Electrokinetic injection (5 kV, 5 s). Applied voltage: 25 kV. Detection: UV absorbance at 234 nm. For other conditions, see text. (b) Coupled ITP–CE of an OPA-derivatized sample of serum spiked with some amino acids. ITP injection: 25 μl of derivatized serum. Injection in CE: electrokinetic (5 kV, 5 s). For other conditions, see text.

a concentration factor of about 5000. A 50-μl injection will result in a zone of 10 nl with a concentration of about 5 mmol/l.

Because of the differences in the I.D. of the two capillaries, a split is made of 1:100, so an absolute volume of 100 pl is injected with a concentration of about 5 mmol/l. In single CE an injection of about 500 nl has to be made to obtain precisely the same amount injected, which will totally overload the system and will make analysis nearly impossible. These aspects of ITP–CE are illustrated in Figs. 3 and 4. Fig. 3a shows the electropherogram of a mixture of a number of amino acids derivatized with OPA, as obtained with single CE, and Fig. 3b is the result of the coupled ITP–CE system. These two figures clearly demonstrate the concentration effect of ITP, as almost no signal can be observed in single CE, whereas the peaks in the ITP–CE run can be quantified easily.

Fig. 4a shows the electropherogram of a serum sample spiked with OPA derivatives of amino acids. Owing to the instability of such derivatives, serum was spiked with relatively high concentrations (0.01–0.1 mmol/l). As the ITP process demands nearly 40 min, endogenous levels of the amino acids (0.01–0.7 mmol/l) could hardly be detected after derivatization with OPA, because the degradation of low concentrations is faster than that of high concentrations. As it was not the intention to develop an amino acid assay for serum samples, but only to explore the potential of this

combined technique, we accepted the spiking of the amino acids in serum. It can be seen from Fig. 4a that in CE analysis the ratio between the rapidly migrating amino acids and the slower serum constituents migrating as an unresolved peak is unfavourable with regard to amino acid analysis. Low concentrations will be affected considerably by this unresolved peak. However, in the coupled system it appears that this ratio has been improved considerably, as can be seen in Fig. 4b. The amino acids have been concentrated by a factor of at least 100, whereas the total amount of the other serum constituents is about the same as in single CE. In fact, the trace amounts of the amino acids have been concentrated while the major components have been diluted, thus enhancing the selctivity of the total system. This example shows the selectivity of the coupled method clearly.

Although in this configuration, with the CE capillary inserted in the ITP capillary, only a small fraction of an ITP zone is transferred to the CE capillary, it must be realized that by applying a concentration-sensitive detector (UV absorbance and fluorescence in this study) the full benefit of ITP concentration of an analyte will be obtained, in combination with favourable CE diameters allowing high voltages. Only in those instances where a mass flow-sensitive detector (*e.g.*, mass spectrometer) is applied will this splitting procedure result in corresponding lower signals.

Quantitative aspects

To demonstrate the quantitative aspects of the method, a calibration plot was constructed. Because the stability of the OPA derivatives is limited we chose FITC derivatives that have fluorescence characteristics that are almost perfectly compatible with the 488-nm lasing line of the argon-ion laser. Fig. 5 shows the electropherograms obtained by single CE and ITP–CE. Although a mixture of only four amino acids was derivatized, many degradation peaks can be observed, hampering trace analysis [17].

A calibration graph was constructed by analysing dilutions of the FITC derivative of Phe at concentrations ranging from 3.5 to 350 μmol/l. In CE the analyte was introduced by electrokinetic injection at 5 kV for 5 s. The correlation coefficient was 0.9999 and the function of the curve was $y = (0.569 \pm 0.004)x + (-1.054 \pm 0.513)$. Another series of dilutions were made ranging from 0.175 to 35.0 μmol/l. From these dilutions a calibration graph was made using on-line ITP as sample pretreatment. The correlation coefficient of this curve was 0.999 and the function of the curve was $y = (-11.15 \pm 0.14)x + (2.52 \pm 1.79)$. The calibration graphs demonstrate that the coupled system can be used quantitatively in a concentration range lower than the minimum detectable amount in separate CE.

Limitations

For optimum injection into the CE system, the ITP zone has to be detected in the ITP system preferably in an identifying way, as matrix compounds can influence the retention time of the various zones. Of course, this is a limitation of ITP. On the other hand, it must be realized that ITP is a concentration technique for trace components, whereas CE for each compound is a dilution technique comparable to chromatography. This implies that by application of similar detection systems, observation of a compound in ITP is not guarantee that this compound will also be observed in CE. When the zone length is smaller than the aperture of the detector cell in the ITP capillary, such a zone will be difficult to detect. In such an event the use of additives functioning as a marker or even as a spacer will be helpful.

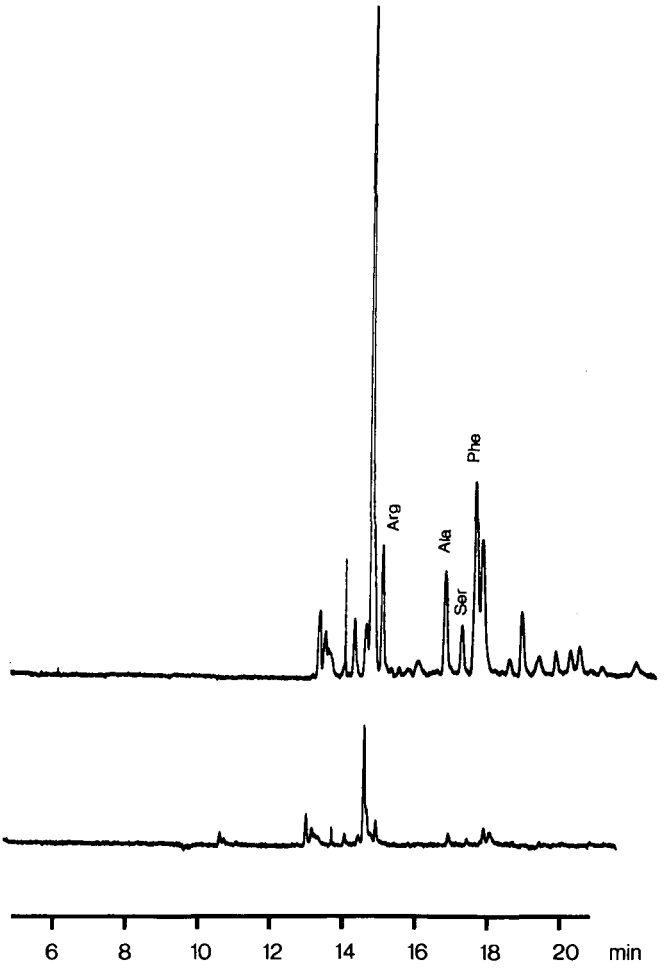

Fig. 5. Electropherograms of an FITC derivatization mixture of some amino acids. Lower trace: single CE. Conditions: electrokinetic injection (5 kV, 5 s) of 10 mmol amino acid–FITC derivative mixture. Applied voltage: 25 kV. Upper trace: coupled ITP–CE. Conditions: ITP injection, 25 μl of derivatization mixture, followed by CE electrokinetic injection (5 kV, 5 s). Applied voltage: in ITP 10 kV and in CE 25 kV. Detection: laser-induced fluorescence at 488/514 nm.

Fig. 3 shows that not all amino acids present in a single CE run also appear in a coupled ITP–CE run. An explanation can be derived from the isotachopherogram of the single ITP system given in Fig. 2. The order of migration is exactly the opposite of that in CE. This is caused by the fact that in ITP the analytes migrate towards the anode and in CE towards the cathode. An injection from the beginning of the sample therefore does not include the less mobile ions.

Another limitation of coupled ITP–CE is that a compromise has to be made between the optimum buffer system for the ITP system and for the CE system. In the combined method one buffer initially acts as a leading buffer in ITP and finally acts as a supporting buffer in CE. For the separation of derivatized amino acids a better

resolution can be obtained when a higher concentration of borate buffer can be used in CE. However, when borate buffers with concentrations higher than 5 mmol/l are used in ITP the heat generation becomes problematic and the analysis times will be long. In the ITP system the use of Tris buffers results in good performance, but is disappointing in the CE system. As a consequence, a buffer has to be chosen that works acceptably in both systems, which is usually not the best buffer for either system.

CONCLUSIONS

ITP can be combined with CE resulting in a gain in sensitivity of at least a factor 100, which is merely limited by the equipment applied such as the detector in the ITP system. The additional selectivity of the coupled ITP–CE system gave promising results concerning the problems of CE with biological matrices.

A limitation of the coupled system is that a compromise has to be made concerning the buffer system that is used in the overall system between analysis time and resolution in both the ITP and the CE stages.

REFERENCES

1 J. W. Jorgenson and L. K. Lukas, *Anal. Chem.*, 53 (1981) 1298.
2 A. S. Cohen and B. L. Karger, *J. Chromatogr.*, 397 (1987) 409.
3 J. H. Knox and K. A. McCormack, *J. Liq. Chromatogr.*, 12 (1989) 2435.
4 S. E. Moring, J. C. Colburn, P. D. Grossman and H. H. Lauer, *LC · GC*, 8 (1990) 34.
5 B. W. Wright, G. A. Ross and R. D. Smith, *J. Microcol. Sep.*, 1 (1989) 85.
6 J. Lui, F. Banks, Jr., and M. Novotny, *J. Microcol. Sep.*, 1 (1989) 136.
7 L. Krivankova, F. Foret, P. Gebauer and P. Boček, *J. Chromatogr.*, 390 (1987) 3.
8 J. Pospichal, P. Gebauer and P. Boček, *Chem. Rev.*, 89 (1989) 419.
9 Th. P. E. M. Verheggen, A. C. Schoots and F. M. Everaerts, *J. Chromatogr.*, 503 (1989) 245.
10 D. Kaniansky and J. Marak, *J. Chromatogr.*, 498 (1990) 191.
11 V. Dolnik, M. Deml and P. Boček, *J. Chromatogr.*, 320 (1985) 89.
12 S. Hjertén, K. Elenbring, F. Kilar, J. L. Liao, A. J. C. Chen, C. J. Siebert and M. D. Zhu, *J. Chromatogr.*, 403 (1987) 47.
13 V. Dolnik, K. A. Cobb and M. Novotny, *J. Microcol. Sep.*, 2 (1990) 127.
14 H. R. Udseth, J. A. Loo and R. D. Smith, *Anal. Chem.*, 61 (1989) 228.
15 J. C. Reijenga, *Thesis*, Eindhoven, 1984.
16 J. L. Beckers and F. M. Everaerts, *J. Chromatogr.*, 508 (1990) 3.
17 C. M. B. van der Beld, U. R. Tjaden, N. J. Reinhoud, D. S. Stegehuis and J. van der Greef, *J. Controlled Release*, 13 (1990) 129.

Journal of Chromatography, 538 (1991) 403–411
Elsevier Science Publishers B.V., Amsterdam

CHROM. 22 820

Isotachophoretic analyser equipped with a scanning ultraviolet photometric detection system

TAKESHI HIROKAWA*, YASURO YOKOTA[a] and YOSHIYUKI KISO
Applied Physics and Chemistry, Faculty of Engineering, Hiroshima University, Kagamiyama 1, Higashi-hiroshima 724 (Japan)
(Received August 14th, 1990)

ABSTRACT

An istoachophoretic analyser with a scanning ultraviolet (UV) photometric detection system was constructed in order to study separation processes. A fused-silica capillary (I.D. 0.53 mm, O.D. 0.66 mm) was scanned over a length of 32 cm with an assembly of a UV lamp and a detector. The assembly was driven by a linear head with a stepping motor. One scanning cycle took 7.027 s and 5333 photometric signals (a UV position spectrum) were acquired. The practical resolution was 0.15 mm. The detection limit of picric acid was 20 pmol. Using the apparatus, the separation of a four-component mixture (SPADNS, monochloroacetic acid, picric acid and acetic acid) was studied using different electrolyte systems and the effect of the pH of leading electrolyte on the separation efficiency is briefly discussed.

INTRODUCTION

One of the important features of capillary isotachophoresis is that computer simulation of several characteristics of sample zones may afford practical guidelines for the optimization of the separation conditions. We are constructing a computer-aided separation-optimizing system utilizing these features. The system is based on the computer simulation of the steady state and the transient state. Especially the determination of dynamic features of the separation such as resolution time depends on the transient state simulation. However, the transient state has not yet been fully clarified, as is apparent from the fact that an analytical method for a three-component sample was reported only very recently [1]. Therefore, in order to improve the reliability of the simulation, the separation process of samples with various components should be observed and compared with the simulated results. In order to observe the separation process, two detection systems may be suitable, a multi-channel detection system, where many detectors are set along a separation tube, and a scanning detection system.

In a previous paper, an isotachophoretic analyser with a multi-channel UV

[a] Present address: Mitsubishi Paper Mills Ltd., Tsukuba Research Laboratory, Wadai 46, Tsukuba, Ibaraki, Japan.

0021-9673/91/$03.50

detection system was reported [2]. By analysing the electropherograms observed, the velocities of the boundaries of transient mixed zones were measured accurately and were compared with theoretical results to confirm a physical model for the isotachophoretic separation of a three-component system [1,3]. However, the detection system suffered from two practical problems: the separation tube used (16.6 cm) was not long enough to observe the separation process of a complex sample system, which needed a relatively long capillary for separation, and the apparent sensitivity and signal-to-noise ratio of each cell differed significantly owing to the different UV intensities at each cell, because only two deuterium lamps were used as the UV source and the radiation from a lamp was delivered to sixteen photocells using quartz optical fibres. To avoid these problems, a scanning system was selected.

A scanning detection system for measuring the profiles of electric field distribution along the migration direction has been developed by Schumacher and co-workers [4–6]. However we avoided measuring the profiles, as the use of complicated electric circuits was inevitable for isolating potential gradient detector signals from high migration voltages. Considering this point, a scanning UV detector with a detector–amplifier pair was designed and constructed, which enabled a fused-silica capillary to be scanned over a length of 32 cm. This paper describes the design and efficiency of this system in comparison with the previous multi-channel system [2]. A typical performance was demonstrated by the separation of 4,5-dihydroxy-3-(*p*-sulphophenylazo)-2,7-naphthalenedisulphonic acid (SPADNS), monochloroacetic acid, picric acid and acetic acid using several leading electrolytes with different pH values.

EXPERIMENTAL

Apparatus

Fig. 1 shows a schematic diagram of the isotachophoretic analyser with a scanning UV photometric detection system. LE and TE in Fig. 1 are the leading and the terminating electrode compartment, respectively, where the migration current was applied; L and T are the reservoirs for the leading and terminating electrolyte, respectively. Sample solution was injected at the injection port of the sampling valve (SV in Fig. 1). The sample was separated in a fused-silica capillary separation tube (FS). The migration process over a 32-cm capillary length was monitored by a scanning UV detector (DET).

A linear head (LH) equipped with a pulse motor (PM) (Model UPH566LB3-A; Oriental Motor, Tokyo, Japan) was used for repeatitive scanning. An assembly of the detector and a UV source (UVS) was attached to the linear head. The movement of the linear head was accurately controlled by the use of a microcomputer (Model PC-9801 VX21, 80286–80287, clock 12 MHz; NEC, Tokyo, Japan) equipped with an interface board for the pulse motor [PMC-1C(98); Contec, Tokyo, Japan]. One electric pulse corresponded to a 0.72° rotation of the pulse motor, while the linear head moved by 0.02 mm. Therefore, 16 000 pulses should be sent to the pulse motor in order to scan the 32-cm capillary.

The fused-silica capillary (FS) used as a separation tube was obtained from Gasukuro Kogyo (Tokyo, Japan). The inner surface was not chemically modified. The original I.D. and O.D. were 0.53 and 0.75 mm, respectively. The polyimide coating of the fused-silica capillary was removed by burning it out in order to make

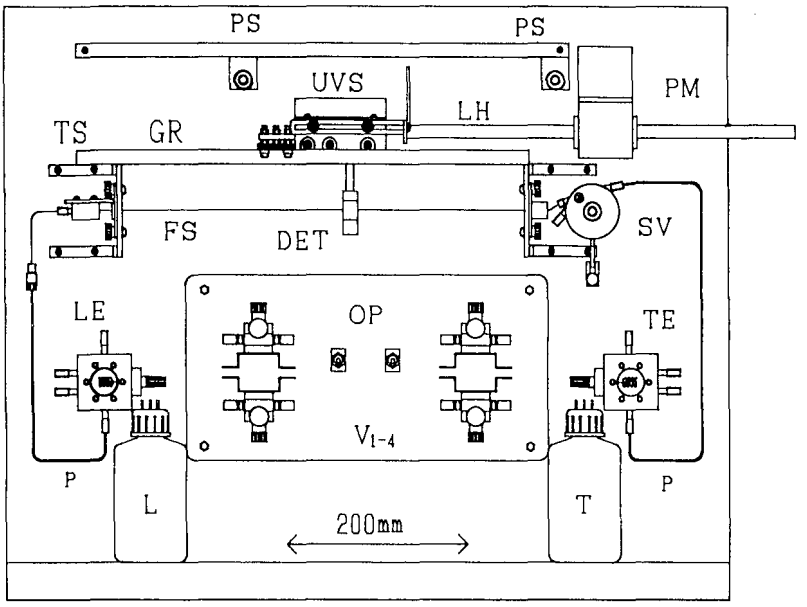

Fig. 1. Schematic diagram of isotachophoretic analyser equipped with a scanning UV photometric detection system. PM = Pulse motor; LH = linear head; UVS = UV source (deuterium lamp); DET = UV detector; FS = separation tube, fused-silica capillary (I.D. 0.53 mm, O.D. 0.66 mm); PS = position sensors; TS = tensioner for the silica capillary; SV = sample injection valve; GR = guide rail for detector assembly; LE = leading electrode compartment; TE = terminating electrode compartment; L and T = leading and terminating electrolyte reservoirs; P = PTFE tube; V_{1-4} = valves to fill or to drain the electrolytes; OP = operation board.

the capillary UV transparent. The O.D. was reduced to 0.66 mm by this treatment. The length of the capillary used was 40 cm and it was joined with PTFE tubes of O.D. 1.0 mm and I.D. 0.5 mm (P).

The silica capillary penetrated a 0.8 mm hole in the PTFE cylindrical block (O.D. 5 mm, length 15 mm) of the scanning UV detector. As the clearance between the capillary and the hole was small and the capillary without a coating was very fragile, slight vertical motion of the scanning detector caused to break it off. The important conditions for smooth scanning were as follows: a guide rail (GR) was used to support the detector assembly, ensuring straight movement of the assembly; and the silica capillary was kept tightened and the tension was adjusted at the end of the capillary by using a simple device (TS).

The UV source was a Hamamatsu deuterium lamp (Model L1626), which was driven by a power supply from a Hamamatsu Model C1518. The UV radiation from the lamp was led to the silica capillary through a short quartz optical fibre after passing through a glass filter (Toshiba Glass, Tokyo, Japan, Model D33S, λ_{max} = 330 nm). The radiation was divided into two paths, one being used for the photometric measurement and the other as the reference signal. The core and cladding diameters of the fibres used were 0.8 and 1.1 mm, respectively. The transmitted UV radiation was led to short-cut optical fibres (*ca.* 10 mm long) which was plugged into the cell.

The fibres acted like an optical slit. At the end of the fibres, a detection element was placed (Hamamatsu Model S1227-16BQ silicone photodiode). The output was connected to a differential amplifier using two LF356N operational amplifiers.

Except for the scanning device, this system had a standard construction. V_{1-4} on an operational board (OP) are valves for rinsing the separation capillary (FS) and filling the electrode compartments (LE and TE). Unless noted otherwise, the main parts used were those of a Shimadzu, (Kyoto, Japan) isotachophoretic analyser (Model IP-1B). The power supply was also that of the IP-1B.

Scanning mode

A single cycle to scan the separation tube and acquire photometric signals took 7.027 s. The speed of the linear head was set constant for the forward and the backward movement. The initial position of the head was set at the nearest position to the sampling valve (SV). An assembly of a small lamp and a photodiode was utilized as a position sensor (PS) in order to determine the initial position exactly. This sensor was also useful for preventing the overshooting of the linear head. The length of the separation tube from the injection port to the initial position of the head was 11.8 cm.

Data acquisition was successively effected during the forward movement (from the terminating side to the leading side) through an analogue-to-digital (A/D) converter. During the backward movement to the initial position, the data were stored in the 3-MB random access memory (a RAM disk system) of the microcomputer. The use of the RAM disk system was necessary in order to treat a large number of data quickly. A/D conversion of the UV signal was made every three electric pulses for the stepping motor. Therefore, the number of the data acquired in a single scan was 5333 (= 16 000/3) and one datum corresponded to 0.06 mm of the separation tube. The resolution was sufficient to obtain the exact position of the boundaries, although a minor correction should be adopted considering that there was a time delay of *ca.* 3.5 s between the first and the last data in a scan.

The scanning and data acquisition were repeated, for example, 200 times or more. After the acquisition was completed, the data in the RAM disk were transferred to a hard disk (80 MB). The data were analysed to obtain the boundary velocities as discussed below. Usually not all of the acquired data were necessary for the evaluation of the boundary velocities.

Samples

The samples were SPADNS, monochloroacetic acid (MCA), picric acid (PIC) and acetic acid (AC). SPADNS and PIC absorb visible and UV radiation. The sodium salt of SPADNS was purchased from Dojin (Kitakyusyu, Japan) in the purest form. The others (extra-pure grade) were obtained from Tokyo Kasei (Tokyo, Japan). Stock sample solutions (*ca.* 10 m*M*) were prepared by dissolution in distilled water without further purification. The sample solution was injected into the terminating electrolyte near the boundary between the leading and the terminating electrolytes.

Operational electrolyte system

The leading electrolyte was 5 m*M* hydrochloric acid. The pH of the leading electrolyte (pH_L) was adjusted to 3.6, 4.4, 4.8 and 6.0 by adding β-alanine, ε-amino-

caproic acid, creatinine and histidine, respectively. The pH measurements were carried using a Horiba (Tokyo, Japan) Model F7ss expanded pH meter.

The terminator was 10 m*M* caproic acid or N-morpholinoethanesulphonic acid (MES). The former was combined with leading electrolyte of pH_L 3.6 and the latter was used with those of pH_L 4.4, 4.8 and 6.0.

Hydroxypropylcellulose (HPC) (0.1%) from Tokyo Kasei was added to the leading and terminating electrolytes to suppress electroendosmosis, which was not negligible in a fused-silica capillary. According to the manufacturer, the viscosity of the 2% aqueous solution is 1000–4000 cP at 20°C. The apparatus was set in a thermostated room and the temperature near the detector was kept at 25 ± 1°C.

RESULTS AND DISCUSSION

Resolution and reproducibility

After inserting a copper wire (O.D. 0.3 mm) into the silica capillary, the capillary was scanned repeatedly and the position spectrum was acquired in order to check the reproducibility. The spectrum was differentiated numerically against the number of data in the scan. Then the numbers expressing the peak position in each scan were compared with each other. No drift was observed, confirming the high stability and reproducibility of the detection system.

The differential peaks had a half-width of 2.5 data (7.5 electric pulses for the stepping motor), which means the edge of the wire was detected with a resolution of 0.15 mm (= 0.02 mm × 7.5). The resolution obtained was sufficient for our purposes. The resolution was checked similarly for an actually migrating sample zone and a similar resolution was obtained.

The accuracy of the stepping distance of the linear head used was checked by measuring repeatedly the data numbers for a copper wire 150.0 mm in length. The number of data between two differential peaks was 2487 with no drift. Apparently

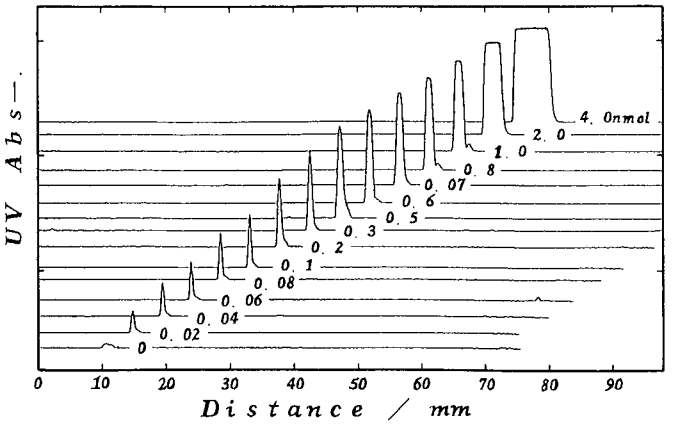

Fig. 2. Detection limit of picric acid by use of the scanning UV photometric detector (20 pmol–4.0 nmol). The leading ion was 5 mM hydrochloric acid (pH 3.6, buffer = β-alanine). The terminator was 10 m*M* caproic acid. The migration current was 49.5 μA. The I.D. of the separation tube (fused-silica capillary) was 0.53 mm.

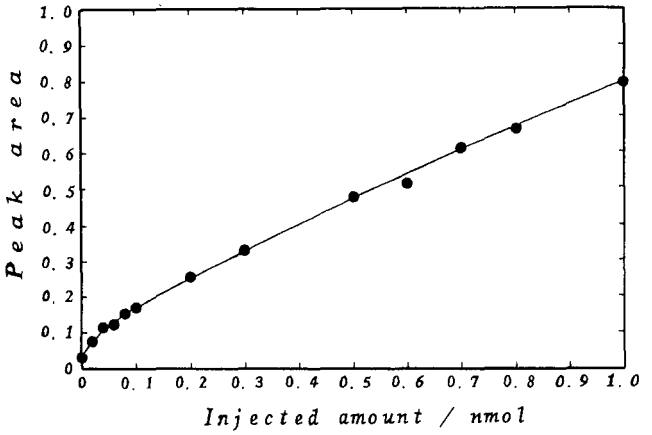

Fig. 3. UV peak area in arbitrary units *vs.* sample amount of picric acid. The sample amount was varied from 0 to 1 nmol. Operational system as in Fig. 2.

from this observation, one datum (three electric pulses) correspond to 0.0603 mm (= 150/2487), confirming the nominal value of 0.06 mm (= 0.02 mm × 3). Time retardation due to inertia effects was not apparent in our observations where the scanning speed was 100 mm/s.

Sensitivity evaluation and analytical utility

Various amounts of picric acid were separated and detected at pH_L 3.6 in order to determine the practical detection limit of the system. The sample amount was varied in the range 20 pmol–4 nmol. The injected sample concentrations were 0.01,

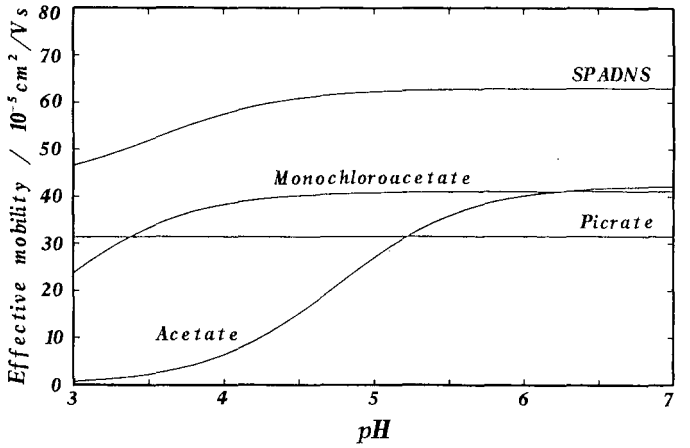

Fig. 4. pH dependence of the effective mobility of SPADNS, monochloroacetic acid, picric acid and acetic acid. Absolute mobility and thermodynamic acid dissociation constant were used. The values were as follows: SPADNS, m_0 = 21 · 10^{-5}, 42 · 10^{-5} and 63 · 10^{-5} and pK_a = −3, −2 and 3.55 (ion-pair formation was assumed for the trivalent anions); monochloroacetic acid, m_0 = 41.1 · 10^{-5} and pK_a = 2.865; picric acid, m_0 = 31.5 · 10^{-5} and pK_a = 0.708; and acetic acid, m_0 = 42.4 · 10^{-5} and pK_a = 4.756.

0.1 and 1 m*M* and the injected sample volume was not less than 2 μl. Fig. 2 shows the observed UV response for the individual sample amounts after the steady state had been achieved. The abscissa is the zone length. The minimum detectable amount was 20 pmol of picric acid, which is comparable to that with the previous system [2] and that reported by Arlinger [7]. The migration current was 49.5 μA.

In a similar manner to the previous work [2], the peak area in arbitrary units was correlated with the sample amount injected. Fig. 3 shows the relationship. Good linearity was found between the peak area and the amount injected in the range 0.1–1 nmol. The gradient of the plots below 0.1 nmol was different from that above 0.1 nmol, where the zone length of picric acid was *ca.* 0.3 mm according to our steady-state simulation.

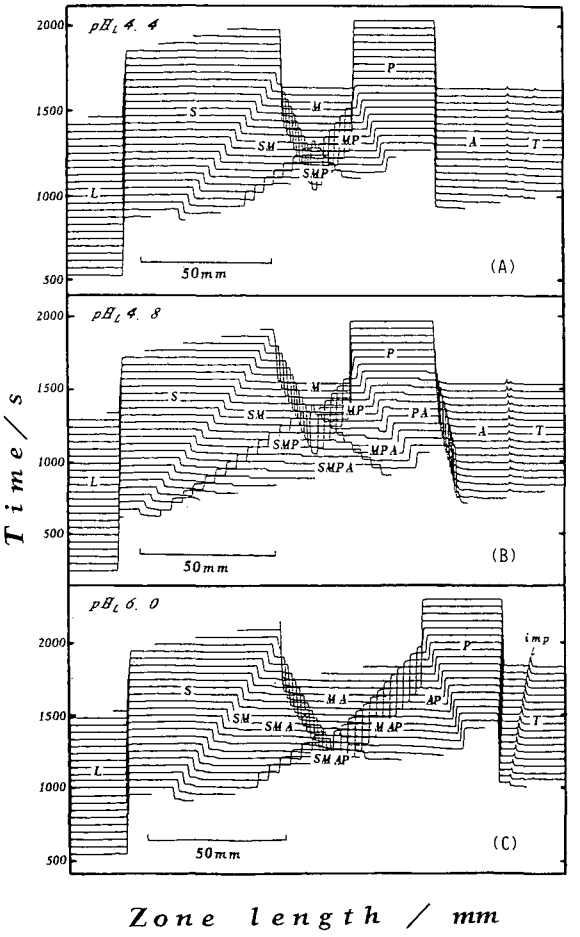

Fig. 5. Transient isotachopherograms of SPADNS, monochloroacetic acid, picric acid and acetic acid obtained by use of the scanning UV photometric detector. The total sample amount was 100 nmol. The leading electrolyte was 5 mM hydrochloric acid. The pH_L was adjusted to (A) 4.4, (B) 4.8 and (C) 6.0 by adding ε-aminocaproic acid, creatinine and histidine, respectively. The terminating electrolyte was 10 m*M* MES. The migration current was 49.5 μA. The I.D. of the separation tube (fused-silica capillary) was 0.53 mm.

Separation of the four-component mixture

Fig. 4 shows the pH dependence of the effective mobility for the components of the treated sample. Under the electrolyte conditions at pH_L 4.4, 4.8 and 6.0, different separation behaviours were expected. It was easily determined from Fig. 4 that the separation order at pH_L 4.4 (SPADNS, MCA, PIC and AC) would be the same with that at pH_L 4.8. However, the separation efficiency of PIC and AC would be higher at pH_L 4.4 than at pH_L 4.8 from the magnitude of the mobility difference. At pH_L 6.0, the migration order would change to SPADNS, MCA, AC and PIC. The separability of MCA and AC would be very low, as is apparent in Fig. 4 from the similar effective mobilities at pH 6.

Fig. 5 shows the observed transient isotacho-pherograms at each pH_L. The total sample amount was the same (100 nmol). The sample volume injected was 10 μl and the pH of the sample solution was adjusted to 3.64 by adding β-alanine. The migration current was 49.5 μA. In Fig. 5, the observed boundaries between the leading and the SPADNS zones were rearranged to the same abscissa position to show clearly the change in the individual zone length at the transient state. Considering that the UV absorption was due to SPADNS and PIC, the concentrations in individual zones were different and all of the width-decreasing zones (triangle form) were transient mixed zones, the different zones found in Fig. 5 were assigned as shown. It should be noted that the total zone length of sample was kept constant during migration and the length was *ca.* 150 mm. At pH_L = 4.4 (Fig. 5A) the SPADNS–MCA–PIC–AC four-component mixed zone (SMPA), the MCA–PIC–AC mixed zone (MPA) and the PIC–AC mixed zone (PA) were not observed, but at pH_L 4.8 (Fig. 5B) all of them were observed, suggesting a low separation efficiency at this pH. At pH_L 6.0 (Fig. 5C), the separation order was different from that in Fig. 5A and B, and no separation was achieved for the MCA–AC mixed zone (MA).

In order to determine the boundary-detected time and subsequently the boundary velocity, the observed UV signals were differentiated with respect to distance (in fact, the number of data in a scan), and the positive and negative peaks of the differentiated signals were searched. Then the distance D and the time t for the Mth datum in the Nth scan were expressed as follows:

$$D = D_{\text{unit}} M \tag{1}$$

$$t = t_{\text{rep}} N + D/V_{\text{scan}} \tag{2}$$

where D_{unit} is the unit length per datum (0.06 mm), t_{rep} is the time needed for one scanning cycle (7.027 s) and V_{scan} is the scanning velocity (100 mm/s). By the use of the time profiles of the boundaries thus obtained, the velocities of the boundaries were obtained by the least-squares method. Table I summarizes the observed resolution time evaluated by solving the boundary equations [2]. The experimental error was less than a few percent. The pH dependence of the separation efficiency is apparent from Table I.

It is concluded that the present apparatus is very useful for the observation of the isotachophoretic transient state of mixtures. This apparatus can be utilized to clarify the factors affecting the separation efficiency, *e.g.*, the number of sample components and the variation of the abundances of components. The results will be reported in due course.

TABLE I

OBSERVED RESOLUTION TIME FOR EQUIMOLAR MIXTURE OF SPADNS, MONOCHLOROACETIC ACID, PICRIC ACID AND ACETIC ACID AT pH 4.4, 4.8 AND 6.0

t_{res} = Resolution time. Zone = mixed zone. S = SPADNS; M = monochloroacetic acid; P = picric acid; A = acetic acid. The leading electrolyte used was 5 m*M* hydrochloric acid and the migration current was 49.5 μA. The sample amount was 25 nmol.

Zone	t_{res} (s)		Zone	t_{res}(s) ($pH_L = 6.0$)
	$pH_L = 4.4$	$pH_L = 4.8$		
SM	1296	1469	SM	1515
MP	1148	1220	MA	–[b]
PA	–[a]	1355	AP	1535
SMP	847	921	SMA	1391
MPA	–[a]	863	MAP	–[c]
SMPA	–[a]	719	SMAP	888

[a] Resolved before starting data acquisition.
[b] Not measured owing to a lack of resolution.
[c] Not measured owing to the unclear boundary.

ACKNOWLEDGEMENT

One of the authors (T.H.) expresses his thanks to the Ministry of Education, Science and Culture of Japan for support of the part of this work under a Grant-in-Aid for Scientific Research (No. 1540482).

REFERENCES

1 T. Hirokawa, K. Nakahara and Y. Kiso, *J. Chromatogr.*, 470 (1989) 21.
2 T. Hirokawa, K. Nakahara and Y. Kiso, *J. Chromatogr.*, 463 (1989) 39.
3 T. Hirokawa, K. Nakahara and Y. Kiso, *J. Chromatogr.*, 463 (1989) 51.
4 E. Schumacher, W. Thormann and D. Arn, in F. M. Everaerts (Editor), *Analytical Isotachophoresis*, Elsevier, Amsterdam, 1981, pp. 33–39.
5 E. Schumacher, D. Arn and W. Thormann, *Electrophoresis*, 4 (1983) 390.
6 W. Thormann, D. Arn and E. Schumacher, *Electrophoresis*, 5 (1984) 323.
7 L. Arlinger, *J. Chromatogr.*, 91 (1974) 785.

Journal of Chromatography, 538 (1991) 413–423
Elsevier Science Publishers B.V., Amsterdam

CHROM. 22 819

Study of isotachophoretic separation behaviour of metal cations by means of particle-induced X-ray emission

I. Separation of twenty metal cations using an acetic acid buffer system and α-hydroxyisobutyric acid complex-forming system

TAKESHI HIROKAWA*, JIAN-YING HU, SHINSUKE EGUCHI, FUMITAKA NISHIYAMA and YOSHIYUKI KISO

Applied Physics and Chemistry, Faculty of Engineering, Hiroshima University, Kagamiyama 1, Higashi-hiroshima 724 (Japan)

(Received August 14th, 1990)

ABSTRACT

Twenty metal ions were separated isotachophoretically and the zones were fractionated and analysed off-line by particle-induced X-ray emission (PIXE). The recovery, migration order and separation efficiency were studied in relation to the use of a complexing agent, α-hydroxyisobutyric acid (HIB). The migration order using the WNH_4Ac system [aqueous solution (W) of NH_4^+ as the leading ion and acetate (Ac) ion as the pH-buffering counter ion, pH = 4.8] was Ba, Sr, Ca, Na, Mg, (Mn, Fe^{II}, Co), Ni, Zn, La, Ce, Cd, Y, Li, Lu, Gd, (Cu, Pb) and ($Zr^{IV}O$, Fe^{III}). The order using the WNH_4Ac–HIB system was Ba, Sr, Ca, Na, Mg, Mn, Fe^{II}, Cd, Co, Li, Ni, Zn, La, Pb, Ce, Gd, Cu, Y, $Zr^{IV}O$, Lu. The recovery of the metal cations was 100% with both electrolyte systems, except for Fe^{II} and $Zr^{IV}O$. The low recovery of $Zr^{IV}O$ was due to hydroxyl complex formation and that of Fe^{II} to hydroxyl complex formation of Fe^{III}, the oxidation product of Fe^{II}. For these ions, the recovery with the WNH_4Ac–HIB system was lower than that with the WNH_4Ac system.

INTRODUCTION

Preparative capillary isotachophoresis (ITP) is a useful technique for the separation and purification of ionic substances. A dilute component in a sample is concentrated according to Kohlrausch's regulating function and correspondingly the concentrated sample is diluted. Such a separation mode is advantageous especially for the fractionation of minor components in a sample.

The other important feature of preparative isotachophoresis is that the recovery of sample components is in principle 100% as the components migrate between the leading and terminating zones, because no packings are used in the separation tube and the separation is carried out in a free electrolyte solution. In fact this is valid for many

0021-9673/91/$03.50

ionic substances, as exemplified for several organic acids by the agreement between the observed zone lengths and the theoretical estimates [1]. However, in the analysis of metal ions which usually form variously charged ion pairs with a complex-forming reagent and hydroxyl ions, the recovery depends on the reagent selected, its concentration and the pH of the leading solution. As discussed by Kaniansky and Everaerts [2], the reactions in complex-forming equilibria must be rapid enough to allow migration as a homogeneous zone, and the ion pair formed must be sufficiently soluble in the solvent used. If not, part of the sample will not migrate isotachophoretically and consequently the recovery will be reduced. This results in an unsuitable sample for isotachophoresis, *e.g.*, Fe^{III}, which easily forms hydroxyl complexes at isotachophoretically safe pH values. In order to confirm the recovery of metal cations, the separated zones must be fractionated and analysed directly by another independent method. This has not yet been carried out, as far as we know.

In addition to the recovery, the isotachophoretic separability of metal ions and the order of migration are also important from the viewpoint of the preparative strategy in isotachophoresis. The separation behaviour and the step heights eighteen metal cations were reported by Everaerts *et al.* [3] using a thermometric detector and a conductivity detector. They discussed the separability of the metal cation using the step heights with several leading electrolytes. Strictly, however, as exemplified by Mikkers *et al.* [4], the same effective mobility at the steady state does not always mean that no separation is possible. Thus the separability should not be simply discussed on the basis of the difference in the step heights at the steady state (*i.e.*, the difference in the effective mobilities), although the difference is usually a good measure of separation. We found this situation for some metal ions, as discussed later.

In order to study such a separation behaviour of metal ions, a new detection method should be applied, because universal detectors and a UV detector are not useful for the present purpose. We utilized an off-line combination of ITP and particle-induced X-ray emission (PIXE), which is a multi-elemental method with high sensitivity [5]. As the latter method is based on the characteristic X-rays emitted by target elements, it has a high specificity for the determination of the elements even if they are not separated. Amount of sample necessary depends on the element but it is usually of the order of submicrograms.

By the use of a preparative isotachophoretic analyser [6], sample zones were fractionated dropwise (one drop x 5 μl) and the fractions were analysed by PIXE. In this paper, the separation behaviour is discussed in relation to the use of a complexing agent, α-hydroxyisobutyric acid (HIB), which is the most effective agent for the separation of rare earth ions [7,8] and other heavy metal ions [9,10].

EXPERIMENTAL

Samples

The metal ions treated were monovalent Li and Na, bivalent Mg, Ca, Mn, Fe, Co, Ni, Cu, Zn, Sr, Cd, Zr^{IV} O, Ba and Pb and trivalent Y, La, Ce, Gd and Lu. Stock solutions were prepared using the chlorides, which were obtained from Tokyo Kasei (Tokyo, Japan). The solution analysed was a mixture of twenty metal ions (0.30–0.5 m*M* each). The water used was purified with a PURIC-R ion exchanger (Japan Organo, Tokyo, Japan). The specific resistance of the water was $18.3 \cdot 10^6$ Ω/cm. The

TABLE I

ELECTROLYTE SYSTEM USED IN ISOTACHOPHORESIS

HIB = α-Hydroxyisobutyric acid; CARH = carnitine hydrochloride; HPC = hydroxypropylcellulose.

Component	WNH_4Ac	WNH_4Ac–HIB
Leading electrolyte	20 m*M* ammonia solution	20 m*M* ammonia solution
Complexing agent	None	10 m*M* HIB
pH-Buffering agent	Acetic acid	Acetic acid
pH of leading electrolyte	4.8	4.8
Terminating electrolyte	10 m*M* CARH	10 m*M* CARH
Additive	0.2% HPC	0.2% HPC

pH of the sample mixture was adjusted to 3 by adding hydrochloric acid to suppress the oxidation of Fe^{II} to Fe^{III}. The sample was prepared just before fractionation. Small amounts of two cationic dyes, toluidine blue (TB) and astrazon pink (AP) were added to the sample solution as position markers in fractionation.

Electrolyte system

The electrolyte systems used are summarized in Table I. The notations proposed by Everaerts *et al.* [3] are used in this paper. For example WNH_4Ac defines an aqueous solution (W) of NH_4^+ as the leading ion and acetate ion (Ac) as the pH- buffering counter ion. The WNH_4Ac system was essentially the same as that of WKAc [3], as the absolute mobility of K^+ and NH_4^+ are approximately equal ($m_K = 79.1 \cdot 10^{-5}$, $m_{NH_4} = 76.8 \cdot 10^{-5}$ cm^2 V^{-1} s^{-1}). The WNH_4Ac system was used owing to the practical requirement for the rapid collection of the sample signals in PIXE measurement, which will be detailed later.

The use of a complex-forming reagent is a traditional technique for improving separablity, especially that of metal ions. We used HIB, which is useful for the separation of rare earth elements [7,8]. The concentration of the complex-forming agent (HIB) is very important for obtaining good separations. Taking into account the results of preliminary experiments and the results of simulation, a leading electrolyte containing 10 m*M* HIB was used in this work (WNH_4Ac–HIB). The leading electrolyte was 20 m*M* ammonia solution and pH_L was adjusted to 4.80 by adding acetic acid. The terminating electrolyte was a 10 m*M* solution of carnitine hydrochloride. The actually migrating terminator was H^+.

Hydroxypropylcellulose (HPC) was added to the leading electrolytes and the terminating electrolyte (0.2%) in order to suppress electroendosmosis. It was obtained from Tokyo Kasei and the viscosity of a 2% solution was given as 1000–4000 cP at 20°C.

Preparative equipment

The preparative isotachophoretic analyser used and the method of fractionation have been reported in a previous paper [6]. The principle was of the Arlinger type [11], except for the dropwise fractionation. Dropwise fractionation (*ca.* 5 μl) was carried out by applying a counter-flow of the leading electrolyte with a syringe pump. A coupled separation tube was used (16 cm × 1 mm I.D. × 2 mm O.D. and 30 cm × 0.5 mm I.D.

× 1 mm O.D.), which connected the injection valve and a potential gradient detector. The volume of the coupled tube was 0.184 cm^3. A typical single run took about 50 min. The migration current was 300 μA for the first 22 min, then it was decreased to 150 μA. The potential gradient detector and the fractionating compartment were connected by a PTFE tube of (16 cm × 0.5 mm I.D. × 1 mm O.D.). After being monitored by the potential gradient detector, sample zones were sliced by the counter-flow of the leading electrolyte applied by a syringe pump. The drops fell onto target holders, where a Nuclepore filter (thickness 5 μm, pore size 0.1 μm) was mounted on an aluminium frame. In a typical experiment 50 fractions were obtained in 9 min. The amount of metal elements in each fraction was 3–5 nmol. The fractions were dried in a desiccator. The residues were analysed individually as the PIXE target.

PIXE analysis

PIXE spectra of the fractions were measured by bombarding the targets with a 2-MeV H^+ beam energized by a Van de Graaff accelerator (Nisshin High Voltage, Model AN-2500). The beam current was typically 40 nA. The detector used was a high-purity Ge detector (Ortec, Model GLP-10180) and the multi-channel analyser was a Laboratory Equipment Model AMS-1000. A single run took ca. 230 s. Owing to the limitations of the detection system used, the light elements with atomic numbers less than 14 (Si) could not be detected. In the present experiment, therefore, Li, Na and Mg were not analysed. The assignment of these ions was carried out isotachophoretically.

The element with maximum sensitivity in the PIXE measurement is Cl or K.

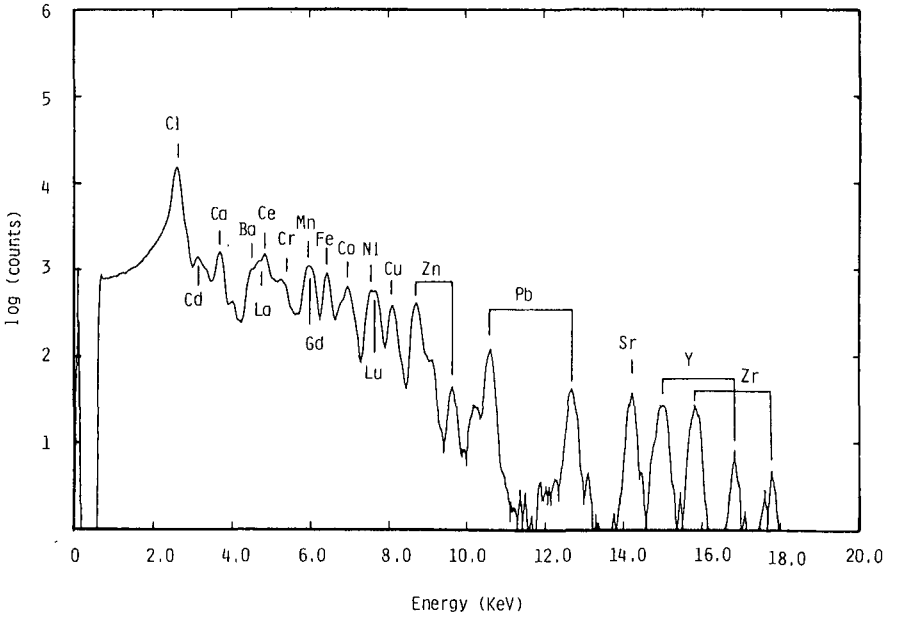

Fig. 1. PIXE spectrum of a mixture of chlorides of Ca, Mn, Fe, Co, Ni, Cu, Zn, Sr, Y, Zr, Cd, Ba, La, Ce, Gd, Lu and Pb. E_p = 2 MeV, 40 nA, 10 μC. The total sample amount was 200 nmol.

Both elements appear frequently in ITP as the leading ions. When the WKAc system was used, each fraction contained considerable amounts of K^+, because the counter-flow used to slice the sample zones should be the same as the leading electrolyte. Not only did it disturb the accurate determination of the neighbouring Ca which was present in our sample, but it also reduced the data acquisition speed owing to the limit of the X-ray counting rate of the detection system. Fig. 1 shows the PIXE spectra of the present sample before separation.

The data reduction software PIXS (developed by the authors) with a relative intensity database of characteristic X-rays was used in the analysis of the PIXE spectra [12]. The calculations were carried on an NEC PC-9801RA microcomputer (80386–80387, 16 MHz). It took *ca.* 100 s to deconvolute the spectra.

RESULTS AND DISCUSSION

Separability

First a mixture of twenty metal cations, Li, Na, Mg, Ca, Mn, Fe^{II}, Co, Ni, Cu, Zn, Sr, Y, $Zr^{IV}O$, Cd, Ba, La, Ce, Gd, Lu and Pb, was separated and fractionated using the WNH_4Ac system (pH_L = 4.8). The sample volume was 25 μl (0.3–0.5 m*M* each) and the total sample amount was *ca.* 200 nmol. Fig. 2 shows the isotachopherogram obtained with the use of the potential gradient detector. The total time-based zone length of the sample zones was 9 min (migration current = 150 μA). The electric charge integrated through the migration process was 0.594 C. Apparently from Fig. 2, the

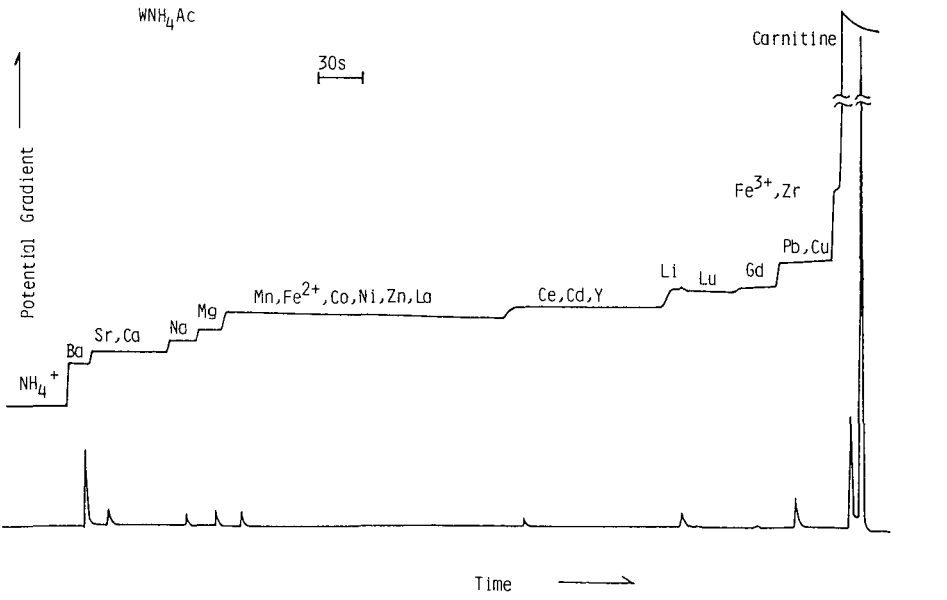

Fig. 2. Isotachopherogram of twenty metal cations (Li, Na, Mg, Ca, Mn, Fe^{II}, Co, Ni, Cu, Zn, Sr, Y, $Zr^{IV}O$, Cd, Ba, La, Ce, Gd, Lu and Pb) with the WNH_4Ac system (pH_L = 4.8). Concentration of leading NH_4^+ = 20 m*M*. Migration current = 150 μA. Coupled separation tube: 16 cm × 1 mm I.D. × 2 mm O.D. and 30 cm × 0.5 cm I.D. × 1 mm O.D.

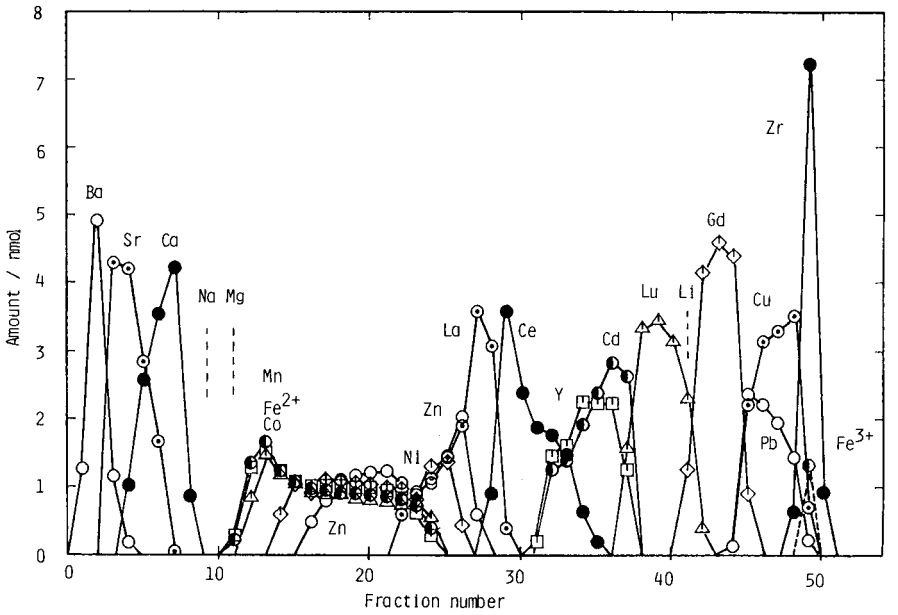

Fig. 3. Analytical result for the fractions with the WNH_4Ac system using PIXE. For the electrolyte conditions, see Fig. 2. The electric charge integrated through the migration process was 0.594 C.

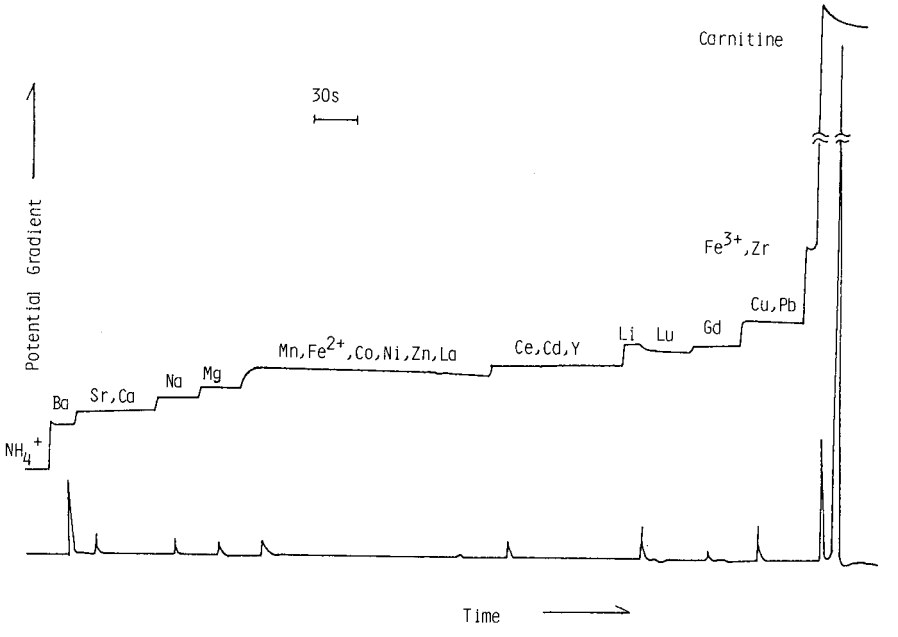

Fig. 4. Isotachopherogram of twenty metal cations (as in Fig. 2) with the WNH_4Ac system ($pH_L = 4.8$) with extended separation tube. Concentration of leading $NH_4^+ = 20$ mM. Migration current = 150 μA. Coupled separation tube: 32 cm × 1 mm I.D. × 2 mm O.D. and 30 cm × 0.5 mm I.D. × 1 mm O.D.

potential gradients of several components were almost identical, suggesting that the separability was not good. Fig. 3 shows the result of PIXE analysis for the fractions except for Li, Na and Mg. Several mixed zones were observed in the fractions, suggesting that the separation was in the transient state.

As it seemed that the applied electric charge was insufficient for separation, the separation tube was extended to give a better resolution for the same amount of sample. The coupled tube was 32 cm × 1 mm I.D. × 2 mm O.D. and 30 cm × 0.5 mm I.D. × 1 mm O.D. Figs. 4 and 5 show the isotachopherogram and the analytical results for the fractions. Although the electric charge integrated was twice as large as in the previous experiment (1.053 C), no distinct difference was observed between the isotachopherogram in Figs. 4 and 2. In contrast to the pessimistic estimation of poor separability from the agreement of the potential gradient trace, as shown in Fig. 5, PIXE analysis revealed that an extended capillary was very effective in the separation of Ni, Zn, La, Ce, Cd and Y. The separation of Mn, Fe^{II} and Co was not improved, although the lengh of the mixed zone was shortened. This suggested that the effective mobilities of these elements in the mixed zone were almost identical under the electrolyte condition used. Similarly, the separation of Cu and Pb was not improved. It was confirmed that the same step heights in an isotachopherogram with a potential gradient detector at the steady state does not always mean that no separation is achieved [4].

It is interesting that two Fe zones with different effective mobilities were detected in this system. The first Fe zone to appear was undoubtedly due to Fe^{II}. The second

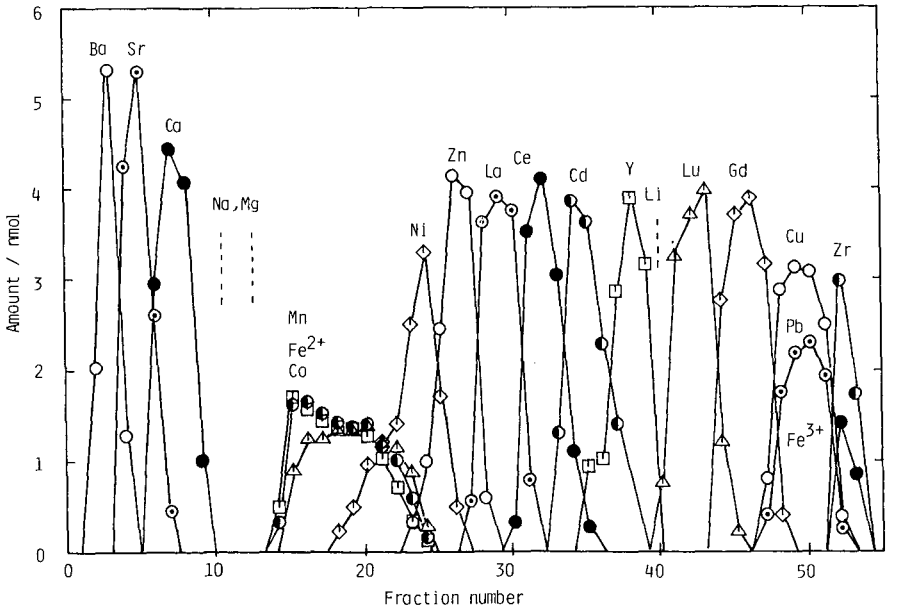

Fig. 5. Analytical result for the fractions with the WNH_4Ac system using PIXE, with extended separation tube. For the electrolyte conditions, see Fig. 4. The electric charge integrated through the migration process was 1.053 C.

zone can probably be assigned to Fe^{III}, as we made similar observations for an Fe^{III} sample. However, as the injected iron sample was nominally Fe^{II}, the Fe^{III} zone found represented the oxidation product of Fe^{II}. It has been accepted that Fe^{III} ion cannot be measured by isotachophoresis because it forms a hydroxyl complex and is deposited at isotachophoretically safe pH values [3]. As suggested, we could not observe the step corresponding to Fe^{III} when its solution was injected. However, by means of PIXE analysis we confirmed that Fe^{III} migrated just at the front end of the terminating zone.

The migration order with the WNH_4Ac system was Ba, Sr, Ca, Mg, Na, (Mn, Fe^{II}, Co), Ni, Zn, La, Ce, Cd, Y, Li, Lu, Gd, (Cu, Pb) and ($Zr^{IV}O$, Fe^{III}). In general, the quality of separation with the WNH_4Ac system was not good, but the system is still useful for the separation of a considerable number of metal ions.

It may be interesting to compare the migration order with that at pH_L 5.4 (WKAc system, 10 m*M* K^+) [3]. The order was Ag (18), Ba (59), Sr (73), Ca (86), Na (100), Mg (102), Fe^{II} (108), La (109), Mn (114), Co (114), Ni (115), Zn (130), Cd (142), Cu (169), Cr (175), Pb (179), Li (194), Sn^{II} (1083), where the figures in parentheses are the reported relative step heights using a conductivity detector. The difference in the migration order is due to the differences in the pH_L values and the leading ion concentrations. The latter factor is not so small because the effective mobility of polyvalent ions is affected more than hat of monovalent ions by a change in ionic strength.

As discussed previously, good separability of metal cations was achieved by adding HIB to the leading electrolyte of an acetic acid buffer system [7–10]. Figs. 6 and

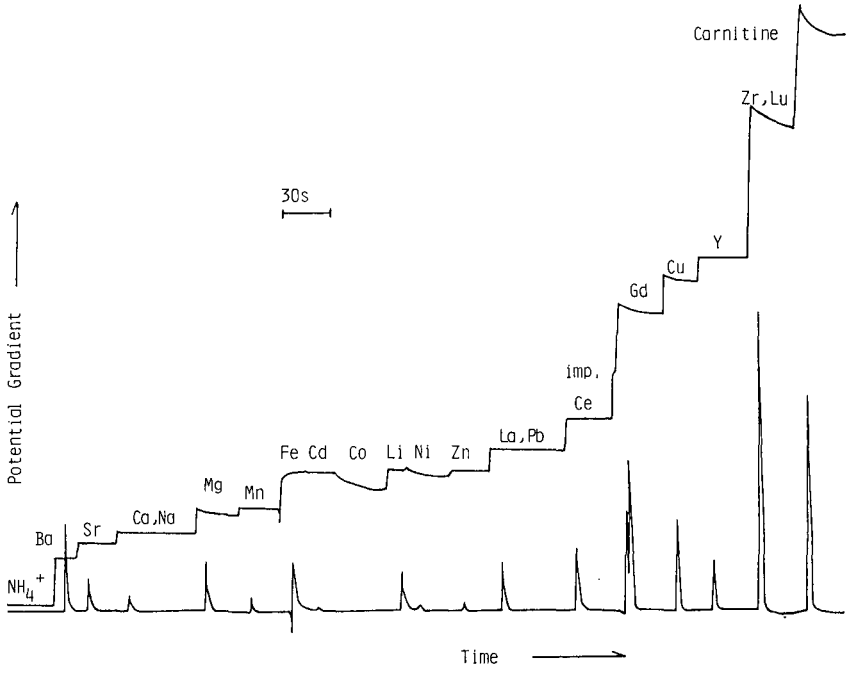

Fig. 6. Isotachopherogram of 20 metal cations (as in Fig. 2) with the WNH_4Ac–HIB system (pH_L = 4.8). Concentration of HIB = 10 m*M* and leading NH_4^+ = 20 m*M*. Migration current = 150 μA.

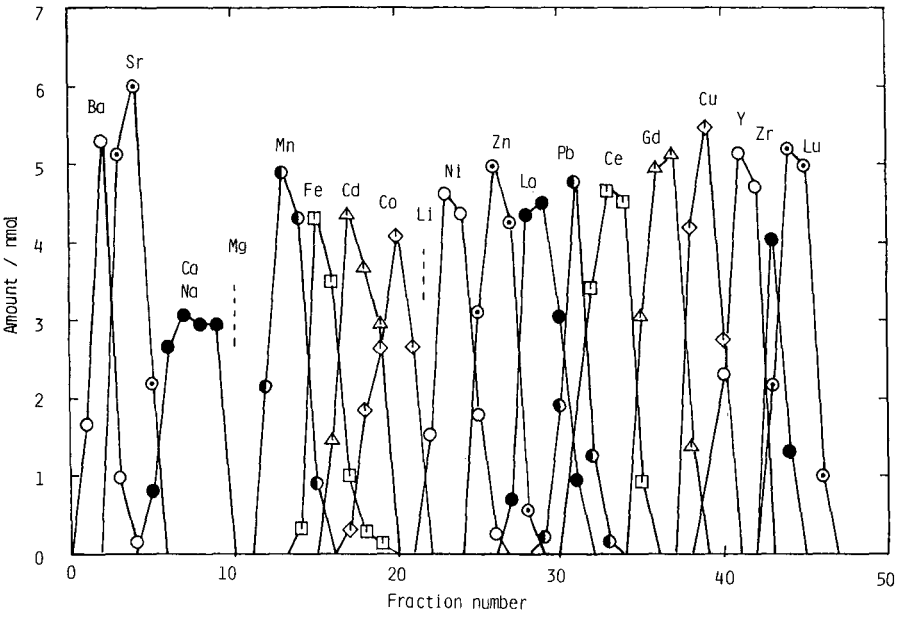

Fig. 7. Analytical result for the fractions with the WNH_4Ac–HIB system using PIXE. For the electrolyte conditions, see Fig. 6. The electric charge integrated through the migration process was 0.567 C.

7 show the isotachopherogram and the analytical results for the fractions. The migration time and the applied current were the same as those with the first WNH_4Ac system. The electric charge integrated through the migration process was 0.567 C, which was similar to that for Figs. 2 and 3. Apparently from Figs. 6 and 7, the separability was considerably improved by adding HIB. Good separation was achieved even for Fe^{II}, Co, Ni, Pb and Cu, although they were difficult to separate with the WNH_4Ac system by applying twice as much electric charge as with the WNH_4Ac–HIB system.

The migration order with the present WNH_4Ac–HIB system was Ba, Sr, (Ca, Na), Mg, Mn, Cd, Fe^{II}, Co, Li, Ni, Zn, La, Pb, Ce, Gd, Cu, Y, $Zr^{IV}O$ and Lu. In this system the Fe^{III} zone was not detected, in accordance with the previous report [9]. It should be noted that the step heights of La and Pb are identical but the separation was again complete.

Recovery

The recovery of metal cations was evaluated on the basis of PIXE analysis, defined as

$$\text{recovery (\%)} = \frac{\text{analysed amount of element in fractions}}{\text{analysed amount of element injected}} \cdot 100$$

where the analysed amount was obtained using PIXE.

In isotachophoresis, the sample should migrate between the leading and the terminating zones forming homogeneous zones. If not, isotachophoretic migration

TABLE II

RECOVERY (%) OF FRACTIONATED METAL CATIONS EVALUATED BY MEANS OF PIXE

For the electrolyte system used, see text.

Z	Metal ion	Electrolyte system		
		WNH_4Ac (0.594 C)	WNH_4Ac (1.053 C)	WNH_4Ac–HIB (0.567 C)
20	Ca	98	104	100
25	Mn	103	102	97
26	Fe^{II}	100[a]	102[b]	71
27	Co	99	102	103
28	Ni	102	102	98
29	Cu	104	102	99
30	Zn	98	103	101
38	Sr	101	98	99
39	Y	100	99	101
40	$Zr^{IV}O$	67	37	40
48	Cd	100	100	104
56	Ba	100	102	98
57	La	101	104	103
58	Ce	102	103	104
64	Gd	103	102	102
71	Lu	102	100	97
82	Pb	100	100	100

[a] 10% was found as Fe^{III}.
[b] 17% was found as Fe^{III}.

does not take place and then complete recovery cannot be expected. In these experiments the concentration of complexing agent and the pH of the leading solution were determined to obtain good recoveries considering the above restriction of isotachophoretic migration. With the WNH_4Ac electrolyte system, most of metal cations considered form weak 1:1 ion pairs with acetate ion. The stability constants (log *K*) of the ion pairs are small for most of the metal ions treated, *e.g.*, those of $BaAc^+$, $CaAc^+$ and $MgAc^+$ are < 1 and at most *ca.* 2 for $CuAc^+$. On the other hand, with the WNH_4Ac–HIB electrolyte system, metal ions form multi-coordinated ion pairs with HIB ion, including mixed ligand ion pairs, *e.g.*, LuHIB, $Lu(HIB)_2$, $Lu(HIB)_3$ and $LuAc(HIB)_2$. The abundance of such ion pairs is considerably higher than that with the WNH_4Ac system as simulated previously [8].

Table II summarizes the evacuated recovery for three runs. Apparently, the recovery of almost all the metal cations treated could be regarded as 100%, taking into account the possible error of a few percent in PIXE analysis. However, the recovery of ZrO was affected by both the electric charge (or migration time) and the electrolyte system used. This observation suggested that the abundance of the ion pairs with low mobility increased gradually and the complex-forming equilibria were not rapid enough to allow migration as a homogeneous zone. Although we have no direct information of the chemical form of the lost Zr compound, the most plausible explanation is that the formation of immobile hydroxyl complexes reduced the recovery. From Table II, it is apparent that the oxidation of Fe^{II} to Fe^{III} took place even

during migration. It should be noted that the recovery of Fe as a whole was 100% with the WNH_4Ac system. On the other hand, the recovery of Fe was reduced when the WNH_4Ac–HIB system was used, because the Fe^{III} zone migrating at the front end of the terminating zone in the WNH_4Ac system no longer migrated, suggesting that the hydroxyl complex of Fe^{III} interacted more strongly with HIB ion than acetate ion.

In conclusion, PIXE is a useful method for revealing the separation behaviour of metal cations in isotachophoresis. The migration order and the recovery of metal ions are very important, especially from the viewpoint of the preparative strategy, as confirmed by the use of a PIXE detector. More detailed studies by means of PIXE of the separation of metal cations which easily form hydroxyl complexes, *e.g.*, Fe^{III} and Ga^{III}, are in progress.

It should be noted that the difference in mobilities at the steady state is a good measure of separation but it is not always necessary for separation. The separation is successful when the mobility of the sample differs sufficiently at the transient mixed zones. However, a problem is that this situation is difficult to detect when universal detectors or a UV detector are used.

REFERENCES

1 T. Hirokawa and Y. Kiso, *J. Chromatogr.*, 312 (1984) 11.
2 D. Kaniansky and F. M. Everaerts, *J. Chromatogr.*, 148 (1978) 441.
3 F. M. Everaerts, J. L. Beckers and Th. P. E. M. Verheggen, *Isotachophoresis*, Elsevier, Amsterdam, 1976.
4 F. E. P. Mikkers, F. M. Everaerts and J. A. F. Peek, *J. Chromatogr.*, 168 (1979) 317.
5 S. A. E. Johansson and T. B. Johansson, *Nucl. Instrum. Methods*, 137 (1976) 473.
6 T. Hirokawa, J.-Y. Hu, K. Umeda, G. Kimura, H. Ikeda, F. Nisiyama and Y. Kiso, *J. Chromatogr.*, 513 (1990) 297.
7 I. Nukatsuka, M. Taga and H. Yosida, *J. Chromatogr.*, 205 (1981) 95.
8 T. Hirokawa, N. Aoki and Y. Kiso, *J. Chromatogr.*, 312 (1984) 11.
9 F. M. Everaerts, Th. P. E. M. Verheggen and J. C. Reijenga, G. V. A. Aben, P. Gebauer and P. Bocek, *J. Chromatogr.*, 320 (1985) 263.
10 T. Hirokawa, N. Matsuki, H. Takemi and Y. Kiso, *J. Chromatogr.*, 280 (1983) 233.
11 L. Arlinger, *J. Chromatogr.*, 119 (1976) 9.
12 T. Hirokawa, F. Nishiyama and Y. Kiso, *Nucl. Instrum. Methods*, B31 (1988) 525.

Journal of Chromatography, 538 (1991) 424–430
Elsevier Science Publishers B.V., Amsterdam

CHROM. 22 913

Short Communication

Identification and analysis of trimethylbiphenyls in petroleum

R. ALEXANDER*, S. H. NGO and R. I. KAGI
Centre for Petroleum and Environmental Organic Geochemistry, GPO Box U1987, Perth 6001, Western Australia (Australia)
(Received August 3rd, 1990)

ABSTRACT

Trimethylbiphenyl isomers (17) have been identified in three Australian crude oils using capillary gas chromatography–mass spectrometry (MRM) techniques. Total concentrations of trimethylbiphenyls in the crude oils ranged from 100 to 600 μg/g and in all cases the most abundant isomers were those with substituents in the *meta* and *para* positions. The elution order of all the isomeric trimethylbiphenyls is reported for four capillary columns with a range of stationary phases.

INTRODUCTION

Alkylbiphenyls are widespread in sedimentary organic matter and have been reported in crude oils [1–3], coal tar [4] and shale oil [5]. More recently, detailed studies on crude oils and sediments [6–8] have led to identification of all the isomers of methylbiphenyl, ethylbiphenyl and dimethylbiphenyl.

Reports on the distributions of alkylbiphenylisomers in sedimentary sequences have shown that isomers with *ortho* substituents are depleted relative to those without *ortho* substituents as the depth and maturity of sediments increase [8]. In the case of methylbiphenyls, the relative abundance of 2-methylbiphenyl moves further from the equilibrium value [9] with increase in sample maturity. This effect has been attributed to a thermally induced cyclisation reaction in which the *ortho* alkyl group forms an incipient free radical which undergoes further reaction to displace a hydrogen radical from the *ortho* position of the adjacent aromatic ring forming fluorenes [10]. These processes have been suggested to have applications for reconstructing the thermal history of sediments [6,11].

In this note we report on the identification and analysis of isomeric trimethylbiphenyls (TMBPs) in some Australian crude oils.

0021-9673/91/$03.50

EXPERIMENTAL

TMBP standards

TMBPs were prepared by the Gomberg reaction as described by Novrocik *et al.* [12] or from the higher-yielding modification of this reaction described by Korzeniowski *et al.* [13]. The compounds were prepared using the coupling reaction between a diazotised aryl amine and an aromatic hydrocarbon:

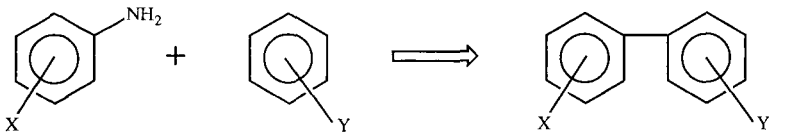

ARYL AMINE AROMATIC HYDROCARBON ALKYL BIPHENYL

The trimethylbiphenyls were isolated from the reaction mixture by column chromatography using a mixed bed of activated silica gel (40 g) and alumina (10 g) with light petroleum–dichloromethane (95:5) as eluent. Individual isomers were then isolated by high-performance liquid chromatography (HPLC) on a silica column using hexane as eluent.

Isolation of alkylbiphenyl fractions from crude oil

A dinuclear aromatic fraction was isolated from each of the three crude oils (Table I) using preparative thin-layer chromatographic methods described previously [14].

Gas chromatography (GC) and GC–mass spectrometry (MS)

GC was performed using a Hewlett-Packard 5890 chromatograph equipped with 50 m × 0.22 mm I.D. capillary columns coated with either BP-1, BP-5, BP-10 (SGE, Australia) or CP Wax 57 CB (Chrompack). Hydrogen was used as the carrier gas at a linear flow velocity of 30 cm/s. The oven was programmed from 70 to 190°C at 2°C/min and then at 10°C/min to 300°C or to the upper temperature limit of the column. Peaks in the chromatograms were assigned on the basis of co-chromatography with standard compounds.

GC–MS was carried out using a VG-TS 250 system equipped with a 50 m × 0.2 mm I.D. capillary column with a BP-5 coating and an autosampler facility. The GC

TABLE I

GEOLOGICAL DATA FOR THE CRUDE OILS

Crude oil	Location Australian sedimentary basin	Age of source	Source rock type	Ref.
Barrow No. 1	Carnarvon	Jurassic	Marine shale	16
Blina No. 1	Canning	Devonian	Marine/lacustrine shale	17
Tuna No. 4	Gippsland	Cretaceous	Coal/shale	18

oven was held at 70°C for 1 min and then programmed from 70 to 190°C at 2°C/min and from 190 to 300°C at 15°C/min. The mass spectrometer was operated in the MRM mode with a source temperature of 200°C, an electron voltage of 70 eV and a dwell time of 100 ms.

RESULTS AND DISCUSSION

Preparation of authentic TMBPs

For those reactions where two or more TMBPs were produced, each TMBP was separately prepared using the alternative combination of substituted reagents. For example, 3,5,3′-TMBP was prepared from the reaction of 3,5-dimethylaniline and toluene and from *m*-toluidine and *m*-xylene. The TMBP common to both reactions was assigned as 3,5,3′-TMBP. In a similar manner structures were assigned to 2,5,3′-, 3,4,3′-, 2,3,3′-, 2,4,3′-, 2,6,3′-, 3,4,2′-, 2,3,2′-, 2,5,2′-, 2,4,2′-, 3,5,2′-, 2,6,2′-, 2,5,4′-, 2,4,4′-, 3,5,4′-, 2,6,4′-, 3,4,4′- and 2,3,4′- TMBPs.

The remaining six isomers all have the methyl substituents in one ring and were prepared from aniline and the appropriate trimethylbenzene. For reactions that gave multiple products, *e.g.* aniline with 1,2,3-trimethylbenzene (two products: 2,3,4- and 3,4,5-TMBPs) and with 1,2,4-trimethylbenzene (three products: 2,3,6-, 2,3,5- and

TABLE II

COMPARISON OF THE GC ELUTION ORDER OF ISOMERIC TRIMETHYLBIPHENYLS USING FOUR STATIONARY PHASES

BP-1	BP-5	BP-10	CP Wax 57 CB
2,6,2′	2,6,2′	2,6,2′	2,6,2′
2,5,2′	2,5,2′	2,5,2′	2,5,2′
2,4,2′	2,4,2′	2,4,2′	2,6,3′
2,6,3′	2,6,3′	2,6,3′	2,4,2′
2,6,4′+2,4,6	2,4,6	2,4,6	2,6,4′
	2,6,4′	2,6,4′	2,4,6
2,3,2′	2,3,2′	2,3,2′	2,3,2′
2,3,6	2,3,6	2,3,6	2,3,6
3,5,2′	3,5,2′	3,5,2′	3,5,2′
2,5,3′	2,5,3′	2,5,3′	2,5,3′
2,4,3′	2,4,3′	2,4,3′	2,4,3′
2,5,4′	2,5,4′	2,5,4′	2,5,4′
2,4,4′	2,4,4′	2,4,4′	2,4,4′
2,3,3′	2,3,3′	2,3,3′+2,3,5	2,3,3′
2,3,5	2,3,5		2,3,5
3,4,2′	3,4,2′	3,4,2′	3,4,2′
2,3,4′+2,4,5	2,4,5	2,4,5	2,3,4′
	2,3,4′	2,3,4′	2,4,5
2,3,4	2,3,4	2,3,4	2,3,4
3,5,3′	3,5,3′	3,5,3′	3,5,3′
3,5,4′	3,5,4′	3,5,4′	3,5,4′
3,4,3′	3,4,3′	3,4,3′	3,4,3′
3,4,4′	3,4,4′	3,4,4′	3,4,4′
3,4,5	3,4,5	3,4,5	3,4,5

2,4,5-TMBPs), each product was separated using HPLC and the structure of each was assigned on the basis of its GC retention behaviour.

Retention behaviour of various chloro-substituted biphenyls has been reported by Mullin and Pochinl [15]. They reported that the position of substitution has a predictable affect on retention behaviour: those compounds with *ortho* substituents have shortest retention times and usually the *para*-substituted isomers have the longest retention times. Similar effects were observed in this study when the trimethylbiphenyls with substituents in both rings were analysed using GC techniques (Table II).

The trimethylbiphenyls with all three methyl groups in one ring which were obtained as mixtures in this study were therefore assigned structures using these principles, *e.g.* TMBPs with two *ortho* substituents were assumed to elute before compounds with one *ortho* substituent. In cases where compounds differed only in *meta* or *para* substituents the compound with the longest retention time was assigned the *para* structure.

GC and GC–MS

Table II and Fig. 1 show the GC retention behaviour of all 24 TMBPs. From these results it is apparent that separation of all isomers could be achieved using either a BP-5 or a CP Wax 57 CB column, and further, *ortho*-substituted isomers have lower retention times with all four columns. Fig. 1 shows a partial gas chromatogram of the all-isomer mixture obtained using a BP-5 coated column. Although all isomers can be distinguished on the trace, only partial resolution was achieved between 2,4,6-TMBP and 2,6,4′-TMBP and between 2,4,5-TMBP and 2,3,4′-TMBP.

Fig. 2 shows the results obtained by using MRM GC–MS techniques to analyse an all-isomer mixture of TMBPs and an aromatic fraction of the Blina crude oil. The mass chromatograms show compounds that underwent a 196-to-181 mass transition. Peaks marked in the mass chromatogram from the Blina crude oil represent compounds with similar retention behaviour and mass spectra compared to the standards. The small differences in retention times between the standards and the compounds in the Blina crude oil which are apparent for compounds eluting after 50

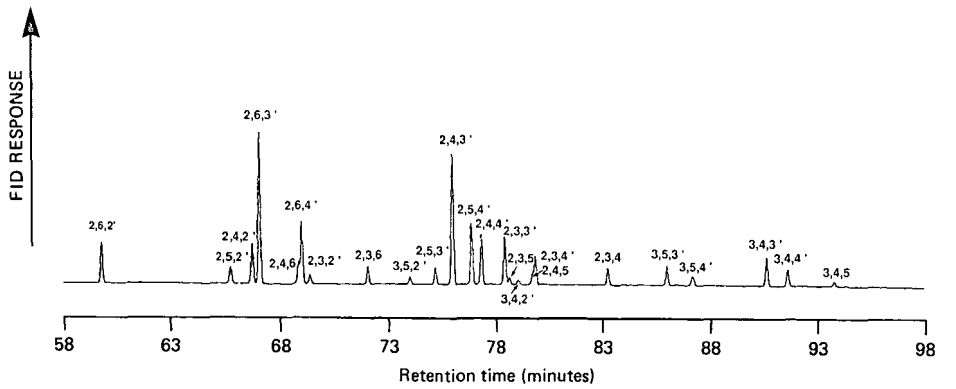

Fig. 1. Partial capillary gas chromatogram showing separation of an all-isomer mixture of TMBPs using a BP-5 capillary column. FID = Flame ionization detection.

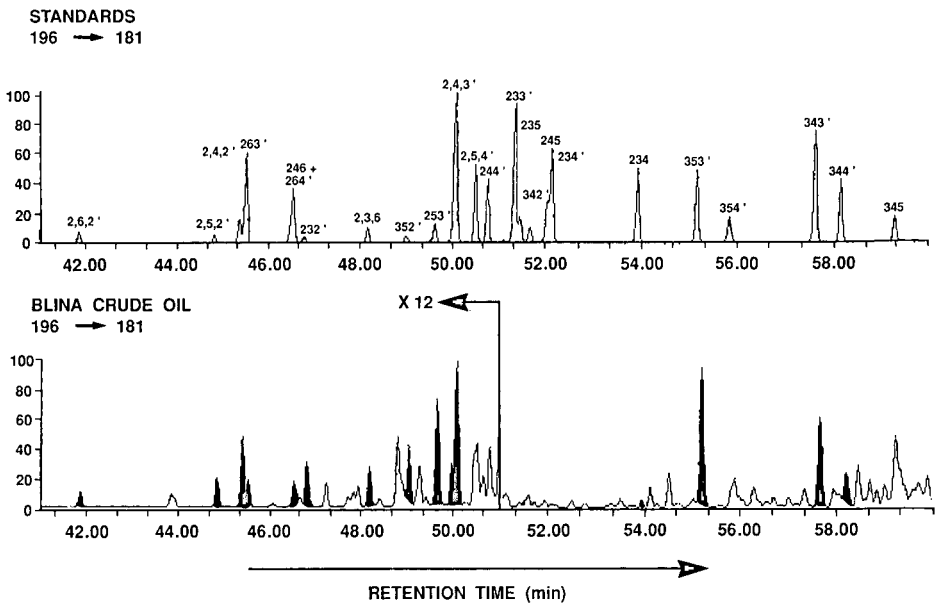

Fig. 2. MRM (196 → 181) mass chromatograms obtained from analysis of an all-isomer mixture of TMBPs and an aromatic fraction of the Blina 1 crude oil.

min is attributed to minor differences in operating conditions between the two analyses. Similar analyses were also carried out using aromatic fractions from the Barrow crude oil and the Tuna 4 crude oil. Table III shows the TMBPs identified in the oils. The concentrations of total TMBPs in the crude oils varied from 100 μg/g for the Blina crude to 600 μg/g for the Barrow crude. This compares with a typical concentration range of 200–300 μg/g reported for methylbiphenyls in crude oils [1,7]. It is apparent from these analyses that the most abundant isomers in these crude oils are those with substituents in the *meta* and *para* positions. Compounds with one, two and three substituents in *ortho* positions have been identified but it is apparent from Fig. 2 and Table III that such compounds are in lower abundance than compounds with fewer *ortho* substituents. In the case of dimethylbiphenyls, the lower abundance of *ortho*-substituted isomers in crude oils and mature sediments has been attributed to their higher reactivity, in that they undergo cyclisation to form fluorenes under the thermal conditions required for oil formation in sediments [8]. Similar processes may be responsible for the depletion of *ortho*-substituted TMBPs observed in these crude oils.

Origins of alkylbiphenyls

The origins of alkylbiphenyls in crude oils and sediments is uncertain. The most likely sources are natural products with the biphenylcarbon skeleton. Compounds of this type, such as ellagic acid (**I**), are usually derived from phenolic coupling processes rather than the processes responsible for sterane and terpane biosynthesis. An alternative explanation —that the biphenyls arise from oxidative degradation of the 9–10 bonds of substituted phenanthrenes —is not favoured, as we have been unable to

TABLE III

TMBP ISOMERS IDENTIFIED IN CRUDE OILS

Double crosses indicate the most abundant isomer(s).

TMBP isomer	Blina No. 1	Barrow No. 1	Tuna No. 4
2,6,2′	+	+	+
2,5,2′	+	+	+
2,4,2′	+		+
2,6,3′	+		+
2,4,6+2,6,4′	+	+	+
2,3,2′	+	+	+
2,3,6	+	+	
3,5,2′	+	+	+
2,5,3′	+	+	+
2,4,3′	+	+	+
2,5,4′			
2,4,4′		+	+
2,3,3′			
2,3,5			
3,4,2′	+	+	+
2,4,5+2,3,4′			
2,3,4	+	+	+
3,5,3′	++	++	++
3,5,4′			
3,4,3′	+	+	++
3,4,4′	+	+	+
3,4,5			

identify significant amounts of the alkylbiphenyls that can be unambiguously related to alkylphenanthrenes by this process in samples containing high concentrations of alkylphenanthrenes.

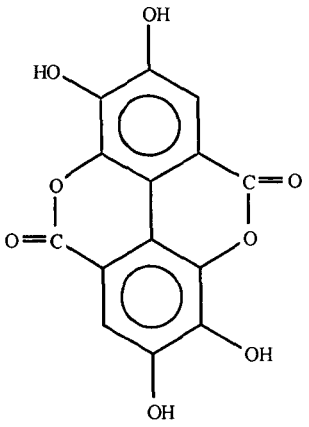

I

Although the three crude oils analysed in this study were derived from different source materials and differ widely in age and location (Table I), the isomer distributions of their TMBP components is similar. As already noted, maturity no doubt has a significant effect on the abundance of *ortho*-substituted isomers; however, the presence of similar distributions in a crude oil with a major contribution from higher plants (Tuna No. 4), in a crude oil originating from marine organic matter (Barrow No. 1) and in a crude oil (Blina No. 1) whose source predates the widespread distribution of higher plants, suggests a ubiquitous microorganism as their source.

ACKNOWLEDGEMENTS

The Chemistry Centre of Western Australia is acknowledged for providing access to the VG-TS 250 GC–MS system. Mr. N. West is thanked for providing technical assistance.

REFERENCES

1 B. J. Mair and T. J. Mayer, *Anal. Chem.*, 36 (1964) 351.
2 F. F. Yew and B. J. Mair, *Anal. Chem.*, 38 (1966) 231.
3 N. G. Adams and D. M. Richardson, *Anal. Chem.*, 25 (1953) 1073.
4 Mostecky, M. Popl and J. Kriz, *Anal. Chem.*, 42 (1970) 1132.
5 C. E. Rovere, P. T. Crisp, J. Ellis and P. D. Bolton, *Fuel*, 62 (1983) 1274.
6 R. Alexander, S. J. Fisher and R. I. Kagi, in L. Mattavelli and L. Novelli (Editors), *Advances in Organic Geochemistry 1987*, Pergamon, Oxford, 1988, p. 833.
7 K. M. Cumbers, R. Alexander and R. I. Kagi, *J. Chromatogr.*, 361 (1986) 385.
8 K. M. Cumbers, R. Alexander and R. I. Kagi, *Geochim. Cosmochim. Acta*, 51 (1987) 3105.
9 G. A. Olah and J. C. Lapierre, *J. Org. Chem.*, 31 (1966) 1271.
10 R. I. Kagi, R. Alexander and E. Toh, in F. Behar *et al.* (Editors), *Advances in Organic Geochemistry 1989*, Pergamon, Oxford, 1990, in press.
11 R. Alexander, R. I. Kagi, E. Toh and W. van Bronswijk, in P. Purcell and R. R. Purcell (Editors), *North West Shelf Symposium*, Petroleum Exploration Society of Australia, 1988, p. 633.
12 J. Novrocik, M. Novrocikova and M. Titz, *Collect. Czech. Chem. Commun.*, 45 (1980) 3140.
13 S. H. Korzeniowski, L. Blum and G. W. Gokel, *Tetrahedron Lett.*, 22 (1977) 1871.
14 R. Alexander, R. I. Kagi and P. N. Sheppard, *J. Chromatogr.*, 267 (1983) 367.
15 M. D. Mullin and C. M. Pocinl, *Environ. Sci. Technol.*, 18 (1984) 468.
16 J. K. Volkman, R. Alexander, R. I. Kagi, R. A. Noble and G. W. Woodhouse, *Geochim. Cosmochim. Acta*, 47 (1984) 2091.
17 R. Alexander, M. Cumbers and R. I. Kagi, in P. G. Purcell (Editor), *The Canning Basin, W. A. Proceedings of Geol. Soc. Aust./Pet. Expl. Soc. Aust. Symposium*, Perth, 1984, p. 343.
18 B. J. Burns, A. T. James and J. K. Emmett, *APEA J.*, 24 (1984) 217.

Journal of Chromatography, 538 (1991) 431–434
Elsevier Science Publishers B.V., Amsterdam

CHROM. 22 847

Short Communication

Direct determination of acetic acid in strongly acidic hydrolysates of chitin and chitin-containing biological products by capillary gas chromatography

G. STOEV*
Institute of Organic Chemistry with a Centre of Phytochemistry, Bulgarian Academy of Sciences, Block 9, 1113 Sofia (Bulgaria)
and
A. VELICHKOV
Institute of Microbiology, Bulgarian Academy of Sciences, Block 26, 1113 Sofia (Bulgaria)
(First received June 26th, 1990; revised manuscript received October 28th, 1990)

ABSTRACT

Laboratory-made capillary columns with high effectiveness and inertness were used for the determination of N-acetyl groups in chitin-containing biological products by liberation of acetic acid in 4 *M* HCl hydrolysates. The quantitative gas chromatographic analysis is fast, requiring only 2 min, with good precision and accuracy. After a long working period of more than 1000 analyses the capillary column retained its high effectiveness and inertness.

INTRODUCTION

In the analysis of chitin-containing biological products, the determination of N-acetyl groups is based on the measurement of acetic acid liberated after acidic or alkaline hydrolysis of the sample. Holan *et al.* [1] proposed a method for the gas chromatographic (GC) determination of acetic acid in 4 *M* HCl by direct injection into glass columns packed with Porapak Q. The resin had been previously treated according to the method of Mahadevan and Stenroos [2]. In the GC analysis of volatile organic acids Porapak Q columns give satisfactory resolution [1,3].

Progress in capillary GC, however, has allowed inert capillary columns to be constructed that give highly satisfactory resolution and accuracy in the quantitative determination of organic acids [4]. We therefore studied the possibility of using a capillary column for the direct determination of acetic acid in a strongly acidic medium (4 *M* HCl) in the GC determination of acetyl groups in chitin-containing biological materials.

0021-9673/91/$03.50

EXPERIMENTAL

Materials

The experiments were carried out with chitin, chitosan and alkali-insoluble residue derived from the mycelium of the fungus *Humicola lutea*. Crustacean chitin was purchased from Koch-Light (0996H Chitin pract.).

Commercial chitin was used in the preparation of chitosan by hydrolysis with 40% NaOH (ratio 1:10) by boiling for 24 h. Chitosan was separated by filtration, washed with hot distilled water to neutral pH of the filtrates and purified by twice dissolving it in ice-cold 0.1 *M* HCl, followed by titration with 1 *M* NaOH to pH 8.0. The final product was filtered off, washed with hot distilled water and dried by successive washing with absolute ethanol and diethyl ether.

Freeze-dried mycelium of *Humicola lutea* was hydrolysed with 30% NaOH (ratio 1:10) by boiling for 3 h. The alkaline-insoluble residue was separated by filtration and washed with water and organic solvents as described above.

Sample preparation

Deacetylation of the samples was carried out according to the method of Holan *et al.* [1] with 4 *M* HCl. Propionic acid was used as an internal standard.

The glucosamine released after hydrolysis of 15 mg of each sample with 5 ml of 6 *M* HCl in sealed ampoules for 16 h at 105°C, was determined by the spectrophotometric method of Tsuji *et al.* [5].

The percentages of acetic acid and glucosamine were calculated taking into account the ash content of the samples.

Gas chromatography

Duran capillaries were leached with 18% HCl at 170°C for 16 h, rinsed with 1% HCl and dried with nitrogen at 230°C for 4 h. After deactivation with PEG 20M at 280°C for 16 h the capillaries were statically coated with a 0.2-μm film of vinyl-modified PEG 20M (Ohio Valley). The columns had been tested with Grob's test mixture [6].

All analyses were carried out with a Perkin-Elmer Sigma 300 gas chromatograph under the following conditions: column temperature, 120°C; injector and flame ionization detector temperatures, 250°C; carrier gas, nitrogen at a linear velocity of 50 cm/s; and splitting ratio, 1:80. The results obtained were calculated by mean of a Shimadzu CR-1B computing integrator.

RESULTS AND DISCUSSION

The GC determination of acetic acid at concentration below 0.1% is usually accompanied by many disadvantages, including non-linear calibration graphs, inadequate detection limits and the appearance of ghost peaks [7,8]. The acidic hydrolysates used in this investigation represented complex mixtures of organic substances with different physico-chemical properties, where the liberated acetic acid was present at low concentrations (0.01–0.07%). Because of its high efficiency, the capillary column permitted the separation of acetic and propionic acids from the other components of the mixture and allowed quantitative analysis with satisfactory accuracy and precision.

TABLE I

PRECISION AND ACCURACY OF THE GC DETERMINATION OF ACETIC ACID

Concentration (g/l)		Precision, V (%)[a]	Accuracy, A (%)[b]
Model mixture	Calculated value ± standard deviation		
0.80	0.85 ± 0.06	7.1	6.25
0.40	0.42 ± 0.03	7.1	5.0
0.20	0.18 ± 0.02	11.1	10.0
0.10	0.08 ± 0.01	12.5	20.0

[a] $V(\%) = (\bar{x}/S) \cdot 100$ $(n=8)$; S = calculated value; $\bar{x}$ = standard deviation. Limit of detection 0.05 g/l.

[b] $A(\%) = \dfrac{[CH_3COOH]_{actual} - [CH_3COOH]_{calculated}}{[CH_3COOH]_{actual}} \cdot 100.$

Data on the accuracy and precision of the GC determination of acetic acid in model mixtures of 4 *M* HCl with propionic acid as an internal standard are presented in Table I. The concentration of acetic acid in the model mixtures was chosen to be near those usually found in the investigated acidic hydrolysates (below 0.1%). Calibration graphs were generated by plotting the peak-area ratio *versus* the concentration of acetic acid in the concentration range 1.0–0.05 g/l. In all instances the calibration graphs were linear with a correlation coefficient of 0.998 passed through the origin. Values of unknown sample concentrations were determined by comparison with the calibration graph.

The results obtained for acetic acid content in chitin, chitosan and alkali-insoluble residue from the mycelium of *Humicola lutea* are given in Table II. The average values of these results and their standard deviations were calculated for four hydrolysates prepared independently of one another ($n=4$). The molecular ratio between acetic acid and D-glucosamine gave the degree of acetylation of the poly-D-glucosamine in the samples.

The capillary column allowed the rapid analysis of each sample in only 1.5 min. Further, the column showed high stability against strong mineral acids. In analyses of

TABLE II

CONCENTRATION OF ACETIC ACID AND DEGREE OF ACETYLATION OF POLY-D-GLUCOSAMINE IN THE INVESTIGATED SAMPLES

Sample	Acetic acid concentration ± standard deviation (%)	D-Glucosamine (%)	Molecular ratio
Chitin	22.24 ± 0.36	76.82	0.86
Chitosan	2.92 ± 0.57	96.73	0.09
Alkali-insoluble residue from *H. lutea* mycelium	2.20 ± 0.42	15.97	0.41

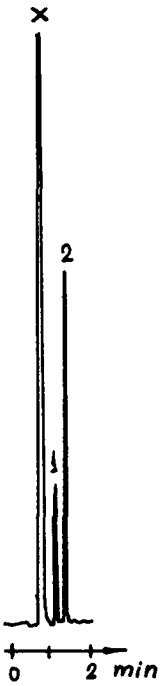

Fig. 1. Chromatogram of acidic hydrolysate from alkali-insoluble residue from *H. lutea* mycelium. Peaks: 1 = acetic acid; 2 = propionic acid; × = volatile impurities.

the acidic hydrolysates it withstood more than 1000 injections, whereas the lifetime of a Porapak Q column was about 150 injections [1].

A chromatogram of the acidic hydrolysate of the fungal alkali-insoluble residue is presented in Fig. 1. The analysis was carried out with a column already used for 1200 injections. This chromatogram illustrates the satisfactory resolution of acetic and propionic acids and the short time needed for analysis.

REFERENCES

1 Z. Holan, J. Vortuba and V. Vlasakova, *J. Chromatogr.*, 190 (1980) 67.
2 V. Mahadevan and L. Stenroos, *Anal. Chem.*, 39 (1967) 1952.
3 M. Henderson and T. Steedman, *J. Chromatogr.*, 244 (1982) 337.
4 G. Schomburg, G. Husman and H. Behlan, *J. Chromatogr.*, 203 (1981) 179.
5 A. Tsuji, T. Kinoshita and M. Hoshino, *Chem. Pharm. Bull.*, 17 (1969) 1505.
6 K. Grob and K. K. Grob, *J. Chromatogr.*, 156 (1978) 1.
7 K. Williams and J. Mazur, *Am. Ind. Hyg. Assoc. J.*, 41 (1980) 1.
8 C. van Eenaeme, J. Bienfait, O. Lambot and A. Pondat, *J. Chromatogr. Sci.*, 12 (1974) 398.

Journal of Chromatography, 538 (1991) 435–440
Elsevier Science Publishers B.V., Amsterdam

CHROM. 22 833

Short Communication

Determination of phosgene as its N,N,N′,N′-tetraethylurea derivative by gas chromatography

SOLOMON E. MASSIL*
Makhteshim Chemical Works Ltd., Department of Analytical Research, Research and Development Division, P.O. Box 60, Beer-Sheva 84100 (Israel)
and
DAVID OVADIA
Makhteshim Chemical Works Ltd., Department of Organic Research, Research and Development Division, P.O. Box 60, Beer-Sheva 84100 (Israel)
(First received March 28th, 1990; revised manuscript received September 17th, 1990)

ABSTRACT

A gas chromatographic method with flame-ionization for the determination of free phosgene as its N,N,N′N′-tetraethylurea derivative and the application of the method to the determination of excess phosgene either in solution or in a reaction mixture is described. The detection limit is 5 ppm.

INTRODUCTION

The commercial applications of phosgene in chemical synthesis are widely known. Extensive information is available regarding the detection and determination of phosgene, mostly in air and gas mixtures, using gas chromatography (GC) [1–6], spectrophotometry [3,7–9], electrochemical methods [10,11] and aniline in bromometric titrations [12]. More recently, the determination of low concentrations of phosgene in air by GC using di-*n*-butylamine coated on a solid sorbent [13] and high-performance liquid chromatography for determining the conversion efficiecy of phosgene into *sym*-diphenylurea [14] have been investigated.

Recently, we have been engaged in the synthesis of benzyl chloroformate by the reaction of phosgene with benzyl alcohol, and efforts have been directed to developing a GC method for the determination of excess phosgene in the reaction mixture. For this purpose, diethylamine has been used selectively as a derivatizing agent to convert phosgene into N,N,N′,N′-tetraethylurea (TEU) as a stable product. The relative strengths of phosgene in toluene solvent at elevated temperatures have also been investigated.

0021-9673/91/$03.50

The GC determination of phosgene as the TEU derivative with flame ionization detection gave good recoveries. To our knowledge, this is the first report of a gas chromatographic assay of phosgene in solution or in a reaction mixture. The method described here is simple and convenient for personal monitoring.

EXPERIMENTAL

Chemicals and reagents

Diethylamine, dichloromethane, toluene and benzyl alcohol were purchased from Aldrich. Phosgene gas and N,N.N',N'-tetraethylurea, N,N-diethyl benzylcarbamate and diethylamine hydrochloride standards were supplied by Makhteshim Chemical Works.

Instrumentation

A Varian Model 3700 gas chromatograph with a flame-ionization detector, equipped with a 6 ft. × 3 mm I.D. glass column filled with a 1:1 mixture of 10% QF-1 and 15% DC-200 on Gas-Chrom Q (80–100 mesh) was used. The column temperature was maintained at 150°C, the injector at 230°C and the detector at 240°C. The carrier gas was helium at a flow-rate of 35 ml/min. A 5-μl sample was injected each time by means of a 10-μl Hamilton syringe. Chromatograms and peak areas were recorded on a Spectra-Physics Model 4720 integrator.

Procedure for derivatization

A stock solution of 10% (v/v) diethylamine in dichloromethane was prepared and 40 ml of this solution was transferred into a 100-ml volumetric flask which was stoppered and weighed. This flask was allowed to stand in the cold (5°C) then the sample (0.5–1 g) containing phosgene was added with a disposable pipette and the flask was shaken manually. After leaving it for 20 min at room temperature, the flask was reweighed to determine the exact sample weight taken. Then the flask was filled to the mark with dichloromethane. Injections of 5 μl each time were then made in the sequence TEU standard and derivatized sample.

Preparation of spiked samples

A stream of phosgene was passed for some time into a previously weighed 100-ml volumetric flask containing about 70 ml of toluene. The flask was reweighed to determine the weight of phosgene added before filling to the mark with toluene. Samples of 25 ml were removed in duplicate and converted into the TEU derivative as described above. Likewise, five spiked samples were treated separately. The results obtained are given in Table I.

Synthetic reaction mixture

Benzyl chloroformate was prepared by passing phosgene into benzyl alcohol at 5°C. The excess phosgene was evaporated by passing a stream of nitrogen through the reaction mixture, during which time the temperature was allowed to rise at room temperature. Six test samples were removed at intervals of 20 min and converted into the TEU derivative as described above. The results ranged from 0.02% (minimum) to 12% (maximum) of phosgene in the reaction mixture.

Relative strengths of phosgene in toluene at elevated temperatures

First, phosgene was passed into 250 ml of toluene in a 500-ml flask until it was saturated at room temperature (24–25°C). Before removing the test samples in duplicate, a steady temperature was maintained for 20 min at each stage during an increase, *e.g.*, at 30, 40, 50, 65 and 80°C. The test samples were then converted into the TEU derivative as described above. The results of the relative strengths of phosgene in solvent toluene at elevated temperatures are given in Table II.

RESULTS AND DISCUSSION

The TEU derivative of phosgene has good GC properties, as shown in Fig. 1. The linearity of the calibration graph, tested in the range 6–110 mg per 100 ml, was very good, with a correlation coefficient of 0.9998 and a relative standard deviation of 0.7% (nine measurements). To evaluate the analytical applicability of the GC method, samples of known amounts of phosgene in toluene were converted into the TEU derivative as described above and analysed as shown in Table I. The recoveries of phosgene ranged from 93 to 97%, which confirmed that the conversion of phosgene into the TEU derivative was instantaneous.

Further experiments were made on the recovery of phosgene from the benzyl chloroformate reaction mixture. Samples were removed at intervals and treated with diethylamine. In these samples there was the possibility of not only free phosgene but

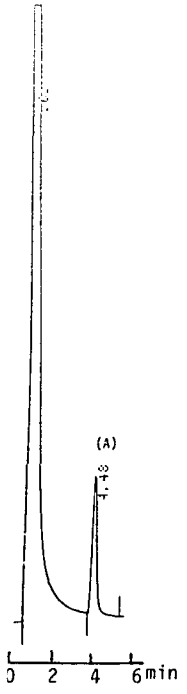

Fig. 1. Chromatogram of the N,N,N′,N′-tetraethylurea (TEU) derivative of phosgene. Attenuation, $16 \cdot 10^{-10}$; other conditions as given under Experimental.

TABLE I

RECOVERY OF PHOSGENE FROM SPIKED SAMPLES

Sample No.	Amount added (g per 100 ml)	Average recovery (g per 100 ml) (n = 2)	Recovery (%)[a]
1	2.731	2.541	93
2	4.144	3.928	94.8
3	3.342	3.175	95
4	5.179	4.956	95.7
5	9.892	9.595	97

[a] R.S.D. (all results) = 1.53%.

also benzyl chloroformate reacting with diethylamine to form N,N-diethyl benzylcarbamate and diethylamine hydrochloride as impurities. The TEU derivative of the test samples was then subjected to GC and no interference from the above impurities was observed. A chromatogram for the separation is shown in Fig. 2. The minimum and maximum recoveries of phosgene from the benzyl chloroformate reaction mixture were in the range 0.02–12%.

The relative strengths of phosgene in toluene solvent were studied at elevated temperatures. It was observed that the stability of phosgene in toluene decreased with

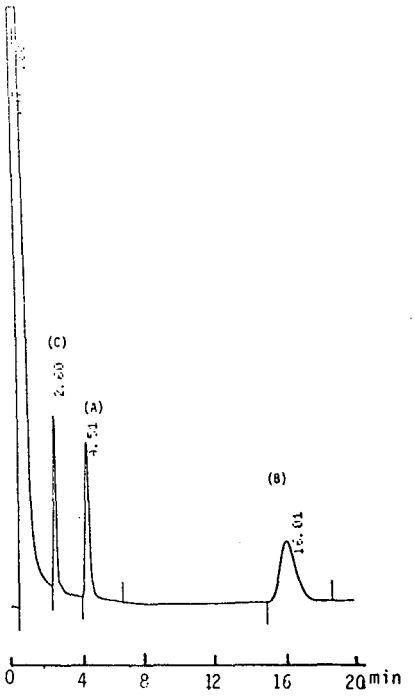

Fig. 2. Chromatogram showing the separation of impurities such as N,N-diethyl benzylcarbamate (B) and diethylamine hydrochloride (C) from the main peak of the TEU derivative (A) of phosgene. GC conditions as in Fig. 1.

TABLE II

RELATIVE STRENGTHS OF PHOSGENE IN TOLUENE SOLVENT AT ELEVATED TEMPERATURES

Temperature (°C)	Average phosgene content (g/100 ml) ± S.D. (n = 2)
24–25 (saturated)	77.8 ± 1.8
30	72.1 ± 0.9
40	48.6 ± 1.1
50	35.8 ± 1.2
65	22.2 ± 1.5
80	13.3 ± 1.2

increase in temperature; the results obtained are given in Table II. Such studies of the solubility of phosgene in toluene are important for practical application in organic synthesis.

Determination of phosgene at the ppm level was achieved using a flame ionization detector sensitivity of 10^{-11}. At this sensitivity, it was possible to detect the TEU derivative of phosgene at a level of 5 ppm ($2.5 \cdot 10^{-5}$ mg), as shown in Fig. 3.

In conclusion, the GC method described here is simple and convenient and is proposed as an alternative procedure for the determination of the extremely corrosive and toxic phosgene.

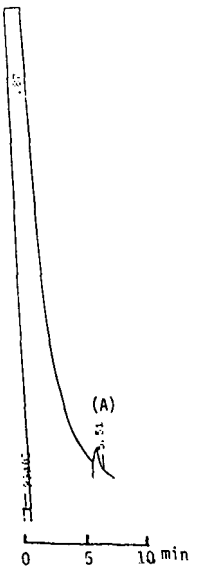

Fig. 3. Chromatogram of TEU derivative at a minimum level of 5 ppm (2.5×10^{-5} mg). Attenuation, $8 \cdot 10^{-11}$; helium flow-rate, 30 ml/min; other conditions as in Figs. 1 and 2.

ACKNOWLEDGEMENT

We thank Mr. Lambert Fuss for providing excellent technical assistance during this investigation.

REFERENCES

1 J. A. Dahlberg and I. B. Kihlman, *Acta Chem. Scand.*, 24 (1970) 644.
2 P. K. Basu, C. J. King and S. Lynn, *J. Chromatogr. Sci.*, 10 (1972) 479.
3 G. G. Esposito, D. Lillian, G. E. Podolak and R. M. Tuggle, *Anal. Chem.*, 49 (1977) 1774.
4 A. Baiker, H. Geisser and W. Richarz, *J. Chromatogr.*, 147 (1978) 453.
5 D. Reicher, U. Spengler and D. Henschler, *J. Chromatogr.*, 179 (1979) 181.
6 A. Kuessner, *J. Chromatogr.*, 204 (1981) 159.
7 S. I. Obtemperanskaya and T. A. Shinskoya, *Vestn. Mosk. Univ. Khim.*, 24 (1969) 73.
8 S. I. Obtemperanskaya, Yu. N. Tikhonov, N. S. Moroz, T. A. Shinskaya, A. G. Egorova, V. N. Likhosherstova, E. G. Chalenko and I. Ya. Tsypkina, *Probl. Anal. Khim.*, 1 (1970) 220.
9 M. H. Noweir and E. A. Pfitzer, *Am. Ind. Hyg. Assoc. J.*, 32 (1971) 163.
10 O. Petersen and H. D. Schmidt, *Ger. Offen.*, 2 627 487, 1977; *C.A.*, 88 (1978) 78418d.
11 J. Kroupa, Z. Bohac, V. Chmatal and M. Vesely, *Czech. Pat.*, 171 308, 1978; *C.A.*, 90 (1979) 8116w.
12 L. Sobolova and M. Souiek, *Czech. Pat.*, 169 579, 1977; *C.A.*, 88 (1978) 11489j.
13 J. P. Hendershott, *Am. Ind. Hyg. Assoc. J.*, 47 (1986) 742.
14 M. Hori, T. Furuya and Y. Kabayashi, *Bunseki Kagaku*, 34 (1985) 211; *C.A.*, 104 (1986) 14171j.

Journal of Chromatography, 538 (1991) 441–446
Elsevier Science Publishers B.V., Amsterdam

CHROM. 22 887

Short Communication

Determination of patulin by capillary gas chromatography of the heptafluorobutyrate derivative

EDWARD J. TARTER[a]

Field Operations Directorate, Health Protection Branch, Health and Welfare Canada, Scarborough, Ontario M1P 4R7 (Canada)

and

PETER M. SCOTT*

Bureau of Chemical Safety, Food Directorate, Health Protection Branch, Health and Welfare Canada, Ottawa, Ontario K1A 0L2 (Canada)

(First received June 8th, 1990; revised manuscript received October 2nd, 1990)

ABSTRACT

Formation and capillary gas chromatography of patulin heptafluorobutyrate is reported for the first time. The derivative was identified by gas chromatography–mass spectrometry ($M^+ = 350$). Electron-capture detector response for patulin heptafluorobutyrate was linear in the range 0.05 to 0.5 ng. This sensitive and reproducible derivatization technique was applied to the determination of patulin in apple juice by capillary gas chromatography–electron-capture detection. The overall method recovery averaged 84% and ≤ 10 μg/l could be detected.

INTRODUCTION

Patulin (Fig. 1) is a toxic mold metabolite produced by several species of *Aspergillus* and *Penicillium* and by *Byssochlamys nivea* [1]. It is frequently found in apple juice [1–3] and is regulated in that product in several European countries at a tolerance level of 50 μg/kg [4].

Although liquid chromatography (LC) is currently the method of choice for determination of patulin in apple juice and other foods [2,5], there are numerous methods utilizing gas chromatography (GC). Most of these involve derivatization of patulin to its trimethylsilyl (TMS) ether, for which both electron-capture detection (ECD) [6–9] and mass spectrometry (MS) [3,10–13] offer sub-nanogram sensitivity not

[a] Present address: P.O. Box 623, Thornhill, Ontario L3T 4A5, Canada.

0021-9673/91/$03.50

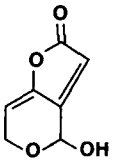

Fig. 1. Chemical structure of patulin.

possible with flame ionization detection [14–17]. Other derivatives of patulin that have been used for GC analysis are the acetate and chloroacetate [16–20], but the lowest reported detection limit was only 12 ng (for the chloroacetate by ECD [16]). Derivatization of patulin to the trifluoroacetate or heptafluorobutyrate (HFB) with trifluoroacetic anhydride and heptafluorobutyric anhydride, respectively, was not satisfactory, according to Bergner-Lang *et al.* [20]. We nevertheless report here for the first time the formation and capillary GC–ECD of patulin HFB, a highly sensitive analytical technique which was applied to the determination of patulin in apple juice.

EXPERIMENTAL

Derivatization of patulin

Patulin working standard solution (10.0 μg/ml chloroform) (200 μl) was evaporated to dryness under nitrogen in a 3.7-ml vial. The HFB derivative was formed by a procedure similar to that used for trichothecenes [21]. After addition of toluene–acetonitrile (95:5) (500 μl) and heptafluorobutyrylimidazole (HFBI) (25 μl), the vial was closed with a PTFE-lined screw cap, mixed 20–30 s on a vortex mixer, and heated in a heating block at 60°C for 10–15 min. After cooling to room temperature (it was later found that derivatization occurred within 1 min without heating), 5% sodium bicarbonate solution (1.0 ml) and toluene–acetonitrile (95:5) (500 μl) were added, shaken 45–60 s on the vortex mixer, and the layers allowed to separate (if the top layer was not clear, additional mixing for 15–20 s was necessary). Using an adjustable Eppendorf pipet, 250 μl of the top layer was added to *n*-heptane (4.75 ml) containing 50 ng hexachlorobenzene (HCB)/ml as internal standard in an 11-ml vial. The vial was closed with a PTFE-lined screw cap and shaken 5 s on the vortex mixer. This solution contained patulin HFB at a concentration corresponding to 0.1 μg patulin/ml; 2.0 μl (or another suitable volume) were injected into the gas chromatograph.

Gas chromatography

Capillary GC was carried out on a Varian 6000 gas chromatograph equipped with an autosampler, a split–splitless injector (250°C) operating in the splitless mode, a J&W Scientific DB-5 fused-silica capillary column (30 m × 0.32 mm I.D., 0.25 μm film thickness), and a ^{63}Ni electron-capture detector (at 350°C). Column temperature programs used are given in the captions to Figs. 2 and 3. The carrier gas was helium (34.6 cm/s) and the make-up gas was nitrogen (20 ml/min). Attenuation was 64 at range 10.

Gas chromatography–mass spectrometry

The mass spectrum of patulin HFB was recorded on a VG Micromass ZAB-2F mass spectrometer operated at 1500 resolution and 70 eV electron energy and interfaced with a Varian 3700 gas chromatograph equipped with splitless injection (180°C) and a 25 m × 0.25 mm I.D. DB-5 fused-silica capillary column (0.25 μm film thickness). The column was programmed from 80°C (after 1 min) to 220°C at 5°C/min. The amount of patulin injected (as HFB) was 80 ng.

Analysis of apple juice

Apple juice was extracted with ethyl acetate and cleaned up on a silica gel column according to the official method of the Association of Official Analytical Chemists [22,23]. Extracts were first analysed by two-dimensional thin-layer chromatography (TLC) [23]. The extract from 45 g apple juice was then evaporated, derivatized, and analysed by GC–ECD as described above, using the column temperature program given in the caption to Fig. 3 for both sample and patulin standard and quantitating by peak-area ratios.

RESULTS AND DISCUSSION

Patulin HFB had a retention time of 11.8 min under the column programming conditions described in Fig. 2. The peak was identified by GC–MS, with a molecular ion at m/z 350, ions at m/z 197 ($C_3F_7CO^+$) and 169 ($C_3F_7^+$) that confirmed the

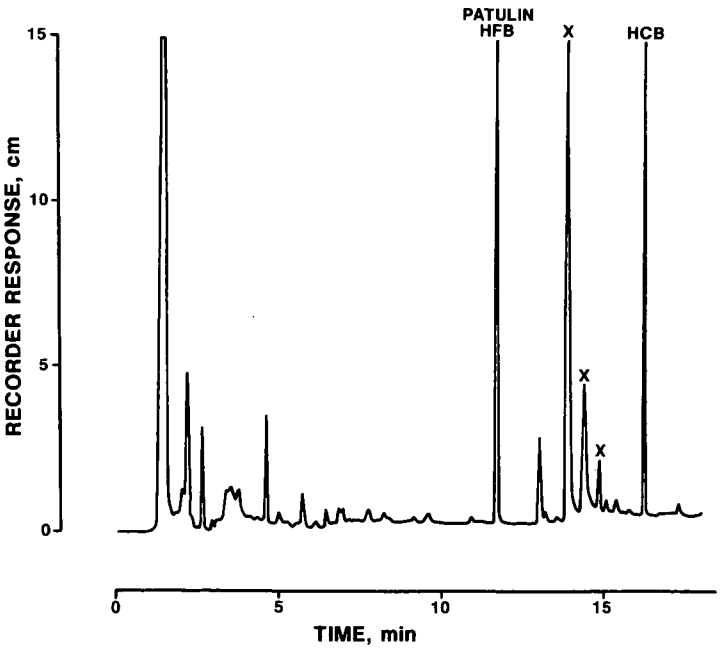

Fig. 2. Gas chromatogram of patulin HFB (0.2 ng patulin injected). Peaks marked × arise from the HFBI reagent; hexachlorobenzene (HCB) is internal standard. Column temperature program: 80°C (1 min), 5°C/min to 140°C, 20°C/min to 210°C.

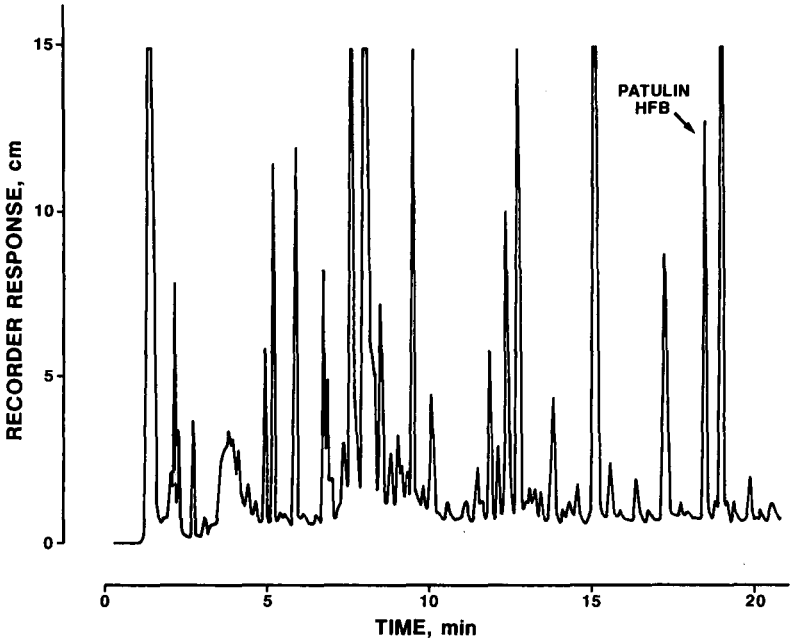

Fig. 3. Gas chromatogram of HFBI-derivatized extract of apple juice estimated to contain 38 μg patulin/l. Column temperature program: 80°C (1 min), 2°C/min to 120°C.

presence of the HFB moiety, and other ions at *m/z* 153, 136, 125, 110, 97, 82, 71, 69, 55 and 53 that were consistent with a patulin-H moiety [24,25] (Fig. 4). The later eluting peaks in the chromatogram were from the reagent blank; the two major ones had molecular ions at *m/z* 461 and 370.

The derivatization reaction was highly reproducible. When 2.0 μg patulin was derivatized and the equivalent of 0.2 ng injected, mean integrator area counts for a duplicate series of injections from 6 reactions were 202 818 and 200 172 with coefficients of variation (C.V.) of 1.9 and 4.0%, respectively. By comparison, mean area counts for 0.1 ng HCB used as internal standard were 324 634 (n = 6, C.V. 2.1%) and 316 456 (n = 6, C.V. 3.4%). The patulin HFB derivative was stable in n-heptane solution for up to 35 h at room temperature.

The ECD response for patulin HFB was linear in the range 0.05 ng to 0.5 ng patulin. In fact, it would be possible to detect and measure considerably less than 0.05 ng patulin, in view of the detector range and attenuation used in this study. Thus, the HFB derivative is probably more sensitive for ECD than the TMS derivative, for which the minimum determinable amount of patulin was reported as 0.1 ng, albeit on a packed column [7,9]. Sensitivity appears to be similar to that of the TMS derivative determined by capillary GC–MS [3] and is achieved with less expensive and more readily available instrumentation. By comparison, the lowest level of patulin reported to be detectable by LC was 1 ng [5].

The HFB derivatization technique was applied to determination of patulin in apple juice. For this analysis, a GC temperature program with a slower heating rate

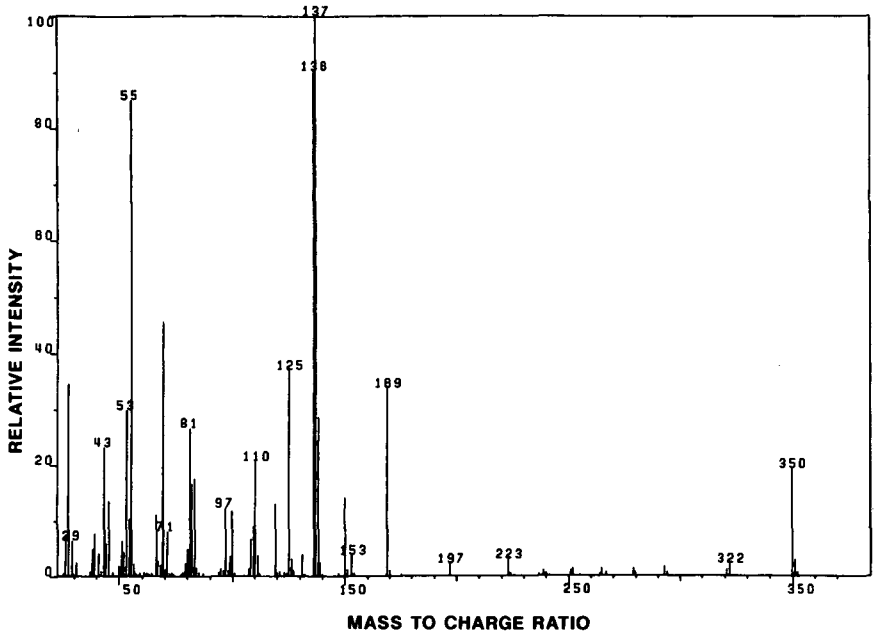

Fig. 4. Mass spectrum of patulin HFB after separation by GC.

was preferable and the retention time for patulin HFB was 18.7 min (Fig. 3). Two naturally contaminated samples determined to contain 78 and 38 μg/l by TLC were found to contain 99 and 38 μg/l, respectively, when the extracts were analysed by GC–ECD. The detection limit by GC was $\leqslant 10$ μg/l. Recovery of patulin from apple juice spiked at 100 μg/l averaged 85% ($n = 6$, range 73–95%); in a second set of experiments (where derivatization was carried out at room temperature), the mean recovery was 83% ($n = 6$, C.V. 6.3%).

In conclusion, GC–ECD of patulin HFB is a sensitive and reproducible procedure for quantitative determination of patulin that can be used for analysis of apple juice.

ACKNOWLEDGEMENTS

The authors thank W. Ng, B. P. C. Kennedy and S. R. Kanhere for technical assistance and W. F. Sun and P.-Y. Lau for GC–MS.

REFERENCES

1 *IARC Monographs on the Evaluation of the Carcinogenic Risk of Chemicals to Humans; Vol. 40, Some Naturally Occurring and Synthetic Food Components, Furocoumarins and Ultraviolet Radiation*, International Agency for Research on Cancer, Lyon, 1986, p. 83.
2 S. J. Kubacki, in P. S. Steyn and R. Vleggaar (Editors), *Mycotoxins and Phycotoxins*, Elsevier, Amsterdam, 1986, p. 293.
3 D. N. Mortimer, I. Parker, M. J. Shepherd and J. Gilbert, *Food Addit. Contam.*, 2 (1985) 165.
4 H. P. van Egmond, *Food Addit. Contam.*, 6 (1989) 139.

5 P. M. Scott, in J. F. Lawrence (Editor), *Trace Analysis*, Vol. 1, Academic Press, New York, 1981, p. 193.
6 T. Suzuki, Y. Fujimoto, Y. Hoshino and A. Tanaka, *J. Chromatogr.*, 105 (1975) 95.
7 Y. Fujimoto, T. Suzuki and Y. Hoshino, *J. Chromatogr.*, 105 (1975) 99.
8 A. Andersson and E. Josefsson, *Var Foeda*, 31 (1979) 365.
9 D. Skierska and W. Martinek, *Rocz. Panstw. Zakl. Hig.*, 35 (1984) 69.
10 J. P. Chaytor and M. J. Saxby, *J. Chromatogr.*, 214 (1981) 135.
11 M. Kellert, W. Baltes, W. Blaas and M. Wittkowski, *Fresenius Z. Anal. Chem.*, 315 (1983) 245.
12 K. R. Price, *Biomed. Mass Spectrom.*, 6 (1979) 573.
13 J. D. Rosen and S. R. Pareles, *J. Agric. Food Chem.*, 22 (1974) 1024.
14 R. W. Pero, D. Harvan, R. G. Owens and J. P. Snow, *J. Chromatogr.*, 65 (1972) 501.
15 T. Suzuki, Y. Fujimoto, Y. Hoshino and A. Tanaka, *Agric. Biol. Chem.*, 38 (1974) 1259.
16 A. E. Pohland, K. Sanders and C. W. Thorpe, *J. Assoc. Off. Anal. Chem.*, 53 (1970) 692.
17 T. Suzuki, M. Takeda and H. Tanabe, *J. Food Hyg. Soc. Jpn.*, 12 (1971) 489.
18 G. M. Ware, C. W. Thorpe and A. E. Pohland, *J. Assoc. Off. Anal. Chem.*, 57 (1974) 1111.
19 J. W. Ralls and R. M. Lane, *J. Food Sci.*, 42 (1977) 1117.
20 B. Bergner-Lang, M. Kächele and E. Stengel, *Dtsch. Lebensm.-Rundsch.*, 79 (1983) 400.
21 P. M. Scott, P.-Y. Lau and S. R. Kanhere, *J. Assoc. Off. Anal. Chem.*, 64 (1981) 1364.
22 P. M. Scott, in K. Helrich (Editor), *Official Methods of Analysis of the Association of Official Analytical Chemists*, Vol. 2, Association of Official Analytical Chemists, Arlington, VA, 15th ed., 1990, p. 1184.
23 P. M. Scott, *J. Assoc. Off. Anal. Chem.*, 57 (1974) 621.
24 A. I. Scott and M. Yalpani, *Chem. Commun.*, (1967) 945.
25 P. M. Scott, W. F. Miles, P. Toft and J. G. Dubé, *J. Agric. Food Chem.*, 20 (1972) 450.

Journal of Chromatography, 538 (1991) 447–451
Elsevier Science Publishers B.V., Amsterdam

CHROM. 22 923

Short Communication

Release of 2-aminofluorene from N-(deoxyguanosin-8-yl)-2-aminofluorene by hydrazinolysis

JOTHI BAKTHAVACHALAM[a], SAMY ABDEL-BAKY and ROGER W. GIESE*
Department of Medicinal Chemistry in the College of Pharmacy and Allied Health Professions, and Barnett Institute of Chemical Analysis and Materials Science, Northeastern University, Boston, MA 02115 (U.S.A.)
(First received May 23rd, 1990; revised manuscript received October 16th, 1990)

ABSTRACT

High temperature (160°C) hydrazinolysis is demonstrated to be a useful chemical transformation reaction for releasing an aminopolyaromatic hydrocarbon, 2-aminofluorene, from a parent DNA adduct, N-(deoxyguanosin-8-yl)-2-aminofluorene.

INTRODUCTION

Inherent structural changes are sometimes made in an analyte as part of sample pretreatment in order to improve its separation and/or detection properties in an analytical procedure. This general strategy can be called "chemical transformation". Examples are the oxidation of cholesterol [1], the deamination of N7-(2-hydroxyethyl)guanine [2], the acidic reduction of tryptophan [3] and the alkaline reduction of thymine glycol [4] in methods used to quantify these substances.

We are interested in broadening the usefulness of gas chromatography (GC) with electron capture negative ion mass spectrometry (ECNI-MS) for the sensitive detection of DNA adducts by using chemical transformation as part of sample pretreatment. DNA adducts are trace analytes which constitute the covalent damage to *in vivo* DNA when an animal or human is exposed to toxic chemical or physical conditions. Conventional derivatization reactions are adequate to convert many small DNA adducts (*e.g.*, damage to DNA by methylating agents) into products which can be detected by GC–ECNI-MS [5]. However, for large DNA adducts (*e.g.*, damage to DNA by polyaromatic hydrocarbons), chemical transformation is needed because the low volatility and thermal stability of such adducts for GC purposes cannot be adequately overcome by conventional derivatization.

[a] Present address: Polaroid and Behringwerke Diagnostic Systems, Westwood, MA 02090, U.S.A.

0021-9673/91/$03.50

Here we introduce a new reaction, in terms of the substrate and conditions, which achieves the release of 2-aminofluorene from the polyaromatic hydrocarbon DNA adduct, N-(deoxyguanosin-8-yl)-2-aminofluorene. The overall goal is to establish a method by which this adduct can be measured using GC–ECNI-MS. In the proposed method, 2-aminofluorene is released from the adduct by this chemical transformation reaction, converted into an electrophoric derivative, and detected by GC–ECNI-MS.

Polyaromatic hydrocarbon DNA adducts can be measured by immunoassay [6], ^{32}P-post labeling [7] and fluorescence [8] procedures. These methods do not always provide sufficient scope, sensitivity and precision. For example, different values can be obtained when they are applied to the measurement of a given DNA adduct, or class of adducts, in the same samples [9,10]. Potentially some improvements over existing methods for the measurement of polyaromatic hydrocarbon DNA adducts can be achieved by using GC–ECNI-MS.

EXPERIMENTAL

Reagents

Anhydrous hydrazine (Aldrich, Milwaukee, WI, U.S.A.) was treated with 20% (w/w) of KOH overnight, followed by distillation under anhydrous conditions. The fraction that distilled at 110°C was collected. 2-Aminofluorene (98%) was from Aldrich. High-performance liquid chromatography (HPLC) solvents were from Burdick & Jackson (American Scientific, Boston, MA, U.S.A.). N-(Deoxyguanosin-8-yl)-2-aminofluorene (dGAF) and N-(deoxyguanosin-8-yl)-2-acetylaminofluorene were kindly provided by Dr. F. A. Beland (National Center for Toxicological Research, Jefferson, AR, U.S.A.).

Hydrazinolysis procedure

A methanolic solution (5 μl from a more concentrated stock solution) of dGAF (116.5 ng) was evaporated in a 1 ml ampule, followed by the addition of 20 μl of anhydrous hydrazine. The ampule was flame-sealed and heated at 180°C for 24 h in a Reacti-Block aluminium block E-1 (13 ampule capacity; Pierce, Rockford, IL, U.S.A.). This heating was achieved by placing the block in a Pyrex crystallizing dish (50 × 75 mm I.D.) which had been filled to a depth of 3.5 cm with silicone oil. Each hole in the heating block had been filled to a depth of 1.5 cm with sea sand, in order to heat primarily the bottom of the ampule. The ampule was cooled to room temperature, its top removed, and the excess reagent was evaporated to dryness using a Speed-Vac. After the addition of 100 μl of acetonitrile–water (2:1, v/v) 10 μl was injected into an HPLC system.

RESULTS AND DISCUSSION

Previously we optimized the derivatization of aminopolyaromatic hydrocarbons (amino-PAHs), such as 2-aminofluorene, for the purpose of detecting such compounds by GC–ECNI-MS [11]. Electrophoric derivatives were formed, and the most promising one was a pentafluorobenzylidene derivative. In order to use this methodology to measure corresponding DNA adducts, in which an amino-PAH

moiety is covalently attached to DNA, it is necessary to first liberate the amino-PAH. Towards this goal, we subjected the DNA adduct, N-(deoxyguanosin-8-yl)-2-aminofluorene, to a wide range of acidic and basic hydrolysis conditions (data not shown). While the desired product, 2-aminofluorene (2-AF), was always observed by HPLC, the yield never rose much above 10%.

A somewhat higher yield of 2-AF was formed (20%) when the parent adduct (*e.g.*, 10 μg) was subjected to hydrazinolysis under conventional conditions (100°C, 24 h). Increasing the reaction temperature (but not the time) up to 200°C increased the yield to 65%. The recovery of the product itself, 2-AF, subjected to hydrazinolysis under these conditions was 86 $\pm$ 3%. These collective observations suggested that the lower yields of 2-AF from the adduct at lower temperature were not due to instability of the 2-AF product under the reaction conditions. Instead a higher temperature apparently favored the formation of product, 2-AF, over unknown side products.

Thus we have achieved the following new chemical transformation.

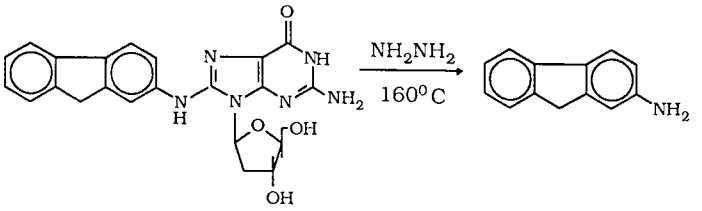

Changing the reaction vessel from a capped vial to a flame-sealed ampule improved the precision of the yield by overcoming variation from one vial to another in leakage of the hydrazine through the vial seal. This did not present a safety problem because small volumes (20 μl) of hydrazine were employed.

The yield of 2-AF from the adduct was about 10% higher when other forms or derivatives of hydrazine were tested: hydrazine hydrochloride, carbohydrazide, hydroxyethyl-hydrazine, *p*-hydrazinobenzoic acid and 2-hydrazino-2-imidazoline hydrobromide. However, the increase in yield was small with these other reagents, and hydrazine can be removed at the end of the reaction by evaporation. (In our method, we either do this, or remove the hydrazine by HPLC after dilution of the reaction mixture with water and methanol.) Thus we selected hydrazine for additional study.

In the optimized, overall procedure that we developed, the parent DNA adduct is subjected to hydrazinolysis at 160°C for 24 h. The reaction shows promise for being applied to a trace amount of analyte. For example, the yield of 2-AF (by HPLC) starting from 115 ng of the adduct is 62 $\pm$ 2%. The related adduct, N-(deoxyguanosin-8-yl)-2-acetylaminofluorene, also forms 2-AF in the same yield. As shown in Fig. 1, aside from non-retained, polar compounds, analysis of the crude reaction mixture by HPLC shows only a single peak, which is the product.

We have also extended our earlier work [11] on the detection of 2-AF by GC–ECNI-MS. As shown in Fig. 2, 10 fg (25 amol) of the pentafluorobenzylidine derivative of the compound can be detected by this technique. DNA adducts, such as N-(deoxyguanosin-8-yl)-2-aminofluorene, may need to be measured in this range when biological samples are encountered. Thus, in our future work, we need to

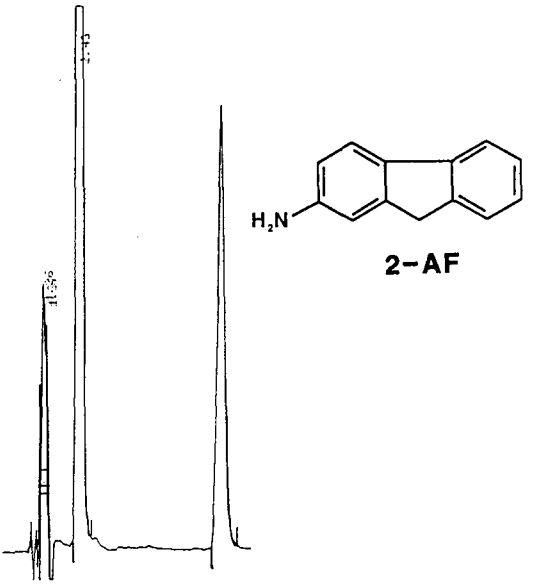

Fig. 1. HPLC separation of the hydrazinolysis reaction. N-(Deoxyguanosin-8-yl)-2-aminofluorene (5 μg) was subjected to hydrazinolysis in 150 μl of hydrazine. The reaction mixture was treated with 100 μl of water and 150 μl of methanol, then 10 μl of this solution were injected into the HPLC. Column: Brownlee (Rainin Instruments, Woburn, MA, U.S.A.) analytical cartridge, RP-8 reversed-phase, (10 cm × 4.6 mm I.D.), 5 μm particle size. Mobile phase: acetonitrile–10 m*M* potassium dihydrogen phosphate adjusted to pH 6.6 with 5 m*M* triethylamine (45:55, v/v) at 1 ml/min. Detection at 280 nm. Retention time 6.8 min.

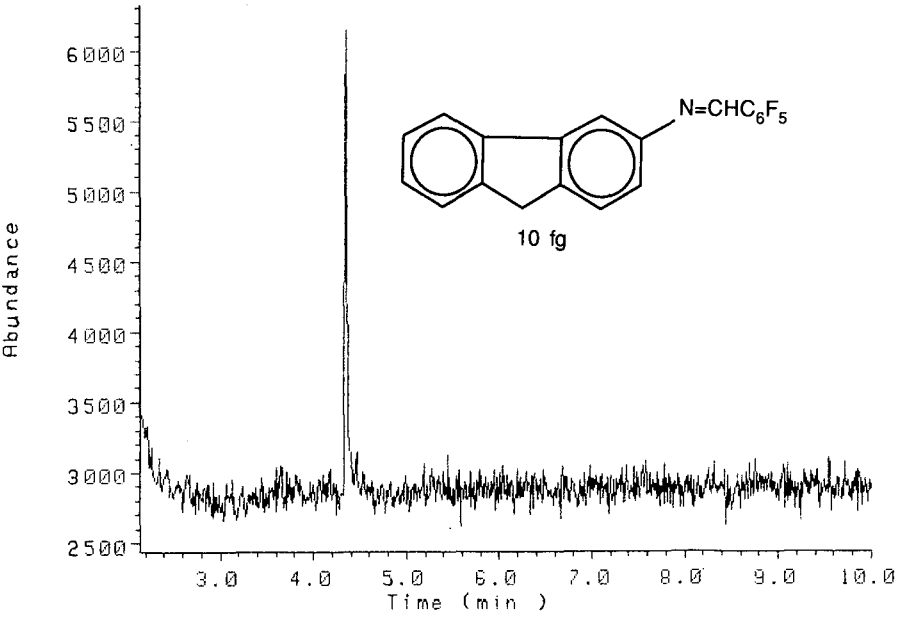

Fig. 2. Detection of N-pentafluorobenzylidenyl-2-aminofluorene by GC–ECNI-MS. Sample: 1 μl of toluene containing 10 fg of analyte. Instrument: Hewlett-Packard (Andover, MA, U.S.A.) Model 5890/5988A. Injection: splitless mode with splitless valve open after 0.8 min. Column: 12 m × 0.2 mm I.D., 0.33 μm film, Ultra-1 (Hewlett-Packard) fused-silica capillary, with 20 p.s.i. helium carrier gas. Conditions: 2 Torr of methane in the source; electron energy 240 eV, source temperature 200°C, emission current 300 μA, interface between GC and MS at 280°C, initial GC oven temperature 100°C then ramp to 280°C at 60°C/min and hold for 5 min. Signal-to-noise ratio 40.

combine and extend the steps presented here to achieve the detection of this adduct in such samples. The effectiveness of the hydrazinolysis reaction on other adducts of this type will also be studied. It is encouraging that others have found the reaction to similarly transform a corresponding 4-aminobiphenyl DNA adduct [12].

ACKNOWLEDGEMENTS

The research described in this article was conducted in part under contract to the Health Effects Institute (HEI) an organization jointly funded by the United States Environmental Protection Agency (EPA) (Assistance Agreement X-812059) and automotive manufacturers. The specific grant was HEI Research Agreement 86-82. The contents of this article do not necessarily reflect the views of the HEI, nor do they necessarily reflect the policies of the EPA or automotive manufacturers. Contribution No. 465 from the Barnett Institute.

REFERENCES

1 E. A. Stein, in N. W. Tietz (Editor), *Textbook of Clinical Chemistry*, Saunders, Philadelphia, PA, 1986, p. 882.
2 K. Allam, M. Saha and R. W. Giese, *J. Chromatogr.*, 499 (1990) 571.
3 W. S. D. Wong, D. T. Osuga, T. S. Burcham and R. E. Feeney, *Anal. Biochem.*, 143 (1984) 62.
4 K. A. Schellenberg and J. Shaeffer, *Biochemistry*, 25 (1986) 1479.
5 M. Saha, G. M. Kresbach, R. W. Giese, R. S. Annan and P. Vouros, *Biomed. Environ. Mass Spectrom.*, 18 (1989) 958.
6 R. B. Everson, E. Randerath, R. M. Santella, R. C. Cefalo, T. A. Avitts and K. Randerath, *Science (Washington, D.C.)*, 231 (1980) 54.
7 E. Randerath, T. A. Avitts, M. V. Reddy, R. H. Miller, R. B. Everson and K. Randerath, *Cancer Res.*, 46 (1986) 5869.
8 K. Vahankangas, A. Haugen and C. C. Harris, *Carcinogenesis (London)*, 6 (1985) 1109.
9 N. Koga, P. B. Inskeep, T. M. Harris and F. P. Guengerich, *Biochemistry*, 25 (1986) 2192.
10 K. Savela, K. Hemminki, A. Hewer, D. H. Phillips, K. L. Putman and K. Randerath, *Mutat. Res.*, 224 (1989) 485.
11 J. Bakthavachalam, R. S. Annan, F. A. Beland, P. Vouros and R. W. Giese, *J. Chromatogr.*, 500 (1990) 373.
12 F. Kadlubar, personal communication.

Journal of Chromatography, 538 (1991) 452–455
Elsevier Science Publishers B.V., Amsterdam

CHROM. 22 830

Short Communication

Rapid method for the detection and determination of artemisinin by gas chromatography

A. T. SIPAHIMALANI*, D. P. FULZELE and M. R. HEBLE

Bio-Organic Division, Plant Biotechnology Section, Bhabha Atomic Research Centre, Trombay, Bombay 400 085 (India)

(First received June 12th, 1990; revised manuscript received August 24th, 1990)

ABSTRACT

Artemisinin, an antimalarial principle of *Artemisia annua*, is thermally unstable and decomposes on the column to give two peaks under various gas chromatographic conditions. A simple and rapid method was developed for its indirect detection and determination, at nanogram levels, both in plants and in tissue cultures developed from the plants. It is based on the linear relationship obtained between the concentration of artemisinin and the respective peak areas for either of the two thermally degraded products.

INTRODUCTION

Artemisinin (Qinghaosu, QHS) is a naturally occurring antimalarial principle isolated from *Artemisia annua* L. (Compositae) [1]. This compound has attracted great attention because it can offer effective control, against the strains of *Plasmodium falciparum* that have, over the years, developed resistance to chloroquin treatment and also against cerebral malaria in humans [2,3]. *A. annua* is native to China, but in recent years it has been successfully cultivated in the U.S.A., Europe and India. Many

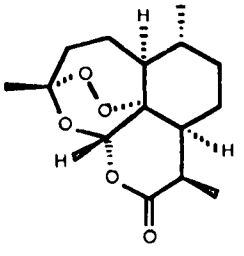

Artemisinin

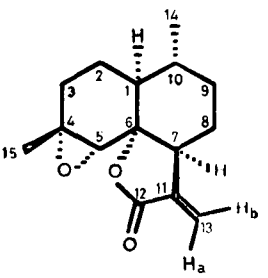

Arteannuin-B

0021-9673/91/$03.50

laboratories are engaged in developing tissue culture technology [4] for the production of the active principle. Hence it is necessary to develop a suitable technique for its detection and determination at micro- or nanogram levels in both plants and tissue cultures.

High-performance liquid chromatography (HPLC) for the detection and determination of artemisinin requires the use of an electrochemical detector [5], which is not commonly available in many laboratories. The alternative choice of the widely used UV detector has limitations as the compound does not possess UV absorption and has to be derivatized to a UV-absorbing compound [6]. Gas chromatography (GC) method has not been attempted, possibly because of the unstable nature of the endoperoxy group. Thermal stability studies [7,8] have indicated that artemisinin is stable up to 150°C but degrades into number of products when heated at 180–200°C. We have developed a simple and rapid GC method that is based on the indirect detection and determination of artemisinin on the basis of its thermally degraded products, eluted from the column.

EXPERIMENTAL

Materials

Artemisinin was kindly donated by Dr. D. L. Klayman (Walter Reed Army Institute of Research, Washington, DC, U.S.A.). Aretannuin-B was obtained from Dr. R. S. Thakur (Central Institute of Medicinal and Aromatic Plants, Lucknow, India). OV-17 and Gas-Chrom Q (80–100 mesh) were purchased from Applied Science Labs. (State College, PA, U.S.A.).

Gas chromatography

GC was performed on a Shimadzu GC-16 A gas chromatograph fitted with a flame ionization detector. A glass column (2 m × 3.2 mm I.D., silanized) was packed in the laboratory with 3% OV-17 on Gas-Chrom Q (80–100 mesh). Nitrogen was used as the carrier gas at a flow-rate of 40 ml/min. The detector temperature was maintained at 250°C whereas the injector temperature was varied from 200 to 240°C and was maintained at the same level as column temperature. Analyses were carried out isothermally (200, 210, 220, 230 and 240°C) and with temperature programming (100 to 240°C at 4°C/min).

Linear calibration graphs were plotted as the peak areas of the decomposition products *versus* the respective concentrations of the parent compound.

Mass spectral (MS) analyses (electron impact mode) were carried out on a Shimadzu GC-MS QP 1000 mass spectrometer. GC–MS analyses were performed on a 3% OV-17 analytical column with helium as the carrier gas at a flow-rate of 55 ml/min. Both artemisinin and arteannuin-B were analysed using a direct insertion (DI) probe and the GC mode. Artemisinin, in the GC mode, gave a fragmentation pattern for two peaks, A and B. Arteannuin-B gave the same MS pattern in the DI and GC modes. The respective fragmentation patterns were as follows: artemisinin, DI mode, m/z 282 (M^+), 250, 232 and 192 and GC mode peak A 282, 269, 224, 211, 195, 192 and 179 and peak B 284, 269, 253, 236, 222 and 204; arteannuin-B, DI and GC modes, m/z 248 (M^+), 230, 220, 215, 206 and 190.

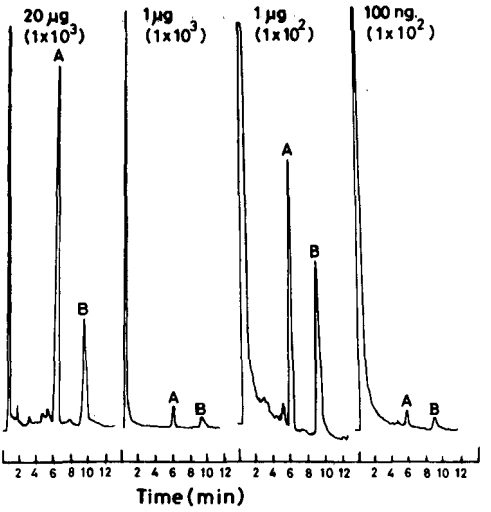

Fig. 1. Isothermal runs on artemisinin (240°C). Different concentrations at two sensitivities (1×10^3 and 1×10^2). A (5.93 min) and B (9.10 min) are the two decomposition products of artemisinin.

RESULTS AND DISCUSSION

The isothermal run with artemisinin (240°C) showed the presence of two peaks, A and B (Fig. 1). The mass fragmentation patterns of A and B, as obtained by GC–MS, did not correspond to that of parent compound. Hence these were artifacts of artemisinin, formed during thermal degradation in the column. With a view to studying the effect of temperature on the thermal stability of the compound, the isothermal runs were repeated at a lower temperature of 200°C and also with temperature programming from 100 to 240°C at 4°C/min. Care was taken to maintain the injector temperature the same as the column temperature. Each time, two peaks were obtained (A and B).

Various concentrations were subjected to GC. A linear relationship was observed between the concentration of artemisinin and the peak areas of its degradation products A and B (Fig. 2). Hence either of the two peaks could be utilized for the detection and determination of artemisinin in unknown samples. Working at the normal sensitivity level (1×10^3), the detection limit was about 1 μg and linearity was observed between 1 and 20 μg of sample. At a higher sensitivity setting (1×10^2), the detection limit was as low as 100 ng.

A problem arises if the plants or the tissue extracts also contain arteannuin-B, because it has the same retention time as A under both isothermal and temperature-programmed conditions. The GC–MS data of arteannuin-B and compound A indicated that the two compounds are different. The presence of arteannuin-B could easily be deduced as it would increase the proportion of A with respect to B. In that event, artemisinin can be determined on the basis of the linear calibration graph for compound B only. Arteannuin-B possesses UV absorption and can easily be detected and determined, at nanogram levels, by HPLC.

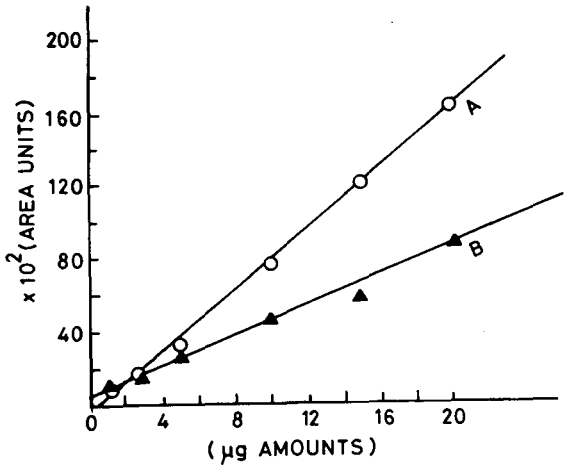

Fig. 2. Linear calibration graph for the two decomposition products (A and B) of artemisinin obtained in an isothermal run (240°C) at 1×10^3 attenuation.

This method was applied [9] to the detection and determination of artemisinin in *A. annua* plants and in plantlet cultures developed under different conditions.

REFERENCES

1 X.-D. Luo and C.-C. Shen, *Med. Res. Rev.*, 7 (1987) 29–52.
2 China Cooperative Research Group on Qinghaosu and Its Derivatives as Antimalarials, *J. Trad. Chin. Med.*, 2 (1982) 17 and 45.
3 G. Li, X. Guo, R. Jin, H. Jian and Z. J. Li, *J. Trad. Chin. Med.*, 2 (1982) 125.
4 B. C. Martinez and E. J. Staba, *Adv. Cell Cult.*, 6 (1988) 69–87.
5 N. Acton, D. L. Klayman and I. J. Rollman, *Planta Med.*, 51 (1985) 445–446.
6 S.-S. Zhao and M.-Y. Zeng, *Yaowu Fenxi Za Zhi*, 6 (1986) 3–4.
7 A. J. Lin, D. L. Klayman, J. M. Hock, J. V. Silverston and C. F. George, *J. Org. Chem.*, 50 (1985) 4504–4508.
8 X.-D. Luo, H. J. C. Yeh, A. Brossi, J. L. Flippen-Anderson and R. Gilardi, *Heterocycles*, 23 (1985) 881–887.
9 D. P. Fulzele, A. T. Sipahimalani and M. R. Heble, *Phytother. Res.*, (1990) in press.

Journal of Chromatography, 538 (1991) 456–461
Elsevier Science Publishers B.V., Amsterdam

CHROM. 22 843

Short Communication

Mild hydrophobic interaction chromatography: prediction of chromatographic behaviour by preliminary analysis by "partition between aqueous two-phase systems"

R. MATHIS, P. HUBERT* and E. DELLACHERIE
Laboratoire de Chimie-Physique Macromoléculaire, URA CNRS 494, ENSIC, BP 451, 54001 Nancy Cedex (France)
(First received April 3rd, 1990; revised manuscript received July 6th, 1990)

ABSTRACT

Mildly hydrophobic stationary phases prepared by coupling amino derivatives of various polyoxyalkylene glycols to Sepharose 6B have previously proved successful for the separation of three closely related enzymes present in the same crude extract. A preliminary analysis of the crude mixture of proteins in aqueous biphasic systems consisting of a polyoxyalkylene glycol-rich top phase and a saline bottom phase affords valuable information that can be exploited to predict experimental conditions for optimum resolution by chromatography.

INTRODUCTION

Mild hydrophobic polymers may be covalently immobilized onto inert supports to afford chromatographic stationary phases that are less denaturing towards biomolecules than those generally used in traditional hydrophobic interaction chromatography [1–7]. Such stationary phases were prepared by coupling amino derivatives of various polyoxyalkylene glycols of increasing hydrophobicity [polyoxyethylene (POE) < Pluronic (copolymer of polyoxyethylene and polyoxypropylene) < polyoxypropylene (POP)] to Sepharose 6B previously activated by carbonyldiimidazole. The extraction of three closely related enzymes from *Pseudomonas testosteroni* [$\Delta_{5\rightarrow4}$ 3-oxosteroid isomerase (isomerase), 3α-hydroxysteroid dehydrogenase (α-HSD) and 3β,17β-hydroxysteroid dehydrogenase (β-HSD)] with the double challenge of starting from the same crude extract and performing the purification simply by stepwise elution, was described previously [7]. These chromatographic experiments were carried out on Sepharose–POE and Sepharose–Pluronic, with potassium phosphate as the mobile phase [7].

In this paper, we show that a preliminary analysis by "partition between

0021-9673/91/$03.50

aqueous two-phase systems" [8] affords valuable information that can be exploited to explain our chromatographic results. Such a procedure could be used in mild hydrophobic chromatography as a general approach, prior to chromatographic experiments, in order to predict the most satisfactory conditions for optimum resolution.

EXPERIMENTAL

All chemicals used in this study have been described previously [7], as well as the preparation of *Pseudomonas testosteroni* crude extract [5].

Biphasic systems were prepared as follows. Desired amounts of POE 6000, Pluronic, and potassium phosphate were dissolved in water (3 ml) in haemolysis tubes. After addition of *Pseudomonas testosteroni* crude extract (0.25 ml), the mixtures were adjusted to 5 g with water. The overall final content of polyethers (POE + Pluronic) was 10% (w/w), with the desired POE-to-Pluronic ratios (10:0, 9.5:0.5, 9:1 and 8:2). The final content of potassium phosphate was 10, 15 or 20% (w/w). After 30 inversions, the mixtures were allowed to stand at room temperature for 1 h. Aliquots of both phases were then carefully removed by pipette and assayed for the various enzymatic activities according to procedures already described [9,10].

RESULTS

Mild hydrophobic chromatographic experiments have previously been carried out on stationary phases prepared by covalent immobilization of POE or Pluronic on Sepharose, and with potassium phosphate as the mobile phase [7]. In this work, different aqueous two-phase systems were prepared by mixing potassium phosphate (final concentration 10, 15 or 20%, w/w) with POE + Pluronic mixtures (final overall content 10%, w/w) of various compositions (POE-to-Pluronic ratios from 10:0 to 8:2). The resulting biphasic systems are composed of a phosphate-rich bottom phase and a polyether-rich top phase, the hydrophobicity of which increases with increasing amount of Pluronic.

The partition coefficient of an enzyme, taken as the ratio of its concentration in the top phase to that in the bottom phase, is therefore a direct indication of the ability of the considered enzyme to establish interactions with the polyethers. Consequently, when chromatography with Sepharose–POE or Sepharose–Pluronic stationary phases and potassium phosphate as the mobile phase is applied, high partition coefficients ($K > 1$) should correspond to retention or retardation by the stationary phases. Conversely, biomolecules with low partition coefficients ($K < 1$) favour the phosphate-rich bottom phase and should be eluted without retardation.

Fig. 1. shows the variation of the partition coefficients of the three enzymes with the content of Pluronic in the mixture at three different potassium phosphate concentrations. Irrespective of both the amount of Pluronic in the top phase and the potassium phosphate concentration in the bottom phase, $K_{\text{isomerase}} > K_{\beta\text{-HSD}} \gg K_{\alpha\text{-HSD}}$. Interactions of the polyethers with the enzymes therefore decrease in the order isomerase > β-HSD $\gg$ α-HSD. Chromatography of the three enzymes on Sepharose–POE and on Sepharose–Pluronic, with potassium phosphate as the mobile phase should therefore result in elution in the order α-HSD, β-HSD and finally

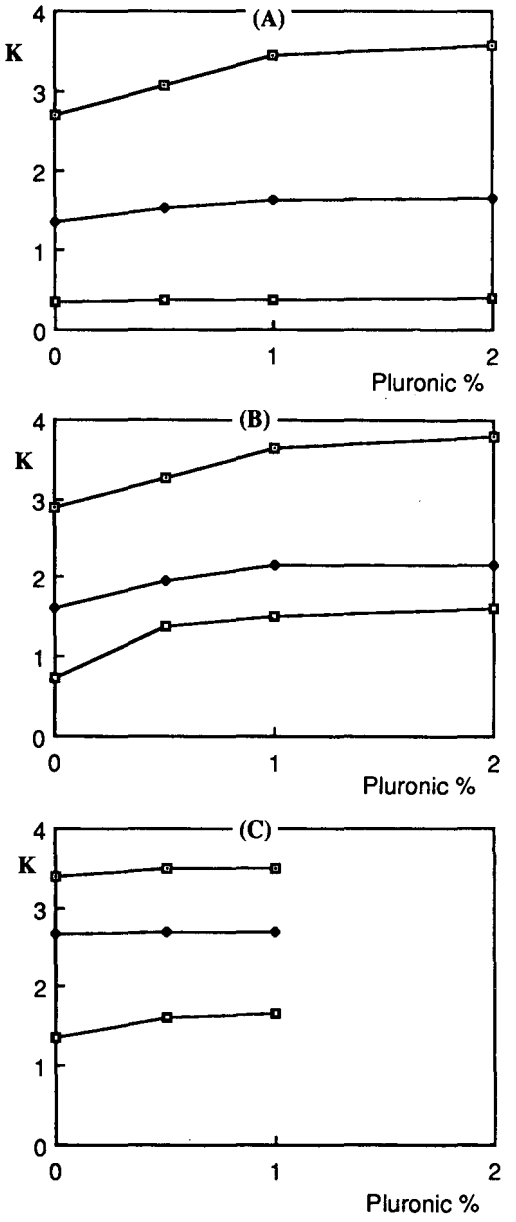

Fig. 1. Partition coefficients (K) of (□) isomerase, (◆) β-HSD and (■) α-HSD *vs.* amount of Pluronic in the biphasic system at different potassium phosphate concentrations: (A) 10, (B) 15, (C) 20% (w/w).

isomerase. This was verified experimentally, as illustrated by elution profiles obtained under various stationary and mobile phases conditions in Figs. 2 and 3.

In addition, the hydrophobic nature of the interactions between the three enzymes and the polyethers is evidenced by two facts. First, all the partition

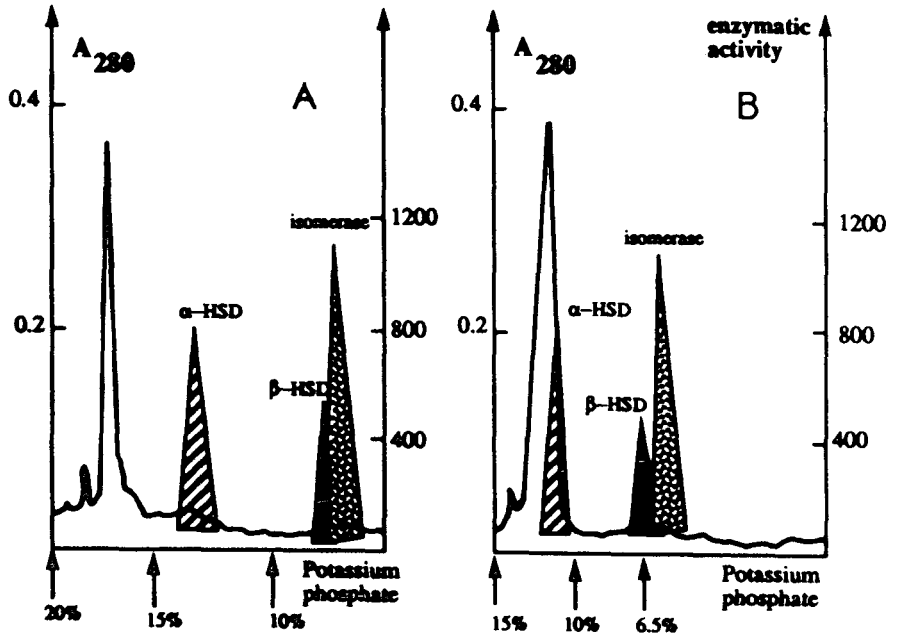

Fig. 2. Results obtained with Sepharose–POE stationary phase. Stepwise elutions of the *Pseudomonas testosteroni* crude extract (0.4 ml) starting with (A) 20% or (B) 15% potassium phosphate (pH 7.0) as the mobile phase (ionic strength changes during the stepwise elutions are indicated by arrows). Column, 38 cm × 1 cm I.D.; flow-rate, 26 ml/h; fractions taken every 5 min; room temperature. The enzymatic activities are indicated in arbitrary units.

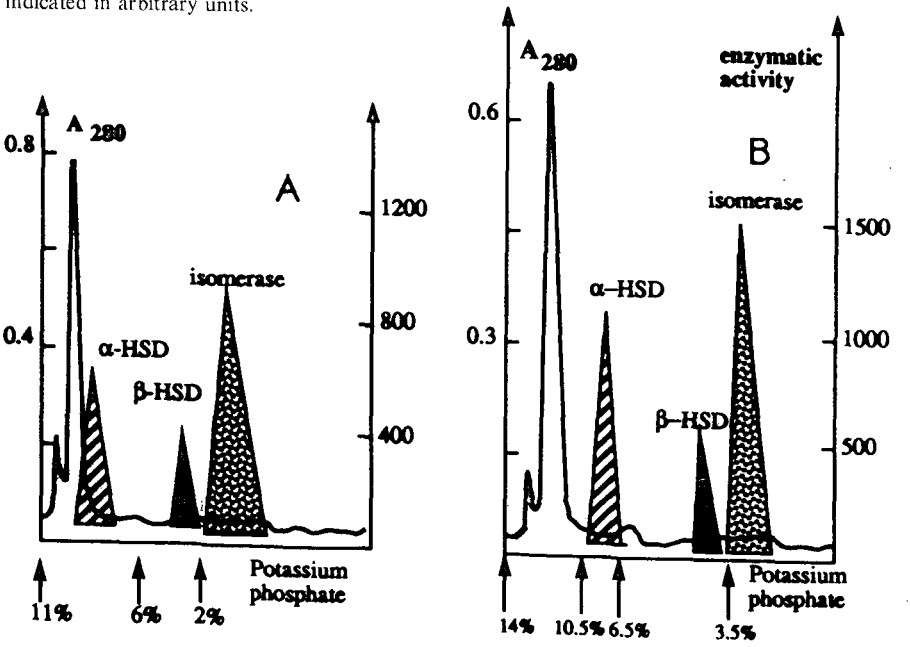

Fig. 3. Results obtained with Sepharose–Pluronic stationary phase. Stepwise elutions of the *Pseudomonas testosteroni* crude extract (0.4 ml) starting with (A) 11% or (B) 14% potassium phosphate as the mobile phase. Column, 29 cm × 1 cm I.D.; other conditions as in Fig. 2.

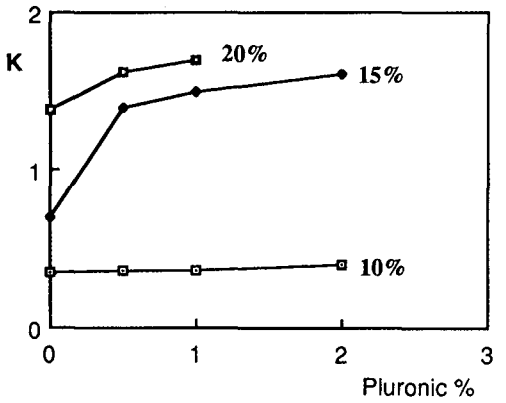

Fig. 4. Partition coefficients of α-HSD *vs.* Pluronic content in the top phase at the three different potassium phosphate concentrations: □ = 10; ◆ = 15 and ◘ = 20% (w/w) (rearrangement from values in Fig. 1).

coefficients increase with increasing amount of Pluronic in the top phase, *i.e.*, as the hydrophobic character of this phase becomes stronger. Second, for any given composition of the top phase, an increase in the phosphate concentration in the bottom phase, *i.e.*, an increase in the ionic strength, results in enhanced partition coefficients. This effect is in agreement with general principles governing hydrophobic interactions.

The second observation concerns α-HSD. Obviously, this enzyme exhibits only a very limited tendency to display hydrophobic interactions with the polyethers ($K \ll 1$ at 10% potassium phosphate) (Fig. 1A). Nevertheless, its partition coefficient can be shifted above 1, under the effect of either a higher ionic strength or an increase in the Pluronic content in the top phase, or a combination of both (Fig. 4). Its chromatographic behaviour is in agreement with these results. On Sepharose–POE, retention of α-HSD requires a 20% potassium phosphate mobile phase (compare Fig. 2A and B). Correspondingly, at 0% Pluronic, $K_{\alpha\text{-HSD}} < 1$ for potassium phosphate concentrations of 10% and 15%; $K_{\alpha\text{-HSD}} > 1$ for a potassium phosphate concentration of 20% (Fig. 4). The slightly stronger hydrophobic character of Sepharose–Pluronic allows retention of this enzyme at only a 14% potassium phosphate concentration in the mobile phase (compare Fig. 3A and B), again in agreement with the partition experiment [*e.g.*, with 0.5% Pluronic, $K_{\alpha\text{-HSD}} < 1$ at 10% potassium phosphate and $K_{\alpha\text{-HSD}} > 1$ at 15% potassium phosphate (Fig. 4)].

Finally, β-HSD and isomerase have $K > 1$ for all cases described in Fig. 1. As a result, both should be retarded or retained on Sepharose–POE or Sepharose–Pluronic, provided that the mobile phase phosphate concentration is at least 10%. Further, as ΔK ($K_{\text{isomerase}} - K_{\beta\text{-HSD}}$) increases with increasing amount of Pluronic, a better separation of these two enzymes should be obtained by chromatography on Sepharose–Pluronic than on Sepharose-POE. The chromatographic profiles obtained with these two stationary phases are in agreement with this expectation (compare Figs. 2 and 3).

The results of these preliminary partition experiments allowed us to develop a strategy for optimum chromatograhic resolution, as illustrated in Fig. 3B. The chromatography of the crude mixture was carried out on Sepharose–Pluronic, starting

with a potassium phosphate concentration in the mobile phase (14%) sufficient to afford total retention of the three enzymes. After removal of the unretarded contaminants, the potassium phosphate concentration was decreased to 10.5%, resulting, as expected in the elution of α-HSD. A further decrease in the potassium phosphate concentration to 6.5% allowed the elution of β-HSD and finally isomerase at 3.5% potassium phosphate.

Under these conditions, good recoveries of the enzymatic activities were obtained (α-HSD 60%, β-MHSD 40%, isomerase 65%) together with almost quantitative removal of the contaminants in each fraction (residual contaminants expressed as a percentage of the total proteins in the starting crude extract: α-HSD 1.5%, β-HSD 2%, isomerase not detectable).

The correlation obtained in this study between the analyses by partition and the chromatographic elution profiles suggests that this procedure might be used more generally in the field of mild hydrophobic interaction chromatography.

REFERENCES

1 S. H. Chang, K. M. Gooding and F. E. Regnier, *J. Chromatogr.*, 120 (1976) 321–333.
2 T. G. I. Ling and B. Mattiasson, *J. Chromatogr.*, 254 (1983) 83–89.
3 N. T. Miller, B. Feibush and B. L. Karger, *J. Chromatogr.*, 316 (1985) 519–536.
4 Y. Shibusawa, U. Matsumoto and M. Takatori, *J. Chromatogr.*, 398 (1987) 153–164.
5 R. Mathis, P. Hubert and E. Dellacherie, *J. Chromatogr.*, 319 (1985) 43–50.
6 R. Mathis, P. Hubert and E. Dellacherie, *J. Chromatogr.*, 347 (1985) 291–296.
7 R. Mathis, P. Hubert and E. Dellacherie, *J. Chromatogr.*, 474 (1989) 396–399.
8 P. A. Albertsson, *Partition of Cell Particles and Macromolecules*, Almquist and Wiksell, Stockholm and Wiley-Interscience, New York, 2nd ed., 1971.
9 P. Talalay and F. S. Wang, *Biochim. Biophys. Acta*, 18 (1955) 300–301.
10 P. I. Marcus and P. Talalay, *J. Biol. Chem.*, 218 (1956) 661–674.

Journal of Chromatography, 538 (1991) 462–468
Elsevier Science Publishers B.V., Amsterdam

CHROM. 22 919

Short Communication

Determination of ptaquiloside in bracken fern (*Pteridium esculentum*)

MICHAEL P. AGNEW* and DENIS R. LAUREN
MAFTech, Ruakura Agricultural Centre, Private Bag, Hamilton (New Zealand)
(First received February 22nd, 1990; revised manuscript received September 18th, 1990)

ABSTRACT

A high-performance liquid chromatography method is described for the analysis of the potent carcinogen, ptaquiloside in bracken fern (*Pteridium esculentum*). The method involves aqueous extraction at room temperature followed by clean-up through a polyamide resin column. An aliquot of the cleaned extract may be analysed directly for ptaquiloside by reversed-phase high-performance liquid chromatography. An alternative analysis is also described using base–acid conversion of ptaquiloside to pterosin B with subsequent high-performance liquid chromatography analysis. The mean recovery of standards through the method was 95% when measured as ptaquiloside, and 89% when measured as pterosin B. Detection limits for the two methods were 30 and 5 mg ptaquiloside/g bracken, respectively. The method has also been used to identify, for the first time, the presence of ptaquiloside in rock fern (*Cheilanthes sieberi*).

INTRODUCTION

Bracken fern (*Pteridium esculentum*) has been linked with several animal health problems world-wide [1–5]. In 1983 workers in Japan [1] and in The Netherlands [3] independently isolated and characterised a carcinogenic norsesquiterpene glucoside, ptaquiloside (Pta, Fig. 1a). Pta is unstable under both acidic and basic conditions. In weak acid Pta is converted to a mixture of compounds such as pterosin B (PtB, Fig. 1b), while in aqueous base, Pta is converted to the conjugated dienone (Fig. 1c) which may then be converted to PtB by weak acid [1]. Analysis is difficult due to the extremely unstable nature of the compound [1–3,6–8].

There was the need to develop an analytical method to quantitate the level of Pta in bracken fern to assist in surveying the toxic potential of bracken from different areas of New Zealand [4]. Published methods for large-scale isolation of Pta have used hot water [1,2] or methanol [3] for extraction followed by multi-step clean-up procedures. These methods gave low recoveries and were unsuitable for analysis. More recently, better recoveries have been reported using water extraction at room temperature [6–8]. However, attempts at high-performance liquid chromatographic (HPLC) analysis

0021-9673/91/$03.50

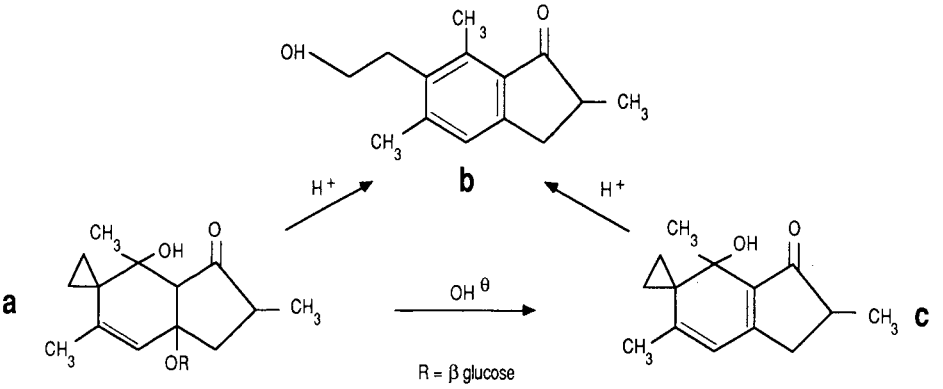

Fig. 1. Structures of ptaquiloside (a), pterosin B (b) and the unstable conjugated dienone (c), and the route by which ptaquiloside is converted to them.

were abandoned due to problems with work-up and low recoveries, although a thin-layer chromatographic assay was devised [8]. When developing our method we decided to try extraction of dried and ground bracken by water at ambient temperature, followed by minimal clean-up prior to analysis by HPLC.

This paper describes a rapid and simple method for the analysis of Pta in bracken fern. It may also be applied for the analysis of other plant materials. The method consists of aqueous extraction followed by clean-up through a polyamide resin column. The sample is then analysed by HPLC with UV detection. The sample may also be reacted to form PtB, then analysed again for confirmation.

EXPERIMENTAL

Materials

Pta was supplied by Professor Kiyoyuki Yamada (Nagoya University, Nagoya, Japan) and stored over silica gel at −20°C. PtB was obtained by reaction of Pta with base, followed by acid, in water. HPLC mobile phases were mixtures of purified water (Millipore Milli-Q) and HPLC-grade methanol (BHD, Poole, U.K.). Polyamide 6 S resin was purchased from Riedel-de Haen (Seelze, Germany).

Preparation of primary standards

Stock solutions of Pta were made in methanol at about 0.1 mg/ml. Working standards (10 μg/ml) were obtained by dilution with water. Both stock and working solutions were stored at −20°C.

For PtB, a solution of Pta in water (0.1 mg/ml) was treated with 75 μl/ml of 1 *M* NaOH and allowed to react for 1 h at 40°C, when 75 μl/ml of 5 *M* HCl was added. This solution was diluted to final volume for working standards. The concentration was calculated on the basis of 100% conversion of Pta to PtB and expressed as Pta equivalents.

Instrumentation and analytical conditions

The HPLC system used was a Spectra-Physics 740B binary pumping system with

either a Rheodyne 7120 manual injector or a Micromeritics 725 autosampler, each fitted with a 50-μl sample loop, a Micromeritics 731 column oven, a Shimadzu SPD-2A UV detector and a Spectra-Physics SP4170 integrator. The analytical column (either Zorbax ODS 5 μm or Chrompak CPSpher C_8; 25 cm × 4.6 mm I.D.) was preceded by a 2-μm in-line filter (Rheodyne) and an MPLC RP-8 guard column (Brownlee Labs, Santa Clara, CA, U.S.A.). All these items were maintained at 35°C in the column oven. The mobile phase was water–methanol (60:40) for Pta or water–methanol (40:60) for PtB. The flow-rate was 1 ml/min. The mobile phases were selected to give retention times of around 10–12 min for both Pta and PtB. Detection was at 220 nm. Concentration calculations were based on both area and height measurements relative to external standards of concentrations in the range 5–15 μg/ml.

Extraction and clean-up

Bracken fern was dried in an air oven (50°C for 5 days) and then ground to pass a 0.6-mm mesh screen. The ground sample (2 g) was shaken with water (100 ml) in a large boiling tube on a flat-bed orbital shaker (350 rpm) for 1 h at room temperature. The extract was filtered through Whatman No. 1 filter paper, and the clear amber filtrate retained.

An aliquot (20 ml) of the filtrate was added to a glass column (25 cm × 12 mm I.D.) dry packed with polyamide 6 S resin (2.5 g). The total eluate (*ca.* 12 ml) was collected and mixed. An aliquot was removed and used for direct determination of Pta. A further aliquot (1 ml) was converted to PtB by the method used for the standard and was then analysed for PtB without further dilution. Concentrations of PtB were expressed as Pta equivalents using a dilution factor of 1.15.

RESULTS AND DISCUSSION

The first extraction solvent tried was methanol. This required evaporation of the extract and dissolving in water prior to clean-up which was time consuming for large numbers of samples. There was also the added risk of degradation of Pta. The proposed method using aqueous extraction and minimal clean-up overcomes these problems. It has given repeatably high recoveries of Pta from bracken over several seasons.

Shaking with water for 1 h at room temperature followed by clean-up through polyamide 6 S resin was found to be suitable (see Table I). In fact, prolonged extraction gave poor recovery of Pta due to breakdown to PtB in aqueous solution. The clean-up column removed all PtB present in the sample extract and thus allowed the development of a confirmatory test based on the conversion of Pta to PtB. As the UV response of PtB was 5–6 times greater than that of Pta, this alternative method was more suitable for determining low levels of Pta. The levels of Pta found in samples ranged from less than 30 μg/g up to 4000 μg/g dry weight, equivalent to from 0.6 μg/ml up to 80 μg/ml in the original extract solutions. The limit of detection was 30 μg/g for Pta and 5 μg/g Pta equivalents after hydrolysis to PtB.

Standards of both Pta and PtB were analysed in the range 0.1–200 μg/ml. Both compounds showed linear response in the range tested. The regression equations for the log-transformed data are for Pta, $\log_{10}$(peak height) = 2.692 + 1.002 $\log_{10}$ (concentration), correlation coefficient 1.000; and for PtB, $\log_{10}$(peak height) = 3.467 + 0.975 $\log_{10}$(concentration), correlation coefficient 0.999.

TABLE I

EFFECT OF EXTRACTION TIME ON Pta AND PtB CONCENTRATIONS IN AQUEOUS EXTRACTS OF BRACKEN

Time shaking (h)	Clean-up	Pta (μg/g)	PtB[a] (μg/g)
1	None	2300	780
1	Polyamide	1590	0
2	Polyamide	1500	0
4	Polyamide	1120	0
24	None	545	>1400

[a] Expressed as Pta equivalents; PtB occurring naturally or from degradation of Pta during extraction is removed by the polyamide clean-up.

The mean recovery of standards in the range 2–35 μg/ml put through the clean-up method was 95% (range 90–100%) when measured as Pta and 89% (range 85–94%) when measured at PtB. Coefficients of variation for five replicate 2- and 10-μg/ml standards put through the clean-up were respectively 2.7% and 3.2% for estimations as Pta and 2.9% and 2.2% for estimations as PtB. The procedure of collecting an aliquot of the eluent from the clean-up column for analysis was shown to be satisfactory by collecting and analysing the eluate from a 10-μg/ml standard in 2-ml

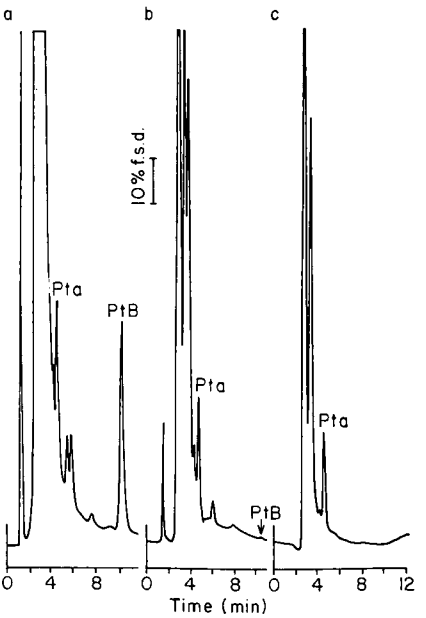

Fig. 2. Chromatograms of crude bracken extract (0.02 g/ml). (a) Without clean-up; (b) after 1-g polyamide 6 S clean-up column; (c) after 2.5-g polyamide 6 S clean-up column. Analysis conditions as in text except for mobile phase, water–methanol (30:70); column temperature, 22°C; UV detection at 220 nm and 0.04 a.u.f.s. Peaks: Pta = ptaquiloside; PtB = pterosin B.

fractions. The first 2-ml fraction showed 6.8 μg/ml while the next five 2-ml fractions showed from 8.9 to 10.2 μg/ml. This result showed that Pta is almost non-retained on the polyamide clean-up medium.

A crude bracken extract was analysed without clean-up and following passage through either a 1-g polyamide column or a 2.5-g polyamide column (see Fig. 2). Comparison of Fig. 2a and Fig. 2c shows complete removal of any PtB naturally present in the sample. In this experiment the estimated amount of Pta after the 1-g and 2.5-g polyamide columns had reduced to 77% and 71%, respectively, of the estimate for the crude extract. An accurate estimate on the crude material was difficult, however, due to co-extractive interferences. The 2.5-g polyamide column (Fig. 2c) gave superior clean-up and was used in the final method. Collection and analysis of the column eluent in 2-ml fractions gave a similar pattern to that seen with standards. Reproducibility of the method was tested on both replicates ($n = 6$) of a bulk extract and on replicate extractions ($n = 5$), in each case analysed both as Pta and PtB. The coefficients of variation were all in the range of 0.8–2.7%.

Fig. 3 shows the results of both immature and mature bracken fronds analysed using the method. Figs. 3a and b show analysis of Pta directly, and Figs. 3c and d show the analysis of the same extracts after base–acid conversion of Pta to BtB.

The reaction conditions required to convert Pta to PtB were studied. Pta may be converted to PtB in either acidic or basic conditions [1]. It was found that reaction of Pta with acid gave two or more products with ratios varying according to solvent composition. Table II shows the results of Pta breakdown under acid conditions in

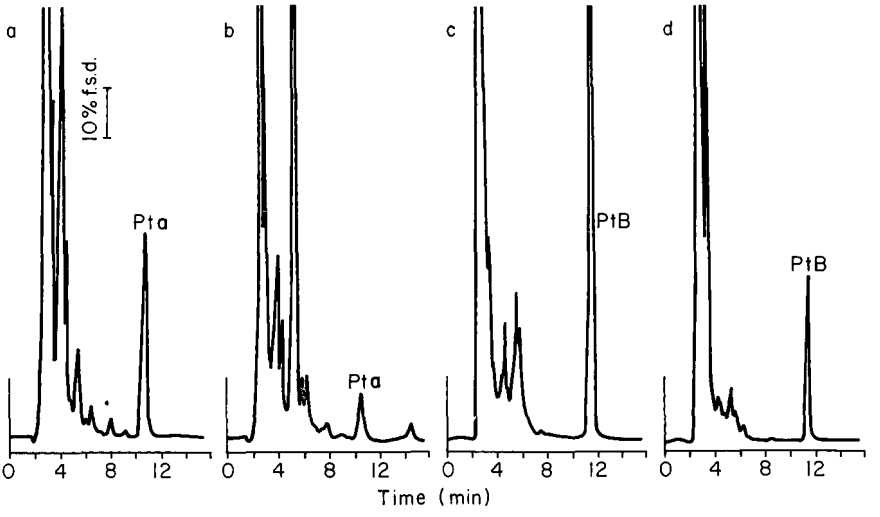

Fig. 3. Chromatograms of (a) extract of immature bracken fronds (0.02 g/ml); shows 28.6 μg/ml Pta, equal to 1430 μg/g in the bracken sample; (b) extract of mature bracken fronds; shows 6.65 μg/ml Pta, equal to 332 μg/g; (c) extract as in (a) after base–acid treatment; shows 26.8 μg/ml Pta equivalents as PtB, equal to 1610 μg/g in the bracken sample; and (d) extract as in (b) after base–acid treatment; shows 7.5 μg/ml Pta equivalents as PtB, equal to 450 μg/g. Analysis conditions as in text with mobile phase water–methanol (60:40) and detector attentuation 0.08 a.u.f.s. for (a) and (b), and mobile phase water–methanol (40:60) and detector attenuation 0.16 a.u.f.s. for (c) and (d).

TABLE II

REACTION OF PTAQUILOSIDE AT pH 1.5

Reaction of Pta standard (100 μg/ml) in water–methanol (1:1) at 24°C. Analysis conditions were as in text except for mobile phase water–methanol (30:70) with a 20-μl sample loop.

Time (min)	f.s.d. at 0.16 a.u.f.s. (%)		
	Ptaquiloside	Pterosin B	Pterosin O
0	37	1	0
15	26	30	38
30	14	46.5	58
45	8	56	70
60	5.5	61.5	77.5
75	3.5	63	79.5

water–methanol (1:1). Even using 100% water as the reaction solvent, a mixture of PtB, a product presumed to be the methoxy derivative pterosin O (PtO) [1], and a third unidentified product resulted. On the other hand, initial reaction with base to convert Pta to the conjugated dienone (Fig. 1c) followed by acid treatment to produce PtB [1] was tried and yielded a single product (HPLC) with reproducible results. This reaction proved to be consistent from one experiment to the next, and was used to prepare a stock solution of PtB. As HPLC of the solution did not reveal any peaks other than PtB the conversion was assumed quantitative. The estimates of Pta measured by direct

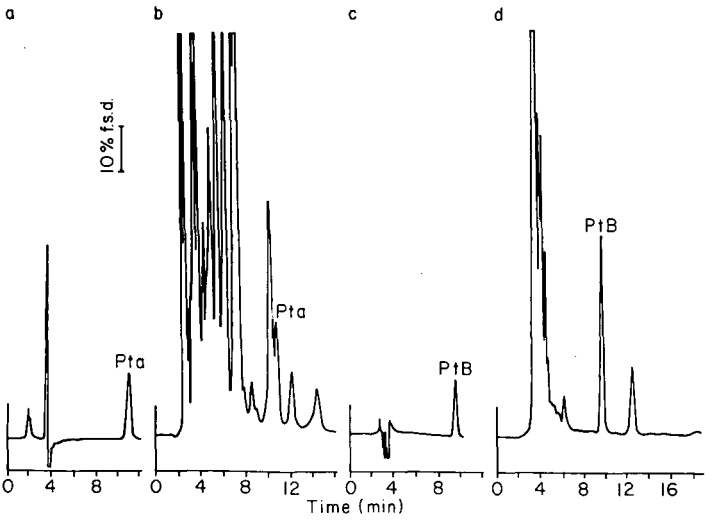

Fig. 4. Chromatograms of (a) ptaquiloside (Pta) standard, 8.25 μg/ml; (b) extract of Australian rock fern (0.02 g/ml); (c) pterosin B (PtB) standard, 4.8 μg/ml; and (d) extract of Australian rock fern (0.02 g/ml) as in (a) after base–acid treatment. Analysis conditions as for Fig. 3 except for detector attenuation for (c) and (d) of 0.32 a.u.f.s.

analysis as Pta or by indirect analysis as PtB generally agreed within 15%. This suggests that the two methods are comparable.

The method has also been used to analyse other species of fern for Pta. Fig. 4 shows results from analysis of *Cheilanthes sieberi* (rock fern). In this species, compounds interfering in the determination of Pta are still present after clean-up (Fig. 4b), although full separation can be achieved by changing the HPLC mobile phase. However, after conversion to PtB (Fig. 4d), no interference remains. This shows a further use for the indirect analysis method as the principal method for difficult samples.

For rock fern the estimates of PtB as Pta equivalents were generally much higher than the direct estimates of Pta. This suggests that some of the interferences for the direct analysis could be compounds similar to Pta which are also able to produce PtB after base–acid treatment. Such compounds may also be expected to be toxic [7,8].

Finally, as shown in Fig. 2a, PtB occurs naturally in samples of bracken containing Pta. In some instances it may be required to measure this naturally occurring PtB. The PtB is removed from the extract by the polyamide clean-up, but may be eluted from the polyamide column with methanol (2 × 5 ml) after first washing excess extract from the column with water. Crude bracken extracts should not be analysed directly as they will quickly destroy the HPLC column.

CONCLUSION

The methods described for analysis of Pta and its principal degradation product PtB are rapid and easy to use. They allow large numbers of bracken samples to be processed with minimum delay between extraction and analysis. The indirect estimate by analysis of PtB produced by base–acid treatment of the cleaned-up extract allows confirmation of the direct analysis results as well as offering an alternative analytical approach for difficult samples and for Pta precursers or conjugates.

REFERENCES

1 H. Niwa, M. Ojika, K. Wakamatsu, K. Yamada, I. Hirono and K. Matsushita, *Tetrahedron Lett.*, 24 (1983) 4117.
2 I. Hirono, K. Yamada, H. Niwa, Y. Shizuri, M. Ojika, S. Hosaka, T. Yamaji, K. Wakamatsu, H. Kigoshi, K. Niiyama and Y. Uosaki, *Cancer Lett.*, 21 (1984) 239.
3 J. C. M. van der Hoeven, W. J. Lagerweij, M. A. Posthumus, A van Veldhuizen and H. A. J. Holterman, *Carcinogenesis*, 4 (1983) 1587.
4 B. L. Smith, P. P. Embling, M. P. Agnew, D. R. Lauren and P. T. Holland, *N.Z. Vet. J.*, 36 (1988) 56.
5 A. Hopkins, *Br. Vet. J.*, 146 (1990) 316.
6 M. Ojika, H. Kigoshi, H. Kuyama, H. Niwa and K. Yamada, *J. Natl. Prod.*, 48 (1985) 634.
7 M. Matoba, E. Saito, K. Saito, K. Koyama, S. Natori, T. Matsushima and M. Takimoto, *Mutagenesis*, 2 (1987) 419.
8 K. Saito, T. Nagao, M. Matoba, K. Koyama, S. Natori, T. Murakami and Y. Saiki, *Phytochemistry*, 28 (1989) 1605.

Journal of Chromatography, 538 (1991) 469–473
Elsevier Science Publishers B.V., Amsterdam

CHROM. 22 846

Short Communication

Fractionation of egg and soybean phosphatidylcholines by silver resin chromatography

R. ADLOF
U.S. Department of Agriculture, Agricultural Research Service, Northern Regional Research Center, 1815 North University Street, Peoria, IL 61604 (U.S.A.)
(Received August 8th, 1990)

ABSTRACT

Samples of egg and soybean phosphatidylcholines were fractionated by total number of double bonds on silver ion-saturated resin columns using solvent programming (acetonitrile in methanol). Stainless-steel columns were packed with 15-μm resin which had been isolated by air elutriation. Methods of column packing, silver ion incorporation, solvent–resin interactions and resin regeneration are also discussed.

INTRODUCTION

Silver-loaded, macroreticular, divinylbenzene copolymer sulfonic acid resins have been useful in the separation of unsaturated compounds, particularly by number or configuration of the double bonds [1–5]. This concept has been extended to the separation of polyunsaturated compounds by use of mixed solvent systems [6–8]. Our studies in the metabolism of configurational and positional fatty acids in humans required preparation of highly unsaturated phospholipid standards. Earlier thin-layer chromatography (TLC) work [9–11] using silver nitrate-saturated silica indicated such fractionation of phospholipids was possible. Further fractionation by total number of carbon atoms can, if required, be accomplished by reversed-phase high-performance liquid chromatography (HPLC) [12,13]. The development of an analytical silver resin column for fractionation of 0.1 to 10 mg phospholipid samples is therefore reported.

EXPERIMENTAL[a]

Materials

Rohm & Haas XN1010 sulfonic acid resin (16–50 mesh) was obtained from

[a] The mention of firm names or trade products does not imply that they are endorsed or recommended over other firms or similar products not mentioned.

Aldrich (Milwaukee, WI, U.S.A.). Egg and soybean phosphatidylcholines (PCs, 99% pure; 100 mg/ml chloroform) were obtained from Sigma (St. Louis, MO, U.S.A.). All chromatography solvents were HPLC grade; all other chemicals were used as received.

Methods

Methods for grinding and sieving of the resin [14] and for use of mixed solvent systems [6–8] have been described previously. The wet-sieved (through 400 mesh) resin was washed with acetone and dried in a vacuum oven (60 mmHg/50°C) for 14 h. The dried resin was then fractionated by air-elutriation by the method of Ekman *et al.* [15]. An 8 l/min fraction was isolated and the resin size determined on a Hitachi H-500 electron microscope. The size of the irregular particles (15 ± 6 μm) was calculated as (length + width)/2. The resin was neutralized with 0.5 *M* sodium hydroxide, slurry packed into a stainless-steel (SS) column and flushed with a 50% excess of 0.5 *M* aqueous silver nitrate. After the resin was washed with water and then acetone, the column was unpacked and the resin was dried in a vacuum oven as described above. The dried resin was packed into a 25 cm × 4.6 mm SS column in small increments with tapping, then the column was flushed with methanol. Column selectivity was determined by the separation of methyl elaidate and methyl oleate.

The HPLC system consisted of a Spectra-Physics Model 8700 solvent delivery system, a Rheodyne 7125 injector (10 μl sample loop) and an Isco Model 1840 ultraviolet detector. Samples (10-μl) of PCs (10 mg/ml chloroform) were injected and detected by UV at 206 nm. The phospholipid fractions were converted to fatty acid methyl esters (FAMEs) by HCl–methanol as described previously [16].

The FAMEs were analyzed in a Packard Model 428 gas chromatograph equipped with a 100 m × 0.25 mm (0.2 μm coating) SP 2560 fused-silica capillary column (Supelco, Bellefonte, PA, U.S.A.). Helium carrier gas and a flame ionization detector were used. The oven temperature was programmed from 200–220°C at 10°C/min after an initial hold of 15 min.

RESULTS AND DISCUSSION

The PC were fractionated with a mobile phase consisting of varying amounts of acetonitrile in methanol. Soybean PC (10 μl of 10 mg PC/ml in chloroform) was fractionated in solvent-programmed (1.0 ml/min) runs in which, after an initial hold of 5 min, the acetonitrile concentration was increased from 0 to 25% in methanol over 40 min as shown in Fig. 1; the FAME composition of the eluted fractions is tabulated in Table I. The fractionation pattern for egg PCs (same sample size and solvent conditions as used for the fractionation of soybean PCs) is shown in Fig. 2 and the FAME composition in Table II. Several authors [17–19] have described the fatty acid (FA) composition and distribution in a variety of both plant and animal phospholipids. They found that saturated FAs predominated in the 1-position while unsaturated FAs were primarily located in the 2-position. Comparison of the FA distributions of the eluted fractions with this data allowed us to assign structures for the primary phospholipid in each fraction. (See Tables I and II, bottom). The PC species were fractionated based on the number of double bonds in their FA components. The FA patterns differed significantly for soybean and egg PCs. While

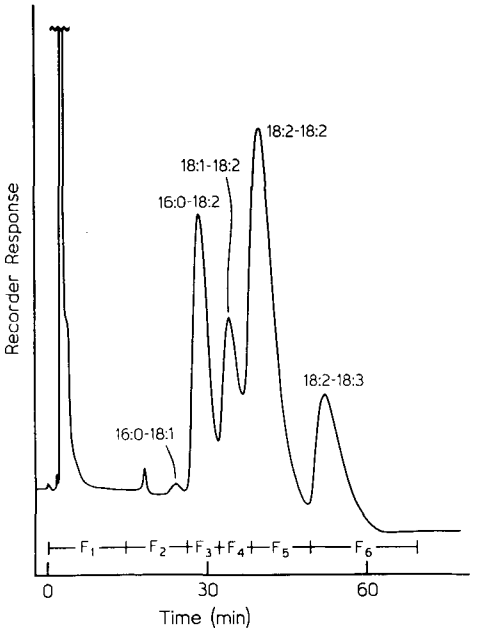

Fig. 1. Fractionation of soybean PCs. Sample size = 10 μl of 10 mg PC/ml chloroform solution. Flow-rate = 1.0 ml/min programmed, after a 5-min hold, from 100% methanol to acetonitrile–methanol (25:75) over 40 min, followed by a hold till the end of the run. F_1–F_6 represent the fractions collected.

soybean PC was composed primarily of 18:2–18:2 PC, fresh egg PC contained mostly sat-18:2 and sat-20:4. Sat-18:2 is defined as a saturated FA (16:0, 18:0 etc.) that is located in the number 1 position of the PC and 18:2 is located at the 2-position. The number 3 position is considered to be occupied by the phosphorus-containing moiety.

During preparation of the resin columns, several points of interest were noted. (1) Column diameter as well as resin particle size are important. Methyl elaidate and

TABLE I

COMPOSITION OF SOYBEAN PHOSPHATIDYLCHOLINE FRACTIONS OBTAINED BY HPLC AND ANALYZED BY GAS CHROMATOGRAPHY

FAME	Composition (%)					
	Standard	F_2	F_3	F_4	F_5	F_6
16:0	14.6	41.5	34.0	6.5	3.0	–
18:0	5.5	12.8	12.4	2.5	1.1	–
18:1ω9	10.5	38.7	7.1	32.8	2.8	–
18:1ω7	2.1	2.0	1.4	7.6	0.5	–
18:2	62.7	5.1	45.1	44.5	89.5	56.6
18:3	5.2	–	–	6.2	4.2	43.4
Primary component(s)		18:0–18:1 16:0–18:1	16:0–18:2 18:0–18:2	18:1–18:2 16:0–18:3	18:2–18:2 18:1–18:3	18:2–18:3 –

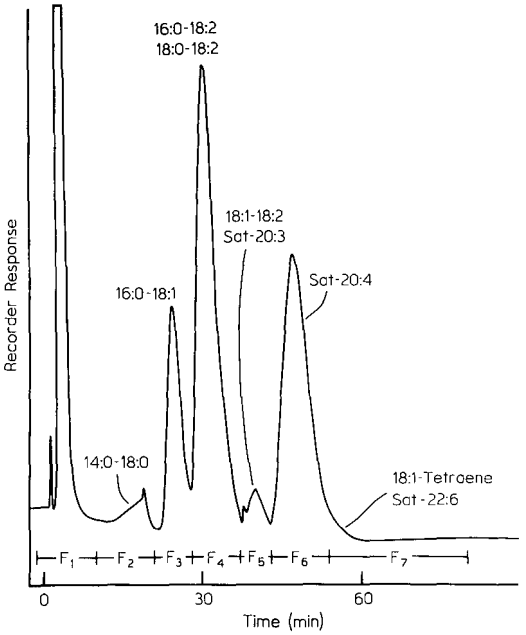

Fig. 2. Fractionation of egg PCs. Sample size and conditions as in Fig. 1.

methyl oleate were poorly separated on a 25 cm × 2.3 mm I.D., silvered resin column (dry-packed) as compared to one of 4.6 mm I.D. Also, if resin particles of < 15 μm were used poor resolution resulted. Apparently the macroreticular structure of the resin was destroyed by very fine grinding. (2) Slurry packing always yielded poorer

TABLE II

COMPOSITION OF EGG PHOSPHATIDYLCHOLINE FRACTIONS OBTAINED BY HPLC AND ANALYZED BY GAS CHROMATOGRAPHY

FAME	Composition (%)					
	Standard	F_3	F_4	F_5	F_6	F_7
14:0	0.4	0.6	0.5	3.1	0.7	1.6
16:0	33.6	40.1	30.8	12.4	17.4	17.1
16:1	1.1	0.8	1.5	3.6	3.1	2.2
18:0	12.5	10.3	12.2	6.6	22.2	5.9
18:1	29.8	46.9	15.2	10.6	5.4	18.2
18:2	15.5	–	36.9	17.3	7.4	3.2
20:2	0.2	–	0.4	–	–	–
20:4ω6	3.6	–	–	–	37.5	28.3
24:1	0.3	–	–	–	2.6	–
22:4	1.0	–	–	–	1.5	7.1
22:6ω3	4.0	–	–	–	–	–
Primary component(s)		16:0–18:1	16:0–18:2 18:0–18:2	18:1–18:2	16:0–20:4 18:0–20:4	18:1–20:4 16:0–22:6

results than dry packing. (3) An attempt to prepare a silver resin column from a dry-packed resin column (unsilvered) by changing the solvents and reagents *in situ* led to the creation of voids and poor resolution. The voids were created because XN1010 resin volume changes with solvent polarity. This problem is more pronounced in the very finely ground resin. (4) A gradual increase of column pressure was noted over a several week period when solvent programming was used. This was apparently caused by solvent-induced fracturing of the resin and the resultant release of fines. This problem was alleviated by reversing the column (no loss of resolution noticed) and/or cleaning the frits periodically. No significant loss of silver ions was noted. (5) Continuous solvent programming and/or "dirty" samples eventually (6–8 months) led to loss of resolution. However, the resin could be regenerated as described previously [8].

Samples which had been eluted through the column were analyzed by gas chromatography (for the presence of FAMEs)to determine if any transesterification had occurred, *e.g.*, catalyzed by residual sulfonic acid groups [20]. No evidence of this reaction was found.

This procedure allowed us to prepare analytical standards of highly unsaturated PCs of known and reproducible composition. Due to the strong affinity of the silver ions to the sulfonic acid groups of the XN1010 resin, no loss of silver ions was noted, even when such polar solvents as methanol and acetonitrile were used. Under these conditons, silver ion loss is a problem with silver nitrate–silica gel columns. Due to the high silver loading capacity of silver-ion saturated XN1010 resin (*ca.* 36%, w/w, for a 100% Ag^+ resin), semi-preparative separations are possible. Currently, a system composed of two 60 cm × 7.5 mm SS columns connected in tandem, has been used to fractionate 200-μl samples of soybean PCs (50% in methanol) at an acetonitrile–methanol (10:90) flow-rate of 3.0 ml/min (isocratic).

REFERENCES

1 E. A. Emken, C. R. Scholfield and H. J. Dutton, *J. Am. Oil Chem. Soc.*, 41 (1964) 388.
2 C. R. Scholfield and E. A. Emken, *Lipids*, 1 (1966) 235.
3 C. R. Scholfield and T. L. Mounts, *J. Am. Oil Chem. Soc.*, 54 (1977) 319.
4 E. A. Emken, C. R. Scholfield, V. L. Davison and E. N. Frankel, *J. Am. Oil Chem. Soc.*, 44 (1967) 373.
5 E. A. Emken, J. C. Hartman and C. R. Turner, *J. Am. Oil Chem. Soc.*, 55 (1978) 561.
6 A. C. Lanser and E. A. Emken, *J. Chromatogr.*, 256 (1984) 460.
7 W. J. DeJarlais, R. O. Adlof and E. A. Emken, *J. Am. Oil Chem. Soc.*, 60 (1983) 975.
8 R. O. Adlof and E. A. Emken, *J. Am. Oil Chem. Soc.*, 62 (1985) 1592.
9 S. M. Hopkins, G. Seehan and R. L. Lyman, *Biochim. Biophys. Acta*, 164 (1968) 272.
10 G. A. E. Arvidson, *J. Lipid. Res.*, 6 (1965) 574.
11 D. A. Kennerly, *J. Chromatogr.*, 363 (1986) 462.
12 C. Demandre, A. Tremolieres, A. Justin and P. Mazliak, *Phytochemistry*, 24 (1985) 481.
13 H. A. Norman and J. B. St. John, *J. Lipid Res.*, 27 (1986) 1104.
14 R. O. Adlof, H. Rakoff and E. A. Emken, *J. Am. Oil Chem. Soc.*, 57 (1980) 273.
15 R. Ekman, B. G. Johansson, U. Ravnskov, *Anal. Biochem.*, 70 (1976) 828.
16 R. O. Adlof, *J. Am. Oil Chem. Soc.*, 67 (1990) 52.
17 A. Kuksis and L. Marai, *Lipids*, 2 (1967) 217.
18 B. J. Holub and A. Kuksis, *Lipids*, 4 (1969) 466.
19 J. L. Harwood, *Phytochemistry*, 15 (1976) 1459.
20 R. O. Adlof and E. A. Emken, *J. Am. Oil Chem. Soc.*, 57 (1980) 276.

Journal of Chromatography, 538 (1991) 474–479
Elsevier Science Publishers B.V., Amsterdam

CHROM. 22 955

Short Communication

High-performance liquid chromatography of oligoguanylates at high pH

ROSCOE STRIBLING[a]
Department of Zoology, University of California at Davis, Davis, CA 95616 (U.S.A.)
(Received August 10th, 1990)

ABSTRACT

Because of the stable self-structures formed by oligomers of guanosine, standard high-performance liquid chromatography techniques for oligonucleotide fractionation are not applicable. Previously, oligoguanylate separations have been carried out at pH 12 using RPC-5 as the packing material. While RPC-5 provides excellent separations, there are several limitations, including the lack of a commercially available source. This report describes a new anion-exchange high-performance liquid chromatography method using HEMA-IEC BIO Q, which successfully separates different forms of the guanosine monomer as well as longer oligoguanylates. The reproducibility and stability at high pH suggests a versatile role for this material.

INTRODUCTION

It has been shown that polynucleotides can direct the synthesis of complementary oligomers by non-enzymatic mechanisms [1–4]. These reactions follow standard Watson–Crick pairing rules and have been used as models of the earliest replicating systems on the primitive Earth. The most successful synthesis occurs when polycytidylic acid [poly(C)] is used as a template to direct the condensation of the activated monomer, guanosine 5′-phospho-2-methylimidazole (2MeImpG). Oligomerization efficiency exceeds 80% and can produce oligomers up to the 40-mer which are detectable with high-performance liquid chromatography (HPLC) [2].

Since oligomers of guanosine form extremely stable self-structures at neutral pH ranges [5], standard techniques for oligonucleotide fractionation are not applicable. The reactions described above were analyzed by HPLC on an RPC-5 column [6] using a sodium perchlorate gradient at pH 12. At this pH, the oligomers are completely deprotonated, with strand separation driven by charge repulsion.

[a] Present address: Cancer Research Institute, UCSF Medical Center, San Francisco, CA 94143-0128, U.S.A.

0021-9673/91/$03.50

While the pH stability of RPC-5 permits its use in oligoguanylate fractionation, it is not widely used in other oligonucleotide separations because the adsorbed quaternary ammonium ion (Andogen 464) is readily stripped off the solid support with resulting loss in resolution. Additionally, the RPC-5 column is not commercially available and the support materials, Kel-F or Plaskon, are not readily available. (See Usher [7] for a more complete discussion.) Because of these limitations, RPC-5 is not ideal for oligonucleotide separation, although no other HPLC option has been available for the analysis of oligomers of guanosine.

More recently, Kanavarioti and Doodokyan [8] have shown that products from the decomposition and oligomerization of 2MeImpG can be analyzed using reversed-phase HPLC on a commercially available, silica-based C_{18} column. This method is superior to RPC-5 when investigating reaction products that do not exceed the guanosine tetramer. However, since the column material is not stable at high pH, it cannot be used to fractionate longer oligomers.

I now report on a new anion-exchange HPLC method that separates different forms of guanosine monomers as well as longer oligomers. The column material is stable at pH 12 and separations are achieved using a sodium perchlorate gradient similar to that used with RPC-5.

EXPERIMENTAL

Materials

Guanosine, guanosine 5′-monophosphate (GMP), poly(C), sodium perchlorate, and bovine pancreatic ribonuclease A were obtained from Sigma (St. Louis, MO, U.S.A.). Poly(G) was obtained from P-L Biochemicals (Milwaukee, WI, U.S.A.). 2MeImpG was a gift from Leslie Orgel of the Salk Institute for Biological Studies, La Jolla, CA, U.S.A. Water was obtained from a NANOpure II system with at least a 17.6 MΩ · cm purity. HPLC solvents were prepared and passed through a 0.2-μm filter under reduced pressure prior to use.

HPLC analysis

Chromatography was performed with a solvent delivery system composed of two Alltex 110A pumps and an Axxiom 710 controller. The eluate was monitored at 254 nm by an Isco V^4 variable-wavelength detector attached to a Linear chart recorder. The analytical (150 × 4.6 mm I.D.) and guard columns were generously provided by Alltech (Deerfield, IL, U.S.A.) and were packed with HEMA-IEC BIO Q, which consists of a quaternary trimethylamino group covalently bound to a pH stable support. Chromatographic conditions were as follows. Mobile phase: solvent A, 2 m*M* Tris–perchlorate, pH 12; solvent B, 2 m*M* Tris–perchlorate, pH 12, 0.4 *M* sodium perchlorate. Gradient elution, 2 to 30% B in 15 min; 30 to 100% B in 87.5 min. The initial steeper gradient is needed to decrease the retention time of the shorter products, while the slower gradient of 0.8% B min^{-1} provides convenient separation of the longer oligomers. A flow-rate of 1 ml min^{-1} was used and produced a system pressure of about 800 p.s.i.

Sample preparation

Separation of guanosine, GMP and 2MeImpG. Approximately 0.5 absorption

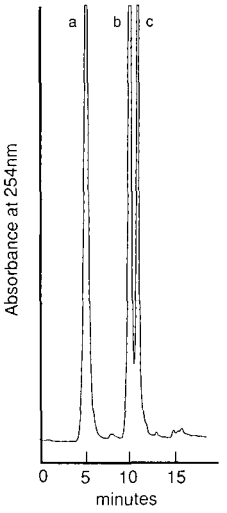

Fig. 1. HPLC elution profile of guanosine (a), 2MeImpG (b) and GMP (c). Column, HEMA-IEC BIO Q; mobile phase: solvent A, 2 m*M* Tris–perchlorate (pH 12); solvent B, 2 m*M* Tris–perchlorate (pH 12), 0.4 *M* sodium perchlorate; gradient elution, 2 to 30% B in 15 min, 30 to 100% B in 87.5 min. The flow-rate was 1 ml min^{-1}, with the chart speed set at 30 cm h^{-1} and the detector scaled to 0.2 a.u.f.s.

units of each were mixed with solvent A and directly injected. Individual peaks were identified by comparison of retention times with authentic samples. The chromatogram shown in Fig. 1 was included for direct comparison with the other elution profiles, but better resolution could be obtained with a slower gradient (not shown).

Poly(G) hydrolysis products. A 3 m*M* solution of poly(G) was adjusted to pH 12 with KOH and heated at 70°C for 40 min. A 50-μl volume was diluted to 200 μl with solvent A and directly injected.

2MeImpG oligomerization reactions. Reaction mixtures were prepared which contained 1.0 *M* NaCl, 0.2 *M* $MgCl_2$, 0.1 *M* Tris–perchlorate, pH 8.5, 0.04 *M* 2MeImpG, and, where necessary, 0.02 *M* poly(C). After mixing, the samples were kept at 4°C. At predetermined times, aliquots were withdrawn and the reaction quenched by mixing with an excess of EDTA, pH 9. Prior to analysis, surviving imidazolides were hydrolyzed (pH 5) for 12 h at room temperature. The poly(C) template was degraded by incubation at 37°C with bovine pancreatic ribonuclease A, which hydrolyzes internucleotide linkages on the 3′ side of pyrimidine residues. The aliquots were diluted with solvent A prior to injection.

RESULTS AND DISCUSSION

Although excellent separations of long oligomers of guanosine can be achieved with RPC-5, the difficulties described above limit its general use. The HEMA-IEC BIO Q material used in the present study overcomes many of those problems. Fig. 1 shows that different monomers of guanosine can be efficiently separated with this technique. The separation of 2MeImpG from GMP is particularly useful since GMP is the major product of 2MeImpG decomposition [8]. The main focus of this study was to

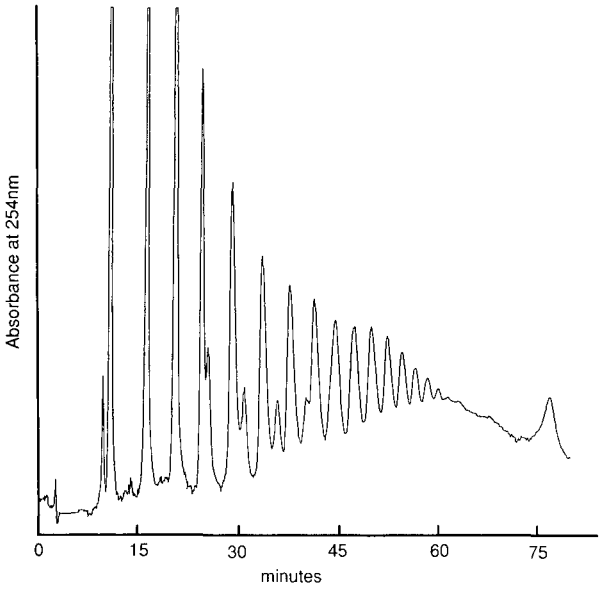

Fig. 2. HPLC elution profile of poly(G) hydrolysis products. The chromatographic conditions are the same as in Fig. 1 except with a chart speed of 20 cm h^{-1} and 0.1 a.u.f.s.

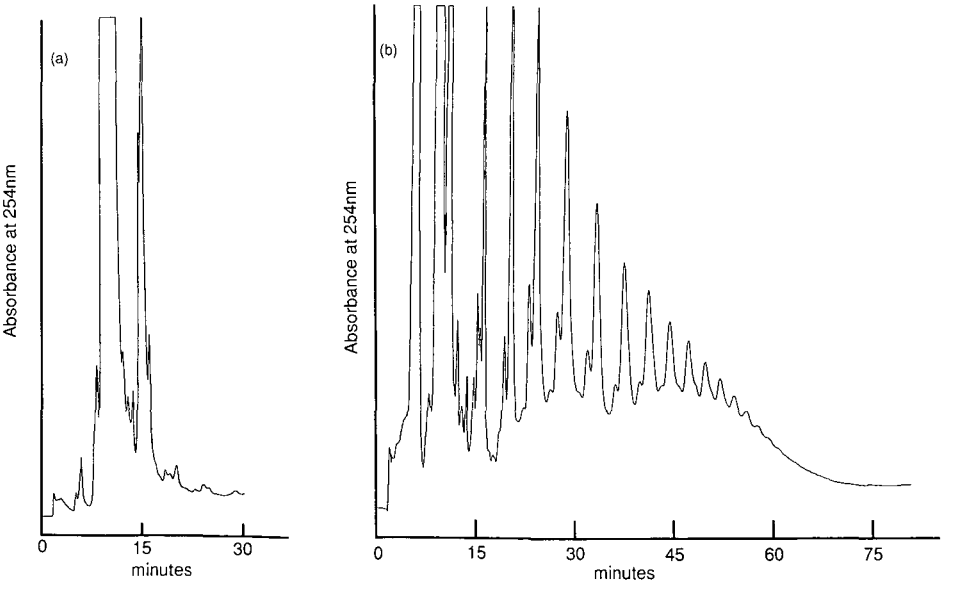

Fig. 3. HPLC elution profiles of 2MeImpG oligomerization reactions using HEMA-IEC BIO Q. Reaction conditions are described in the text. These profiles are of aliquots taken after incubation at 4°C for 6 days. The chromatographic conditions are the same as in Fig. 1 except with a chart speed of 20 cm h^{-1} and 0.05 a.u.f.s. (a) 2MeImpG alone; (b) 2MeImpG in the presence of poly(C).

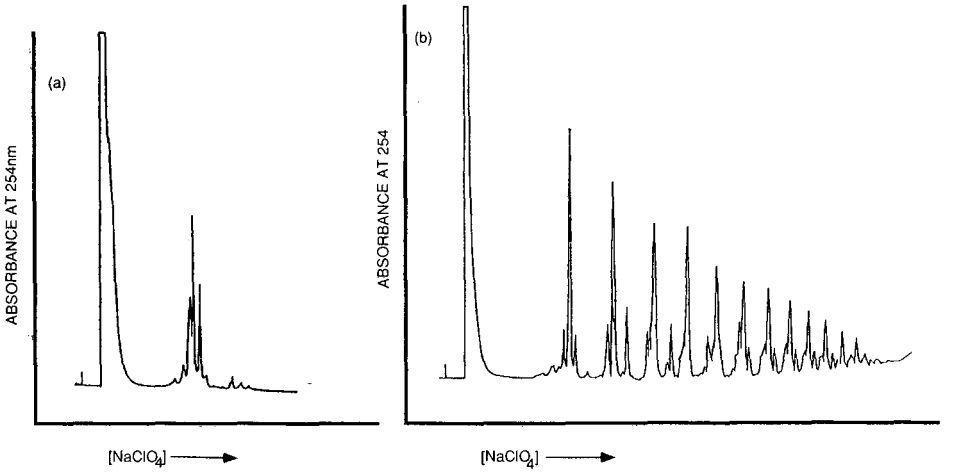

Fig. 4. HPLC elution profiles of 2MeImpG oligomerization reactions using RPC-5. The reaction and sample preparation conditions used here are from previous work [9], and are similar to those described in the text except that the incubation was at −18°C for 4 weeks. The chromatography was performed using a Beckmann solvent delivery system composed of two 110B pumps and an NEC 8300 gradient controller at pH 12 using a linear gradient of sodium perchlorate (0 to 0.06 *M* in 90 min) and a flow-rate of 1 ml min^{-1}. The eluate was monitored at 254 nm by a Kratos spectroflow 757 variable-wavelength detector attached to a Soltec Model 1242 recorder. (a) 2MeImpG alone; (b) 2MeImpG in the presence of poly(C).

find ways to separate longer oligomers, and it is likely that better resolution can be obtained with investigations of other mobile phase conditions.

Fig. 2 shows the elution profile produced when poly(G) is subjected to partial base-catalyzed hydrolysis. At least some of the peak broadening seen in the longer oligomers is due to the preparative flow cell used in the UV detector. This result can be directly compared with the 2MeImpG oligomerizations shown in Fig. 3. Finally, similar oligomerizations analyzed by RPC-5 are shown in Fig. 4. It should be noted that the profiles in Fig. 4 are from previously published work [9] which employed reaction conditions different from those described in this study. More efficient reaction conditions can be found elsewhere [2].

It is clear from the results reported here that HEMA-IEC BIO Q is useful for separating oligonucleotides at high pH. Its stability and reproducibility, as well at its ability to separate both long and short oligonucleotides suggest a versatile workhorse role for this type of column.

ACKNOWLEDGEMENTS

I am indebted to Dr. David Deamer for his support and critical comments. This work was supported by ONR grant N00014-90-1121.

REFERENCES

1 J. Sulston, R. Lohrmann, L. E. Orgel and H. T. Miles, *Proc. Natl. Acad. Sci. U.S.A.*, 59 (1968) 726.
2 T. Inoue and L. E. Orgel, *J. Mol. Biol.*, 162 (1982) 201.

3 T. Inoue and L. E. Orgel, *Science (Washington, D.C.)*, 219 (1983) 859.
4 J. Ninio and L. E. Orgel, *J. Mol. Evol.*, 12 (1978) 91.
5 P. O. P. Ts'o, *Basic Principles in Nucleic Acid Chemistry*, Academic Press, New York, 1974, Ch. 6.
6 R. L. Pearson, J. F. Weiss and A. D. Kelmers, *Biochim. Biophys. Acta*, 228 (1971) 770.
7 D. A. Usher, *Nucleic Acids Res.*, 6 (1979) 2289.
8 A. Kanavarioti and D. L. Doodokyan, *J. Chromatogr.*, 389 (1987) 334.
9 R. Stribling and S. L. Miller, *J. Mol. Evol.*, in press.

Journal of Chromatography, 538 (1991) 480–483
Elsevier Science Publishers B.V., Amsterdam

CHROM. 22 834

Short Communication

Liquid chromatographic determination of carbendazim in the presence of some normal soil constituents with photodiode-array detection

F. SÁNCHEZ-RASERO*, T. E. ROMERO and C. G. DIOS
Estación Experimental del Zaidín, CSIC, c/Profesor Albareda 1, 18008 Granada (Spain)
(First received February 16th, 1990; revised manuscript received August 1st, 1990)

ABSTRACT

A reversed-phase high-performance liquid chromatographic method was developed for the determination of carbendazim in the presence of some normal soil constituents (kaolinite, montmorillonite and peat). Spiked aqueous soil samples were injected after centrifugation and filtration. Quantitative recoveries were observed and good precision was obtained. The concentration range studied, 1.6716–8.3580 mg/l, is the most suitable for adsorption–desorption studies of carbendazim on soil and soil constituents.

INTRODUCTION

Carbendazim (methyl benzimidazol-2-ylcarbamate) is a systemic fungicide which controls a wide range of pathogens of cereals, vegetables, fruits grapes and ornamental plants. Its solubility in water at pH 6–6.5 is about 10 ppm.

In some solvents [1] and in contact with water or under moist conditions in soil [2], dissociation of benomyl occurs to form carbendazim. The EPA [3] has pointed to the possible mutagenicity, teratogenicity and reduction in spermatogenic activity of benomyl under certain conditions, which increases the toxicological interest in carbendazim.

Because of the possible toxicity of carbendazim for man, through contaminated plants and waters, we decided to study the adsorption–desorption mechanisms of this fungicide on kaolinite, montmorillonite and peat, in order to be able to predict its behaviour in different soils and in the environment.

Gorbach [4] published a review of analytical methods for carbendazim, benomyl and related fungicides, and many other papers (*e.g.*, [5–8]) have subsequently appeared on the same topic.

A reversed-phase high-performance liquid chromatographic (HPLC) method with methanol–water as the eluent has been developed for the direct determination of

0021-9673/91/$03.50

carbendazim in supernatants of aqueous solutions of carbendazim and soil constituents. This was done in order to avoid either preconcentration steps [9] or derivatization processes necessary in gas–liquid chromatography [5], to eliminate organic solvents [10] of low polarity which would make difficult the interpretation of the adsorption–desorption process of carbendazim on soil and to minimize small changes in pH [8] which could influence both retention times and peak areas if acidic or basic substances were present in the mobile phase.

EXPERIMENTAL

Apparatus

A Hewlett-Packard Model 1090 liquid chromatograph, equipped with a 4.5-μl spectrometer cell, a diode-array detector and DPU multi-channel integrator, as described in a previous paper [11], was used. A Hewlett-Packard 799160D-552 stainless-steel column (100 mm × 2.1 mm I.D.) packed with ODS-Hypersil (5 μm) was used.

The Millex filters (Millipore, Bedford, MA, U.S.A.) used were Type HV_4, 4 mm, pore size 0.45 μm.

Soil constituents

Kaolinite from Lage, montmorillonite from Almería and peat from Padul (all in Spain) were used.

Reagents

Methanol of HPLC grade was obtained from Panreac (Madrid, Spain). Water was purified with a Milli-Q water purification system (Millipore). Carbendazim samples, as analytical standards of known purity, were gifts from BASF (Limburgerhof, F.R.G.) DuPont (Wilmington, DE, U.S.A.) and Hoechst (Frankfurt am Main, F.R.G.).

Calibration solutions

A solution of carbendazim standard in water was prepared at 8.3580 mg/l and four other solutions were prepared by dilution with water at 6.6864, 5.0148, 3.3432 and 1.6716 mg/l. Taking into account the very low solubility of carbendazim in water (10 ppm), a wider range of concentrations is not feasible.

Sample solutions

Approximately 0.2 g of peat, or 1.0 g of the other soil constituents, was weighed (to the nearest 0.1 mg). A 20-ml volume of carbendazim solution at a concentration within the range 1.6716–8.3580 mg/l was added and shaken mechanically for a certain period (the time necessary for the study of adsorption–desorption behaviour). The solution was then centrifuged at 12 062 *g* for 20 min and an aliquot of the supernatant was filtered through a Millex HV_4 filter into a small vial fitted with a cap.

Chromatography

The chromatographic conditions were as follows: mobile phase, methanol–water (65-35); flow-rate, 0.3 ml/min; column temperature, 40°C; detection wave-

lengths, 285 and 243 nm (bandwidth 4 nm); reference wavelength, 550 nm (bandwidth 100 nm); range, automatic; and injection volume, 10 μl.

RESULTS AND DISCUSSION

The calibration graph, obtained by plotting absorbance *versus* carbendazim concentration, was linear over the range 1.6716–8.3580 mg/l for 10-μl injections and passed through the origin. The straight line obtained corresponds to the equation $y = 86.5166x + 4.0979$, with a correlation coefficient of 0.9999.

The chromatography of various samples is shown in Fig. 1. The carbendazim peak area is about 250 milliabsorbance units. The separation of carbendazim from impurities seems to be adequate in each instance and no peak was observed at the retention time of carbendazim when blank samples of montmorillonite, kaolinite and peat were chromatographed under the same conditions.

UV spectra measured for each chromatographic peak prior to, at and after the carbendazim maximum were very similar, demonstrating the purity of the carbendazim peak. This purity was also demonstrated by the linear relationship between the signals obtained at 285 and 243 nm.

The standard addition technique was used to test the ability of the HPLC system to determine accurately carbendazim added to a peat carbendazim supernatant. To five 2-ml aliquots of peat carbendazim supernatant, at a concentration of 0.5841 mg/l, were added 0, 1, 2, 3 and 4 ml of a 14.700 mg/l carbendazim solution in methanol and correspondingly 4, 3, 2, 1 and 0 ml of methanol. The detector response to carbendazim,

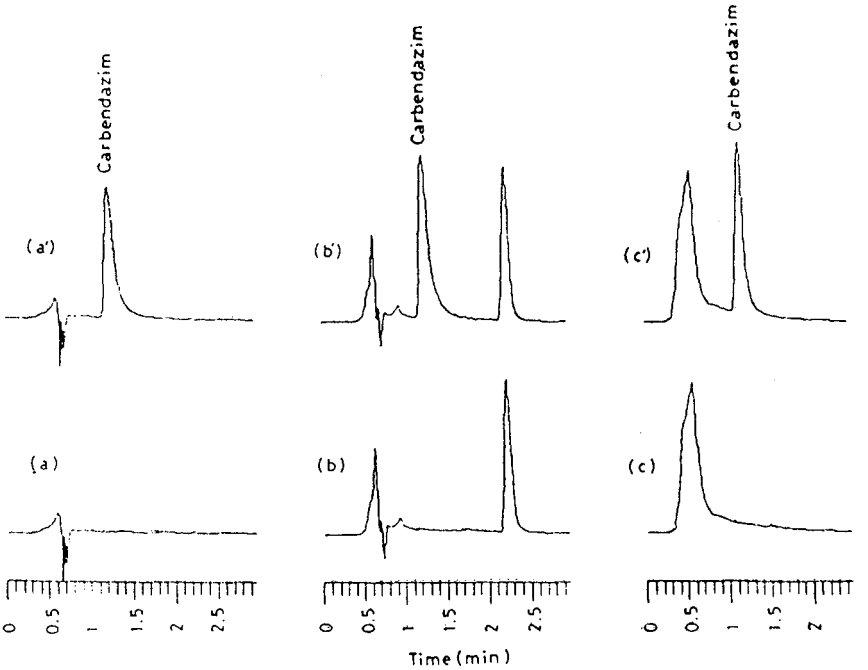

Fig. 1. Chromatography of (a), (b) and (c) montmorillonite, kaolinite and peat samples (blanks), and of (a'), (b') and (c') montmorillonite–carbendazim, kaolinite–carbendazim and peat–carbendazim samples.

in the presence of coextracted constituents of the peat soil, ranged from 97.9% to 102.9 of theoretical. A peat carbendazim sample was chosen for this experiment because the components of peat extracts are chromatographically separated from carbendazim with more difficulty than those of either montmorillonite or kaolinite, as can be seen in Fig. 1.

The relative standard deviations for eleven repeated injections of two carbendazim samples at 0.5760 and 8.7709 mg/l were 1.05 and 0.54%, respectively.

The detection limit, for a standard sample, defined as the amount which produces a signal equal to three times the background noise level, was 0.06 ng of carbendazim, equivalent to 10 μl of solution of concentration 6 μg/l.

ACKNOWLEDGEMENTS

We gratefully acknowledge support for this work by grant PR84-0160-C04-02 from the Comisión Asesora de Investigación Científica y Técnica (CAICYT). The valuable technical assistance of M^{a}. D. Maroto is gratefully acknowledged.

REFERENCES

1 M. Chiba and E. A. Cherniak, *J. Agric. Food Chem.*, 26 (1978) 573.
2 R. P. Singh and M. Chiba, *J. Agric. Food Chem.*, 33 (1985) 63.
3 U.S. EPA, *Fed. Regist.*, 44 (1979) 51166.
4 S. Gorbach, *Pure Appl. Chem.*, 52 (1980) 2567.
5 H. Steinwandter, *Fresenius' Z. Anal. Chem.*, 321 (1985) 599.
6 H. T. Kalinoski, H. R. Hudseth, B. W. Wright and R. D. Smith, *J. Chromatogr.*, 400 (1987) 307.
7 M. B. Thomas and P. E. Sturrock, *J. Chromatogr.*, 357 (1986) 318.
8 M. Chiba and R. Singh, *J. Agric. Food Chem.*, 34 (1986) 108.
9 U. Oehmichen, F. Karrenbrock and K. Haberer, *Fresenius' Z. Anal. Chem.*, 327 (1987) 715.
10 J. E. Farrow, R. A. Hoodless, M. Sargent and J. A. Sidwell, *Analyst (London)*, 102 (1977) 752.
11 F. Sánchez-Rasero and A. Peña-Heras, *J. Assoc. Off. Anal. Chem.*, 71 (1988) 1064.

Journal of Chromatography, 538 (1991) 484–491
Elsevier Science Publishers B.V., Amsterdam

CHROM. 22 865

Short Communication

Simultaneous determination of residual synthetic antibacterials in fish by high-performance liquid chromatography

MASAKAZU HORIE*, KOICHI SAITO, YOJI HOSHINO and NORIHIDE NOSE
Saitama Prefectural Institute of Public Health, 639–1, Kamiokubo, Urawa, Saitama 338 (Japan)
HIROYUKI NAKAZAWA
Department of Pharmaceutical Sciences, National Institute of Public Health, 4–6–1 Shirokanedai, Minato-ku, Tokyo 108 (Japan)
and
YASUHIRO YAMANE
Faculty of Pharmaceutical Sciences, Chiba University, 1–33, Yayoi-cho, Chiba, Chiba 260 (Japan)
(First received May 7th, 1990; revised manuscript received September 24th, 1990)

ABSTRACT

A simple and rapid high-performance liquid chromatographic (HPLC) method for the simultaneous determination of sulphamonomethoxine (SMMX), sulphadimethoxine (SDMX), sulphisozole (SIZ), nalidixic acid (NA), oxolinic acid (OXA), piromidic acid (PMA), furazolidone (FZ) and sodium nifurstyrenate (NFSA) in cultured fish was developed. The drugs were extracted with 0.2% metaphosphoric acid–methanol (6:4), followed by a Bond Elut C_{18} clean-up procedure. The HPLC separation was carried out on an Inertsil ODS column (150 × 4.6 mm I.D.) using 5 m*M* aqueous oxalic acid–acetonitrile (55:45) as the mobile phase with detection at 265 nm (0.04 a.u.f.s.). The calibration graphs were rectilinear from 1 to 20 ng for OXA, from 2 to 50 ng for SMMX, SDMX, SIZ, NA, PMA and FZ and from 5 to 100 ng for NFSA. The recoveries of each drug added to fish were 65.0–89.5%. The detection limits were 0.02 μg/g for OXA, 0.05 μg/g for SMMX, SDMX, SIZ, NA, PMA and FZ and 0.1 μg/g for NFSA.

INTRODUCTION

Various antibiotics and synthetic antibacterials are widely used for the prevention and treatment of infectious diseases in cultured fish. According to the Japanese Food Sanitation Law, no food should contain antibiotics and, in addition, meat, poultry, eggs, fish and shellfish should not contain any synthetic antibacterial substances.

0021-9673/91/$03.50

In a previous paper [1], we reported a method for the simultaneous determination of nalidixic acid (NA), oxolinic acid (OXA) and piromidic acid (PMA) in cultured fish by high-performance liquid chromatography (HPLC). In addition to NA, OXA and PMA, sulphamonomethoxine (SMMX), sulphadimethoxine (SDMX), sulphisozole (SIZ), furazolidone (FZ) and sodium nifurstyrenate (NFSA) are also used in culture fisheries in Japan. HPLC analysis of these antibacterials is being performed individually [2–7] or with specified groups [8–12], because their physico-chemical properties are different from one another. Although individual methods are useful for the accurate detemination of each drug, it is very labour- and time-consuming to inspect one by one every possible drug that might remain in fish. Consequently, it is necessary to establish a reliable method by which many antibacterials can be determined simultaneously and simply and rapidly.

This paper describes a simple and rapid HPLC method for the simultaneous determination of eight kinds of synthetic antibacterials which were considered to be possible residues in fish using Bond-Elut C_{18} cartridges in a clean-up step.

EXPERIMENTAL

Materials and reagents

The edible muscle tissues of yellowtail, eel, sweet fish, rainbow trout and red sea bream served as samples.

SMMX, SDMX and NA were obtained from Daiichi (Tokyo, Japan), FZ and NFSA from Ueno (Osaka, Japan) and OXA, PMA and SIZ from Tanabe (Osaka, Japan), Dainihon (Osaka, Japan) and Takeda (Osaka, Japan) Pharmaceutical, respectively.

Bond Elut C_{18} (500 mg), Baker C_{18} (500 mg) and Sep-Pak C_{18} were purchased from Analytichem (Harbor City, CA, U.S.A.), J. T. Baker (Phillipsburg, NJ, U.S.A.) and Millipore (Milford, MA, U.S.A.), respectively. The cartridges were washed with 5 ml of methanol and then 10 ml of distilled water before use. Hyflo Super-Cel was purchased from Johns-Manville (Denver, CO, U.S.A.). Other chemicals were of analytical-reagent or HPLC grade.

Preparation of standard solutions

Each standard (10 mg) was weighed accurately into a 100-ml volumetric flask and diluted to volume with acetonitrile. Subsequent dilutions were made with the HPLC mobile phase.

Apparatus

The HPLC system consisted of an LC-6A solvent-delivery system, an SPD-6A UV detector operated at 265 nm and a Chromatopack C-R3A data system, all from Shimadzu (Kyoto, Japan). The separation was performed on an Inertsil ODS (5 μm) column (150 × 4.6 mm I.D.) (Gasukuro Kogyo, Tokyo, Japan) with 5 m*M* aqueous oxalic acid–acetonitrile (55:45) as the mobile phase at a flow-rate of 0.5 ml/min at room temperature. An RP-8 Newguard guard column (15 × 3.2 mm I.D.) (Brown Labs., Santa Clara, CA, U.S.A.) was fitted in front of the analytical column.

The other instruments used were a Model 330 spectrophotometer (Hitachi, Tokyo, Japan) and a Model NS-50 Physcotron homogenizer (Niti-on, Chiba, Japan).

Sample preparation

A 5-g amount of sample was homogenized with 100 ml of 0.2% metaphosphoric acid (MPA)–methanol (6:4) as a deproteinizing extractant at high speed for 2 min. The homogenate was filtered through *ca.* 1 mm Hyflo Super-Cel coated on a suction funnel. The filtrate was evaporated under reduced pressure at 40°C. Evaporation was interrupted when *ca.* 10 ml of solution remained in the flask. The flask contents were applied to a Bond Elut C_{18} cartridge. After washing with 10 ml of distilled water, the cartridge was eluted with 10 ml of methanol. The eluate was evaporated to dryness under reduced pressure and the residue dissolved in 1 ml of HPLC mobile phase; 10 μl of the solution were injected for HPLC.

Calibration graphs

Working standard solutions with concentrations of 0.1, 0.2, 0.5, 1.0 and 2.0 μg/ml of OXA, 0.2 0.4, 1.0, 2.0 and 5.0 μg/ml of SMMX, SDMX, SIZ, NA, PMA and FZ and 0.5, 1.0, 2.0, 5.0 and 10.0 μg/ml of NFSA were prepared from stock standard solutions. A 10-μl volume of these solutions was injected into the column. Calibration graphs were obtained by the measurement of peak heights.

RESULTS AND DISCUSSION

Chromatographic conditions

Each of the eight synthetic antibacterials was dissolved in the HPLC mobile phase and their UV spectra were measured. The maximum UV absorptions of each of SMMX, SDMX, SIZ, FZ, NA and OXA were found to be 260–270 nm and those of PMA and NFSA were *ca.* 280 and 290 nm, respectively. On the basis of these results, a wavelength of 265 nm was chosen for the measurement.

It is known generally that NA, OXA and PMA show peak tailing in reversed-phase chromatography [1,12]. In order to prevent such a phenomenon, methylation of samples [6] or addition of counter ions to the mobile phase [7,11] is recommended. However, the methylation method requires a complex procedure and the addition of counter ions cannot prevent the tailing sufficiently. Previously, we reported that such tailing could be prevented by the use of wide-pore ODS column [1]. Therefore, in this study the effect of a wide-pore ODS column on the mutal separation of the eight drugs was evaluated. These drugs, however, could not be separated efficiently with this column because of its weak retention capacity compared with that of the ODS column.

Ikai *et al.* [12] reported that the tailing of NA, OXA and PMA could be prevented by the addition of oxalic acid to mobile phase. Although Ikai *et al.* used a three-component mobile phase (acetonitrile–methanol–aqueous oxalic acid), operation would be easier if a two-component system could be applied. Consequently, the separation conditions for the drugs were examined by applying acetonitrile–aqueous oxalic acid as the mobile phase and by using end-capped Inertsil ODS, Nucleosil $5C_{18}$ (Macherey-Nagel, Düren, F.R.G.) and LiChrosphere RP-18e (E. Merck, Darmstadt, F.R.G.) in the separation column, because it seemed that residual silanol groups on the surface of the stationary phase could cause the tailing of NA, OXA and PMA [1,12]. Inertsil ODS was chosen for subsequent experiment because it gave the best separations and peak shapes.

Next, optimum separation conditions were evaluated by changing the mixing ratio, oxalic acid concentration and the pH of the mobile phase (acetonitrile–aqueous oxalic acid). As the result, 5 m*M* aqueous oxalic acid–acetonitrile (55:45) was chosen as the mobile phase. Fig. 1A shows a typical chromatogram of the eight antibacterials obtained under the chosen conditions.

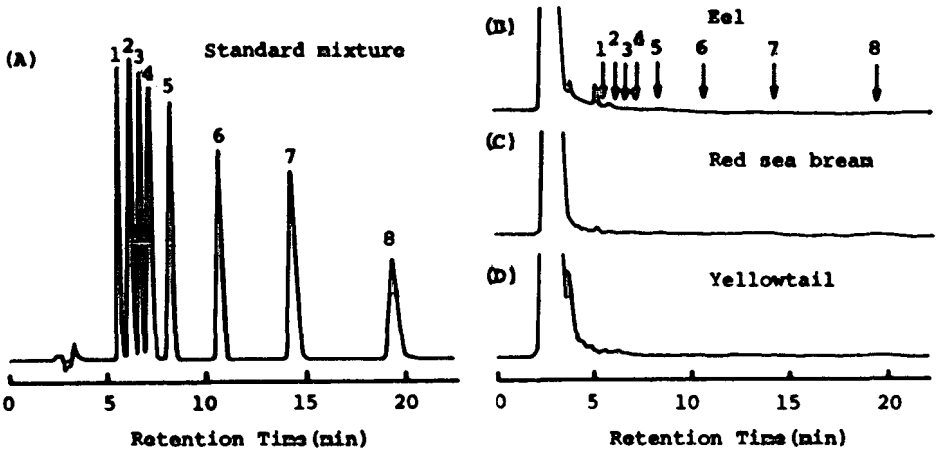

Fig. 1. Typical chromatograms of extracts of cultured fish. (A) Standard mixture. Peaks: 1 = SMMX (10 ng); 2 = SIZ (10 ng); 3 = FZ (10 ng); 4 = OXA (4 ng); 5 = SDMX (10 ng); 6 = NA (10 ng); 7 = PMA (10 ng); 8 = NFSA (20 ng). (B) Eel extract. (C) Red sea bream extract. (D) Yellowtail extract. For chromatographic details, see Experimental.

Clean-up

Various methods have been applied to the extraction and clean-up processes for the HPLC analysis of residual antibacterials in livestock and aquatic products, because their physico-chemical properties are different from one another. In a previous paper [1], we reported the simultaneous determination of NA, OXA and PMA in fish in which samples were extracted with MPA–methanol and cleaned-up using Sep-Pak C_{18} cartridges. Therefore, an evaluation was performed in order to establish whether such a method could be applied to the simultaneous determination of the eight drugs.

The drugs (5 μg each, except for 2 μg of OXA) were added to a yellowtail extract which has been prepared according to the method described under Experimental, and the retention capacity for each drug between the C_{18} cartridges was compared. As shown in Table I, Sep-Pak C_{18} showed a weak SIZ-retaining capacity, resulting in the loss of about 20% of the SIZ. In contrast, the retention capacity of Baker C_{18} for NA, OXA and PMA was so strong that about 20% of each drug could not be eluted. On the basis of these results, it was decided that Bond-Elut C_{18} be used as the cartridge for clean-up.

We have previously reported that the content of methanol in the MPA–methanol extraction solvent affected the recovery of veterinary drugs [1,13]. Here, the effect of methanol on the recovery of the eight drugs was evaluated by changing the content of methanol in the extraction solvent. As shown in Table II, the recovery of these drugs, excluding SIZ, was improved as the content of methanol increased; the recovery of SIZ decreased when the content of methanol exceeded 40%.

TABLE I

COMPARISON OF DISPOSABLE REVERSED-PHASE C_{18} CARTRIDGES

Values are means ± S.D. ($n = 5$). Recoveries of synthetic antibacterials from 10 ml of yellowtail extract. To the samples were added 0.2 μg/ml of oxolinic acid and 0.5 μg/ml of other drugs.

Drug	Recovery (%)		
	Bond Elut C_{18}	Baker C_{18}	Sep-Pak C_{18}
SDMX	91.7 ± 3.1	92.1 ± 2.6	90.5 ± 3.7
SIZ	88.7 ± 3.7	90.6 ± 3.5	73.9 ± 7.7
SMMX	93.2 ± 2.9	92.9 ± 3.7	94.1 ± 4.0
NA	97.0 ± 1.6	74.0 ± 3.1	87.7 ± 2.7
OXA	97.7 ± 1.6	80.5 ± 2.7	91.3 ± 3.3
PMA	97.8 ± 2.2	76.3 ± 2.0	91.9 ± 4.1
FZ	95.8 ± 0.7	93.2 ± 2.2	94.6 ± 1.4
NFSA	91.6 ± 2.8	90.3 ± 3.0	88.7 ± 1.2

The pH of the yellowtail extract prepared according to the method described under Experimental was varied from 2.5 to 7.0 and 5-μg portions of SMMX, SDMX and SIZ were added. As shown in Fig. 2, the recovery of SIZ decreased considerably when the pH exceeded 5.5, probably owing to a weakened retention capacity of the C_{18} cartridge due to the ionization of SIZ at > 5.5. When the content of methanol in the extraction solvent exceeds 50%, the pH of the extract increases to ≥ 5 (Table II). This seems to be a cause of the reduction in SIZ recovery. The pH of the extract and the change in the recovery of SIZ accompaning an increase in methanol concentration are similar for yellowtail as for other kinds of fish (eel, sweet fish, red sea bream and rainbow trout), so that they are independent of the kind of fish. In addition, the peaks on the chromatogram were affected by the coexisting agents when the content of methanol was increased. As a consequence, the content of methanol was fixed at 40%.

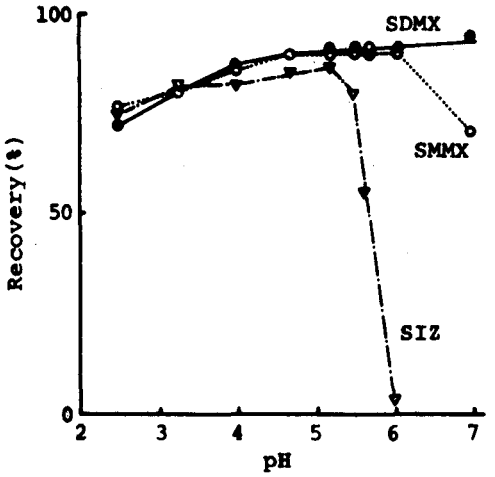

Fig. 2. Influence of pH of yellowtail extract on the recovery of SMMX, SDMX and SIZ.

TABLE II

EFFECT OF METHANOL CONTENT IN EXTRACTING SOLVENT ON THE RECOVERY OF SYNTHETIC ANTIBACTERIALS FROM YELLOWTAIL

Samples were spiked with 0.4 μg/g of oxolinic acid and 1.0 μg/g of other drugs. Mean results of five replicate determinations with relative standard deviations (%) in parentheses.

Extraction solvent	pH[a] of extract	Recovery (%)							
		SDMX	SIZ	SMMX	NA	OXA	PMA	FZ	NFSA
0.2% MPA–methanol(8:2)	3.9	65.3(3.3)	64.5(4.5)	71.1(3.7)	81.5(2.6)	78.0(3.2)	66.5(2.6)	82.4(3.0)	21.7(3.3)
0.2% MPA–methanol(7:3)	4.3	76.1(2.9)	74.0(1.6)	80.0(3.2)	84.2(1.4)	83.7(1.4)	75.6(1.7)	87.5(1.3)	45.7(0.8)
0.2% MPA–methanol(6:4)	4.7	83.8(2.6)	80.1(3.4)	85.8(3.2)	87.3(2.3)	86.4(1.5)	85.4(3.2)	86.1(0.4)	65.3(3.5)
0.2% MPA–methanol(5:5)	5.1	83.7(1.8)	73.6(6.3)	86.1(2.0)	87.8(2.0)	87.3(2.5)	87.3(1.6)	87.3(2.0)	70.9(2.8)
0.2% MPA–methanol(4:6)	5.5	86.9(2.7)	63.4(9.7)	86.9(2.5)	88.6(2.6)	88.5(1.6)	88.8(2.7)	88.6(1.6)	77.9(0.8)

[a] pH of a typical concentrated extract.

TABLE III

EFFECT OF THE CONCENTRATION OF METAPHOSPHORIC ACID IN THE EXTRACTION SOLVENT ON THE RECOVERY OF SYNTHETIC ANTIBACTERIALS FROM YELLOWTAIL

Samples were spiked with 0.4 μg/g of oxolinic acid and 1.0 μg/g of other drugs. Results of five replicate determinations with relative standard deviations (%) in parentheses.

Extraction solvent	Recovery (%)							
	SDMX	SIZ	SMMX	NA	OXA	PMA	FZ	NFSA
0.1% MPA–methanol(6:4)	86.5(1.2)	84.4(4.2)	88.2(1.7)	85.0(1.9)	85.0(1.4)	82.9(2.4)	86.4(2.2)	70.5(4.3)
0.2% MPA–methanol(6:4)	83.8(2.6)	80.1(2.6)	85.8(3.2)	87.3(2.3)	87.9(3.1)	85.4(3.2)	87.5(2.0)	65.3(3.5)
0.5% MPA–methanol(6:4)	76.5(4.5)	76.9(3.4)	80.1(3.0)	89.0(2.7)	86.4(1.5)	85.4(3.6)	85.4(0.4)	53.8(4.9)
1.0% MPA–methanol(6:4)	63.8(5.0)	64.1(3.7)	67.1(3.9)	88.3(1.3)	84.4(1.6)	81.0(4.7)	83.4(1.6)	46.0(3.5)

TABLE IV

RECOVERIES OF SYNTHETIC ANTIBACTERIALS FROM CULTURED FISH

Samples were spiked with 0.4 μg/g of oxolinic acid and 1.0 μg/g of other drugs. Results of five replicate determinations with relative standard deviations (%) in parentheses.

Sample	Recovery (%)							
	SDMX	SIZ	SMMX	NA	OXA	PMA	FZ	NFSA
Yellowtail	83.8(2.6)	80.1(2.6)	85.8(3.2)	87.3(2.3)	87.9(3.1)	85.4(3.2)	87.5(2.0)	65.3(3.5)
Eel	81.7(1.0)	80.5(2.3)	82.9(1.9)	87.9(1.9)	90.2(3.4)	86.4(3.9)	89.0(2.1)	67.8(3.7)
Sweet fish	86.6(1.7)	86.0(4.8)	88.5(2.1)	85.9(2.9)	88.1(1.4)	84.9(1.7)	89.5(3.1)	66.3(1.9)
Red sea bream	85.2(2.2)	82.6(2.7)	86.2(3.0)	87.4(2.7)	89.1(2.0)	87.3(1.8)	89.2(0.7)	66.1(2.7)
Rainbow trout	82.7(2.1)	83.2(2.0)	84.2(2.0)	87.0(3.4)	87.1(2.5)	84.5(2.9)	87.0(2.7)	65.0(1.3)

Table III shows the effect of the MPA concentration on the recovery of the eight drugs. A lower concentration of MPA gave higher recoveries of SMMX, SDMX, SIZ and NFSA, and gave less interfering paks. An extractant of 0.1% MPA–methanol (6:4) was not effective enough with regard to deproteinization. Based on the above experiments, 0.2% MPA–methanol (6:4) was chosen as a deproteinization extractant. Fig. 1B, C and D show typical chromatograms of eel, red sea bream and yellowtail extracts, respectively. Similar chromatograms were obtained from sweet fish and rainbow trout samples.

Recovery

Linear calibration graphs were obtained from 1 to 20 ng for OXA, 2 to 50 ng for SMMX, SDMX, SIZ, FZ, NA and PMA and 5 to 100 ng for NFSA. Table IV summarizes the recoveries of the drugs from commercial samples of yellowtail, eel, sweet fish, red sea bream and rainbow trout fortified with 0.4 μg/g of OXA and 1.0 μg/g of other drugs. Although the recovery of NFSA was low (65.0–67.8%), those of other drugs were higher than 80%, with standard deviations within 5%. The detection limits of the method were 0.02 μg/g for OXA, 0.05 μg/g for SMMX, SDMX, SIZ, FZ, NA and PMA and 0.1 μg/g for NFSA.

REFERENCES

1 M. Horie, K. Saito, Y. Hoshino, N. Nose, E. Mochizuki and H. Nakazawa, *J. Chromatogr.*, 402 (1987) 301.
2 Y. Kasuga, K. Otsuka, T. Sugiya and F. Yamada, *J. Food. Hyg. Soc. Jpn.*, 22 (1981) 479.
3 T. Oida, K. Kouno, H. Katae, S. Nakamura, Y. Sekine and M. Hashimoto, *Bull. Japan. Soc. Sci. Fish.*, 48 (1982) 1599.
4 W. Winterlin, G. Hall and C. Mourer, *J. Assoc. Off. Anal. Chem.*, 64 (1981) 1055.
5 L. H. M. Vroomen, M. C. J. Berghmans and T. D. B. Strujs, *J. Chromatogr.*, 362 (1986) 141.
6 *Official Publication*, Veterinary Sanitation Division, Environmental Health Bureau, Ministry of Health and Welfare, Tokyo, Vol. 2, 1982, No. 5, pp. 1–11.
7 *Official Publication*, Veterinary Sanitation Division, Environmental Health Bureau, Ministry of Health and Welfare, Tokyo, Vol. 2, 1984, No. 7, pp. 11–18.
8 T. Nagata, F. Miyamoto and M. Saeki, *J. Food. Hyg. Soc. Jpn.*, 23 (1982) 278.
9 Y. Kasuga, T. Sugiya and F. Yamada, *J. Food. Hyg. Soc. Jpn.*, 23 (1982) 344.
10 Y. Hori, *J. Food. Hyg. Soc. Jpn.*, 25 (1984) 158.
11 S. Horii, C. Yasuoka and M. Matsumoto, *J. Chromatogr.*, 388 (1987) 459.
12 Y. Ikai, H. Oka, N. Kazumura, M. Yamada, K. Harada, M. Suzuki and H. Nakazawa, *J. Chromatogr.*, 388 (1987) 459.
13 M. Horie, Y. Hoshino, N. Nose and H. Nakazawa, *Eisei kagaku*, 31 (1985) 371.

Journal of Chromatography, 538 (1991) 492–496
Elsevier Science Publishers B.V., Amsterdam

CHROM. 22 839

Short Communication

High-performance liquid chromatographic separation of heterometallic 1,1′-bis(diphenylphosphino)ferrocene-substituted metal carbonyls

KEMMY B. H. LIM, L.-T. PHANG, M. R. KHAN, T. S. ANDY HOR and H. K. LEE*
Department of Chemistry, National University of Singapore, Kent Ridge, Singapore 0511 (Singapore)
(First received May 18th, 1990; revised manuscript received August 21st, 1990)

ABSTRACT

The normal-phase, isocratic high-performance liquid chromatographic analysis of a series of 1,1′-bis (diphenylphosphino)ferrocene (dppf)-substituted metal carbonyl compounds, namely $(OC)_9Mn_2(dppf)M(CO)_5$, where M = Cr, Mo, W; $(OC)_9Mn_2(dppf)Fe(CO)_4$ and $(OC)_9Mn_2(dppf)Mn_2(CO)_9$ is described. A column packed with silica bonded with polar secondary amino–cyano groups was used after preliminary experiments showed that conventional silica columns were unsatisfactory for separation. The mobile phase used was isooctane–chloroform (92:8, v/v). On the basis of the results obtained, the retention behaviour of the compounds studied is discussed.

INTRODUCTION

The first reported separation of organometallic compounds by high-performance liquid chromatography (HPLC) was in 1969 [1]. Since then its use has greatly increased. Although thin-layer chromatography (TLC) is still often used in organometallic chemistry, it suffers from several limitations, including long analysis times, low adequate efficiency of separation and poor detection capability. All of these problems can be circumvented by HPLC. Moreover, HPLC can be applied to compounds prone to instability, whether thermal, oxidative or photochemical, etc. Several reviews of the application of HPLC to the analysis of organometallic and coordination compounds, have been published in recent years [2–5]. In the analysis of organometallics, much attention has been focused on carbonyl complexes, which are important in many synthetic and catalytic processes [6–9]. A review was recently devoted to the HPLC separation of these species [5].

This paper describes the normal-phase, isocratic HPLC separation of five 1,1′-bis(diphenylphosphino)ferrocene (dppf)-substituted metal carbonyl compounds, namely $(OC)_9Mn_2(dppf)M(CO)_5$ (M = Cr, **1**; Mo, **2**; W, **3**); $(OC)_9Mn_2(dppf)Fe(CO)_4$

0021-9673/91/$03.50

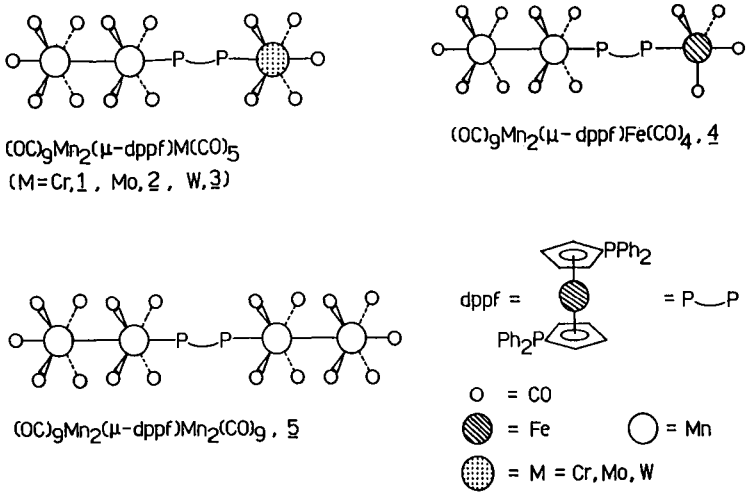

Fig. 1. Structures of the dppf-substituted metal carbonyls studied.

(**4**) and $(OC)_9Mn_2(dppf)Mn_2(CO)_9$ (**5**). Fig. 1 shows the structures of these cluster compounds. A study of these mixed-metal polynuclear complexes allows the examination of the effect of the metal, within a similar ligand environment, on their chromatographic retention behaviour. For comparison purposes, the parent compound, $Mn_2(CO)_{10}$ (**6**), was included in the study.

In addition to the aforementioned problems with TLC, the compounds under consideration here cannot be satisfactorily separated by this technique because of the similarities of their geometrical and chemical properties. An additional advantage of HPLC is that the separation takes only 8 min, as reported below.

EXPERIMENTAL

A Shimadzu LC-6A pump equipped with a Shimadzu Model SPD-6A variable-wavelength UV spectrophotometric detector was used. A Whatman Partisil 5 PAC (5 μm) column (100 mm × 4.6 mm I.D.) was used for separations. Chromatographic data were collected and analysed on a Shimadzu Chromatopac C-R3A data processor. The eluent flow-rate was typically 0.5 ml min^{-1}. The detection wavelength was 254 nm. The mobile phase compositions used in this work included 87:13, 90:10 and 92:8 (v/v) isooctane–chloroform.

All solvents were of HPLC grade from various suppliers, and were filtered through a Millipore membrane filter and degassed by ultrasonication before use. Mobile phases were prepared by measuring exact volumes of the individual components and then mixing them to give the desired compositions.

Sample solutions were filtered before being introduced into the column by means of a Rheodyne Model 7125 injection valve. Typically, 5–10-μl samples were injected. HPLC runs were carried out at least in triplicate. The reproducibility of retention times between runs was $\pm 2\%$ or better.

The metal carbonyl compounds investigated have been previously synthesized

and characterized; details have been reported elsewhere [10,11]. Fresh solutions of the compounds, shielded from sunlight, were used. The integrity of the compounds (in solutions of chloroform), based on their carbonyl absorptions, was checked by infrared spectroscopy.

RESULTS AND DISCUSSION

Owing to their inherently poor solubilities in the traditional solvents used in reversed-phase HPLC such as methanol and acetonitrile (neat or in combination with water), the decision was made to separate the dppf-substituted metal carbonyls by normal-phase HPLC. Conventionally, for normal-phase HPLC, columns packed with silica are used. However, in recent years, the use of columns packed with silica bonded with polar groups has become more popular.

In this work, a column packed with silica bonded with polar secondary amino–cyano groups was used (hence the proprietary description of PAC for the column). The carrier solvent was isooctane, with chloroform making up the binary mixture. Preliminary experiments with conventional (unmodified) silica columns showed that no separation amongst the compounds considered could be achieved. It was surmised that, with the PAC column, the presence of bonded secondary amino–cyano groups on the silica would impart a measure of selectivity to the stationary phase, a selectivity that should be greater than if a column packed with unmodified silica was used. The better selectivity would therefore translate into satisfactory separation of the compounds. This turned out to be the case for some of the compounds considered, as

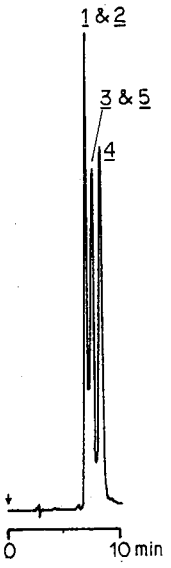

Fig. 2. Normal-phase liquid chromatogram of dppf-substituted metal carbonyls on a Whatman Partisil 5 PAC (5 μm) column (100 mm × 4.6 mm I.D.). Mobile phase, isooctane–chloroform (92:8, v/v); flow-rate, 0.5 ml min^{-1}; detection wavelength, 254 nm. Compounds: **1** = $(OC)_9Mn_2(dppf)Cr(CO)_5$ (k' = 1.49); **2** = $(OC)_9Mn_2(dppf)Mo(CO)_5$ (k' = 1.49); **3** = $(OC)_9Mn_2(dppf)W(CO)_5$ (k' = 1.71); **4** = $(OC)_9Mn_2(dppf)Fe(CO)_4$ (k' = 1.99); **5** = $(OC)_9Mn_2(dppf)Mn_2(CO)_9$ (k' = 1.70).

shown by the chromatogram in Fig. 2, which was obtained using isooctane–chloroform (92:8, v/v) as the eluent. Compounds **2**, **3** and **4** were resolved from one another. However, **1** could not be separated from **2** or **3** from **5**. Apart from isooctane–chloroform, mobile phases such as isooctane–dichloromethane and hexane–dichloromethane were also used in order to separate the recalcitrant pairs, but without success.

In an attempt to arrive at a compromise between resolution and reasonable analysis times, several other isooctane–chloroform compositions were investigated, including 90:10 and 87:13. With the exception of the 90:10 composition, which provided a slightly inferior resolution (but with shorter retention times) of the same three compounds than that afforded by the 92:8 system, the other eluent provided unsatisfactory separation. As expected for normal-phase HPLC, as the proportion of the non-polar component (isooctane) in the mobile phase is raised, an increased retention of the analytes is observed.

Order of elution

Using isooctane–chloroform (92:8) as the eluent, **6** had the shortest elution time; in fact, its capacity factor (k') of 0.03 suggests that it underwent minimal retention, if any, on the column (the use of isooctane–dichloromethane and hexane–dichloromethane as eluents did not improve the retention characteristics of **6**). As shown by the capacity factors in Fig. 2, **2** eluted after **6**, followed by **3** and finally **4**. As described previously, separation of the Cr and Mo complexes (**1** and **2**), and W and Mn_4 complexes (**3** and **5**) could not be achieved under the present conditions.

Several workers have attempted to correlate the chromatographic elution order of similar complexes with cluster size, geometry and electronic environment [12–15]. It is clear, however, that much of the issue remains speculative and more evidence is needed before a general correlation between retention behaviour and such parameters may be arrived at. Nevertheless, it appears that minor changes in the metal and ligand environment are sufficient to alter the retention characteristics of these compounds. Our results show that all the dppf-substituted complexes possess greater retention than the parent binary carbonyl, **6**, an observation in agreement with what has been previously determined for PPh_3 complexes [16]. Earlier work on $M(CO)_6$ (M = Cr, Mo, W) on a Si 60 column failed to resolve these binary carbonyls [17] (that is, carbonyls containing only CO as ligands), although a partial separation in the reversed-phase mode using a C_{18} column was reported. Our finding that the W complex **3**, can be resolved from the other Group 6 congeners is noteworthy, although it is unclear why the W complex should have a greater retention than the Cr (and the co-eluting Mo) complexes {the electronegativity of W being 1.40 (Allred–Rochow scale), which is intermediate between the values for Cr (1.56) and Mo (1.30) [18]}. This observation suggests that caution should be exercised in the use of electronegativity to rationalize the retention behaviour of analogous complexes [17,19]. On the other hand, the greater retention of the W complex may be due to the higher steric requirement of the $W(CO)_5$ moiety. The greater retention of **5** (which co-elutes with **3**) in comparison to **1** and **2** may be understood in terms of the higher nuclearity of the cluster. It should be pointed out that although **5** is the largest cluster studied, its size may not be the sole factor in determining its retention characteristics. The latter may also be attributed to the lower polarity and dipole moment of **5** compared with **1** or **2**, an inherent consequence of the symmetrical diphosphine

bridge in the molecule. This influence of dipole moment is also possibly reflected by the most strongly retained component (**4**) of the series of compounds studied, in which the $Fe(CO)_4$ moeity possesses lower local symmetry than the other $M(CO)_5$ moieties. This therefore results in a higher overall dipole moment for the molecule than that for **5**.

Our choice of the open-form dppf-substituted carbonyl clusters allowed us to examine the effect of the metal on the HPLC characteristics of heterometallic systems. However, more examples of such compounds need to be available before a more meaningful interpretation of their retention behaviour may be made. Nevertheless, at this stage, it is conclusive that HPLC with UV detection offers a sufficiently high sensitivity for the analysis of these compounds, possessing only a slight variation in the metal centre. The obvious benefit that may be gained from the amenability of the compounds to HPLC separation is in the area of preparative liquid chromatography.

ACKNOWLEDGEMENTS

The authors thank the National University of Singapore for financial support and Ms. Tan Geok Kheng and Ms. Leong Ying Phooi for their technical assistance.

REFERENCES

1 H. Veening, J. M. Greenwood, W. H. Shanks and B. R. Willeford, *J. Chem. Soc., Chem. Commun.*, (1969) 1305.
2 H. Veening and B. R. Willeford, *Rev. Inorg. Chem.*, 1 (1979) 281.
3 B. R. Willeford and H. Veening, *J. Chromatogr.*, 251 (1982) 61.
4 H. Veening and B. R. Willeford, *Adv. Chromatogr.*, 22 (1983) 117.
5 A. Casoli, A. Mangia, G. Predieri, E. Sappa and M. Volante, *Chem. Rev.*, 89 (1989) 407.
6 W. A. Herrmann, *J. Organomet. Chem.*, 383 (1990) 21.
7 R. Hoffmann, S. D. Wijeyesekera and S.-S. Sung, *Pure Appl. Chem.*, 58 (1986) 481.
8 M. E. Dry, *J. Organomet. Chem.*, 372 (1989) 117.
9 W. Keim, *J. Organomet. Chem.*, 372 (1989) 15.
10 T. S. A. Hor and L.-T. Phang, *J. Organomet. Chem.*, 381 (1990) 121.
11 T. S. A. Hor and L.-T. Phang, *Polyhedron*, 9 (1990) 2305.
12 A. Casoli, A. Mangia, G. Predieri and E. Sappa, *J. Chromatogr.*, 303 (1984) 404.
13 A. Casoli, A. Mangia, G. Predieri and E. Sappa, *Anal. Chim. Acta*, 176 (1985) 259.
14 C. T. Enos, G. L. Geoffroy and T. H. Risby, *J. Chromatogr. Sci.*, 15 (1977) 83.
15 W. L. Gladfelter and G. L. Geoffroy, *Adv. Organomet. Chem.*, 18 (1980) 249.
16 A. Casoli, A. Mangia, G. Predieri and E. Sappa, *J. Chromatogr.*, 447 (1988) 187.
17 A. Casoli, A. Mangia, G. Predieri and E. Sappa, *J. Chromatogr.*, 355 (1986) 285.
18 J. Emsley, *The Elements*, Clarendon Press, Oxford, 1989, p. 232.
19 A. Mangia, G. Predieri and E. Sappa, *Anal. Chim. Acta*, 152 (1984) 289.

Journal of Chromatography, 538 (1991) 497–503
Elsevier Science Publishers B.V., Amsterdam

CHROM. 22 924

Short Communication

Hollow-fibre membrane-based sample preparation device for the clean-up of brine samples prior to ion chromatographic analysis

PETER E. JACKSON* and WILLIAM R. JONES
Waters Chromatography Division of Millipore, 34 Maple Street, Milford, MA 01757 (U.S.A.)
(First received July 16th, 1990; revised manuscript received October 17th, 1990)

ABSTRACT

A hollow-fibre membrane-based sample preparation device was investigated for the removal of chloride from brine samples prior to ion chromatographic analysis. A device consisting of 150 cm of sulphonated Dupont Nafion® fiber immersed in a counter-ion donating solution of 0.050 *M* silver *p*-toluenesulphonate can remove greater than 99% of chloride and bromide in a sample while giving quantitative recoveries for other inorganic anions of interest. This sample pretreatment approach combined with conventional non-suppressed ion chromatography using conductivity detection gives a detection limit for nitrite of approximately 0.1 ppm in brine samples containing up to 5000 ppm chloride.

INTRODUCTION

Ion chromatography (IC) is now widely used for the determination of anions in water samples [1,2]. While many natural and industrial water samples often only require filtration and/or dilution prior to injection, the determination of trace anions in brines and other samples containing high levels of chloride has typically been achieved using a variety of approaches.

The most common approach is to reduce the chloride concentration by precipitation as the silver salt. This is usually achieved either by directly adding silver form cation-exchange resin to the sample or by passing the sample through a silver form cation-exchanger [3–5]. Any cation-exchange resin used must first be converted to the silver form, usually by soaking in silver nitrate, then rinsed extensively to avoid contamination [3]. Alternatively, a column packed with silver form resin can be placed on-line so that it acts as a halide suppressor, however the halide suppressor only has a finite lifetime as silver chloride precipitation in the column results in increasing backpressure as the column becomes exhausted [6].

Selective detection, such as direct UV absorption or amperometry, has been used

0021-9673/91/$03.50

to achieve the determination of specific anions [7,8] in brines; and the use of a sodium chloride eluent in conjunction with selective detection [9,10] further enhances the ability to determine trace anions in high chloride matrices. Reinjection of unresolved column effluent fractions back into the IC system by means of switching valves has also been shown to allow determination of trace level anions in brine [11], however, all these approaches are somewhat limited in general utility.

It has recently been shown that hollow-fiber ion-exchange membranes offer some advantages over resin-based ion-exchangers for sample pretreatment in terms of ease of use for small sample volumes [12], better recoveries and less ionic contamination [13]. In this paper we discuss the use of a silver form, cation-exchange, hollow-fiber device for reducing chloride interference in the analysis of anions in brines and similar samples by ion chromatography with conductivity detection.

EXPERIMENTAL

Instrumentation

The liquid chromatograph consisted of a Waters (Milford, MA, U.S.A.) Model 510 pump, U6K injector, Model 430 conductivity detector, Model 441 UV detector and either a Waters 840 data station or 745 integrator. The analytical column used was a Waters IC-Pak™ anion HC (150 × 4.6 mm I.D.) methacrylate-based anion-exchanger. The eluent used was the Waters standard borate–gluconate buffer which consisted of 1.3 m*M* gluconate, 1.5 m*M* tetraborate, 5.8 m*M* boric acid, 120 ml/l acetonitrile, 20 ml/l *n*-butanol, pH 8.5 operated at a flow-rate of 2.0 ml/min. The eluent was prepared daily, filtered and degassed with a Waters solvent clarification kit.

Reagents

Eighteen-MΩ water purified using a Millipore Milli-Q™ water purification system (Bedford, MA, U.S.A.) was used for all solutions. Sodium D-gluconate (97%), boric acid (98% ACS reagent) were obtained from Sigma and sodium tetraborate (99% ACS reagent) was obtained from Aldrich. Acetonitrile and *n*-butanol [both high-performance liquid chromatography (HPLC) grade] were obtained from J. T. Baker, as were the analytical grade sodium salts used for the preparation of all the anion standards. Silver nitrate (99%) and silver *p*-toluenesulphonate (99%) used for the counter-ion donating (CID) solutions were also obtained from Aldrich.

Hollow-fiber sample pretreatment device

The strong cation-exchange hollow-fiber (0.87 mm O.D., 0.72 mm I.D.) was made from Nafion® perfluorosulphonate fiber obtained from Permapure Products (Toms River, NJ, U.S.A.). The sample pretreatment device was simply a 150 cm length of this fiber immersed in the CID solution which was housed in a 80-ml plastic sample storage bottle, similar to the experimental device described by Jones and Jandik [13]. A female plastic Luer-Lok® fitting was attached at one end of the fiber to enable the sample to be passed through the fiber with a disposable Luer-tip syringe. A male Luer-Lok fitting was attached at the outlet end of the fiber to allow a Millipore Millex® GV disposable filter to be incorporated into the device to remove any silver chloride precipitation prior to injection.

RESULTS AND DISCUSSION

Selection of an appropriate CID solution

For this application, co-cations in the sample (sodium, potassium, magnesium, etc.) are exchanged across the membrane for silver ions from the CID solution. The silver then precipitates as the chloride salt, to be passed through the fiber along with the sample stream. Silver nitrate (60 ml of 0.025 *M*) was initially selected as the CID solution as this silver salt is typically used for converting cation-exchange resins to the silver form [3]. The fiber was initially rinsed with 20 ml of Milli-Q water then 1 ml of a standard anion mix (10 ppm fluoride, 20 ppm chloride, 40 ppm nitrite, 40 ppm bromide, 40 ppm nitrate, 60 ppm phosphate and 40 ppm sulphate) was passed through the fiber at approximately 1 ml/min with a disposable Luer-tip syringe. The last 0.5 ml of the effluent was retained for injection. This procedure was repeated four times and the average recoveries (%) for the anions in the effluent are shown in Table I.

As was expected, the device completely removed chloride and bromide from the solution. However, the recovery for nitrate was higher than expected, while the remaining anions gave quantitative recoveries. The same anion mix was then allowed to reside in the fiber for 30 min before collection and injection into the IC. Similar recoveries were obtained to those shown in Table I for all ions, except that the recovery for nitrate was 345%. The nitrate ion evidently permeates into the sample from the CID solution, even though the fiber was negatively charged. A similar contamination problem was observed by Jones and Jandik [13] when using sulphuric acid as the CID solution with a hydrogen form, cation-exchange fiber device. The amount of nitrate permeating the fiber was found to be dependent upon the residence time of the sample in the fiber and the concentration of the CID solution.

Silver *p*-toluenesulphonate was then investigated for use as the CID solution, as it has been demonstrated that the greater the molecular weight of the scavenger (or CID co-anion in this case) the less leakage through the membrane occurs [14]. The recoveries for the seven anion mix were determined as previously for the device but using 60 ml of 0.025 *M* silver *p*-toluenesulphonate as the CID solution. Similar recoveries were obtained to those shown in Table I, except that the average recovery (of five) for nitrate was 96.3%. The *p*-toluenesulphonate anion did not appear to permeate the fiber at this CID concentration as no chromatographic peak was ever observed on the UV detector (operated at 214 nm) at the retention time corresponding to that of *p*-toluenesulphonate (*ca.* 15 min). The silver *p*-toluenesulphonate CID

TABLE I

RECOVERIES FOR A SEVEN-ANION MIX PASSED THROUGH THE HOLLOW-FIBER SAMPLE PRETREATMENT DEVICE WITH 60 ml OF 0.025 *M* SILVER NITRATE AS THE CID SOLUTION

The (%) relative standard deviation of the recovery is shown in parenthesis.

Average recovery ($n = 5$)						
F^-	Cl^-	NO_2^-	Br^-	NO_3^-	PO_4^{3-}	SO_4^{2-}
98.9 (0.4)	0.0	94.2 (1.8)	0.0	117.3 (4.6)	96.6 (0.1)	98.6 (0.9)

solution proved to be light sensitive but was stable for several weeks if stored in the absence of light.

Performance of fiber sample pretreatment device for chloride removal

A standard solution containing a high chloride concentration (5000 ppm chloride and 50 ppm each of nitrite, nitrate and sulphate) was prepared to test the performance of the fiber sample pretreatment device. The device was prepared as above (except using 0.050 *M* silver *p*-toluenesulphonate as the CID solution) and rinsed with 5 ml of Milli-Q water before use. The high chloride solution (1 ml) was passed through the device at approximately 1 ml/min, with the last 0.25 ml being retained for injection into the IC. Fig. 1 shows a chromatogram (20 μl injection) of the high chloride solution before being passed through the fiber sample pretreatment device and Fig. 2 shows a chromatogram of the same solution after being passed through the device. The chloride concentration was reduced by over 99% while the other anions all gave quantitative recoveries. Also, the chromatography was greatly

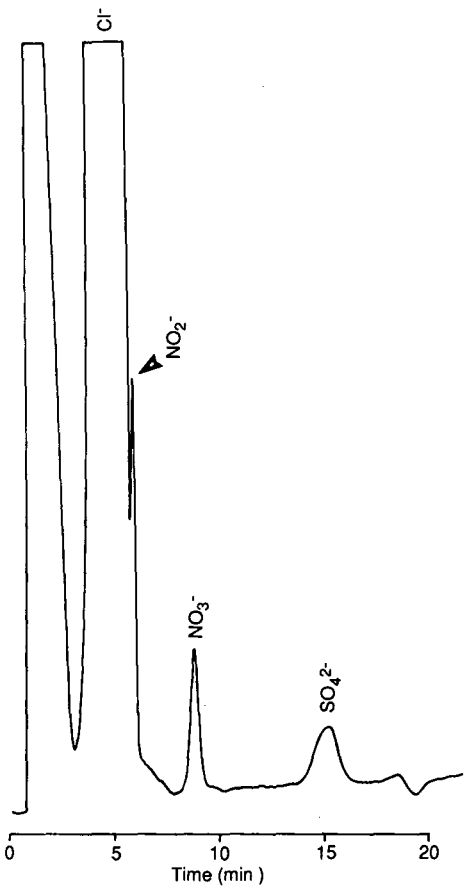

Fig. 1. Chromatogram of standard containing 5000 ppm chloride and 50 ppm each of nitrite, nitrate and sulphate. See Experimental section for conditions.

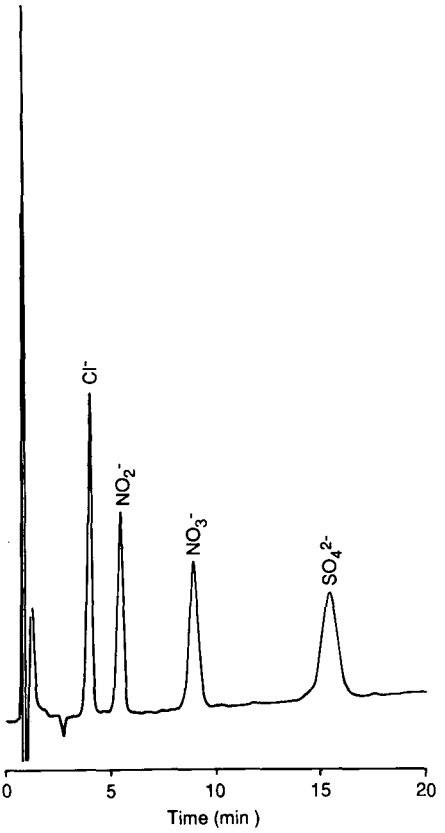

Fig. 2. Chromatogram of standard containing 5000 ppm chloride and 50 ppm each of nitrite, nitrate and sulphate after being passed through fiber sample pretreatment device. See text for details. See Experimental section for conditions.

improved due to the reduction in ionic strength of the sample after being passed through the device.

The fiber sample pretreatment device was applied to the determination of nitrite and nitrate in an industrial brine. A device was prepared as above and 1 ml of the sample was passed through the fiber at approximately 1 ml/min with the last 0.25 ml being retained for direct injection. Fig. 3 shows a chromatogram (20 μl injection) of the brine before being passed through the fiber sample pretreatment device and Fig. 4 shows a chromatogram of the same solution after being passed through the device. The sample contained approximately 1500 ppm chloride, which was almost totally removed (along with bromide) by passage through the device. The detection limit (3 $\times$ signal-to-noise) for nitrite in the presence of up to 5000 ppm chloride is *ca.* 0.1 ppm.

Capacity of fiber sample pretreatment device for chloride removal

The capacity of the device was limited to the removal of approximately 0.5 mequiv. of chloride as the fiber become blocked by precipitated silver chloride with use. However, it was possible to clean-up the fiber *in situ* by passing 2 ml of 1.0 *M*

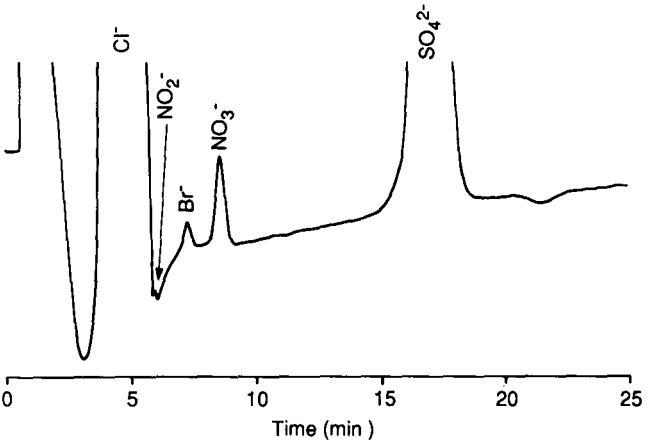

Fig. 3. Chromatogram of industrial brine. See Experimental section for conditions.

ammonium hydroxide through the device via a Luer-Lok syringe. The fiber was then rinsed with 5 ml of Milli-Q water before a new sample was applied and this procedure could be carried out until the CID solution was depleted of free silver ions.

CONCLUSIONS

The removal of chloride from brine samples prior to ion chromatographic analysis can be accomplished using a sample pretreatment device consisting of 150 cm of sulphonated Nafion fiber immersed in a CID solution of 0.050 *M* silver *p*-toluenesulphonate. The device can remove >99% of chloride and bromide at levels up to 5000 ppm in a sample while giving quantitative recoveries for other inorganic anions. The silver chloride which precipitates in the hollow-fiber tubing can be

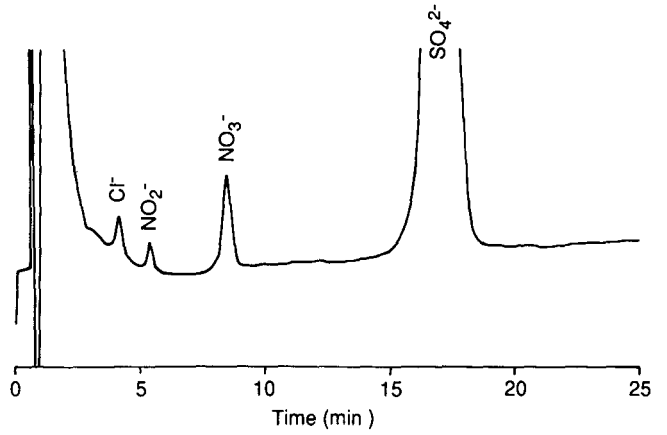

Fig. 4. Chromatogram of industrial brine after being passed through fiber sample pretreatment device. See text for details. See Experimental section for conditions. Nitrite and nitrate were present at 1.4 and 9.6 ppm, respectively.

removed *in situ* with ammonium hydroxide enabling the device to be regenerated and reused until the CID solution is exhausted. This sample pretreatment approach allows the determination of trace levels of nitrite (*ca.* 0.1 ppm) in brine samples containing up to 5000 ppm chloride when using conductivity detection.

REFERENCES

1 O. A. Shpigun and Yu. A. Zolotov, *Ion Chromatography in Water Analysis*, Ellis Horwood, Chichester, 1989.
2 D. T. Gjerde and J. S. Fritz, *Ion Chromatography*, Huthig, Heidelberg, 2nd ed., 1987.
3 R. M. Merril, *Technical Report SAND-84-2297*, Sandia National Laboratories, Albuquerque, NM, 1985.
4 R.-D. Wilken and H. H. Kock, *Fresenius Z. Anal. Chem.*, 320 (1985) 477.
5 M. H. Gaffney and M. Cooke, *Anal. Proc.*, 22 (1985) 25.
6 P. F. Kehr, B. A. Leone, D. E. Harrington and W. R. Bramstedt, *LC · GC*, 4 (1986) 1118.
7 R. G. Gerritse and J. A. Adeney, *J. Chromatogr.*, 347 (1985) 419.
8 K. Itoh and H. Sunahara, *Bunseki Kagaku*, 37 (1988) 292.
9 T. Okada, *Bunseki Kagaku*, 36 (1987) 702.
10 P. Pastore, I. Lavagnini, A. Boaretto and F. Magno, *J. Chromatogr.*, 475 (1989) 331.
11 P. F. Subosa, K. Kihara, S. Rokushika, H. Hatano, T. Murayama, T. Kuboto and Y. Hanaoka, *J. Chromatogr. Sci.*, 27 (1987) 680.
12 J. A. Cox, E. Dabek-Zlotorzynska, R. Saari and N. Tanaka, *Analyst (London)*, 113 (1988) 1401.
13 W. R. Jones and P. Jandik, *J. Chromatogr. Sci.*, 27 (1989) 449.
14 Y. Hanaoka, T. Murayama, S. Muramoto, T. Matsuura and A. Nanba, *J. Chromatogr.*, 239 (1982) 537.

Journal of Chromatography, 538 (1991) 504–505
Elsevier Science Publishers B.V., Amsterdam

CHROM. 22 831

Short Communication

Method for long-term preservation of thin-layer polyacrylamide gels by producing a gelatine coating

K. HOFMANN
Bundesanstalt für Fleischforschung, Institut für Chemie und Physik, Kulmbach (F.R.G.)
(First received August 10th, 1990; revised manuscript received September 20th, 1990)

ABSTRACT

Thin-layer polyacrylamide gels can be preserved and stored for unlimited periods by covering them with a gelatine coating. The method is inexpensive and simple. After air-drying, the gel is immersed in an aqueous 10% solution of highly viscous gelatine between 55 and 60°C. The coated gel is dried by hanging it in air. The method was checked successfully with gels of different thicknesses (0.15–0.50 mm) and after using different staining methods, *e.g.*, with silver, Coomassie Brilliant Blue and pseudoperoxidase.

INTRODUCTION

Thin and ultra-thin polyacrylamide gels after application in electrophoresis and especially isoelectric focusing [1] can normally be stored as a document for only a short period. When the gels are stored for longer periods they are ruptured or changed in an adverse way.

For the long-term preservation of such gels it has been suggested that they be stored in evacuated transparent bags [2], but it is even better to cover them with a gelatine coating as described below. The latter has the advantages that it is very cheap, large gels can be preserved and handled easily and no vacuum sealing machine is needed.

PREPARATION OF A 10% GELATINE SOLUTION

For the production of a smooth gelatine coating, free from air bubbles, it is essential to prepare the gelatine solution using ion-free water that has been boiled beforehand. After boiling, the water is cooled to 60°C in a 600-ml beaker. To 360 ml of the water, 40 g of pulverized highly viscous gelatine (*e.g.*, edible gelatine, 280 Bloom grade, produced by Deutsche Gelatine-Fabriken Stoess, Eberbach, F.R.G.) are added. The solution is stirred continuously until the gelatine has dissolved completely, and the

0021-9673/91/$03.50

temperature should be maintained in the range 55–60°C using a temperature-controlled water-bath. Finally, 2% glycerol (8 ml) and for microbiological stabilization a few drops of a 0.1% percent aqueous solution of sodium azide are added.

COATING THE GELS WITH GELATINE

The hot gelatine solution is transferred carefully into a suitable dish so that the formation of foam is avoided. Then the dry polyacrylamide gel is inserted slowly in the gelatine solution and the foil of the gel is fixed at the margin by a clamp. For this purpose, a staining and destaining dish from Pharmacia–LKB (Cat. No. 2117-109) is recommended (the cover of which limits losses from evaporation).

After immersing the gel for a short period (5–10 s) in the gelatine solution the gel is removed and, after allowing the excess of solution to run off, it is dried by hanging it in air. This procedure has been applied successfully to 0.15–0.50-mm gels of different dimensions (125 × 125 and 245 × 125 mm) after staining the gels with silver [3], Coomassie Brilliant Blue [4] or pseudoperoxidase [5].

STORAGE OF THE GELATINE SOLUTION

After use, the gelatine solution should be returned to the beaker and sealed, *e.g.*, with Parafilm. The solution solidifies when the temperature falls and it can be used again several times after warming to 55–60°C.

REFERENCES

1 A. Görg, W. Postel and R. Westermeyer, *GIT Lab.-Med.*, 2 (1979) 32.
2 K. Hofmann and E. Blüchel, *J. Chromatogr.*, 130 (1977) 444.
3 F. Bauer and K. Hofmann, *Fleischwirtschaft*, 67 (1987) 1141.
4 H. P. Schickle and F. Horneff, Pharmacia-LKB, Freiburg, instructions.
5 F. Bauer and K. Hofmann, *Fleischwirtschaft*, 67 (1987) 861.

Journal of Chromatography, 538 (1991) 506–509
Elsevier Science Publishers B.V., Amsterdam

CHROM. 22 852

Short Communication

Pharmaceutical analysis by capillary zone electrophoresis and micellar electrokinetic capillary chromatography[a]

K. D. ALTRIA*
Pharmaceutical Analysis Department, Glaxo Group Research, Ware, Herts. (U.K.)
and
N. W. SMITH
Chemical Analysis Department, Glaxo Group Research, Greenford, Middlesex (U.K.)
(First received April 12th, 1989; revised manuscript received September 12th, 1990)

ABSTRACT

The techniques of capillary zone electrophoresis and micellar electrocapillary chromatography have been found to be of use for the analysis of pharmaceuticals and separation from related impurities. The methods can give good resolutions and high separation efficiencies in many instances.

INTRODUCTION

Following its introduction in 1981 [1] capillary zone electrophoresis (CZE) is now developing into a useful and viable analytical technique. The high separation efficiencies, rapid run-times, relatively high levels of automation and low sample and solvent requirements make CZE particularly attractive to pharmaceutical analysis; and this potential use has been recognised [2]. This report gives details of some pharmaceutical applications within a commercial environment.

In CZE an electroendosmotic (EEO) flow of liquid occurs when a high voltage is applied across a capillary filled with carrier electrolyte. This EEO flow sweeps solutes along the capillary towards the detector. Therefore, the magnitude and direction of EEO flow affects the analysis times, separation efficiencies and resolution that are possible [3,4].

[a] Presented at the *1st International Symposium on High-Performance Capillary Electrophoresis, Boston, April 10–12, 1989*. The majority of the papers presented at this symposium have been published in *J. Chromatogr.*, Vol. 480 (1989).

0021-9673/91/$03.50

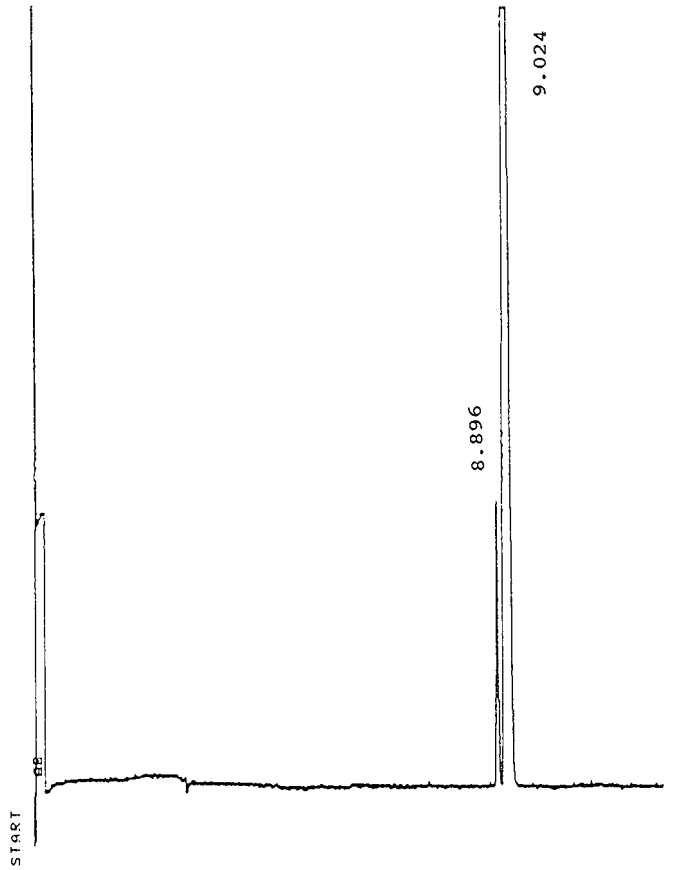

Fig. 1. Electropherogram of GR50360A and its des-5-fluoro analogue. Conditions: sample injection by vacuum for 1 s, detection by UV absorbance at 200 nm, +30 kV applied across the 100 cm × 50 μm capillary, equipment thermostatted at 30°C, 20 m*M* sodium citrate buffer (pH 2.5). Numbers at peaks indicate retention times in min.

EXPERIMENTAL

The electropherograms given in this paper were produced using an Applied Biosystems Model 270A instrument.

Des-5-fluoro analogue of GR50360A

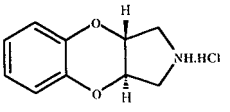

GR50360A

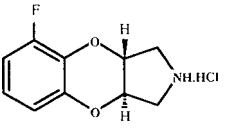

Fig. 2. Molecular structures of GR50360A and its desfluoro analogue.

RESULTS AND DISCUSSION

Fig. 1 shows the baseline separation of the anti-depressant GR50360A from a potential manufacturing impurity, the desfluoro analogue (Fig. 2). This separation is difficult to achieve by high-performance liquid chromatography (HPLC).

Equipment designed for use in CZE can also be applied to micellar electrokinetic capillary chromatographic (MECC) separations. In MECC [5] the stationary phase consists of surfactant micelles which typically move against the direction of EEO flow. Fig. 3 shows the resolution of the *syn* and *anti* isomers of a compound currently being developed for pharmaceutical use. The mobile phase was modified by the addition of 15% methanol to facilitate solubility of the test compound. This use of non-aqueous solvents has been recognised in CZE and MECC [6–8] and will become increasingly important.

A sample of peptide derived material was supplied that had previously been found to give only one peak by HPLC. Fig. 4 shows the electropherogram following

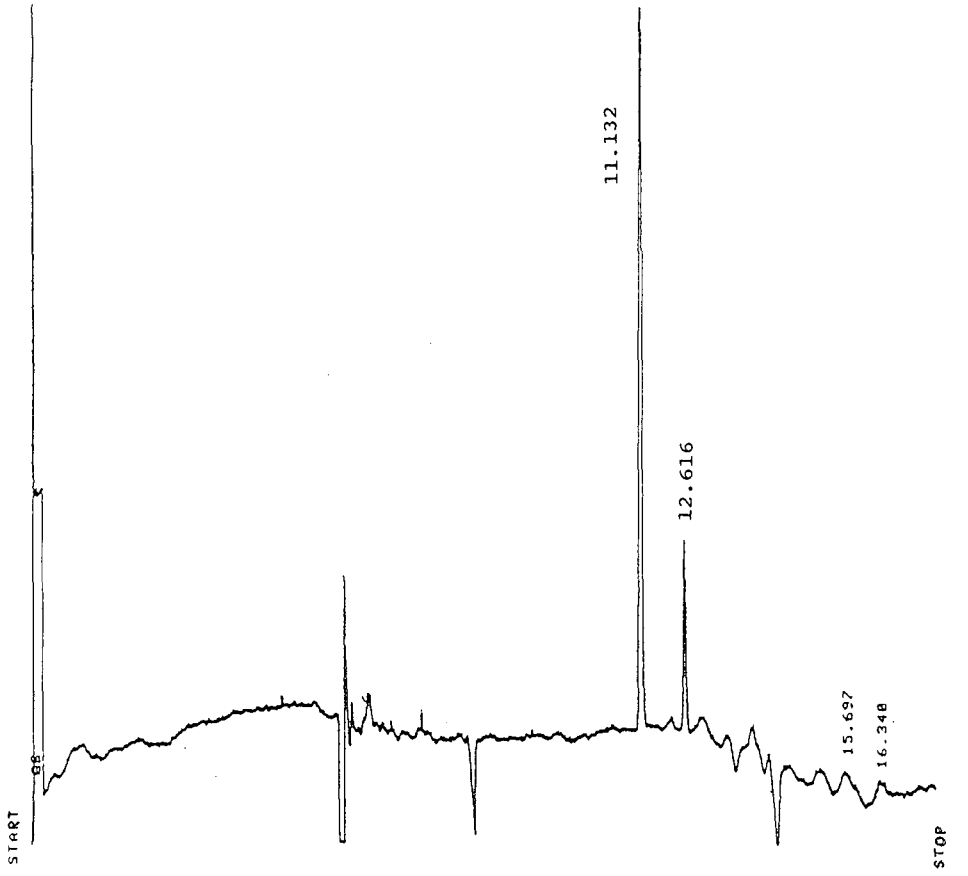

Fig. 3. MECC separation of *syn* and *anti* isomers. Conditions as in Fig. 1, except pH 11.0 [3-cyclohexylamino-1-propanesulfonic acid (CAPS) buffer], 50 m*M* sodium dodecyl sulphate, 15% (v/v) methanol. Numbers at peaks indicate retention times in min.

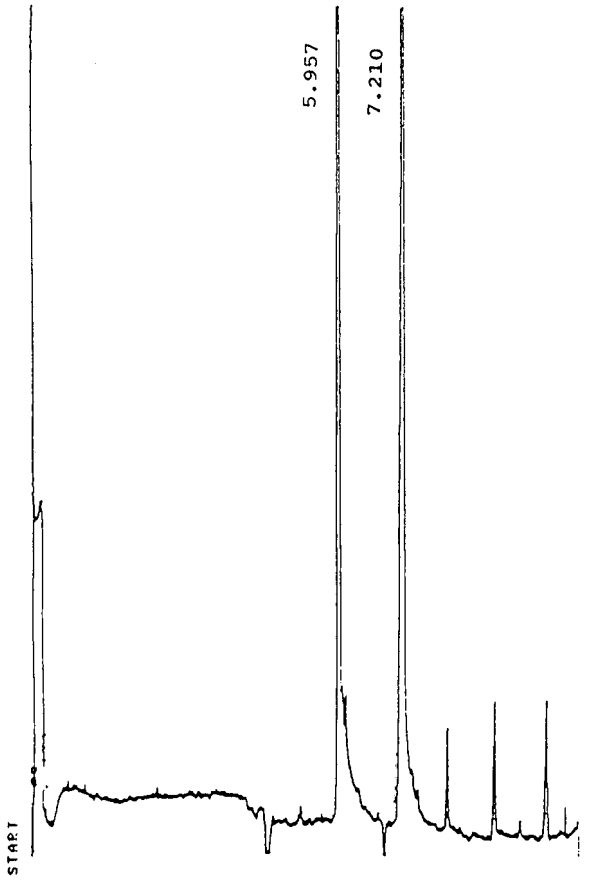

Fig. 4. MECC separation of a peptide. Conditions as in Fig. 3. Numbers at peaks indicate retention times in min.

resolution by MECC, the sample was separated into two principal components and three smaller constituents. This example highlights the alternative separation basis of MECC, compared to HPLC.

REFERENCES

1 J. W. Jorgenson and K. D. Lukacs, *Anal. Chem.*, 53 (1981) 1298.
2 K. D. Altria and C. F. Simpson, presented at *1st Conference on Pharmaceutical and Biomedical Analysis, Barcelona, 1987.*
3 K. D. Altria and C. F. Simpson, *Chromatographia*, 24 (1987) 527.
4 K. D. Altria and C. F. Simpson, *Anal. Proc.*, 23 (1986) 453.
5 S. Terabe, K. Otsuka, K. Ichikawa, A. Tsuchiya and T. Ando, *Anal. Chem.*, 56 (1984) 111.
6 Y. Walbroehl and J. W. Jorgenson, *Anal. Chem.*, 58 (1986) 479.
7 S. Fujiwara and S. Honda, *Anal. Chem.*, 59 (1987) 487.
8 A. T. Balchunas and M. J. Sepaniak, *Anal. Chem.*, 60 (1988) 617.

Journal of Chromatography, 538 (1991) 510–511
Elsevier Science Publishers B.V., Amsterdam

CHROM. 22 888

Book Review

Liquid chromatography/mass spectrometry applications in agricultural, pharmaceutical, and environmental chemistry (ACS Symposium Series, No. 420), edited by M. A. Brown, American Chemical Society, Washington, DC, 1990, XII + 298 pp., price US $ 64.95, ISBN 0-8412-1740-8.

This book, one of the *ACS Symposium Series*, contains material originally presented at a Symposium held by the Division of Agrochemicals during the *197th National Meeting of the American Chemical Society* in Dallas, Texas, April 1989. In a total of 18 chapters it provides state-of-the-art information on recent applications of combined liquid chromatographic–mass spectrometric (LC–MS) techniques in the fields of (A) Pesticide metabolism and degradation, (B) Pharmaceuticals and metabolism and (C) Environmental analysis.

The first chapter briefly reviews the development of LC–MS as a kind of introduction to the different interface and ionization systems, with regard to both their design and performance characteristics.

The following chapters are centred on the LC–MS analysis of agricultural chemicals and their metabolites and describe in some detail the different techniques available to enhance the usually scarce structural information provided by LC–MS data. Some of these techniques are based on the use of immobilized enzyme hydrolysis combined with thermospray ionization (TSP), chemical derivatization, high source temperatures, particle beam methods, tandem MS, wire repellers and modification of solvent adduct ions with novel additives in the LC eluent. Practical examples of how to improve the sensitivity of response with electron-capture negative-ion LC–MS are also described.

The second group of five chapters, under the heading Pharmaceuticals and metabolism, deals with examples on how to approach the qualitative and in some instances quantitative analysis of various types of compounds, such as biliary drug metabolites in their conjugate forms, macrolides, tetracyclines, retinoic acid in human plasma, aminonitrazepam in a *post mortem* blood extract and metoprolol enantiomers, and also the monitoring of *in vivo* acetylation and deacetylation of an anticonvulsant in rat blood.

Six more chapters, grouped under the heading Environmental analysis, close the book. These chapters deal with the use of particle beam (PB) LC–MS for the determination of pollutants in waste samples or of sulphate and glucuronide conjugates of phenols. In this regard, it is interesting that even though the particle beam interface has been praised for its ability to provide electron impact (EI) mass spectra that are readily amenable to identification via existing library search algorithms, only one library match was obtained for diisooctyl phthalate in a drinking water sample, the problem being that there are no EI mass spectra available yet for most organic

compounds in hazardous waste and drinking water samples. There is a chapter on LC–TSP-MS of phenol conjugates showing strong glucuronide and sulphate molecular ions, in contrast to the absence of these ions in PB mass spectra.

One of the chapters in this group presents comparative data on direct liquid introduction (DLI), TSP and fast atom bombardment (FAB) MS for the secondary metabolites of benzo[*a*]pyrene, showing that, as opposed to DLI and TSP, FAB-MS did not cause thermal decomposition and thus gives higher molecular ion responses. Another of the chapters is not really environmentally oriented but describes in some detail the recently developed combined TSP-EI interface, also called the "universal interface". Finally, there is a very interesting description of the use of highly sophisticated MS equipment for structural studies of protein alkylation by electrophilic xenobiotic metabolites.

Overall, the book should not be considered as a treatise on LC–MS but rather a collection of specialized manuscripts reflecting presentations at a meeting. Thus, although the expert may be aware of most of the information that it contains, it should certainly be of interest to all of those looking for an integrated appraisal of the present status of LC–MS with regard to environmental and related applications and including some fundamental information on interface design, ionization mechanisms and structural information, but with a more limited coverage of pharmaceutical applications.

Barcelona (Spain) E. GELPÍ

Author Index

Errata

J. Chromatogr., 515 (1990) 175–182
Pages 180–181: Figs. 4 and 5 should be interchanged (the legends are correct).

J. Chromatogr., 515 (1990) 227–231
Page 227, the third author's name should read Suguru Takatsuto.

PUBLICATION SCHEDULE FOR 1991

Journal of Chromatography and Journal of Chromatography, Biomedical Applications

MONTH	D 1990	J	F	M	
Journal of Chromatography	535/1 + 2	536/1 + 2 537/1 + 2 538/1	538/2 539/1 539/2	The publication schedule for further issues will be published later	
Cumulative Indexes, Vols. 501–550					
Bibliography Section					
Biomedical Applications		562/1 + 2 563/1	563/2	564/1	

INFORMATION FOR AUTHORS

(Detailed *Instructions to Authors* were published in Vol. 522, pp. 351–354. A free reprint can be obtained by application to the publisher, Elsevier Science Publishers B.V., P.O. Box 330, 1000 AH Amsterdam, The Netherlands.)

Types of Contributions. The following types of papers are published in the *Journal of Chromatography* and the section on *Biomedical Applications*: Regular research papers (Full-length papers), Review articles and Short Communications. Short Communications are usually descriptions of short investigations, or they can report minor technical improvements of previously published procedures; they reflect the same quality of research as Full-length papers, but should preferably not exceed six printed pages. For Review articles, see inside front cover under Submission of Papers.

Submission. Every paper must be accompanied by a letter from the senior author, stating that he/she is submitting the paper for publication in the *Journal of Chromatography*.

Manuscripts. Manuscripts should be typed in double spacing on consecutively numbered pages of uniform size. The manuscript should be preceded by a sheet of manuscript paper carrying the title of the paper and the name and full postal address of the person to whom the proofs are to be sent. As a rule, papers should be divided into sections, headed by a caption (*e.g.*, Abstract, Introduction, Experimental, Results, Discussion, etc.). All illustrations, photographs, tables, etc., should be on separate sheets.

Introduction. Every paper must have a concise introduction mentioning what has been done before on the topic described, and stating clearly what is new in the paper now submitted.

Abstract. All articles should have an abstract of 50–100 words which clearly and briefly indicates what is new, different and significant.

Illustrations. The figures should be submitted in a form suitable for reproduction, drawn in Indian ink on drawing or tracing paper. Each illustration should have a legend, all the *legends* being typed (with double spacing) together on a *separate sheet*. If structures are given in the text, the original drawings should be supplied. Coloured illustrations are reproduced at the author's expense, the cost being determined by the number of pages and by the number of colours needed. The written permission of the author and publisher must be obtained for the use of any figure already published. Its source must be indicated in the legend.

References. References should be numbered in the order in which they are cited in the text, and listed in numerical sequence on a separate sheet at the end of the article. Please check a recent issue for the layout of the reference list. Abbreviations for the titles of journals should follow the system used by *Chemical Abstracts*. Articles not yet published should be given as "in press" (journal should be specified), "submitted for publication" (journal should be specified), "in preparation" or "personal communication".

Dispatch. Before sending the manuscript to the Editor please check that the envelope contains four copies of the paper complete with references, legends and figures. One of the sets of figures must be the originals suitable for direct reproduction. Please also ensure that permission to publish has been obtained from your institute.

Proofs. One set of proofs will be sent to the author to be carefully checked for printer's errors. Corrections must be restricted to instances in which the proof is at variance with the manuscript. "Extra corrections" will be inserted at the author's expense.

Reprints. Fifty reprints of Full-length papers and Short Communications will be supplied free of charge. Additional reprints can be ordered by the authors. An order form containing price quotations will be sent to the authors together with the proofs of their article.

Advertisements. Advertisement rates are available from the publisher on request. The Editors of the journal accept no responsibility for the contents of the advertisements.

For Superior Chiral Separation From Analytical To Preparative.

The finest from DAICEL·····

Why look beyond DAICEL? We have developed the finest CHIRALCEL, CHIRALPAK and CROWNPAK with up to 17 types of HPLC columns, all providing superior resolution of racemic compounds.

NEW CHIRALPAK AS

● CHIRALPAK AS

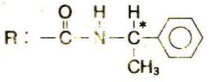

for β-Lactam antibiotics

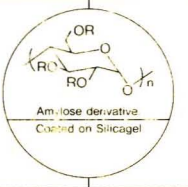

NEW CHIRALPAK AD

● CHIRALPAK AD

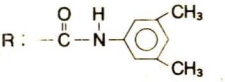

1-Acetoxy-2-azetidine

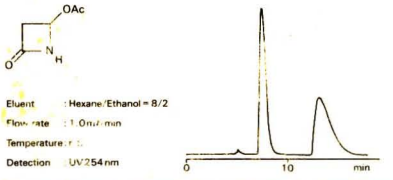

Oxyphencyclimine

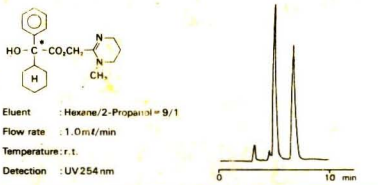

Ofloxacine methyl ester

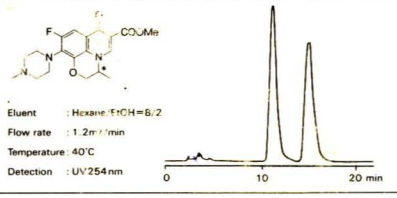

Verapamil

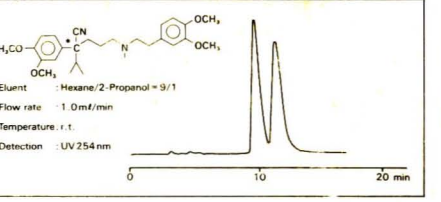

Analytical column 0.46cm×25cm(10μm)

CHIRALCEL OA
OB
OC
OD
OJ
OF
OG
OK

CHIRALPAK AS
AD

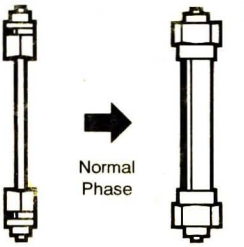

Semi-preparative column 2cm×25cm(10μm)

You can have Pure enantiomer quickly!!

■Separation Service

- A pure enantiomer separation in the amount of 100g~10kg is now available.
- Please contact us for additional information regarding the manner of use and application of our chiral columns and how to procure our separation service.

DAICEL CHEMICAL INDUSTRIES, LTD.

chiral chemicals division.
8-1, Kasumigaseki 3-chome, Chiyoda-ku, Tokyo 100, Japan Phone: 03 (507) 3151 FAX: 03 (507) 3193

DAICEL(U.S.A.), INC.
Fort Lee Executive Park
Two Executive Drive, Fort Lee,
New Jersey 07024
Phone: (201) 461-4466
FAX: (201) 461-2776

DAICEL(U.S.A.), INC.
23456 Hawthorne Blvd.
Bldg. 5, Suit 130
Torrance, CA 90505
Phone: (213) 791-2030
FAX: (213) 791-2031

DAICEL(EUROPA)GmbH
Oststr. 22
4000 Düsseldorf 1, F.R. Germany
Phone: (211) 369848
Telex: (41) 8588042 DCEL D
FAX: (211) 364429

DAICEL CHEMICAL(ASIA)PTE. LTD.
65 Chulia Street #40-07
OCBC Centre, Singapore 0104
Phone: 5332511
FAX: 5326454